

**MOLECULAR CAPSULES
BASED ON IONIC INTERACTIONS
IN POLAR SOLVENTS**

This work was supported by the Council for Chemical Sciences of the Dutch Organization for Scientific Research (CW-NWO), project number JC 99538.

© F. Corbellini, Enschede, 2004

No part of this work may be reproduced by print, photocopy or any other means without the permission in writing of the author.

ISBN 90-365-2040-1

**MOLECULAR CAPSULES
BASED ON IONIC INTERACTIONS
IN POLAR SOLVENTS**

PROEFSCHRIFT

ter verkrijging van
de graad van doctor aan de Universiteit Twente,
op gezag van de rector magnificus,
prof. dr. F.A. van Vught,
volgens besluit van het College van Promoties
in het openbaar te verdedigen
op vrijdag 7 mei 2004 om 16:45 uur.

door

Francesca Corbellini

geboren op 26 oktober 1975
te Leno, Italië

Dit proefschrift is goedgekeurd door:

Promotor:	Prof. dr. ir. D. N. Reinhoudt
Assistent-promotor:	Dr. M. Crego Calama

Contents

Chapter 1

GENERAL INTRODUCTION	1
-----------------------------------	---

Chapter 2

SUPRAMOLECULAR CONTAINERS: SYNTHESIS AND FUNCTIONAL PROPERTIES

2.1 Introduction	6
2.2 Molecular capsules based on covalent frameworks	6
2.3 Capsules <i>via</i> self-assembly	12
2.3.1 Hydrogen-bonded systems	12
2.3.1.1 <i>Glycoluril-derived capsules</i>	13
2.3.1.2 <i>Cyclophane-based capsules</i>	15
2.3.2 Metal-induced self-assembly of molecular containers	23
2.3.2.1 <i>Metal-bridged carceplexes</i>	23
2.3.2.2 <i>Metallo cages based on “molecular paneling”</i>	26
2.3.2.3 <i>Supramolecular metal clusters</i>	28
2.4 Functional properties	30
2.4.1 Molecular capsules for the isolation of reactive species	30
2.4.2 Molecular capsules as reaction chambers	31
2.4.3 Molecular capsules for sensing	33
2.5 Concluding remarks	34
2.6 References	35

Chapter 3

MULTIPLE IONIC INTERACTIONS FOR NONCOVALENT SYNTHESIS OF MOLECULAR CAPSULES IN POLAR SOLVENTS

3.1 Introduction	46
3.2 Results and discussion	48
3.2.1 Synthesis	48
3.2.2 Characterization of the molecular capsules 1a•2a-c	50
3.2.3 Studies on the self-assembly of 1a•2d	56
3.3 Conclusions	61
3.4 Experimental section	61
3.4.1 General information and instrumentation	61
3.4.2 Binding studies	62
3.4.3 Synthesis	62
3.5 References and notes	64

Chapter 4

DETAILED STUDY OF THE GEOMETRY AND THE GUEST ENCAPSULATION PROPERTIES OF AN AMIDINIUM-SULFONATE CALIX[4]ARENE BASED CAPSULE IN METHANOL

4.1 Introduction	70
4.2 Results and discussion	72
4.2.1 Synthesis	72
4.2.2 ¹ H NMR studies on the formation of the molecular capsule 1b•2a	73
4.2.3 Self-assembly of 1b-e•2a : influence of the amidinium side chain size	76
4.2.4 X-ray crystal structure of 1a•2a	78
4.2.5 Guest encapsulation studies with capsule 1b•2a	78
4.2.6 Towards water soluble molecular capsules	83
4.3 Conclusions	84
4.4 Experimental section	85
4.4.1 General information and instrumentation	85
4.4.2 Binding studies	85
4.4.3 Experimental details of the X-ray structure determination	86
4.4.4 Synthesis	87
4.5 References and notes	91

Chapter 5

WATER-SOLUBLE MOLECULAR CAPSULES: SYNTHESIS AND BINDING PROPERTIES

5.1 Introduction	96
5.2 Results and discussion	98
5.2.1 Synthesis	98
5.2.2 Characterization of the molecular capsules 1a•2a-b	99
5.2.3 Guest encapsulation in 1a•2a	105
5.2.3.1 Charged guest: <i>N</i> -methylquinuclidinium	105
5.2.3.2 Neutral molecules: docking study	107
5.3 Conclusions	114
5.4 Experimental section	114
5.4.1 General information and instrumentation	114
5.4.2 Binding studies	115
5.4.3 Docking	116
5.4.4 Synthesis	116
5.5 References and notes	118

Chapter 6

SELF-ASSEMBLY OF MULTICOMPONENT SUPRAMOLECULAR STRUCTURES THROUGH IONIC INTERACTIONS

6.1 Introduction	122
6.2 Results and discussion	123
6.2.1 Synthesis	123
6.2.2 Assembling studies in aqueous solution	124
6.2.3 Assembling studies in methanol	129
6.2.4 X-ray crystal structure of 1a•2a₂	139
6.3 Conclusions	140
6.4 Experimental section	141
6.4.1 General information and instrumentation	141
6.4.2 Binding studies	142
6.4.3 Synthesis	142
6.5 References and notes	143

Chapter 7

**SOLUTION AND SURFACE STUDIES ON THE SELF-ASSEMBLY OF A
NONCOVALENT MOLECULAR CAPSULE BASED ON IONIC INTERACTIONS**

7.1 Introduction	148
7.2 Results and discussion	149
7.2.1 Synthesis	152
7.2.2 Formation of the molecular capsule 1•2 in solution	153
7.2.3 Formation of the molecular capsule 1•2 at the surface	156
7.3 Conclusions	159
7.4 Experimental section	159
7.4.1 General information and instrumentation	159
7.4.2 Binding studies	160
7.5 References and notes	161
<i>Summary</i>	165
<i>Samenvatting</i>	169
<i>Acknowledgements</i>	173
<i>Curriculum Vitae</i>	175

GENERAL INTRODUCTION

Chemists have borrowed from nature the basic principles of molecular recognition¹ and self-assembly^{2,3} and made them integral features of supramolecular chemistry, i.e. the “chemistry beyond the molecule” as defined in 1969 by Jean-Marie Lehn.⁴ Molecular recognition is based on complementarity in size, shape and functional groups between molecules and governs the self-assembly of many biological systems and processes in the living cell. Examples are the pairing of complementary nucleoside bases in the double helix of DNA structure,⁵ the substrate-enzymes recognition process,⁶ and the formation of membranes and ribosomes.

One of the aims in the field of supramolecular chemistry is to design chemical systems that mimic biological processes. To achieve this, the understanding of the principles that govern molecular recognition processes i.e. “the energy and information involved in the binding and selection of substrates, by a receptor molecule”⁴ was actively pursued. This paved the way to the origin of host-guest chemistry⁷ which, like biological systems, exploits and explores a variety of noncovalent forces like hydrogen bonding, π - π stacking, electrostatic, and van der Waals interactions between synthetic receptors or hosts and target ions and molecules.

Over the last decades there has been a considerable interest in the design and synthesis of nanoscale molecular containers. The beginning of the field dates back to the stimulating work of Donald Cram⁸ and his coworkers on carceplexes and hemicarceplexes. These three-dimensional cavity-containing hosts created a new perspective from which to study complexation processes through guest encapsulation and opened the way to a wide range of applications.⁹

More recently, the self-assembly of molecular capsules emerged.¹⁰ Nature offers examples of shell-like containers of nanoscale dimensions like such as viruses and

ferritin,¹¹ the protein for the storage of iron in cells, from which chemists have found inspiration for the synthesis of molecular containers. Synthetic capsules and cages of different sizes and shapes have been obtained from different subunits, containing the instructions to self-assemble through noncovalent interactions into bigger architectures, as happens with natural systems.

So far, the predominant interactions employed in the synthesis of molecular capsules have been hydrogen bonds because of their biological relevance and directionality, and metal ligand interactions because of their strength and compatibility with water. These capsules are not only important because of their fascinating design but also because of their applications in binding, separations and sensing of molecules and ions, the stabilization of reactive intermediates, and catalysis. One of the goals is to create macromolecular capsules for biochemical applications such as drug encapsulation, transport through cell membranes and drug delivery. To achieve these objectives, it becomes obvious that efforts have to be focused on developing systems that form and display a stable association as well as binding properties in aqueous solution.

Electrostatic interactions¹² are often employed as an important attractive force both in biological and artificial molecular recognition.¹³ Nevertheless, these strong interactions have been only marginally used for building molecular capsules. The work presented in this thesis is aimed to prove the effectiveness of multiple ionic interactions as an alternative to hydrogen bonds and metal-ligand coordination for the synthesis of noncovalent supramolecular capsules in aqueous solutions.

Calix[4]arenes¹⁴ were used as building blocks for capsule construction¹⁵ because, when fixed in the *cone* conformation, they possess a well defined shape and they are readily available from cheap starting materials. Very importantly, they are also easily functionalized.

In Chapter 2 an overview of molecular containers i.e. capsules, cages and supramolecular clusters obtained *via* covalent and noncovalent synthesis is given. Of particular interest are those supramolecular containers which have shown guest encapsulation properties in solution.

After a brief introduction describing the examples of self-assembled molecular capsules based on ionic interactions that have appeared in the literature, Chapter 3 reports on the synthesis of oppositely charged calix[4]arenes as building blocks for

bimolecular capsules based on multiple ionic interactions in methanol and methanol/water solutions.

In Chapter 4 a detailed study of the influence of the side chain length of differently substituted tetraamidinium calix[4]arenes on the geometry and thermodynamics of the self-assembled molecular capsules is described. The encapsulation properties of one molecular capsule in methanol are also investigated. Moreover, this chapter reports on structural variations within one of the building blocks to achieve water-solubility of the molecular capsule.

Chapter 5 reports on the formation of molecular capsules made soluble in aqueous solution by the introduction of amino acids in one of the building blocks. A docking procedure has been used to identify possible guest molecules. The binding properties towards both charged and neutral molecules in aqueous solution are discussed.

Aiming at larger molecular capsules than the ones reported in the previous chapters, Chapter 6 describes how the combination of preorganization and of an array of alternating charges can be applied to achieve a multicomponent molecular capsule based on the self-assembly of six components.

The possibility of building a molecular capsule at a surface is the topic of Chapter 7. A multistep approach for this synthesis is reported which involves the attachment of one building block to a “molecular printboard” followed by the self-assembly of the second component at the interface.

References

1. Cram, D. J. *Nature* **1992**, *356*, 29-36.
2. Tecilla, P.; Dixon, R. P.; Slobodkin, G.; Alavi, D. S.; Waldeck, D. H.; Hamilton, A. D. *J. Am. Chem. Soc.* **1990**, *112*, 9408-9410.
3. Whitesides, G. M.; Mathias, J. P.; Seto, C. T. *Science* **1991**, *254*, 1312-1319.
4. Lehn, J.-M. *Supramolecular Chemistry: Concepts and Perspectives*; WILEY-VCH: Weinheim, 1995.
5. Watson, J. D.; Crick, F. H. C. *Nature* **1953**, *171*, 737-738.

6. Fisher, E. *Ber. Dt. Chem. Ges.* **1894**, 27, 2985-2993.
7. Schneider, H.-J.; Yatsimirski, A. *Principles and Methods in Supramolecular Chemistry*; John Wiley & Sons: Chichester 2000.
8. Cram, D. J.; Cram, J. M. *Container Molecules and Their Guests*; Royal Society of Chemistry: Cambridge, 1994.
9. Sherman, J. C. *Tetrahedron* **1995**, 51, 3395-3422.
10. Conn, M. M.; Rebek, J. Jr. *Chem. Rev.* **1997**, 97, 1647-1668.
11. Harrison, P. M.; Arosio, P. *Biochim. Biophys. Acta* **1996**, 1275, 161-203.
12. Warshel, A. *Acc. Chem. Res.* **1981**, 14, 284-290.
13. Diederich, F. *Cyclophanes (Monographs in Supramolecular Chemistry)*; Ed.: J. F. Stoddart, Royal Society of Chemistry: Cambridge, 1991.
14. Gutsche, C. D. *Calixarenes (Monographs in Supramolecular Chemistry)*; Ed.: J. F. Stoddart, Royal Society of Chemistry: Cambridge, 1989.
15. Rebek, J. Jr. *Chem. Commun.* **2000**, 637-643.

Chapter 2

SUPRAMOLECULAR CONTAINERS: SYNTHESIS AND FUNCTIONAL PROPERTIES

The literature review presented in this chapter discusses the more significant examples of molecular containers, i.e. capsules, cages and supramolecular clusters that have appeared in the literature over the last decade, with a particular interest in those systems that have shown guest encapsulation. Supramolecular containers have been obtained using either covalent or noncovalent synthesis. A brief summary of (hemi)carcerands and cryptophanes resulting from the connection of two or more building blocks by means of covalent bonds is given. More extensively discussed are the molecular systems that self-assemble into molecular capsules by means of noncovalent forces viz. hydrogen bonds and metal-ligand interactions. In the last part of this chapter the most important applications of the molecular containers are outlined. Although the use of ionic interactions represents an effective, alternative way for the synthesis of noncovalent assemblies, only a few examples of molecular capsules based on these interactions are found in the literature, which will be reported in Chapter 3.

2.1 Introduction

The interest of organic chemists in three-dimensional, cavity-containing hosts resembling the shape of a box or a capsule started with the work of Cram who reported the first example of a covalently linked molecule (carcerand) having an internal, limited space for the isolation of a molecule from the bulk solvent.¹ Since then the concept of “molecule within molecule” has been widely exploited leading to a large number of examples which are summarized in the following sections.

The advantage of using self-complementary units to accomplish the same purpose, i.e. create a closed space within a molecular framework, soon became an attractive alternative to the covalent approach.² Molecular capsules were generated from the self-assembly of two or more, not necessarily identical, subunits equipped with the correct molecular instructions to drive their recognition in solution and consequently the self-assembly into the desired structure. By virtue of directionality and reversibility, hydrogen-bonds and metal-ligand interactions are the two main noncovalent forces used to bring molecules together into a well-defined superstructure. This approach requires fewer synthetic steps compared to the corresponding covalent synthesis. Due to the weakness of noncovalent interactions a high degree of symmetry and certain conditions, for example a suitable solvent or the presence of a guest molecule, are prerequisites for the self-assembly process to occur. Hydrogen-bonded capsules are easily disrupted in polar solvents while capsules constructed through metal-ligand interactions are stable in water but disassemble in strongly ligating solvents.

2.2 Molecular capsules based on covalent frameworks

In 1983, Cram proposed the idea of a covalently joined supramolecular structure, which would act as a molecular prison for the entrapment of a guest molecule within its interior. The synthesis of such a spherical molecule was achieved a few years later upon linking two identical hemi-spherical cavitands through their aromatic upper rim positions.³ Complexes that permanently imprisoned guests were called *carceplexes* as the guest can only escape by rupture of covalent bonds. *Hemicarceplexes* are like *carceplexes* (i.e. they incarcerate guest molecules at ambient temperature) but they contain portals in their shells large enough to allow the guests to enter and leave the

inner cavity upon heating and without breaking of any covalent bonds. In absence of a guest the closed surface compounds are called *carcerands* and *hemicarcerands*.

Cram and co-workers synthesized a large number of (hemi)carcerands by connecting two cavitands with a variety of four appropriate linkers (Figure 2.1). Each system possesses a unique cavity-size and shape dictated by the bridging unit. The cavity is suitable for the incarceration of guests varying in size and shape from gases, such as Xe, to solids such as C₆₀. For more detailed information the reader is referred to some reviews on this topic.^{4,5}

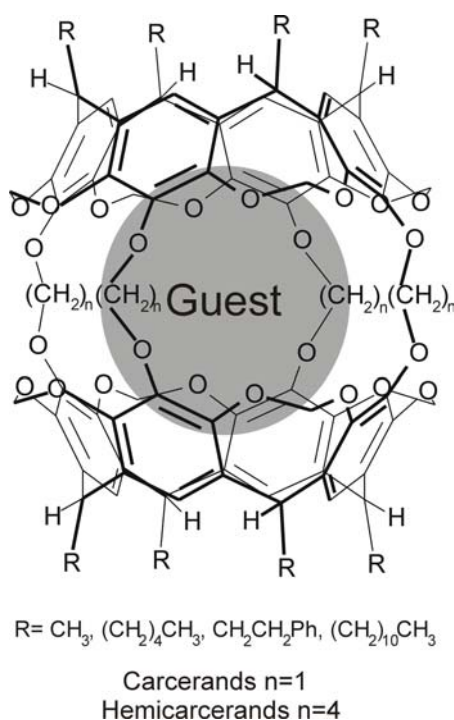


Figure 2.1. Example of Cram's carcerands and hemicarcerands.

An additional step was taken when Cram reported the first water-soluble hemicarceplexes (Figure 2.2) able to complex 14 neutral different guests in D₂O at pH 9.⁶ Deshayes⁷ undertook a calorimetric study of the binding properties of similar water-soluble hemicarceplexes showing the importance of the entropic driving force for complexation in aqueous medium. No complexation was observed for charged molecules indicating that water most probably solvates their charges better than does the host's cavity.

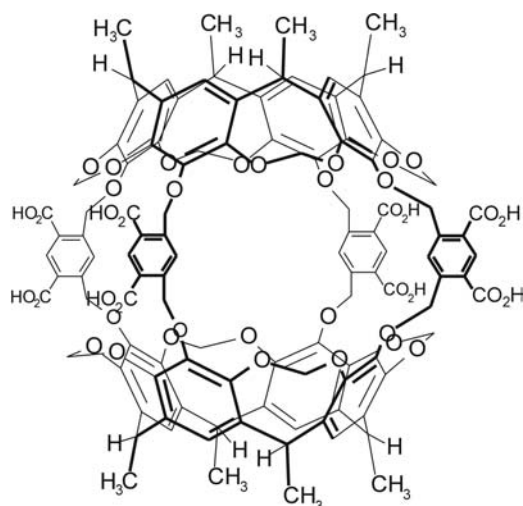


Figure 2.2. Water-soluble hemicarceplex.

An important prerequisite for the formation of carceplexes is the presence of a guest template in the reaction mixture. In the absence of a suitable template guest (or of solvents that are too large to be accommodated in the internal cavity), carceplexes cannot be isolated. The template effect has been widely studied both in the groups of Cram⁸ and Sherman.⁹ Their studies showed that small changes in the guests result in large differences in the relative free energy of binding of the complexes, emphasizing the importance of noncovalent interactions between molecules.

The carceplex of Sherman and al. reported in Figure 2.3a is an example of a guest molecule acting as a template in the formation of a capsule.⁹⁻¹¹ The reaction for the carceplex formation was conducted in *N*-methyl-2-pyrrolidinone (NMP), a solvent which is a poor template, in the presence of a variety of guest molecules and the relative yields of formation of the carceplex were measured. Pyrazine turned out to be the best template molecule with a template ratio of one million over other small molecules. Using the same building block Sherman and coworkers synthesized a side-to-side bis-capsule, where guest molecules, such as pyrazine and methyl acetate, are reversibly encapsulated in adjacent chambers (Figure 2.3b). Formation of the bis-capsule is cooperative as no 1:1 host-guest species was observed. In the absence of a suitable guest, no well-defined capsule was formed and only aggregates were observed.¹² This work was also extended to the hexamer, shown to form a tris-capsule and a tris-carceplex with methyl acetate.¹³

Larger carceplexes of three cavitands units have been synthesized that irreversibly retain three molecules of DMF (Figure 2.3c).¹⁴

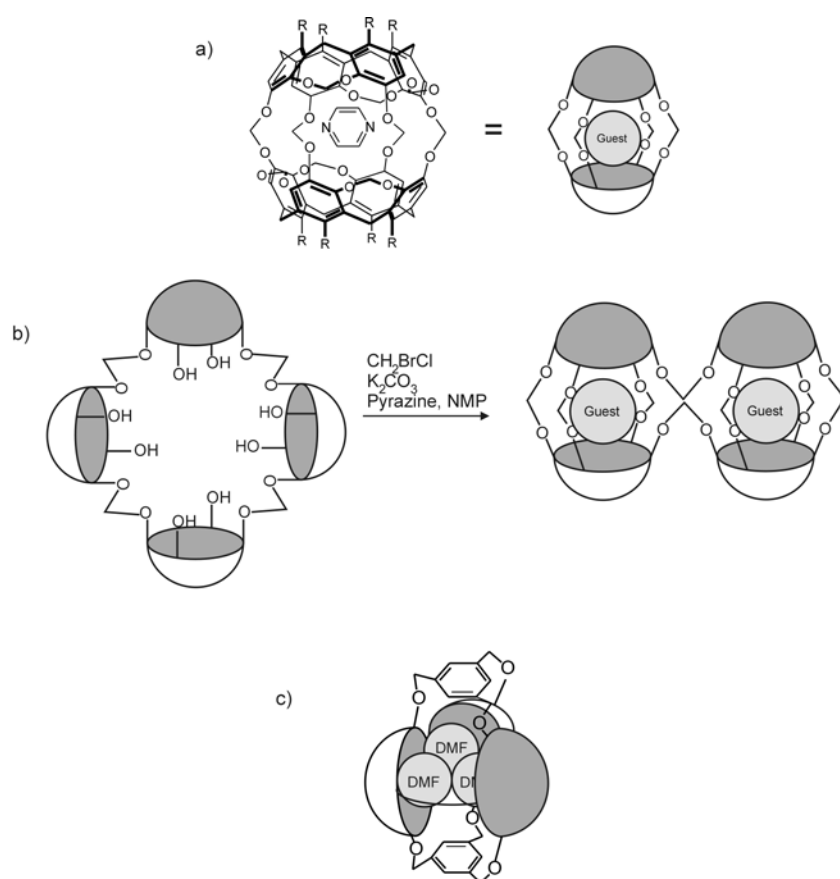


Figure 2.3. a) Carceplex-pyrazine complex; b) schematic representation of the formation of bis-carceplex from the tetramer; c) trimeric carceplex containing three solvent molecules.

Very recently a bigger carceplex was generated by the linkage of two [5]cavitands via disulfide bonds. NMR studies show the inclusion of two molecules of DMF oriented inside the cavity in parallel planes perpendicular to the principle axis of the host.¹⁵

Calixarenes have also been used as building blocks to synthesize covalent molecular capsules. Blanda¹⁶ proposed a symmetric octathiobis(calix[4]arene) cage molecule synthesized by joining two thiomethylated calixarene molecules via a single carbon spacer unit. Other groups¹⁷⁻²⁰ have linked calixarenes “head-to-head” using one or two instead of four linker groups to obtain compounds with large holes. The group of Arduini²¹ explored how the length and rigidity of a single spacer connecting head-to-head two calix[4]arene subunits could influence the cavity size of the resulting capsules.

Recently, dynamic covalent chemistry, i.e. the stepwise breaking and remaking of dynamic covalent bonds, began to make its presence in the field of supramolecular capsules. First Tam-Chang et al. in 1999 reported the dimerization, under equilibrium control, of the parent *tris*-thiol monomer to form a bicyclic capsule.²² A year later the power of dynamic chemistry allowed the conversion of a hemicarceplex into a hemicarcerand.²³

Interesting variations to the prototypical carceplexes have been introduced by the group of Reinhoudt.²⁴⁻²⁷ Heteromeric carceplexes based on a cavitand and a calix[4]arene unit linked through four amide bridges were isolated in quantitative yield (Figure 2.4a). Solvent molecules like DMF, DMSO and ethyl methyl sulfoxide were encapsulated. These assemblies exhibit a new type of isomerism, called *carceroisomerism*, determined by the inherent asymmetry of the host-guest complexes according to which the guest can assume different orientations with respect to the calix[4]arene and cavitand halves of the molecules.

A bigger cavity, named the “holand”, originated by connecting two calix[4]arenes and two resorcin[4]arenes via amido spacers (Figure 2.4b).²⁸ Nevertheless, due to the rigidity of both the building blocks and of the amido bridges no guest complexation was observed.

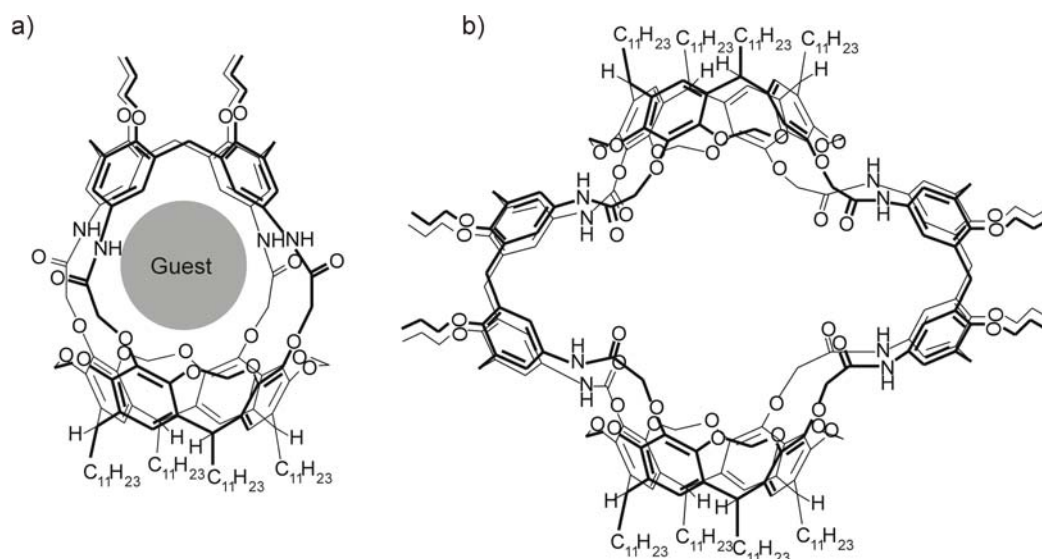


Figure 2.4. a) Heteromeric carceplex; b) “holand”.

Rebek’s group²⁹ has shown that the connection of two self-folding cavitands through extended aromatic spacers provided large unimolecular cavities with an

internal volume of 800 \AA^3 able to encapsulate more than one guest at a time. The guest uptake and release is controlled by the two seams of intramolecular hydrogen bonds. Depending on the nature of the aromatic spacer the host exists in an S-shape isomer, in which the two cavities act independently for the binding of guest molecules, (Figure 2.5a) or in a C-shape isomer that accommodates rigid and long guests (Figure 2.5b).

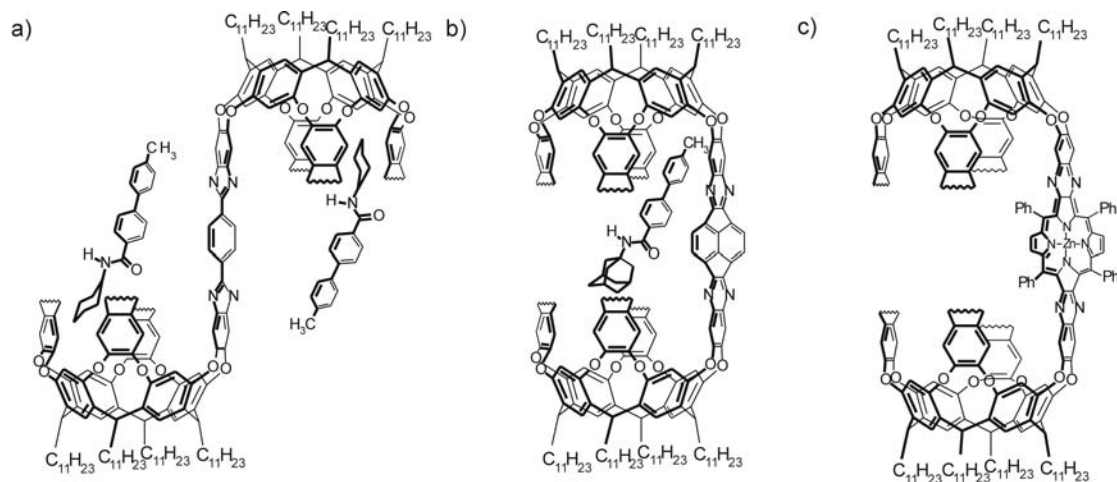


Figure 2.5. S-shape (a) and C-shape (b and c) self-folding containers.

When two cavitands are connected through a Zn-porphyrin wall a huge unimolecular cavity of the dimensions of $10 \times 25 \text{ \AA}^3$ is formed (Figure 2.5c). Encapsulation of adamantyl- and pyridyl containing guests of various lengths was observed. Moreover, the porphyrin functions provide the possibility of meta-catalyzed reactions in this capsule.³⁰

The cyclotrimeratrylene scaffold represents another fundamental building block for the synthesis of molecular capsules.³¹ The covalent linkage of two cone-shaped cyclotrimeratrylene units provides a class of macrocyclic hosts called *cryptophanes* (Figure 2.6), having a preorganized, three-dimensional cavity suitable for accommodating organic substrates. The work of Collet and coworkers entailed a large number of cryptophanes that encapsulate a variety of charged and neutral guests such as tetramethylammonium cations and CHCl_3 .³²⁻³⁵

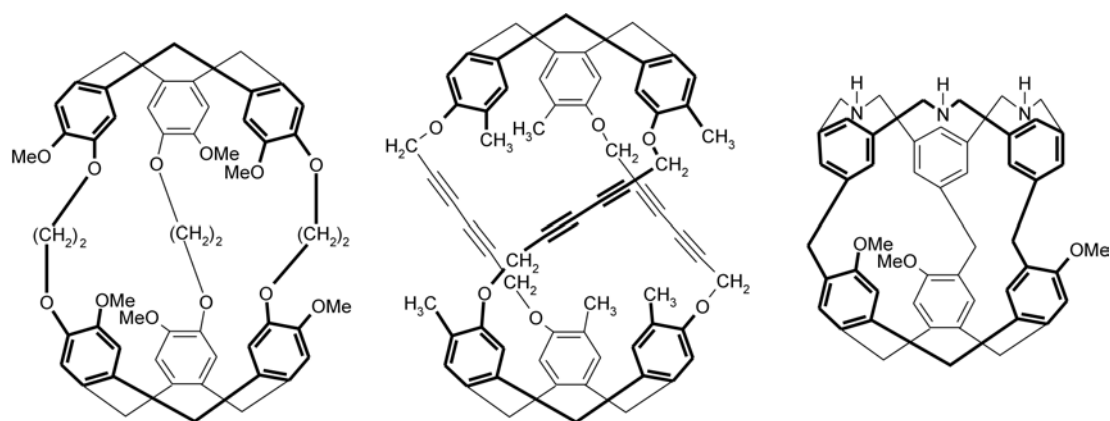


Figure 2.6. Collet's cryptophanes.

2.3 Capsules via self-assembly

Although the carceplexes described in the previous paragraph are of great conceptual importance, the guest cannot usually be removed without the rupture of at least one covalent bond of the host or without heating to increase the opening of the portals.

Consequently, there has been much interest in the utilization of noncovalent interactions to assemble concave building blocks in order to produce cavities. In general, such cages are attractive because the molecular association is reversible under relatively mild conditions. Nevertheless, since noncovalent interactions are generally much weaker than covalent bonds, large areas of complementarity are necessary to allow the self-assembly to occur. In the following paragraphs examples of molecular capsules based on hydrogen bonds and metal-ligand interactions will be discussed.

2.3.1 Hydrogen-bonded systems

Hydrogen bonding is the favorite intermolecular force in self-assembling systems by virtue of its directionality, specificity, and biological relevance. Building blocks possessing an appropriate curvature and functionalized with donor and acceptor hydrogen bonds units have been used to generate molecular capsules of different size and shape. Due to the large number of examples reported in literature on this subject, for clarity this section will be divided into two major parts:

- (a) Glycoluril-derived assemblies, which essentially represent the pioneering work of Rebek in the field of self-assembled molecular capsules, and
- (b) Cyclophane-derived capsules based on calixarene, cavitand and resorcinare scaffolds.

2.3.1.1 Glycoluril-derived capsules

The self-assembly of glycoluril derivatives is a recurrent motif for the synthesis of noncovalent molecular capsules. The reason lies in the self-complementary array of hydrogen bond donor and acceptor sites and on the stereochemical features of the glycoluril functions that impart a curvature to the structure that encourages dimerization. The first assembly in this series is represented by the so-called “tennis-ball”, reported by the groups of Rebek and de Mendoza, consisting of two diphenylglycoluril units linked by a durene spacer (Figure 2.7).³⁶ The assembly is held together by eight hydrogen bonds and has a cavity with a volume of about 50 Å³ that functions as a host for guests like benzene, adamantane and ferrocene derivatives.³⁷

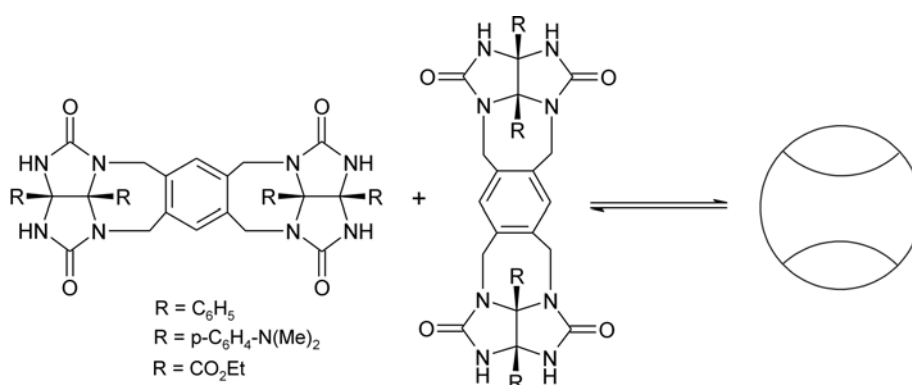


Figure 2.7. Two identical molecules give a closed shell “tennis-ball”.

A library of pseudo-spherical structures with cavities smaller or larger than the originally designed capsule was obtained by variation of the size of the connecting spacer elements.⁴⁰ Selective encapsulation of methane versus ethane,³⁸ noble gases³⁹ and other small molecules in non-polar solvents was achieved. Moreover, to help the guest encapsulation, either electron-rich or electron-deficient surfaces were introduced into the original scaffold.⁴¹

A modification of the “tennis-ball” dimer is the cyclic tetrameric capsule originated from the self-complementary glycoluril and cyclic sulfamide functionalities shown in Figure 2.8.⁴² To assemble the components into discrete tetrameric capsules a noncompetitive solvent, such as CD_2Cl_2 , toluene- d_8 , or benzene- d_6 and a guest molecule of appropriate size and shape are required.⁴³ Special affinity was found for guest molecules containing a carbonyl group, which can participate in the seam of hydrogen bonds of the host. In particular 2,6-adamantandione appeared to be an ideal guest.⁴⁴

The addition of a hydroxyl functionality on the central phenyl ring imparts chirality to each of the subunits and the union of four of these *nonracemic* pieces produces a single enantiomer of a chiral capsule having a special affinity for ketones and able to discriminate between enantiomeric guests in solution.⁴⁵

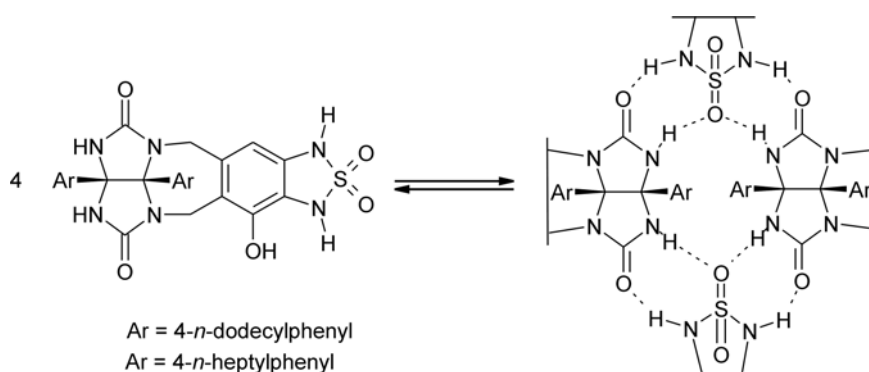


Figure 2.8. Structural depiction of the monomer (left) and pattern of hydrogen bonding in the tetrameric assembly (right).

To develop self-assembled dimers capable of recognizing and binding larger molecules, Rebek and coworkers expanded the size of the spacer between the two glycoluril units.³⁷ The monomers have a tape-like structure of 13 fused rings of which only two are benzenes; the other ring fusion provides the necessary curvature required for the assembly. The two self-complementary subunits are held together by a seam of 16 hydrogen bonds in a roughly spherical “softball-like” assembly. The best guests for the capsule were 1-adamantane carboxylic acid and 1-ferrocene carboxylic acid.

The assembly reported in Figure 2.9 can be regarded as another variation made on the original design of the “tennis-ball”. Appending the glycoluril functionalities to a triphenylene scaffold, a small capsule having the appearance of a “jelly doughnut”

with an unusual symmetry (D_{3d}) and flattened spherical interior cavity was obtained (Figure 2.9).

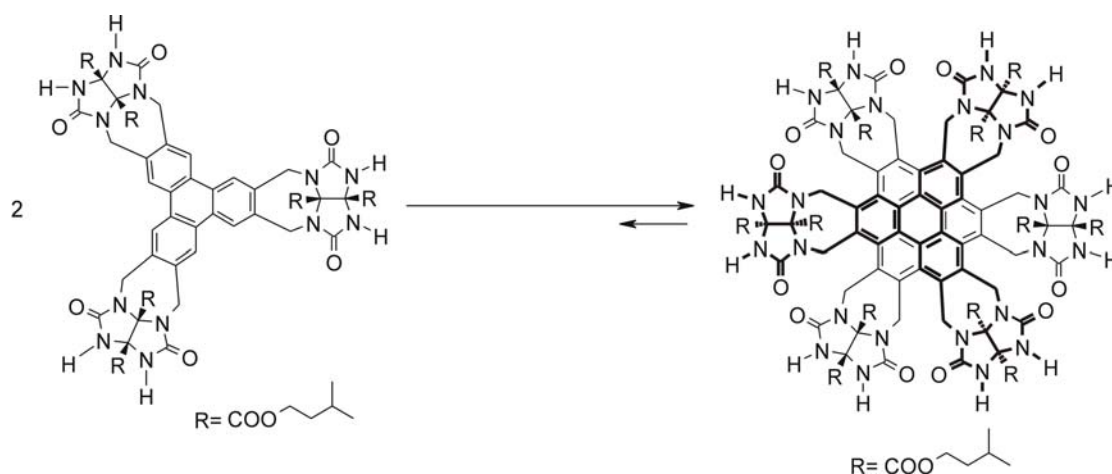


Figure 2.9. Formation and structure of the “jelly doughnut”.

A more rigid capsule was obtained when the glycoluril was appended to a hexa-substituted spacer.⁴⁶

Similar to the previous assemblies, these dimeric structures are capable of encapsulating guest molecules.⁴⁷ The beautiful fit of cyclohexane suggests the use of this capsule as a reaction chamber for a Diels-Alder reaction of ethylene and butadiene or for the Claisen rearrangement.

2.3.1.2 Cyclophane-based capsules

Calixarenes fixed in the cone conformation, cavitands, and resorcinarenes can be regarded as molecular half-spheres. When functionalized with appropriate groups a single unit either dimerizes or self-assembles with a complementary one, giving rise to a single bowl-shaped container possessing an internal cavity normally suitable for encapsulation of a single molecule. When more than two units are involved in the self-assembly process, or when appropriate spacers are acting as connectors between two building blocks, cavities of nanoscale dimensions are generated.

Calix[4]arenes

Rebek and Böhmer⁴⁸⁻⁵⁰ later, studied the dimerization of calix[4]arenes containing ureas at the upper rim.

These molecules are self-complementary and able to associate via hydrogen bonds in apolar organic solvents, forming a completely closed cavity by dimerization (Figure 2.10).⁵¹ X-ray crystallography⁵² showed that all eight ureas interdigitate in a head-to-tail array of 16 intermolecular hydrogen bonds, leaving a sizeable cavity where guests such as benzene, pyridine, fluorobenzene, pyrazine and ammonium cations can be reversibly accommodated with a rate that is slow on the NMR timescale. The encapsulation of other guests such as *p*-difluorobenzene and pyrazine shows that there is a preferable orientation of the guest within the cavity.

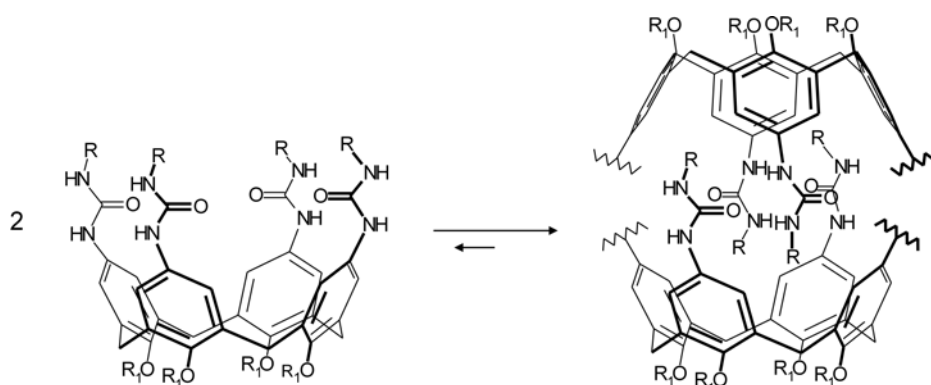


Figure 2.10. The dimerization of the urea-substituted calix[4]arene through the formation of intermolecular hydrogen bonds.

The association of the dimer can be affected by the addition of urea derivatives⁵³ or by the addition of a small percentage of polar solvent responsible for denaturation of the capsule. On the other hand, the entanglement of bulky residues attached to the urea functions generate dimers which are kinetically stable in a hydrogen bond competing solvent like DMSO.⁵⁴

When different functional groups are inserted at the distal urea nitrogen atoms the monomeric units assemble into heteromeric, chiral capsules^{55,56} where chirality is caused by the directionality of the hydrogen bonded belt. Recent studies showed that when hydrogen bonding is the main factor for the stability of the capsule, the change in the directionality of the hydrogen bond belt is a slow process on the NMR time scale. Interestingly, when a charged guest like tetraethylammonium cation is included in the cavity, the hydrogen bonding system is weakened so that the inversion of the directionality of the hydrogen bond belt becomes fast on the NMR time scale and takes place through the rotation of the urea residues within the dimeric capsule.⁵⁷

When amino acids are introduced onto the urea functionalities a second chirality element is added in addition to the urea directionality.⁵⁸ The chirality of the amino acids is transferred upon assembly formation, giving rise to a chiral capsule possessing only one direction of its head-to-tail arrangement of ureas and capable of discriminating between enantiomeric guest molecules. Very recently the group of Böhmer reported examples of supramolecular chirality in tetra-urea dimers generated only by the spatial arrangement of two calixarenes composed on two different phenolic urea units.⁵⁹ Expanded calix[4]arene tetra-urea capsules intended to offer bigger cavities for guest encapsulation have also been reported.⁶⁰⁻⁶²

Interestingly, it has been observed that hydrogen bonding through dimerization can be used to drive the conformational equilibrium of the calix[4]arene skeleton exclusively to the cone conformer. In this way flexible molecules can reversibly self-assemble to give a well-defined receptor cavity.⁶³

Two calix[4]arenes featuring either aryl or sulfonyl urea functionalities were covalently attached at their lower rims through a spacer by Rebek et al. in such a way that the ureas at the upper rim were oriented in opposite directions.⁵⁵ The dimerization led to linear polymers that formed reversibly and that can encapsulate benzene and toluene derivatives (Figure 2.11a). Upon assembly into a “dumbbell” a sense of directionality in the urea functions is also introduced. The “head-to-tail” arrangements of the ureas can be clockwise or counterclockwise, giving rise to cyclo-enantiomers of the complex.

Similarly, calix[4]arene tetra-ureas were connected through their upper rims *via* a hexamethylene spacer which is long enough to reverse the direction of the divergent bonds of the adjacent urea substituents, but short enough to minimize the loss of entropy due to the restriction of freely rotating single bonds. Although this system allows three types of assemblies, ¹H NMR and ESI-MS studies showed that the intramolecularly assembled capsule is primarily formed (Figure 2.11b).⁵¹

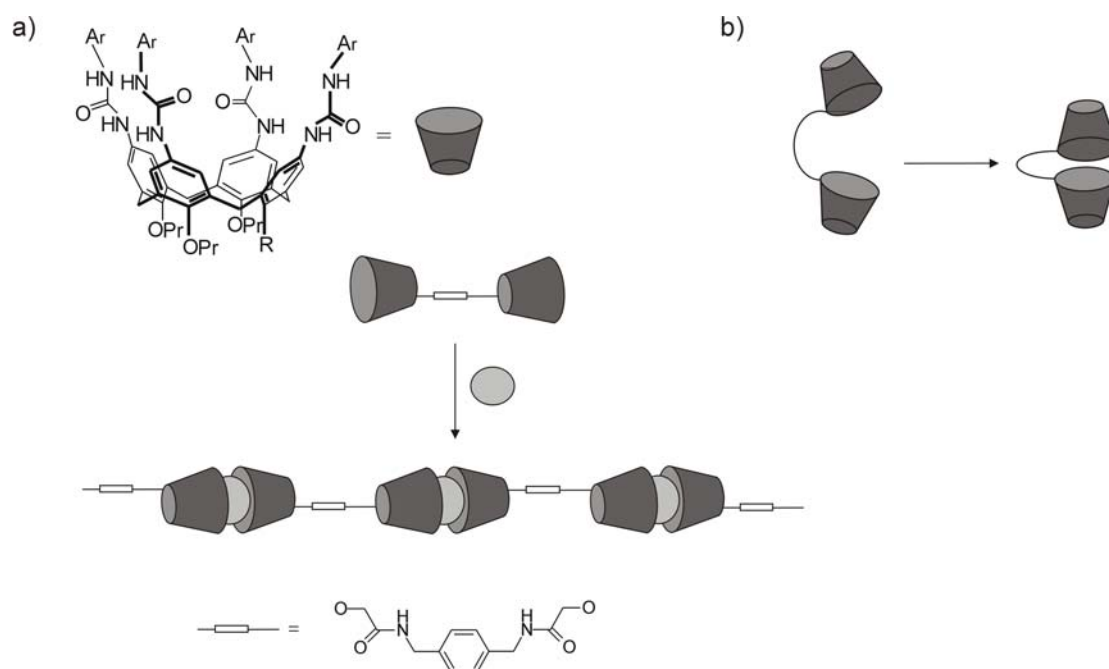


Figure 2.11. a) Two calixarene units covalently bonded through an aromatic spacer lead to linear oligomers; b) bridged calixarene dimer and intramolecularly assembled capsule.

Our group described a well-defined hydrogen-bonded capsule in which a calix[4]arene substituted with carboxylic acids at the upper rim interacts with calix[4]arenes substituted with pyridines at the lower rim (Figure 2.12a).⁶⁴ When the substituent was changed to 2-pyridyl no association was observed. ¹H NMR studies showed that the association is based on hydrogen bonding rather than electrostatic interactions resulting from proton transfer.

The same motif, i.e. carboxylic acids and pyridyl groups, was used by Shinkai to drive the “head-to-head” assembly of two calix[4]arenes (Figure 2.12b). The formation of the self-assembled capsule was confirmed by VPO measurements and by the fluorescence properties arising from the stilbazole units.⁶⁵

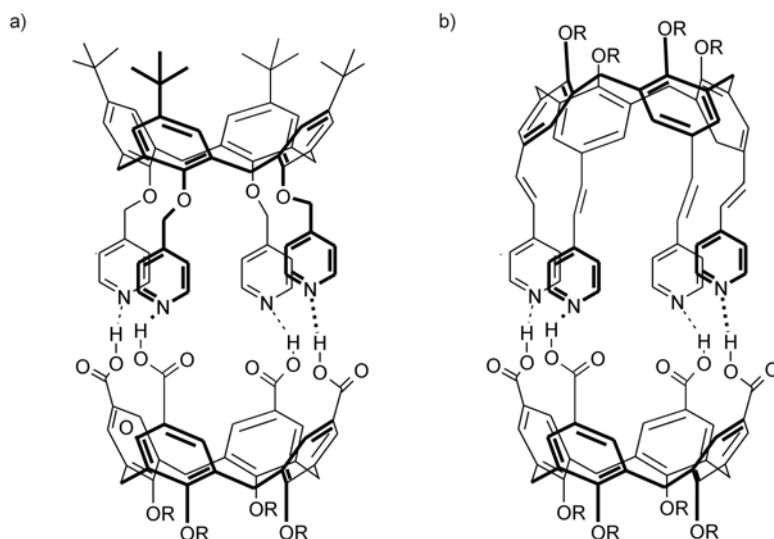


Figure 2.12. a) “Head-to-tail” and b) “head-to-head” hydrogen-bonded capsules.

A calix[4]arene functionalized at the upper rim with alanine moieties has shown to form a dimeric capsule in protic solvents. The formation of the assembly was proven by ^1H NMR and mass spectrometry analysis and was claimed to be due to the formation of hydrogen bonds between the two identical subunits. The dimer is stable in methanol solution containing up to 4% water, while further addition of water resulted in the dissociation of the complex. Figure 2.13 depicts the two possible binding conformations proposed by the authors.⁶⁶

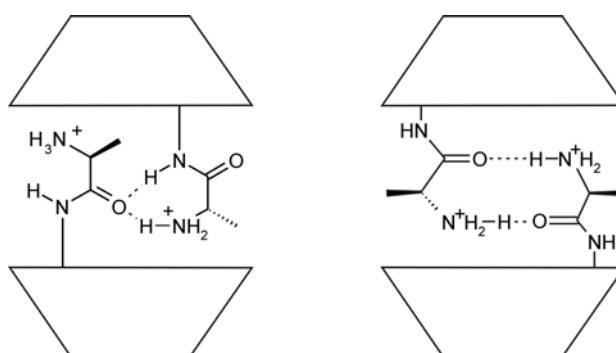


Figure 2.13. Proposed interactions in the tetraalanine calix[4]arene dimer.

Cavitands

Cavitands were used by Rebek and Rudkevich for the synthesis of capsules of nanometer dimensions. As schematically reported in figure 2.14 a capsule is formed by dimerization of two self-folding vase shaped cavitands. Eight bifurcated hydrogen bonds, with the imide hydrogens of one molecule directed between two carbonyl

oxygen of another stabilized the assembly. The capsule has a dimension of about 1.0 nm \times 1.8 nm with an internal cavity of 460 Å³. High conformational stability in solvents like CDCl₃, benzene-*d*₆, and toluene-*d*₈ was observed.

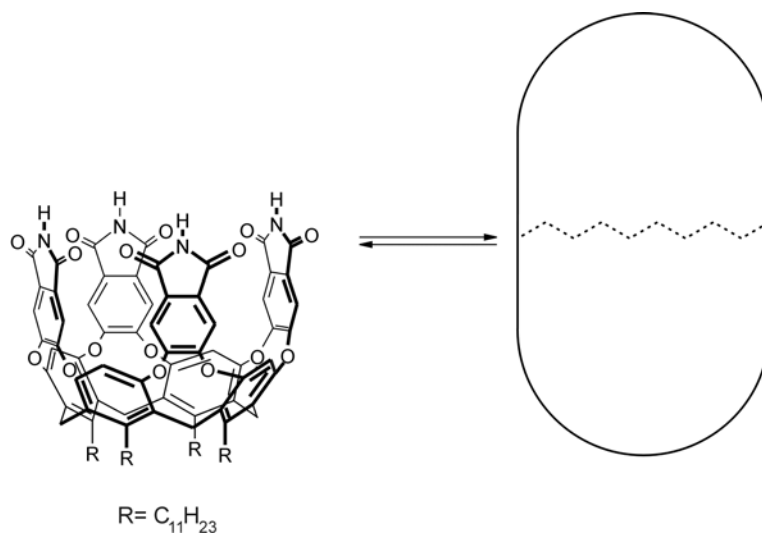


Figure 2.14. Schematic representation of the molecular capsule obtained through dimerization of a self-folding cavitand.

To explore the size and shape selectivity of the encapsulation process, competition experiments were performed involving different solvents. When the solvent is too large or too small for the cavity, added guests that fit well are encapsulated.⁶⁷ Besides solvent molecules, anions⁶⁸ and functionalized amino acids⁶⁹ are also suitable guest molecules for this cylindrical capsule.

Due to the stunning selectivity of the capsule, research was undertaken to determine its capacity for small molecule solvents.^{70,71} Additionally, recent studies have shown that the cylindrical capsule provides an asymmetric environment for encapsulated guest molecules. When a chiral guest is accommodated in the cavity the remaining space becomes chiral.⁷² The orientation of one guest affects the presence and nature of the other, a phenomenon termed *social isomerism*.⁷³

Kobayashi reported on a molecular capsule based on ionic hydrogen bonds involving two molecules of cavitand carboxylic acids and four molecules of 2-aminopyrimidine (AP) (Figure 2.15a).⁷⁴

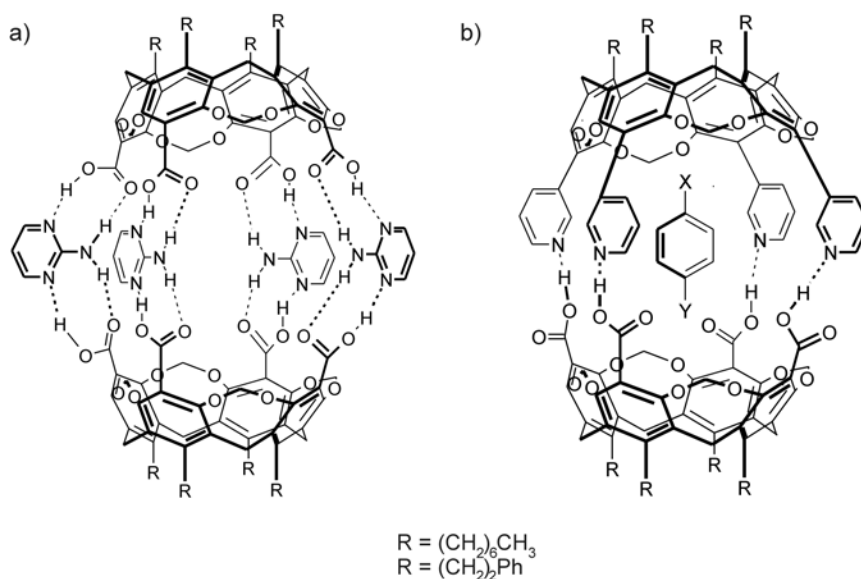


Figure 2.15. Molecular structure of Kobayashi's capsules.

While the cavitand alone has low solubility in CHCl_3 at room temperature, in the presence of two equivalents of 2-AP it becomes very soluble. ^1H NMR titration and an X-ray diffraction study confirmed the expected stoichiometry of 2:4. Upon addition of $\text{DMSO-}d_6$ as a cosolvent, the capsule in CDCl_3 is disrupted. Encapsulation of two molecules of nitrobenzene in an antiparallel fashion was also shown.

Using the same supramolecular motif i.e. hydrogen bonds between carboxylic and pyridyl groups, Kobayashi's group synthesized a molecular capsule whose assembly turned out to be guest-induced (Figure 2.15b).⁷⁵ Single-crystal X-ray analysis and solution studies showed that when one molecule of an appropriate 1,4-disubstituted-benzene guest is present in solution, the exclusive formation of the heteromeric capsule is observed.

A complex-within-complex system was synthesized in Rebek's group. The capsule is the result of the dimerization of a monomeric unit generated by the combination of a cavitand and a glycoluril module and possesses a cavity large enough to accommodate a cryptate.⁷⁶

Resorcinarenes

Resorcinarenes provide scaffolds for dimeric and hexameric hydrogen bonded capsules. Examples in the solid state, reported by Atwood⁷⁷ and Aoki,⁷⁸ showed dimers of resorcinarenes linked by intermolecular hydrogen bonds involving eight molecules of propanol-2-ol or water respectively. Additional intramolecular hydrogen

bonds impart structural rigidity to the resorcinarene scaffold. X-ray analysis showed the important role of the cation- π interaction in the formation of this molecular capsule.

The self-assembly of six resorcinarene units and 8 ordered water molecules in apolar media generates an hexameric capsule (Figure 2.16). The assembly, whose structure was confirmed by X-ray crystallography, is held together by a total of 60 hydrogen bonds⁷⁹ and possesses an internal cavity of about 1375 Å³. The cavity is large enough to encapsulate a tetraethylammonium ion. Rebek's group further investigated the molecular recognition properties of this host structure in wet CDCl₃ claiming that the hexameric structure assembles when appropriately sized tetraalkylammonium or phosphonium salts are present in solution.⁸⁰⁻⁸² Nevertheless, a recent NMR diffusion study demonstrates that the resorcinarene unit contains enough molecular information to self-assemble spontaneously into a hexameric capsule in chloroform without the aid of any guest.⁸³

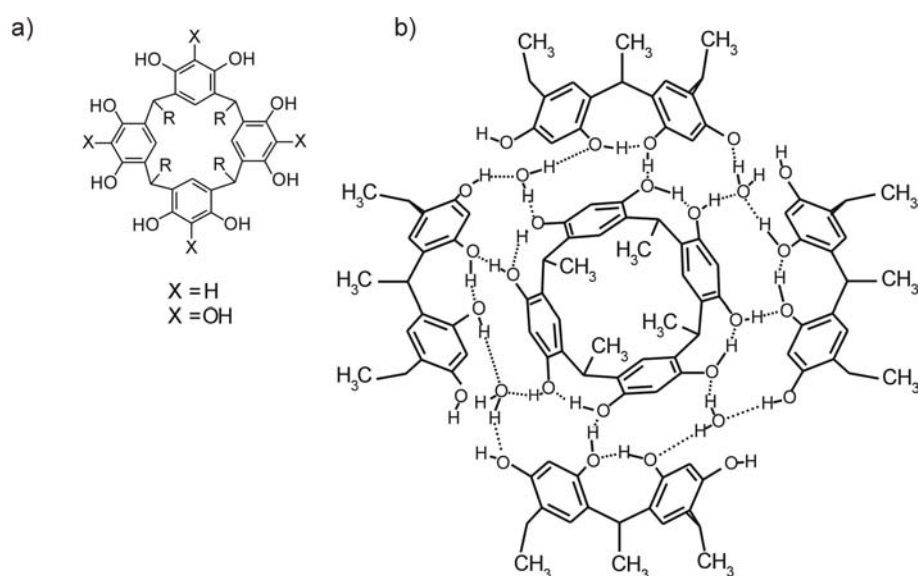


Figure 2.16. a) Building blocks and b) resulting hexameric capsule (for clarity part of the resorcinarene unit is omitted).

Pyrogallo[4]arenes, obtained by the introduction of hydroxyl groups on the resorcinarene unit, provide easy access to new molecular capsules stable in a protic solution. Dimeric capsules are stable both in methanol and wet acetonitrile. Encapsulation of charged guests like tetramethylammonium, quinuclidinium and tropylium cations was also observed.^{82,84}

Even larger hexameric capsules were obtained by the self-assembly of six pyrogallo[4]arene units. Remarkably this capsule has shown high stability even in a 1:1 mixture of acetone-water.⁸⁵

2.3.2. Metal-induced self-assembly of molecular containers

The ability of a metal ion to organize a flexible ligand around its coordination sphere has prompted chemists to use metal-ligand interactions for the assembly of a variety of supramolecular structures e.g. chains, rings, squares and more complicated polymeric structures.⁸⁶⁻⁸⁹ Moreover, as described in the following paragraphs, directionality together with the versatility of the diverse transition-metal complexes have resulted in a number of attractive examples of self-assembled cages⁹⁰ and metal clusters⁹¹ synthesized by the groups of Shinkai, Fujita, Stang, Dalcanale, Raymond and others. Unlike hydrogen-bonded capsules, the strength of the metal ligand interactions allows many of these systems to aggregate in aqueous solutions.

2.3.2.1 Metal-bridged carceplexes

A particularly successful approach for the synthesis of molecular capsules based on metal-ligand coordination is the self-assembly of two identical concave building blocks like calixarenes, cavitands and resorcinarenes, through coordination to metal ions having square-planar geometry.

Dalcanale reported the quantitative self-assembly cage molecules composed of two tetracyanocavitand derivatives connected through four Pd(II) or Pt(II) bistriflates (Figure 2.17a).^{92,93} The cages are stable both in the solid state and in solution and are soluble in chlorinated and aromatic solvents. Moreover the strength of the metal-ligand coordination renders the cages stable even at 100 °C. ¹H NMR studies and ESI mass spectrometry provide evidence for inclusion of the triflate anion, that is too bulky to escape from the equatorial portals of the cage. Control of the self-assembly process was achieved through metal-ligand exchange. Addition of a competing ligand such as triethylamine led to complete disassembly of the cage. Subsequent addition of triflic acid restored the original Pt complex.

The versatility of the cavitands allows their functionalization with different metal-coordinating ligands. When nitrile groups are replaced for pyridines a wider molecular capsule is formed (Figure 2.17b). Moreover, while the addition of an

excess of NEt_3 as competitive ligand results in the disassembly of the Pd cage, under the same conditions the Pt cage remains unchanged due to the stronger Pt-N bonds.⁹⁴

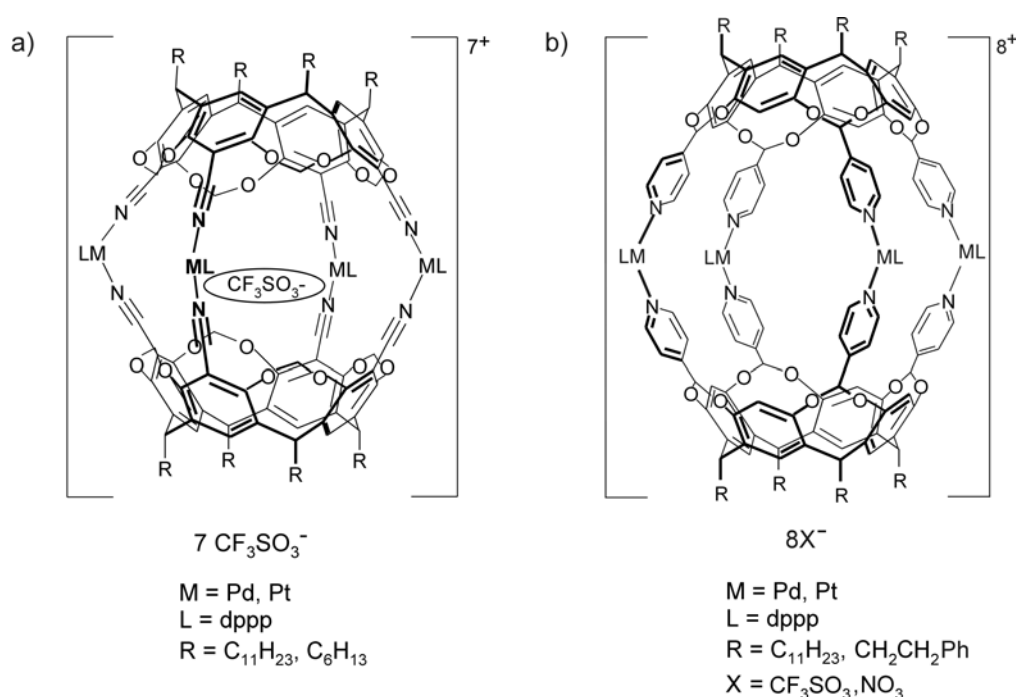


Figure 2.17. Dalcanale's cages.

The same class of interaction has been used by the group of Shinkai to assemble molecular capsules based on calixarenes.⁹⁵ When mixed with three equivalents of a cis-Pd(II) complex, two *p*-pyridyl substituted homo-oxacalix[3]arenes afford the molecular capsule shown in figure 2.18a. This dimer forms a kinetically stable 1:1 complex with C_{60} fullerene. Recently the same group reported how the introduction of a chiral element resulted in a right-handed (*P*) and a left-handed (*M*) capsule.⁹⁶

The same group reported the formation of a novel molecular capsule resulting from the self-assembly of two porphyrin-based building blocks and four cis-Pd(II) complexes (Figure 2.18b). The resulting cavity has shown guest encapsulation towards a bipyridine guest.⁹⁷⁻⁹⁹

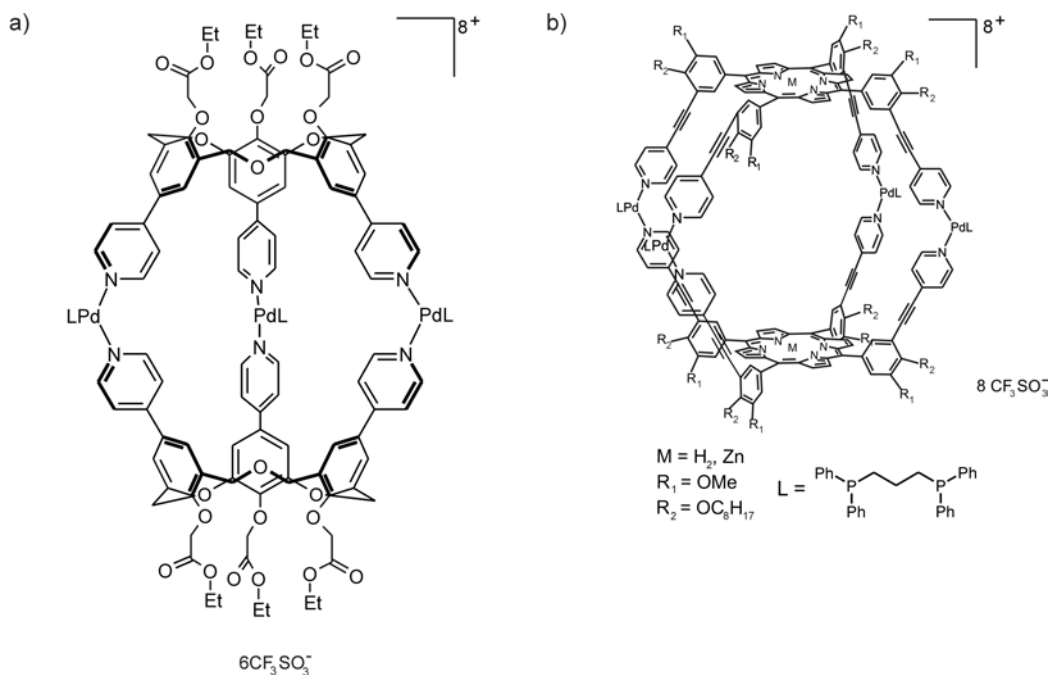


Figure 2.18. Examples of molecular capsules based on metal-ligand interactions synthesized in the group of Shinkai.

Hong et al.¹⁰⁰ reported the formation of a molecular capsule based on two resorcin[4]arenes functionalized at the upper rim with pyridine groups and four square planar metal Pd(II) or Pt(II) complexes. Guest encapsulation through cation- π interactions of *N*-methylpyridinium derivatives in acetone-*d*₆ was observed. Interestingly, addition of the guest after capsule formation did not show any sign of encapsulation as a result of the strong, nearly irreversible, Pd-pyridine bond.

Harrison et al.¹⁰¹ reported an example of a water-soluble, metal-containing resorcinarene cage complex, whose assembly is pH dependent. The cage consists of two identical halves bound together by four divalent cobalt ions. CPK models demonstrate that the cavity is large enough to accommodate a variety of small molecules including acetone, benzene, dioxane, and dichloromethane (Figure 2.19). The pH dependency of the Co(II) coordination to the resorcinarene ligand has been used to explore the ability of the cage molecules to trap and release organic guests such as benzene, hexane and butanol from aqueous solution. Due to the large paramagnetic shifts observed in the proton resonances (30-40 ppm) this type of cage can be regarded as an NMR shift reagent.¹⁰² Moreover, the replacement of Co(II) by Fe(II) resulted in the first iron(II)-containing cage complex formed by the self-assembly of cavitands.¹⁰³

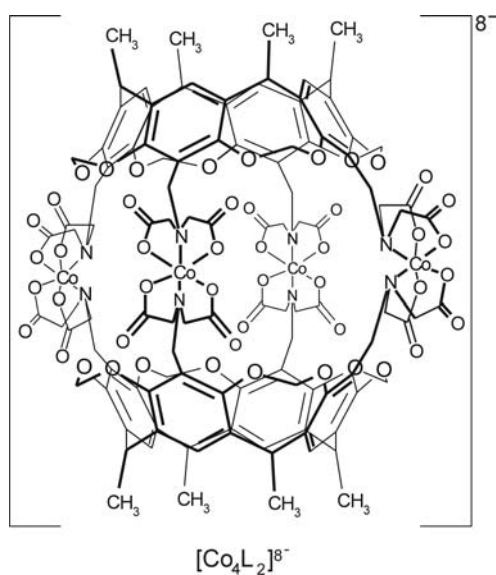


Figure 2.19. Harrison's water soluble molecular capsule.

2.3.2.2. Metallo cages based on "molecular paneling"

The concept of "molecular paneling" has been introduced by Fujita¹⁰⁴ to define the approach for constructing, large 3D structures from 2D organic components *via* metal coordination. Molecular panels based on planar exo-multidentate organic ligands assemble into large three-dimensional assemblies through metal-coordination with *cis*-protected square planar metals, [(en)Pd²⁺ or (en)Pt²⁺ (en = ethylenediamine)].

Mainly triangular panels, having different symmetry imparted by varying the number and the position of the binding sites, were used to assemble molecular cages resembling octahedra, square pyramids, tetrahedra and hexahedra (Figure 2.20).

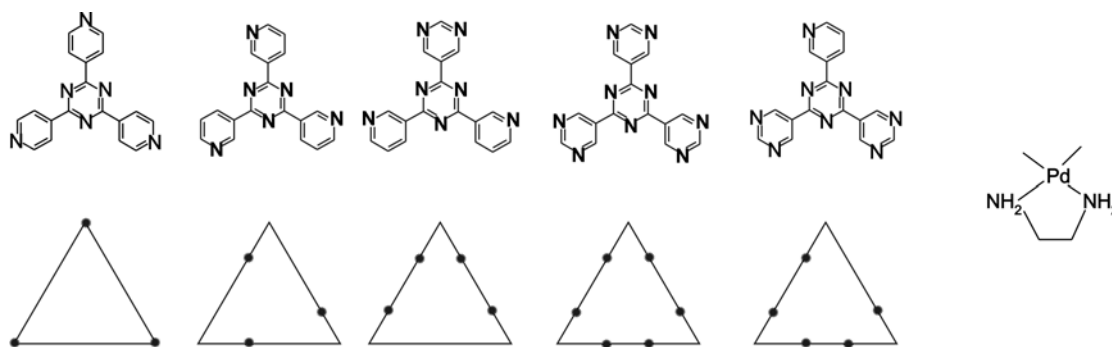


Figure 2.20. Triangular molecular panels and the square planar Pd unit.

A thermodynamically stable octahedral cage was obtained by the self-assembly of six panels with four Pd-based corner units.¹⁰⁵ The nanosize cavity of the M_6L_4 capsule (Figure 2.21a) has shown binding of organic guests like adamantenecarboxylate. Moreover, encapsulation of spherical guest molecules and aromatic compounds in aqueous solvent was also observed.¹⁰⁶ The nature of the metal was shown to determine the stability of the cage. An analogous but kinetically stable cage was in fact obtained when a Pt(II) instead of Pd(II) complex was employed.¹⁰⁷

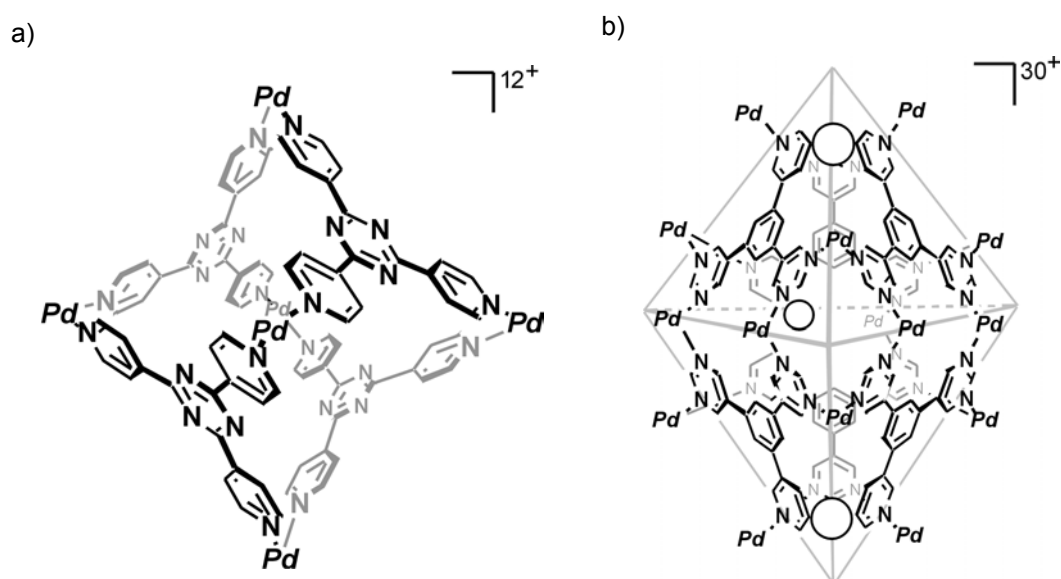


Figure 2.21. Examples of Fujita's cages.

Dimerization of a square pyramidal cone resulted in a dimeric capsule accommodating as many as six organic molecules as confirmed by X-ray analysis.¹⁰⁸ When molecular panels can assemble into different superstructures, the geometry of the assembly is controlled by the size of the guest molecule. An example is M_8L_4 : a square pyramidal cone is formed when a dibenzoyl molecule acts as a guest while CBr_4 templates the formation of a tetrahedron.¹⁰⁹

A bigger hexahedral architecture originating from the combination of 18 metal units and 6 molecular panels is depicted in Figure 2.21b. The molecular cage has an internal cavity of 900 \AA^3 . Its closed and rigid structure makes the encapsulation and the exchange of guest molecules difficult.¹¹⁰ A slight modification of the molecular panel resulted in a similar but more flexible hexahedral capsule having clefts for the reversible inclusion of small molecules like $CHCl_3$, CBr_4 and CH_2Br_2 .¹¹¹

2.3.2.3 Supramolecular metal clusters

Assemblies that can be regarded as small molecular capsules are the supramolecular clusters synthesized in the group of Raymond based on catecholamine as binding units and either tri- or tetravalent metal ions like Ga(III), Fe(III), Ti(IV) and Sn(IV).¹¹² Despite the limited dimension of the cavities, these types of assemblies are very versatile and show interesting binding properties (Figure 2.22). Studies on the energetics of the encapsulation of different alkylammonium guests in aqueous solutions showed that the encapsulation is an endothermic and entropy driven process due to the release of bound water from both the host and the guest into the bulk solvent. Dynamic exchange of guests within the supramolecular cluster cavity was also reported.¹¹³

As for Fujita's molecular cages where the ligand and the metal components can assemble into two different architectures, i.e either a triple helicate or a tetrahedron; the guest induces the organization of the host.¹¹⁴ Structural memory has also been reported for this type of clusters.¹¹⁵

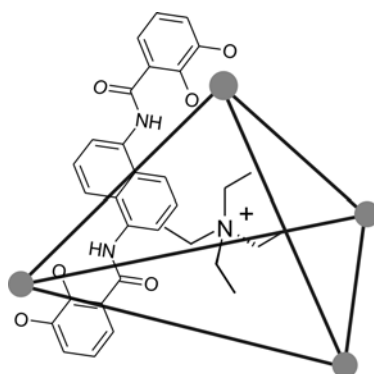


Figure 2.22. Metal cluster with encapsulated ammonium cation.

Hong et al. recently reported the self-assembly of a propeller-shaped supramolecular capsule induced by a rigid chiral tris(oxazoline) unit and Ag(I) metal ions which have tetrahedral coordination geometry.¹¹⁶

Konishi's group reported a novel class of container system in which an inorganic metal nanocluster is confined within an organic cage, composed of metalloporphyrins. The cage possesses a space between the core and porphyrin shell which allows the access of small molecules to the central core through the openings of the cage. This new system has potential for applications in material science.¹¹⁷

The group of Stang⁹⁰ proposed two general strategies for the self-assembly of metallocyclic cages based on metal-ligand coordination (Figure 2.23). The first is the edge-directed self-assembly where tritopic angular components are connected through linear linkers. The other is the face-directed self-assembly where some or all the faces of the target aggregate are spanned by the linkers themselves, which hold together the overall architecture.

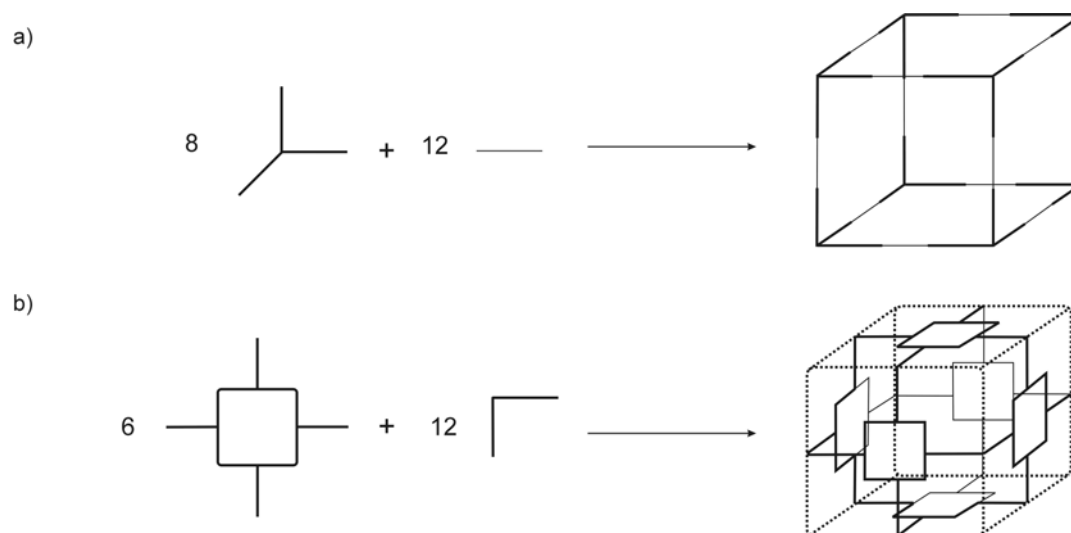


Figure 2.23. a) Edge-directed self-assembly and b) face-directed self-assembly.

Using these approaches nanoscopic cages resembling polyhedra have been reported.¹¹⁸ The synthesis of supramolecular cuboctahedrons was achieved by combining tridentate units (such as 1,3,5-tris(4'-iodophenyl)ethynylbenzene) and bidentate angular components (such as 4,4-bispyridylacetal).¹¹⁹ The tridentate building units must have three donor or acceptor sites located in one plane at 120° relative to each other. Moreover, in order to obtain the closed structure the ratio of bidentate to tridentate ligands must be 3:2 with a total of 20 appropriate subunits. A single dodecahedron molecule was obtained upon formation of 60 metal-ligand bonds and participation of 50 individual molecules providing an internal cavity for potential encapsulation of globular oligomers.^{119,120} Another example is the trigonal-bipyramid cage based on the self-assembly of two angular tritopic pyridine donor linkers and three ditopic platinum acceptors.¹²¹ Although these superstructures are of great conceptual importance, guest encapsulation was never reported.

2.4 Functional properties

The molecular capsules described up to this point have been discussed in the context of structural motifs and interactions. The examples reported below emphasize the applications of these covalent and noncovalent structures.

2.4.1 Molecular capsules for the isolation of reactive species

The stabilization of reactive intermediates is a unique property of molecular capsules. The internal cavity can be regarded as a “safe” closed space where otherwise unstable molecules, sequestered from the bulk solvent, are protected and stabilized.

Incarceration in the inner phase of Cram’s hemicarcerands represents a powerful way to stabilize reactive intermediates by preventing their dimerization.¹²² Other examples are the stabilization of cyclobutadiene, o-benzyne¹²³⁻¹²⁵ and 1,2,4,6-cycloheptatetraene.¹²⁶ Additionally, Rebek et al. reported the stabilization of benzoyl peroxide through encapsulation in a hydrogen-bonded molecular capsule.¹²⁷

Metal-ligand capsules have also been used for the stabilization of unfavored conformations. The molecular cage reported in Figure 2.24 has shown enclathration properties towards dimers of *cis*-isomers of azobenzene and stilbene in D₂O (Figure 2.24a).¹²⁸ The encapsulation stabilizes the *cis*-isomers preventing their conversion to the *trans*-isomers. As the dimensions of the spherical dimer are larger than that of the portals, dimerization most probably occurs within the cavity.

The stabilization of the kinetic, short-lived product trimer deriving from the condensation of trialkoxysilanes was also observed in the molecular cage (Figure 2.24b). Remarkably the complex cage-trimer remains stable even under acidic conditions.¹²⁹

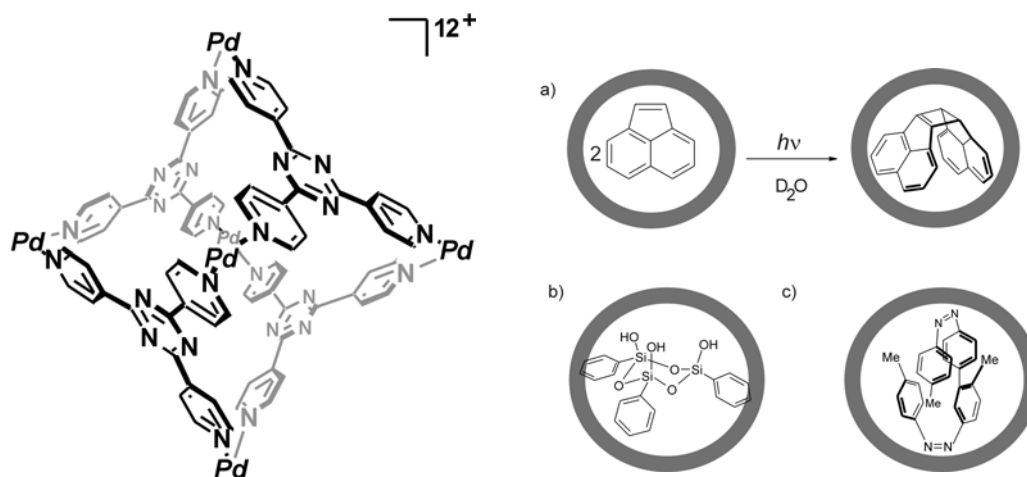


Figure 2.24. Stabilization in a molecular capsule based on metal-ligand interactions.

2.4.2 Molecular capsules as reaction chambers

In addition to photochemical reactions, the internal cavity of the molecular capsules reported in the previous sections represents a unique microchamber in which novel chemical reactions may be explored. The equatorial portals of hemicarcerands allow reactants to enter and exit the inner phase and to undergo either *inner-phase reactions*, when all the reactants are fully incarcerated¹³⁰ or *through-shell reactions* when the reaction takes place in one of the equatorial entryways. Examples are the selective borane reduction and butyllithium addition to benzaldehyde, benzocyclobutenedione and benzilcyclobutenone reported by Warmuth et al.¹³¹ The same group also reported on an *innermolecular* reaction where the encapsulated *o*-benzyne undergoes a Diels-Alder reaction with one of the arene rings lining the cavity wall of the hemicarceplex.¹²⁵ The reaction was found to be very selective and only one product was formed.

An *inner-phase* Diels-Alder reaction between *p*-quinone and cyclohexadiene was studied within Rebek's softball (Figure 2.25).^{132,133} Although the system does not show true catalytic behavior owing to the lack of dissociation, clear evidence for a rate increase of over two orders of magnitude was found. The simultaneous complexation of the two reactants within the capsule and thus the enhancement of their effective molarity was regarded as the reason for the increased reaction rate.

To achieve a real turn-over catalyst, Rebek and coworkers studied the reaction between benzoquinone and thiophene dioxide.¹³⁴ The release of the Diels-Alder adduct is the result of stronger binding of two molecules of benzoquinone by the

capsule compared to the product. Although the acceleration is modest this can be regarded as an example of true supramolecular catalysis.

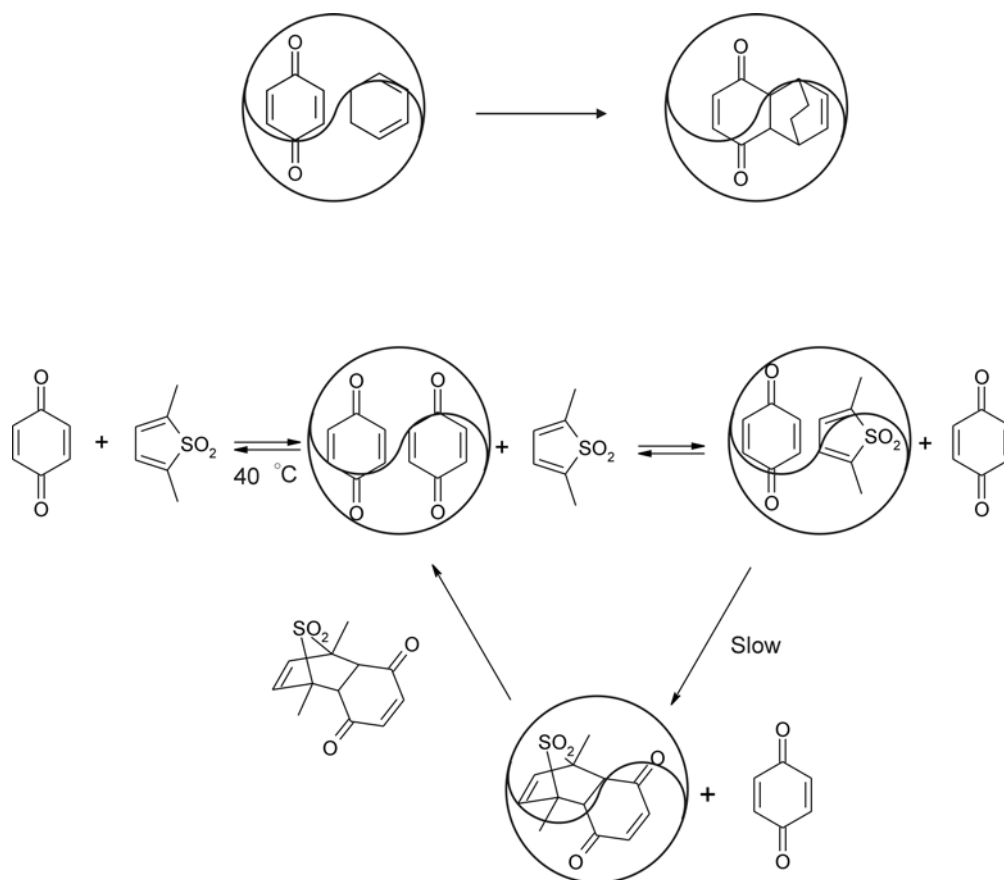


Figure 2.25. Diels-Alder reactions occurring in the interior cavity of Rebek's softball.

The group of Reinhoudt reported on the change of the rate of a thermal retro-Diels-Alder reaction when a suitable substrate is included in the cavity of a capsule (Figure 2.26).^{24,25} Normally the extrusion of SO₂ and butadiene from a free 3-sulfolene takes place at 100-130 °C. Instead, the 3-sulfolene included in the carcerand's cavity gains high thermal stability which causes the extrusion of the products from the carceplex only when the temperature rises to 180 °C as demonstrated by mass spectrometry (EI-MS) and field desorption mass spectrometry (FD-MS). Below this temperature a thermal equilibrium between 3-sulfolene, SO₂, and butadiene was proposed.

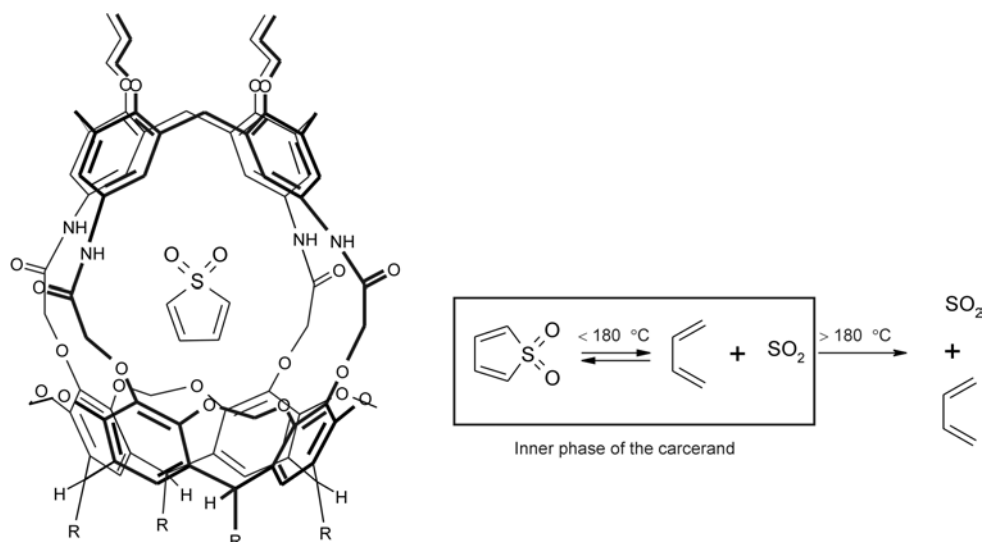


Figure 2.26. Retro-Diels Alder promoted in the inner phase of a carcerand.

Very recently the group of Sherman studied the inner-phase ketonization of a free-standing simple enol incarcerated in a trimer carceplex and found that it ketonizes slowly *via* enolate formation by bound water.¹³⁵

Examples of catalysis have also been reported for molecular capsules based on metal-ligand interactions. The cages reported by Fujita et al. are among the most promising host systems for promoting chemical transformations due to the large size of the internal cavity. Intermolecular [2+2] photodimerization and cross-photodimerization of large olefins was achieved within the coordination cage (see Figure 2.24c). Only *syn* and head to tail isomers were obtained.^{136,137} Other examples are the oxidation of styrene and the isomerization of allylbenzene. When the condensation of trialkoxysilanes was conducted in presence of the cage the exclusive formation of the cyclic trimer was observed.¹³⁸

2.4.3 Molecular capsules for sensing

Molecular capsules can also be used as sensing molecules when equipped with suitable groups that can act as noninvasive reporters of the recognition process.

In the group of Rebek¹³⁹ two calix[4]arenes tetra-urea were functionalized, one with a donor (D) fluorophore and one with an acceptor (A) fluorophore and their dimerization/dissociation processes followed by means of fluorescence resonance energy transfer (FRET) (Figure 2.27). Dimerization brings the fluorophores close enough for energy transfer to take place and the resulting fluorescent signal at $h\nu'$ is

indicative of the assembly of the molecular capsule. Denaturation of the dimer by addition of DMSO restored the donor emission.

More important for sensing purposes is that the assembly process occurs only in the presence of a guest molecule. A FRET signal is generated in chloroform solution, where the solvent is suitable for encapsulation. Contrarily in *p*-xylene, a solvent too bulky to be included in the cavity, the assembly takes place only when 3-methylcyclopentanone is added to the solution.

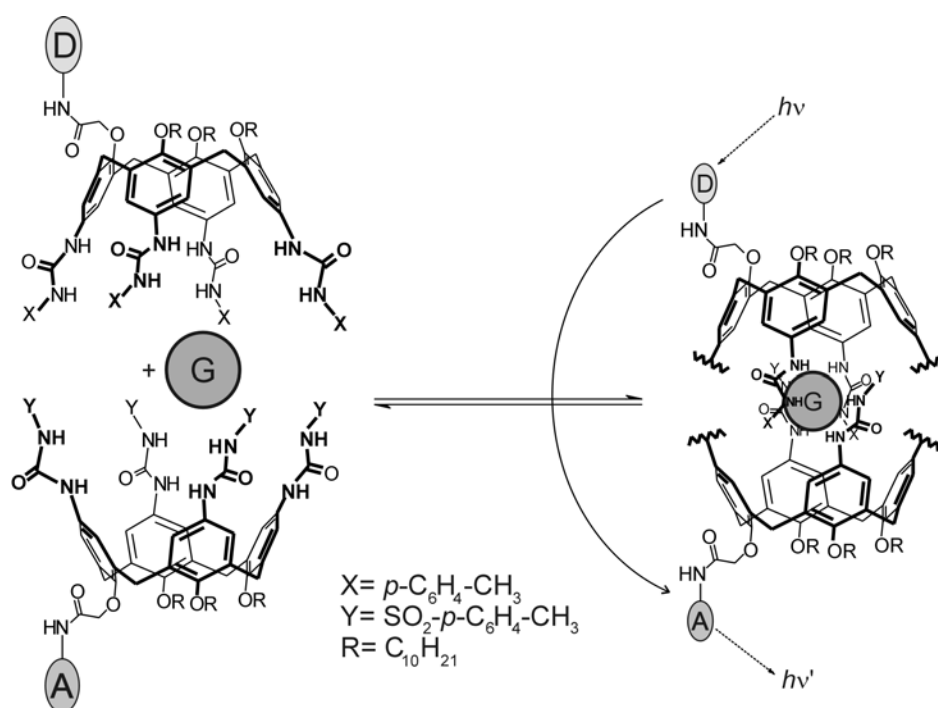


Figure 2.27. Encapsulation-dependent sensing of a guest. Part of the assembly is omitted by clarity.

Another system that can be regarded as an optical sensor for complexation is the chiral hemicarcerand reported by Warmuth.¹⁴⁰ Coumarin groups attached at one opening of the hemicarcerand are able to sense binding of chiral guests in aqueous solution.

2.5 Concluding remarks

Taking advantage of the large number of building blocks at the disposal of chemists, molecular capsules have been obtained either by means of *covalent* or *noncovalent* interactions. As shown in this chapter both approaches provide frameworks possessing cavities capable of entrapping atomic and/or molecular sized

guests. The properties of these systems allow applications in chemistry (stabilization of reactive intermediates and catalysis) and material science (sensing), as reported in the last section of the chapter. Nevertheless, as molecular recognition is rapidly moving towards molecular biology for application like encapsulation of drugs and their active transport/delivery through cell membranes, *noncovalent* molecular capsules are preferable. This tendency is currently inspiring the design of new reversible and water compatible containers. This thesis deals with the use of multiple electrostatic interactions for the self-assembly of highly stable molecular capsules in polar organic solvents and in aqueous solutions. Thus far only a limited number of molecular containers based on ion pairing have been published. These will be described in Chapter 3.

2.6 References

1. Cram, D. J.; Cram, J. M. *Container Molecules and Their Guests*; Royal Society of Chemistry: Cambridge, 1994.
2. Rebek, J. Jr. *Acc. Chem. Res.* **1999**, *97*, 278-286.
3. Cram, D. J.; Karbach, S.; Kim, Y. H.; Baczynskyj, L.; Kalleyman, G. W. *J. Am. Chem. Soc.* **1985**, *107*, 2575-2576.
4. Sherman, J. C. *Tetrahedron* **1995**, *51*, 3395-3422.
5. Jasat, A.; Sherman, J. C. *Chem. Rev.* **1999**, *99*, 931-967.
6. Yoon, J.; Cram, D. J. *Chem. Commun.* **1997**, 497-498.
7. Piatnitski, E. L.; Flower, R. A. II.; Deshayes, K. *Chem. Eur. J.* **2000**, *6*, 999-1006.
8. Cram, D. J.; Tanner, M. E.; Thomas, R. *Angew. Chem. Int. Ed. Engl.* **1991**, *30*, 1024-1027.
9. Chapmann, R. G.; Olovsson, G.; Trotter, J.; Sherman, J. C. *J. Am. Chem. Soc.* **1998**, *120*, 6252-6260.
10. Nakamura, K.; Sheu, C.; Keating, A. E.; Houk, K. N. *J. Am. Chem. Soc.* **1997**,

- 119, 4321-4322.
11. Chapman, R.; Sherman, J. C. *J. Am. Chem. Soc.* **1995**, *117*, 9081-9082.
 12. Chopra, N.; Naumann, C.; Sherman, J. C. *Angew. Chem. Int. Ed.* **2000**, *39*, 194-196.
 13. Mungaroo, R.; Sherman, J. C. *Chem. Commun.* **2002**, 1672-1673.
 14. Chopra, N.; Sherman, J. C. *Angew. Chem. Int. Ed.* **1999**, *38*, 1955-957.
 15. Naumann, C.; Place, S.; Sherman, J. C. *J. Am. Chem. Soc.* **2002**, *124*, 16-17.
 16. Blanda, M. T.; Griswold, K. E. *J. Org. Chem.* **1994**, *59*, 4313-4315.
 17. Araki, K.; Hayashida, H. *Tetrahedron Lett.* **2000**, *41*, 1209-1213.
 18. Araki, K.; Watanabe, T.; Oda, M.; Hayashida, H.; Yasutake, M.; Shinmyouzu, T. *Tetrahedron Lett.* **2001**, *42*, 7465-7468.
 19. Bottino, A.; Cunsolo, F.; Piattelli, M.; Garozzo, D.; Neri, P. *J. Org. Chem.* **1999**, *64*, 8018-8020.
 20. Neri, P.; Bottino, A.; Cunsolo, F.; Piattelli, M.; Gavuzzo, E. *Angew. Chem. Int. Ed.* **1998**, *37*, 166-169.
 21. Arduini, A.; Pochini, A.; Secchi, A. *Eur. J. Org. Chem.* **2000**, *12*, 2325-2334.
 22. Tam-Chang, S.-W.; Stehouwer, J. S.; Hao, J. *J. Org. Chem.* **1999**, *64*, 334-335.
 23. Ro, S.; Rowan, S. J.; Pease, A. R.; Cram, D. J.; Stoddart, J. F. *Org. Lett.* **2000**, *13*, 2411-2414.
 24. Timmerman, P.; Verboom, W.; van Veggel, F. C. J. M.; van Hoorn, W. P.; Reinhoudt, D. N. *Angew. Chem. Int. Ed. Engl.* **1994**, *33*, 1292-1295.
 25. van Wageningen, A. M. A.; Timmerman, P.; van Duynhoven, J. P. M.; Verboom, W.; van Veggel, F. C. J. M.; Reinhoudt, D. N. *Chem. Eur. J.* **1997**, *3*, 639-654.

26. Timmerman, P.; Verboom, W.; van Veggel, F. C. J. M.; van Duynhoven, J. P. M.; Reinhoudt, D. N. *Angew. Chem. Int. Ed. Engl.* **1994**, *33*, 2345-2348.
27. van Wageningen, A. M. A.; van Duynhoven, J. P. M.; Verboom, W.; Reinhoudt, D. N. *Chem. Commun.* **1995**, 1941-1942.
28. Timmerman, P.; Nierop, K. G. A.; Brinks, E. A.; Verboom, W.; van Veggel, F. C. J. M.; van Hoorn, W. P.; Reinhoudt, D. N. *Chem. Eur. J.* **1995**, *2*, 132-143.
29. Lücking, U.; Tucci, F. C.; Rudkevich, D. M.; Rebek, J. Jr. *J. Am. Chem. Soc.* **2000**, *122*, 8880-8889.
30. Starnes, S. D.; Rudkevich, D. M.; Rebek, J. Jr. *J. Am. Chem. Soc.* **2001**, *123*, 4659-4669.
31. Collet, A.; Dutasta, J.-P.; Lozach, B.; Canceill, J. *Top. Curr. Chem.* **1993**, *165*, 103-129.
32. Lang, J.; Dechter, J. J.; Effemey, M.; Kowalewski, J. *J. Am. Chem. Soc.* **2001**, *123*, 7852-7858.
33. Collet, A. *Tetrahedron* **1987**, *43*, 5725-5759.
34. Garel, L.; Dutasta, J.-P.; Collet, A. *Angew. Chem. Int. Ed. Engl.* **1993**, *32*, 1169-1171.
35. Canceill, J.; Lacombe, L.; Collet, A. *J. Am. Chem. Soc.* **1985**, 6993-6996.
36. Wyler, R.; de Mendoza, J.; Rebek, J. Jr. *Angew. Chem. Int. Ed. Engl.* **1993**, *32*, 1699-1701.
37. Meissner, R. S.; Rebek, J. Jr.; de Mendoza, J. *Science* **1995**, *270*, 1485-1488.
38. Valdés, C.; Toledo, L. M.; Spitz, U.; Rebek, J. Jr. *Chem. Eur. J.* **1996**, *2*, 989-991.
39. Branda, N.; Grotzfeld, R. M.; Valdés, C.; Rebek, J. Jr. *J. Am. Chem. Soc.* **1995**, *117*, 85-88.

40. Valdés, C.; Spitz, U. P.; Toledo, L. M.; Kubik, S. W.; Rebek, J. Jr. *J. Am. Chem. Soc.* **1995**, *117*, 12733-12745.
41. Garcías, X.; Rebek, J. Jr. *Angew. Chem. Int. Ed. Engl.* **1996**, *35*, 1225-1228.
42. Martín, T.; Obst, U.; Rebek, J. Jr. *Science* **1998**, *281*, 1842-1845.
43. Hof, F.; Nuckolls, C.; Craig, S. L.; Martín, T.; Rebek, J. Jr. *J. Am. Chem. Soc.* **2000**, *122*, 10991-10996.
44. Johnson, D. W.; Hof, F.; Iovine, P. M.; Nuckolls, C.; Rebek, J. Jr. *Angew. Chem. Int. Ed.* **2002**, *41*, 3793-3796.
45. Nuckolls, C.; Hof, F.; Martín, T.; Rebek, J. Jr. *J. Am. Chem. Soc.* **1999**, *121*, 10281-10285.
46. Szabo, T.; O'Leary, B. M.; Rebek, J. Jr. *Angew. Chem. Int. Ed.* **1998**, *37*, 3410-3413.
47. Grotzfeld, R. M.; Branda, N.; Rebek, J. Jr. *Science* **1996**, *271*, 487-489.
48. Shimizu, K. D.; Rebek, J. Jr. *Proc. Natl. Acad. Sci. U.S.A.* **1995**, *92*, 12403-12407.
49. Hamann, B. C.; Shimizu, K. D.; Rebek, J. Jr. *Angew. Chem. Int. Ed. Engl.* **1996**, *35*, 1326-1329.
50. Mogck, O.; Böhmer, V.; Vogt, W. *Tetrahedron* **1996**, *52*, 8489-8496.
51. Brody, M. S.; Schalley, C. A.; Rudkevich, D. M.; Rebek, J. Jr. *Angew. Chem. Int. Ed.* **1999**, *38*, 1640-1644.
52. Mogck, O.; Paulus, E. F.; Böhmer, V.; Thondorf, I.; Vogt, W. *Chem. Commun.* **1996**, 2533-2534.
53. Hamann, B. C.; Shimizu, K. D.; Rebek, J. Jr. *Angew. Chem. Int. Ed. Engl.* **1996**, *35*, 1326-1329.
54. Vysotsky, M. O.; Thondorf, I.; Böhmer, V. *Chem. Commun.* **2001**, 1890-1891.

55. Castellano, R. K.; Rebek, J. Jr. *J. Am. Chem. Soc.* **1998**, *120*, 3657-3663.
56. Castellano, R. K.; Hyeon Kim, B.; Rebek, J. Jr. *J. Am. Chem. Soc.* **1997**, *119*, 12671-12672.
57. Vysotsky, M. O.; Pop, A.; Broda, F.; Thondorf, I.; Böhmer, V. *Chem. Eur. J.* **7**, 4403-4410.
58. Castellano, R. K.; Nuckolls, C.; Rebek, J. Jr. *J. Am. Chem. Soc.* **1999**, *121*, 11156-11163.
59. Pop, A.; Vysotsky, M. O.; Saadioui, M.; Böhmer, V. *Chem. Commun.* **2003**, 1124-1125.
60. Lag Cho, Y.; Rudkevich, D. M.; Rebek, J. Jr. *J. Am. Chem. Soc.* **2000**, *122*, 9868-9869.
61. González, J. J.; Ferdani, R.; Albertini, E.; Blasco, J. M.; Arduini, A.; Pochini, A.; Prados, P.; de Mendoza, J. *Chem. Eur. J.* **2000**, *6*, 73-80.
62. Rincón, A. M.; Prados, P.; de Mendoza, J. *J. Am. Chem. Soc.* **2001**, *123*, 3493-3498.
63. Castellano, R. K.; Rudkevich, D. M.; Rebek, J. Jr. *J. Am. Chem. Soc.* **1996**, *118*, 10002-10003.
64. Vreekamp, R. H.; Verboom, W.; Reinhoudt, D. N. *J. Org. Chem.* **1996**, *61*, 4282-4288.
65. Araki, K.; Shinkai, S. *Tetrahedron Lett.* **1994**, *35*, 8255-8258.
66. Brewster, R. E.; Beckham Shucker, S. *J. Am. Chem. Soc.* **2002**, *124*, 7902-7903.
67. Heinz, T.; Rudkevich, D. M.; Rebek, J. Jr. *Nature* **1998**, *394*, 764-766.
68. Hayashida, O.; Shivanyuk, A.; Rebek, J. Jr. *Angew. Chem. Int. Ed.* **2002**, *41*, 3423-3426.

69. Ohayashida, O.; Sebo, L.; Rebek, J. Jr. *J. Org. Chem.* **2002**, *67*, 8291-8298.
70. Shivanyuk, A.; Rebek, J. Jr. *Chem. Commun.* **2002**, 2326-2327.
71. Shivanyuk, A.; Rebek, J. Jr. *Angew. Chem. Int. Ed. Engl.* **2003**, *42*, 684-686.
72. Scarso, A.; Shivanyuk, A.; Hayashida, O.; Rebek, J. Jr. *J. Am. Chem. Soc.* **2003**, *125*, 6239-6243.
73. Shivanyuk, A.; Rebek, J. Jr. *J. Am. Chem. Soc.* **2002**, *124*, 12074-12075.
74. Kobayashi, K.; Shirasaka, T.; Yamaguchi, K.; Sakamoto, S.; Horn, E.; Furukawa, N. *Chem. Commun.* **2000**, 41-42.
75. Kobayashi, K.; Ishii, I.; Sakamoto, S.; Shirasake, T.; Yamaguchi, K. *J. Am. Chem. Soc.* **2003**, *125*, 10615-10624.
76. Lutzen, A.; Renslo, A. R.; Schalley, C. A.; O'Leary, B. M.; Rebek, J. Jr. *J. Am. Chem. Soc.* **1999**, *121*, 7455-7456.
77. Rose, K. N.; Barbour, L. J.; Orr, G. W.; Atwood, J. L. *Chem. Commun.* **1998**, 407-408.
78. Murayama, K.; Aoki, K. *Chem. Commun.* **1998**, 607-608.
79. MacGillivray, L. R.; Atwood, J. L. *Nature* **1997**, *389*, 469-472.
80. Shivanyuk, A.; Rebek, J. Jr. *Proc. Natl. Acad. Sci. U.S.A.* **2001**, *98*, 7662-7665.
81. Shivanyuk, A.; Rebek, J. Jr. *Chem. Commun.* **2001**, 2424-2425.
82. Shivanyuk, A.; Rebek, J. Jr. *Chem. Commun.* **2001**, 2374-2375.
83. Avram, L.; Cohen, Y. *J. Am. Chem. Soc.* **2002**, *124*, 15148-15149.
84. Shivanyuk, A.; Friese, J. C.; Döring, S.; Rebek, J. Jr. *J. Org. Chem.* **2003**, *68*, 6489-6496.
85. Atwood, J. L.; Barbour, L. J.; Jerga, A. *Chem. Commun.* **2001**, 2376-2377.

86. Linton, B.; Hamilton, A. D. *Chem. Rev.* **1997**, *97*, 1669-1680.
87. Stang, P. J.; Olenyuk, B. *Acc. Chem. Res.* **1997**, *30*, 502-518.
88. MacGillivray, L. R.; Atwood, J. L. *Angew. Chem. Int. Ed.* **1999**, *38*, 1018-1033.
89. Leininger, S.; Olenyuk, B.; Stang, P. J. *Chem Rev.* **2000**, *100*, 853-908.
90. Russel-Seidel, S.; Stang, P. J. *Acc. Chem. Res.* **2002**, *35*, 972-983.
91. Caulder, D. L.; Raymond, K. N. *Acc. Chem. Res.* **1999**, *32*, 975-982.
92. Jacopozi, P.; Dalcanale, E. *Angew. Chem. Int. Ed. Engl.* **1997**, *36*, 613-615.
93. Fochi, F.; Jacopozi, P.; Wegelius, E.; Rissanen, K.; Cozzini, P.; Marastoni, E.; Fiscaro, E.; Manini, P.; Fokkens, R.; Dalcanale, E. *J. Am. Chem. Soc.* **2001**, *123*, 7539-7552.
94. Pirondini, L.; Bertolini, F.; Cantadori, B.; Ugozzoli, F.; Massera, C.; Dalcanale, E. *Proc. Natl. Acad. Sci. USA* **2002**, *99*, 4911-4915.
95. Ikeda, A.; Udzu, H.; Yoshimura, M.; Shinkai, S. *Tetrahedron* **2000**, *56*, 1825-1832.
96. Ayabe, M.; Yamashita, K.; Sada, K.; Shinkai, S.; Ikeda, A.; Sakamoto, S.; Yamaguchi, K. *J. Org. Chem.* **2003**, *68*, 1059-1066.
97. Ikeda, A.; Ayabe, M.; Shinkai, S.; Sakamoto, S.; Yamaguchi, K. *Org. Lett.* **2000**, *2*, 3707-3710.
98. Kawaguchi, M.; Ikeda, A.; Shinkai, S. *Tetrahedron Lett.* **2001**, *42*, 3725-3728.
99. Ikeda, A.; Sonoda, K.; Shinkai, S. *Chem. Lett.* **2000**, 1220-1221.
100. Park, S. J.; Hong, J.-H. *Chem. Commun.* **2001**, 1554-1555.
101. Fox, D. O.; Dalley, N. K.; Harrison, R. G. *J. Am. Chem. Soc.* **1998**, *120*, 7111-7112.

102. Fox, O. D.; Leung, J. F. Y.; Hunter, J. M.; Dalley, N. K.; Harrison, R. G. *Inorg. Chem.* **2000**, *39*, 783-790.
103. Fox, O. D.; Dalley, N. K.; Harrison, R. G. *Inorg. Chem.* **1999**, *38*, 5860-5863.
104. Fujita, M.; Umemoto, K.; Yoshizawa, M.; Fujita, N.; Kusukawa, T.; Biradha, K. *Chem. Commun.* **2001**, 509-518.
105. Fujita, M.; Oguro, D.; Miyazawa, M.; Oka, H.; Yamaguchi, K.; Ogura, K. *Nature* **1995**, *378*, 469-471.
106. Kusukawa, T.; Fujita, M. *Angew. Chem. Int. Ed.* **1998**, *37*, 3142-3144.
107. Ibukuro, F.; Kusukawa, T.; Fujita, M. *J. Am. Chem. Soc.* **1998**, *120*, 8561-8562.
108. Yu, S.-Y.; Kusukawa, T.; Biradha, K.; Fujita, M. *J. Am. Chem. Soc.* **2000**, *122*, 2665-2666.
109. Umemoto, K.; Yamaguchi, K.; Fujita, N. *J. Am. Chem. Soc.* **2000**, *398*, 794-795.
110. Takeda, N.; Umemoto, K.; Yamaguchi, K.; Fujita, M. *Nature* **1999**, *398*, 794-796.
111. Umemoto, K.; Tsukui, H.; Kusukawa, T.; Biradha, K.; Fujita, M. *Angew. Chem. Int. Ed.* **2001**, *40*, 2620-2622.
112. Parac, T. N.; Caulder, D. L.; Raymond, K. N. *J. Am. Chem. Soc.* **1998**, *120*, 8003-8004.
113. Caulder, D. L.; Powers, R. E.; Parac, T. N.; Raymond, K. N. *Angew. Chem. Int. Ed.* **1998**, *37*, 1840-1843.
114. Scherer, M.; Caulder, D. L.; Johnson, D. W.; Raymond, K. N. *Angew. Chem. Int. Ed.* **1999**, *38*, 1588-1592.
115. Ziegler, M.; Davis, A. V.; Johnson, D. W.; Raymond, K. N. *Angew. Chem. Int. Ed.* **2003**, *42*, 665-668.

116. Kim, H. J.; Moon, D.; Lah, M. S.; Hong, J. I. *Angew. Chem. Int. Ed.* **2002**, *41*, 3174-3177.
117. Inomata, T.; Konishi, K. *Chem. Commun.* **2003**, 1282-1283.
118. Stang, P. J. *Chem. Eur. J.* **1998**, *4*, 19-27.
119. Olenyuk, B.; Whiteford, J. A.; Fechtenkötter, A.; Stang, P. J. *Nature* **1999**, *398*, 796-799.
120. Olenyuk, B.; Levin, M. D.; Whiteford, J. A.; Shield, J. E.; Stang, P. J. *J. Am. Chem. Soc.* **1999**, *121*, 10434-10435.
121. Radhakrishnan, U.; Schweiger, M.; Stang, P. J. *Org. Lett.* **2001**, *3*, 3141-3143.
122. Cram, D. J.; Cram, J. M. *Container Molecules and Their Guests*; Royal Society of Chemistry: Cambridge, 1994.
123. Cram, D. J.; Tanner, M. E.; Thomas, R. *Angew. Chem. Int. Ed. Engl.* **1991**, *30*, 1024-1027.
124. Warmuth, R. *Angew. Chem. Int. Ed. Engl.* **1997**, *36*, 1347-1350.
125. Warmuth, R. *Chem. Commun.* **1998**, 59-60.
126. Warmuth, R.; Marvel, M. A. *Angew. Chem. Int. Ed.* **2000**, *39*, 1117-1119.
127. Körner, S. K.; Tucci, F. C.; Rudkevich, D. M.; Heinz, T. *Chem. Eur. J.* **2000**, *6*, 187-195.
128. Kusukawa, T.; Fujita, M. *J. Am. Chem. Soc.* **1999**, *121*, 1397-1398.
129. Yoshizawa, M.; Kusukawa, T.; Fujita, M.; Yamaguchi, K. *J. Am. Chem. Soc.* **2000**, 6311-6312.
130. Warmuth, R. *J. Incl. Phenom. Mac. Chem.* **2000**, *37*, 1-38.
131. Warmuth, R.; Maverick, E. F.; Knobler, C. B.; Cram, D. J. *J. Org. Chem.* **2003**, *68*, 2077-2088.

132. Kang, J.; Hilmersson, G.; Santamaria, J.; Rebek, J. Jr. *J. Am. Chem. Soc.* **1998**, *120*, 3650-3656.
133. Kang, J.; Rebek, J. Jr. *Nature* **1997**, *385*, 50-52.
134. Kang, J.; Santamaria, J.; Hilmersson, G.; Rebek, J. Jr. *J. Am. Chem. Soc.* **1998**, *120*, 7389-7390.
135. Makeiff, D. A.; Vishnumurthy, K.; Sherman, J. C. *J. Am. Chem. Soc.* **2003**, *125*, 9558-9559.
136. Yoshizawa, M.; Takeyama, Y.; Kusukawa, T.; Fujita, M. *Angew. Chem. Int. Ed.* **2002**, *41*, 1347-1349.
137. Yoshizawa, M.; Takeyama, Y.; Okano, T.; Fujita, M. *J. Am. Chem. Soc.* **2003**, *125*, 3243-3247.
138. Kusukawa, T.; Yoshizawa, M.; Fujita, M. *Angew. Chem. Int. Ed.* **2001**, *40*, 1879-1884.
139. Castellano, R. K.; Craig, S. L.; Nuckolls, C.; Rebek, J. Jr. *J. Am. Chem. Soc.* **2000**, *122*, 7876-7882.
140. Singh, H.; Warmuth, R. *Tetrahedron* **2002**, *58*, 1257-1264.

MULTIPLE IONIC INTERACTIONS FOR NONCOVALENT SYNTHESIS OF MOLECULAR CAPSULES IN POLAR SOLVENTS

*The work presented in this chapter reports the formation and characterization of a novel type of capsules resulting from the self-association between oppositely charged calix[4]arenes in polar solvents like MeOH and MeOH/H₂O. The multiple ionic interactions allow the self-assembly of the complementary calix[4]arenes **1a** and **2a-c** into 1:1 complexes. ¹H NMR, ESI-MS, and ITC provide evidence for the formation of the assemblies. The self-assembly between the conformationally flexible thiacalix[4]arene **2d** and calix[4]arene **1a** is also investigated.*

3.1 Introduction

Building molecular structures that are able to encapsulate guest molecules in solution is one of the objectives in supramolecular chemistry.¹⁻³ The design of such structures has been achieved using either covalent⁴⁻⁷ or noncovalent synthesis.^{1,8,9} As described in Chapter 2 different approaches have been used to obtain capsules via noncovalent interactions. Multiple hydrogen bonding represents one of the most widely employed tools in the construction of predefined molecular containers.¹⁰⁻²⁴ Most of these systems, however, are restricted to non-polar solvents. Nevertheless, capsules that are stable in polar organic solvents²⁵⁻²⁷ have recently been obtained by combining hydrogen bonds with other weak noncovalent interactions, like cation- π and π - π stacking. Metal ions have also been widely used for the self-assembly of supramolecular host capsules.²⁸⁻⁴¹ This has the advantage that guest molecules can be bound by vacant coordination sites on the metal centers.^{42,43}

Surprisingly, when our work started only a few examples of stable cage-like complexes using multiple ionic interactions have been reported in the literature. The group of Hong⁴⁴ synthesized a three-dimensional molecular capsule based on charged hydrogen-bonding interactions between carboxylates and ammonium groups located at the upper rim of two cyclotrimeratrylene (CTV) monomers (Figure 3.1a). The formation of the self-assembled molecular capsule was confirmed by irreversible inclusion of neutral guests, such as chloroform and tetramethylsilane, in DMSO-*d*₆.

Another example is the capsule resulting from ionic interactions between two oppositely charged β -cyclodextrins in water. Dynamic ¹H NMR studies were used to demonstrate the formation of the molecular assembly.⁴⁵ A spherical assembly^{46,47} was reported by Schrader and coworkers by combining triply charged complementary building blocks based on ammonium or amidinium and phosphate ions (Figure 3.1b). The assemblies are stable in solvents like methanol ($K_a \sim 10^6 \text{ M}^{-1}$) and water ($K_a \sim 10^3 \text{ M}^{-1}$). Calculations of the van der Waals surfaces revealed a very small internal cavity of approximately the size of a diatomic molecule. However, encapsulation was not reported.

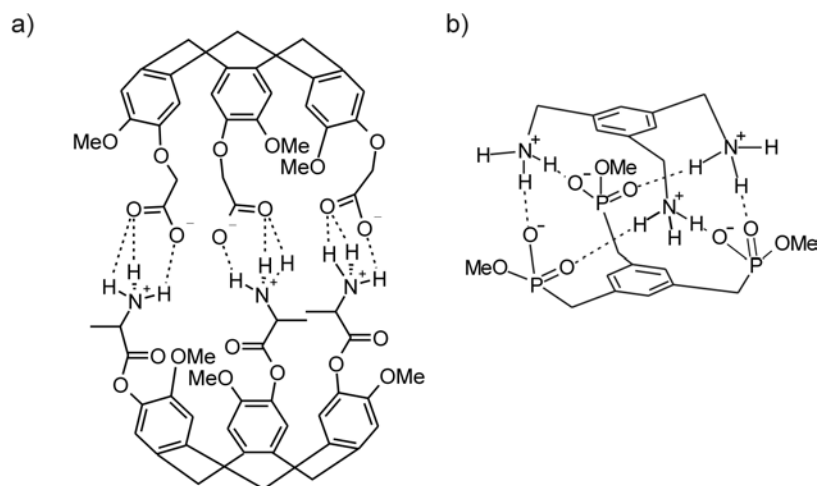


Figure 3.1. Molecular capsules based on ionic interactions.

Only very recently a number of publications have followed these first examples.

A self-assembled, helical, capsule-like assembly composed of two tris(imidazoline) bases and three tartaric acids linked through charged hydrogen bonds in aqueous solution has been reported by Hong et al. (Figure 3.2a).⁴⁸

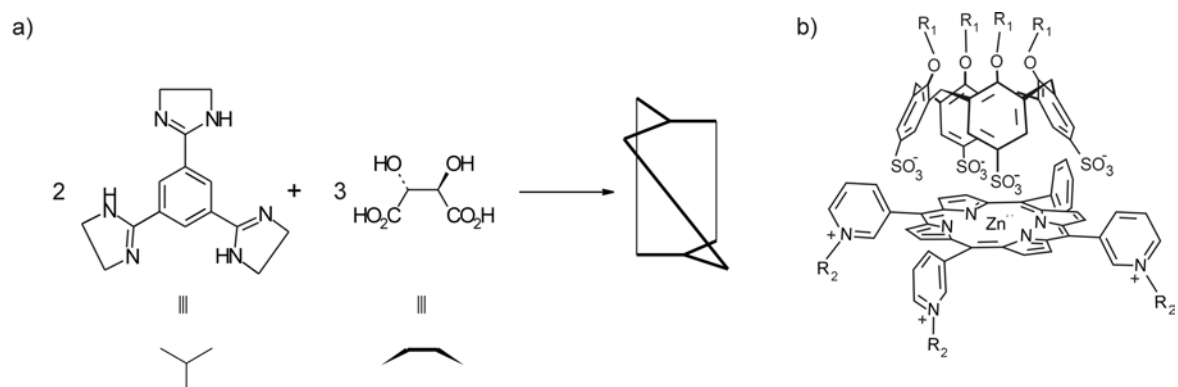


Figure 3.2. a) Helical capsule-like assembly through charged hydrogen bonds; b) calix[4]arene capped porphyrin.

Cage-like complexes based on tetracationic Zn(II) porphyrinates and tetraanionic calix[4]arenes were studied in our group⁴⁹ (Figure 3.2b). In parallel with our study, the synthesis of molecular capsules based on ionic interactions between oppositely charged calix[4]- and calix[6]arenes has been very recently published by the group of Schrader.^{50,51} In this chapter it is shown that the strong association between oppositely charged calix[4]arenes **1a** and **2a-c**, functionalized at the upper rim with amidinium and either sulfonate, carboxylic acid and phosphate moieties respectively, results in the formation of

a novel type of 1:1 molecular capsule (Figure 3.3). The assemblies are stable in solutions containing up to 40 mol% water, most likely as the result of preorganization of the charges on the calix[4]arene scaffold. The conformationally flexible thiacalix[4]arene **2d** (Figure 3.3) also forms a very strong complex with the oppositely charged calix[4]arene **1a**. As discussed in the last section of this chapter, no definitive indication was found for the conformation adopted by **2d** in **1a•2d** in solution, which can be either *cone* or *1,3-alternate*.

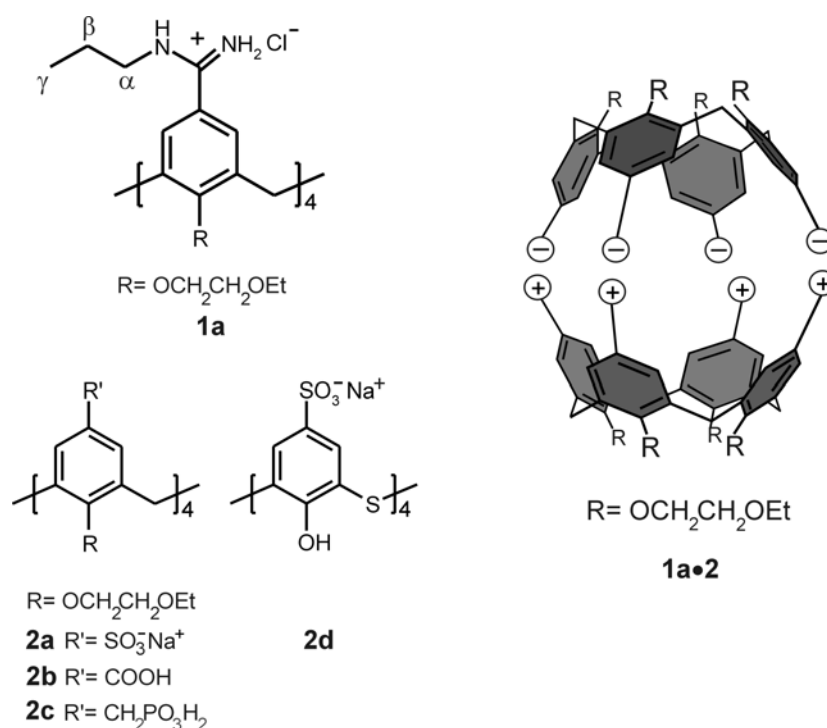


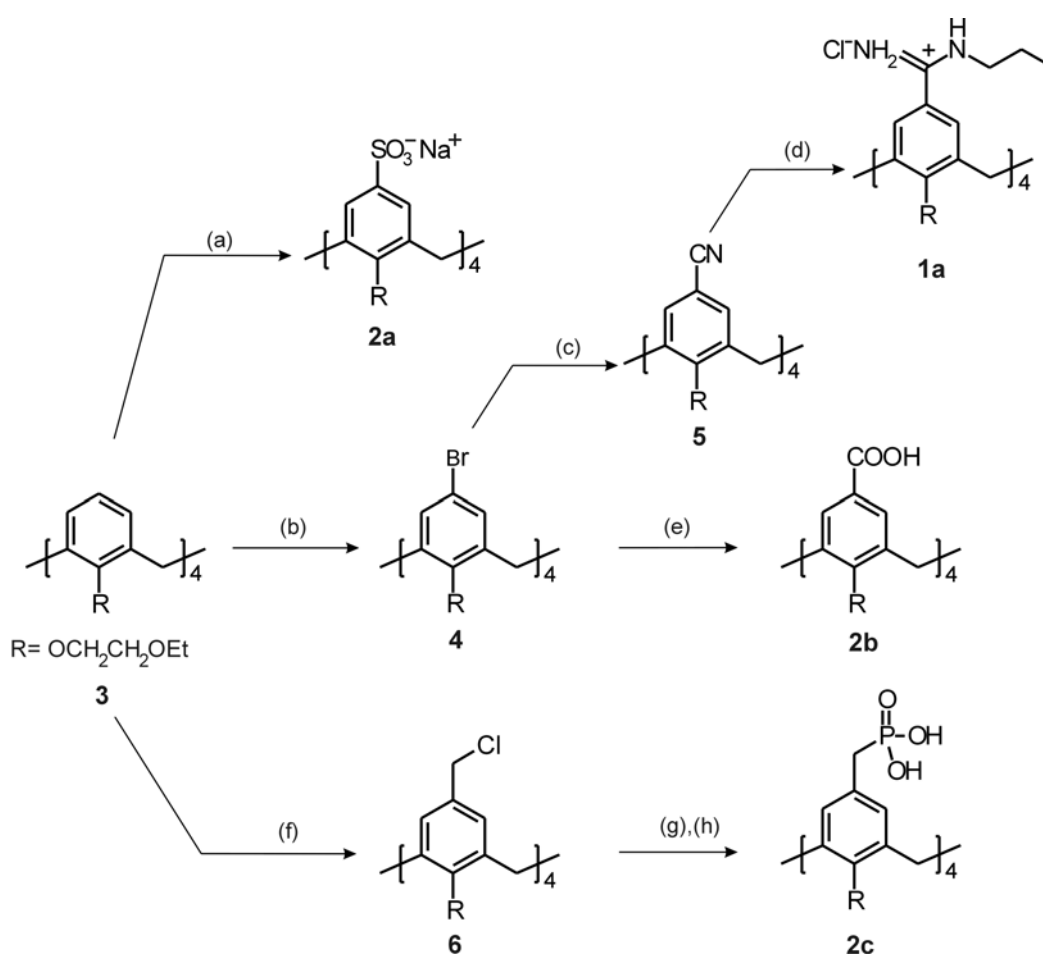
Figure 3.3. Molecular structures of the building blocks and schematic representation of the resulting molecular capsule.

3.2 Results and discussion

3.2.1 Synthesis

Calix[4]arene fixed in the *cone* conformation by *O*-alkylation at the lower rim offers a preorganized cavity which is easy to functionalize in various ways by substitution at the upper rim.⁵² Calix[4]arene **1a**, with tetraamidinium groups directly attached to the upper rim, was synthesized using a modified one step literature procedure.^{53,54} The introduction of the amidinium moieties was achieved by reacting the alkylchloroaluminium amide, generated from Et_2AlCl and propyl amine, with **5** in fluorobenzene (Scheme 3.1). The

chloride salt of **1a** was obtained after reverse phase chromatography and ion exchange chromatography in 65% yield. Compound **2a** was obtained as previously described⁵⁵ by treating compound **3** with concentrated H_2SO_4 (Scheme 3.1). Tetracarboxy calix[4]arene **2b** was obtained in 70% yield in a Br-Li exchange reaction on the precursor compound **4** with *t*-BuLi in THF at $-78\text{ }^\circ\text{C}$ followed by quenching with CO_2 (Scheme 3.1). The reaction of chloromethylated calix[4]arene **6** with triethylphospite, in the typical conditions of the Arbuzov reaction, and subsequent de-esterification with TMSBr afforded calix[4]arene **2c** in a 54% yield (Scheme 3.1). Thiocalix[4]arene **2d** was synthesized according to a literature procedure.⁵⁶



Scheme 3.1. Reagents and conditions: (a) H_2SO_4 conc., 2h, rt then $\text{NaOH}/\text{H}_2\text{O}$, yield 80%; (b) NBS, ethylmethyl ketone, 36h, rt, yield 85%; (c) CuCN , N-methylpyrrolidinone, 6h reflux, yield 78%; (d) Et_2AlCl , propylamine, fluorobenzene, 5 days, $80\text{ }^\circ\text{C}$, yield 65%; (e) *t*-BuLi, CO_2 , 30 min., rt, HCl 6M, yield 72%; (f) *p*-HCOH, HCl , CH_3COOH , H_3PO_4 , 1,4-dioxane, 3 days, reflux, 45%; (g) $(\text{EtO})_3\text{P}$, 12h reflux; (h) TMSBr, 24h rt, then MeOH yield 54%.

Compounds **1a** and **2a-c** give sharp ^1H NMR spectra in CD_3OD , showing that they do not aggregate in solution, and clearly reveal C_{4v} -symmetry common to tetrasubstituted *cone* calix[4]arenes. Unlike the analogous calix[4]arene **2a**, which is fixed in the *cone* conformation by the alkylation of the phenolic oxygens, compound **2d** could exist in solution in four different conformations (Figure 3.4). Nevertheless, the ^1H NMR spectrum of thiacalixarene **2d** in CD_3OD shows only a single peak for the aromatic protons most probably as averaged signal of rapid interconversion among the four conformers.

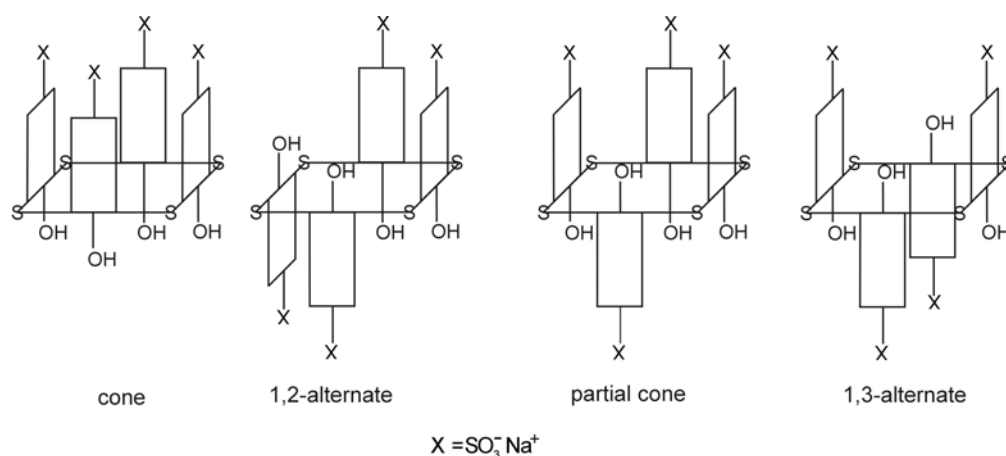


Figure 3.4. Schematic representation of the four conformations of thiacalix[4]arene **2d**.

3.2.2 Characterization of the molecular capsules **1a•2a-c**

^1H NMR spectroscopy. Isolation of the 1:1 complexes **1a•2a-c** was achieved by precipitation in water. While all the isolated building blocks are soluble, the mixtures of the two corresponding components were insoluble in water at room temperature. The white precipitates were filtered, washed with water, dried and re-dissolved in CD_3OD . Integration of the ^1H NMR resonances revealed in each case the 1:1 (or $n:n$) stoichiometry of the complexes. Interestingly, the proton signals of the amidinium propyl chains of compound **1a**, H_α , H_β and H_γ , shifted upfield upon assembly formation, (Figure 3.5 and Table 3.1). This upfield shift is probably due to (partial) self-inclusion of the propyl side chains of calix[4]arene **1a** in the interior of the cavity formed by the capsule **1a•2** (see Chapter 4). For assembly **1a•2a** only small changes were observed for all the other signals ($\Delta\delta < 0.1$ ppm) while for the assembly **1a•2b** downfield changes were observed also for the methylene bridge hydrogens ($\Delta\delta = 0.12$ ppm). Downfield shifts accompanied by

broadening were also detected for the first CH₂ group of the ethoxyethyl chains at the lower rim of **2b** ($\Delta\delta = 0.15$ ppm).

Assembly **1a•2c** shows only minor changes in the resonances of the propyl side chain protons (Table 3.1). Most likely the hindrance caused by the bulkier phosphate groups precludes the access of the propyl chain(s) to the cavity of the calix[4]arene **1a**. Nevertheless small changes are detectable for the signals of the aromatic protons and the methylene bridge hydrogens of **1c** ($\Delta\delta \sim 0.05$ ppm).

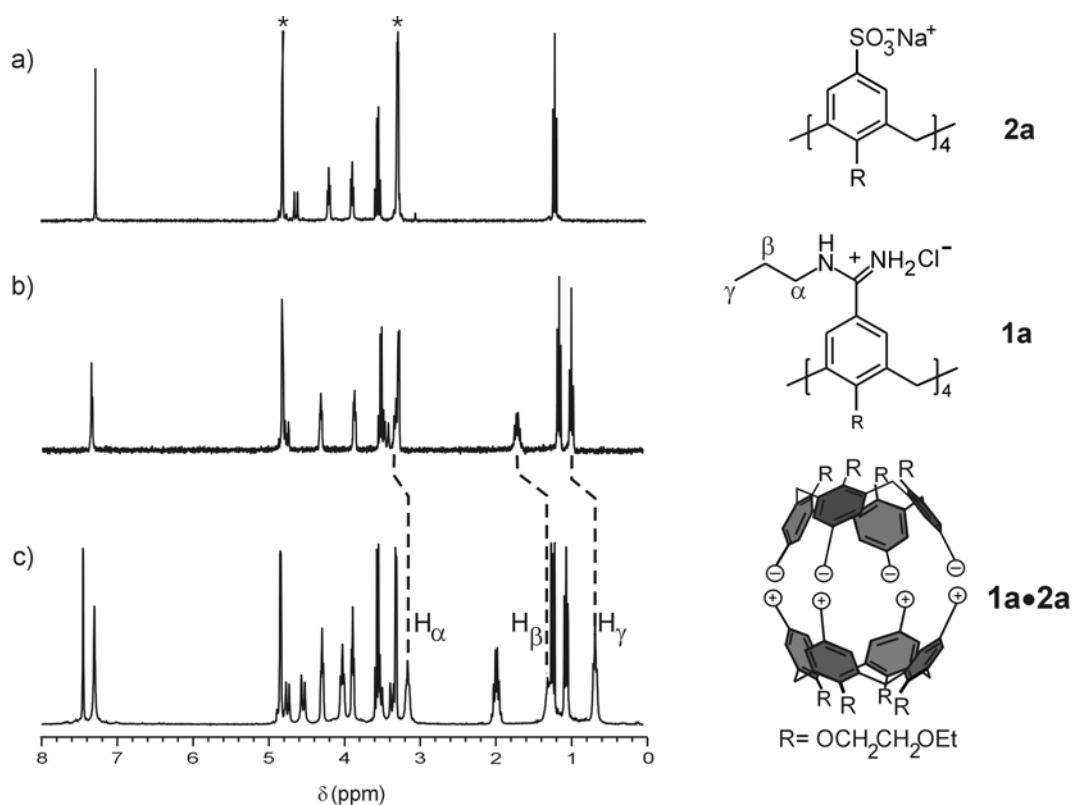


Figure 3.5. ¹H NMR spectra (CD₃OD, 298 K) of a) **2a**; b) **1a**; and c) capsule **1a•2a** obtained by precipitation upon mixing solutions of **1a** and **2a** in H₂O. Asterisks indicate solvent signals.

Table 3.1. ^1H NMR chemical shift changes for the protons of the propyl chain of **2a** upon formation of the complexes **1a•2a-d**, ($T = 298\text{K}$, CD_3OD). (For assignment of H_α , H_β and H_γ see Figure 3.5).

Assembly	$\Delta\delta_{\text{H}_\alpha}$	$\Delta\delta_{\text{H}_\beta}$	$\Delta\delta_{\text{H}_\gamma}$
1a•2a	0.23	0.53	0.33
1a•2b	0.13	0.16	0.25
1a•2c	-	0.03	0.04
1a•2d	0.46	0.45	0.32
1a•2d ^(a)	0.27	0.35	0.30

^(a) $\text{DMSO-}d_6$

ESI mass spectrometry. Formation of the complexes was also studied by electrospray mass spectrometry (ESI-MS). Equimolar solutions of the different assemblies were analyzed and in all cases the presence of a doubly charged peak for the capsule was observed. Peaks for the isolated building blocks were also detected.

The spectrum of an equimolar solution of **1a** and **2a** in MeOH shows the doubly charged signals of the capsule at m/z 1064.8 corresponding to $[(\mathbf{1a}\cdot\mathbf{2a})+2\text{Na}]^{2+}$. A peak at m/z 717.5 for $[(\mathbf{1a}\cdot\mathbf{2a})+3\text{Na}]^{3+}$ is also present. The spectrum of an equimolar solution of **1a** and **2b** in MeOH shows the doubly charged signals of the capsule at m/z 969.7 and m/z 987.8 corresponding to $[(\mathbf{1a}\cdot\mathbf{2b})+2\text{H}]^{2+}$ and $[(\mathbf{1a}\cdot\mathbf{2b})+\text{H}+\text{Na}]^{2+}$ respectively, together with a peak at m/z 1049.5 for $[\mathbf{1a}-4\text{HCl}+\text{H}]^+$ and two peaks at 911.2 and 933.8 for $[\mathbf{2b}-3\text{Na}+4\text{H}]^+$ and $[\mathbf{2b}-2\text{Na}+3\text{H}]^+$ respectively (Figure 3.6).

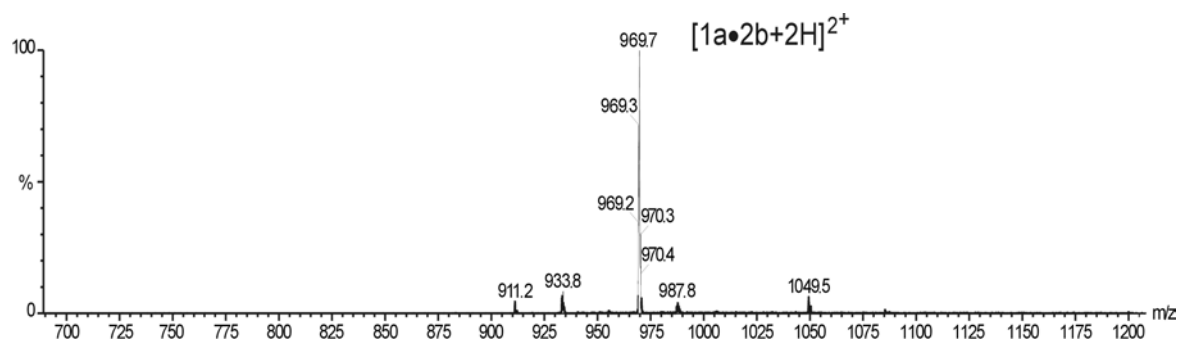


Figure 3.6. ESI-MS spectrum for assembly of **1a•2b**.

Analogously, the measured ESI-MS spectrum of an equimolar solution of **1a** and **2c** in MeOH shows the $[(\mathbf{1a}\cdot\mathbf{2c})+\text{Na}+\text{H}]^{2+}$ and $[(\mathbf{1a}\cdot\mathbf{2c})+2\text{Na}]^{2+}$ ions at m/z 1079.5 and m/z 1090.5 together with signals at m/z 1049 and 911.3 for $[\mathbf{1a}\cdot 4\text{HCl}+\text{H}]^+$ and $[\mathbf{2c}\cdot 3\text{Na}+4\text{H}]^+$, respectively.

Isothermal titration calorimetry (ITC). was used to study the thermodynamics of association between **1a** and **2a-d**. This technique gives directly the association constant and moreover, allows the dissection of the free energy into its enthalpic and entropic components.

The titrations were carried out by adding aliquots of calix[4]arene tetraamidinium **1a** to a solution of calix[4]arenes **2a-d** at 298 K in MeOH/H₂O ($x_{\text{water}} = 0.4$) in the presence of either tetrabutylammonium perchlorate (Bu_4NClO_4 , $I = 0.01$ M) or borate buffer ($\text{Na}_2\text{B}_4\text{O}_7$, $I = 0.01$ M and $I = 0.03$ M).

The titration curves showed an inflection point around 1.0 equivalent of **1a** added, which confirms the formation of complexes with 1:1 stoichiometry (Figure 3.7). The titration data were fitted to a 1:1 binding model using a non-linear least squares fitting procedure. The corresponding association constants and thermodynamic parameters are listed in Table 3.2.

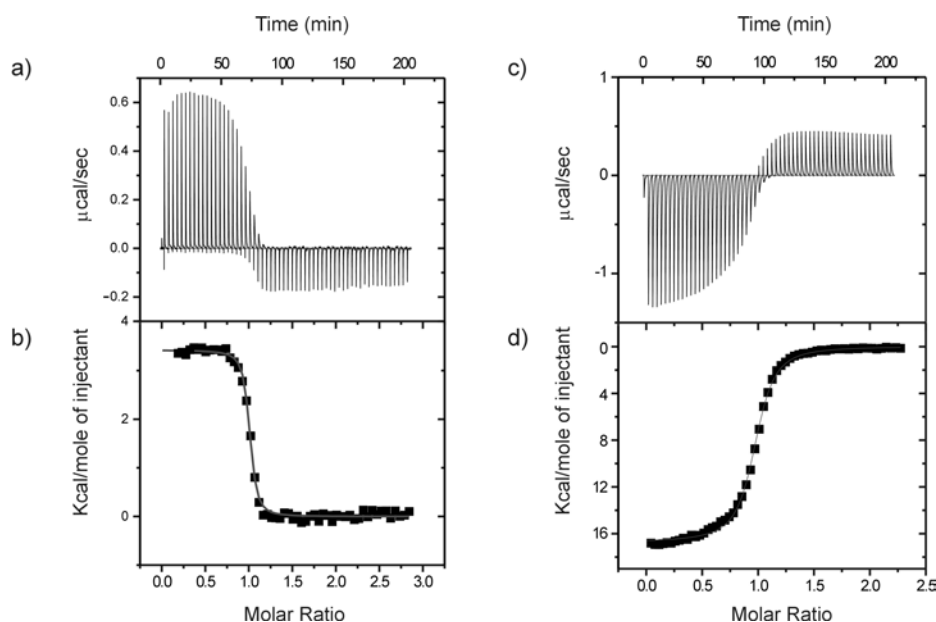


Figure 3.7. Calorimetric titration of **2a** (0.1 mM) with **1a** (1.0 mM) in MeOH/H₂O ($x_{\text{water}} = 0.4$) at 298 K in presence of Bu_4NClO_4 , $I = 0.01$ M (left), and $\text{Na}_2\text{B}_4\text{O}_7$, $I = 0.01$ M, pH=9.2 (right). a) and c) heat evolution per injection of **1a**; b) and d) resulting binding curve and best fit curve.

Table 3.2. Association constants and thermodynamic parameters for the formation of assemblies **1a•2a-d** as determined by ITC in MeOH/H₂O ($x_{\text{water}} = 0.4$) at 298 K.

Assembly	K_a (M ⁻¹)	ΔH° (kJ mol ⁻¹)	ΔS° (J K ⁻¹ mol ⁻¹)
1a•2a ^(a)	$(8.5 \pm 1.4) \times 10^6$	14.1 ± 0.1	180 ± 2
1a•2a ^(b)	$(1.2 \pm 0.1) \times 10^6$	-69.9 ± 0.2	-118 ± 1
1a•2a ^(c)	$(1.1 \pm 0.1) \times 10^5$	-58.2 ± 0.4	-98 ± 2
1a•2b ^(a)	$(8.6 \pm 1.9) \times 10^6$	17.1 ± 0.2	190 ± 2
1a•2b ^(b)	$(1.5 \pm 0.1) \times 10^6$	-57.9 ± 0.1	-76 ± 1
1a•2b ^(c)	$(1.8 \pm 0.1) \times 10^5$	-49.7 ± 0.4	-66 ± 2
1a•2c ^(a)	-	-	-
1a•2c ^(b)	$(4.5 \pm 0.2) \times 10^4$	-55.3 ± 0.1	-96 ± 1
1a•2c ^(c)	$(6.7 \pm 0.1) \times 10^3$	-40.9 ± 0.3	-63 ± 1
1a•2d ^(a)	$(1.0 \pm 0.1) \times 10^7$	25.9 ± 0.1	221 ± 1

^{a)} Background electrolyte: 1×10^{-2} M Bu₄NClO₄ ($I = 0.01$); ^{b)} background electrolyte: 0.33×10^{-2} M Na₂B₄O₇ ($I = 0.01$, pH=9.2); ^{c)} background electrolyte: 1×10^{-2} M Na₂B₄O₇ ($I = 0.03$, pH=9.2).

In the presence of 1×10^{-2} M ($I = 0.01$ M) of Bu₄NClO₄ as background electrolyte, association constants on the order of 10^6 M⁻¹ for **1a•2a** and **1a•2b** were determined. The association process is strongly driven by entropy, most likely due to the release of highly ordered solvent molecules into the bulk solvent. The positive values obtained for the enthalpies are ascribed to the energy needed to desolvate the charged groups, which overrides the negative enthalpic contribution due to the formation of the assemblies.⁵⁷⁻⁶⁰ These results are in agreement with the binding of dicarboxylate to diamidinium receptors in methanol reported by Diederich.⁵⁹

The binding curve obtained for assembly **1a•2c** displayed only a very small endothermic effect that precluded accurate curve fitting. This was attributed to possible intramolecular interactions between the phosphate groups of **2c**. These interactions could compete with the assembly of the molecular capsule. An ITC experiment for assemblies **1a•2c** was performed in the presence of borate buffer (Na₂B₄O₇). The measurements were performed at two different concentrations of borate buffer ($c = 1 \times 10^{-2}$ M and $c = 0.33 \times 10^{-2}$ M), leading to ionic strengths of $I = 0.03$ M and $I = 0.01$ M respectively. For

comparison, the titrations of **1a** with **2a**, and **1a** with **2b** were also studied under the same conditions, i.e. using the borate salt as background electrolyte.

A number of general observations can be made from these data. Compared to **1a•2a** and **1a•2b**, assembly **1a•2c** shows the lower association constants ($K_a = 4.5 \times 10^4 \text{ M}^{-1}$ or $K_a = 6.7 \times 10^3 \text{ M}^{-1}$, Table 3.2). This is most probably the result of a lower degree of preorganization of **2c** due to the freedom of rotation around the C-P bond. A working hypothesis is that the formation of the capsule causes a reduction in this torsional entropy which overrides the gain in entropy, which is determined by the desolvation of the charged groups as reflected in the negative values for the ΔS° .⁶¹

The enthalpograms for titrations performed in the presence of the two different background electrolytes (Bu_4NClO_4 vs borate buffer) but at the same ionic strength ($I = 0.01 \text{ M}$) show opposite signs of the heat effects, which indicate a change in thermodynamics of association. Going from Bu_4NClO_4 to borate buffer the overall process occurring in solution changes from endothermic and entropy driven to exothermic and enthalpy driven with the overall curve showing a negative contribution both from the ΔH° and ΔS° (Figure 3.7). It is well known that the heat effect varies depending on the particular electrolyte employed. Different solvation modes of the charged moieties are of importance for the differences in the thermodynamics of binding.⁶²

More interesting is to notice how the heat effect varies depending on the specific electrolyte concentration in solution.⁶³ The association constant decreases on increasing the ionic strength. For example, for assembly **1a•2a** the K_a goes from $1.2 \times 10^6 \text{ M}^{-1}$ at $I = 0.01 \text{ M}$ to $K_a = 1.1 \times 10^5 \text{ M}^{-1}$ at $I = 0.03 \text{ M}$. This can be rationalized taking into account two aspects *viz.* the strength of the electrostatic interactions and the degree of solvation of the charged groups. Increasing the ionic strength in general weakens the electrostatic interactions. When a higher concentration of salt is present in solution, the Coulombic attractive forces between the two building blocks are considerably shielded and the binding is weakened. This is reflected in a less negative value of the ΔH° . Moreover, higher concentration of salt results in a less ordered solvent shell around the ionic groups meaning that, when the desolvation process occurs, a lower gain in entropy is observed. This is reflected in a less negative value for the ΔS° . Although the observed K_a decreases by increasing the salt concentration, a change in the mode of binding is not expected as no change in the stoichiometry of interaction was observed.

3.2.3 Studies on the self-assembly of **1a•2d**

Capsule formation with the larger and less preorganized building block **2d** has also been investigated. As suggested by molecular modeling studies, the four sulfur atoms in thiacalix[4]arene **2d** provide an enlargement of the skeleton of the calix[4]arene scaffold and therefore of the resulting capsule (Figure 3.8). Unlike the analogous calix[4]arene **2a**, compound **2d** is not fixed in the *cone* conformation and therefore the aromatic rings are free to rotate, giving rise to a number of different conformers (Figure 3.4).

The solid state structure of **1a•2d** shows a 1:1 three-dimensional network in which **2d** adopts a *1,2-alternate* conformation. However, in solution ¹H NMR, 2D NMR and ITC studies show evidence for the formation of a 1:1 complex. By comparison with the results obtained for **1a•2a**, in solution, a discrete assembly is very likely.

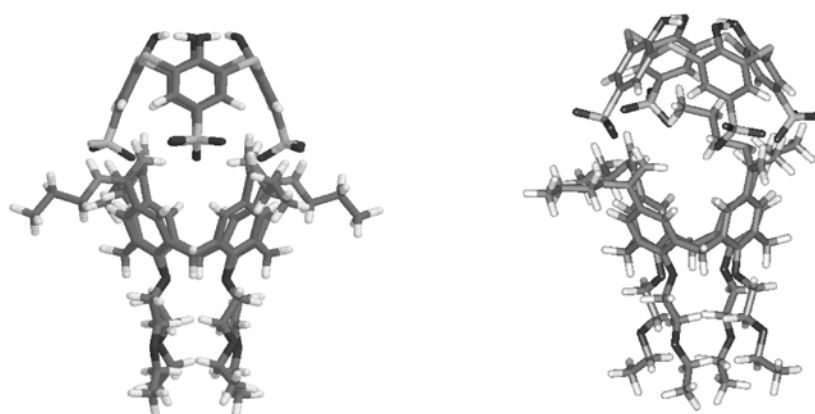


Figure 3.8. Molecular simulation (CHARMm 24.0) of assembly **1a•2d** assuming a *cone* conformation for thiacalix[4]arene **2d**. The alkyl chains are pointing outside (left); one of the alkyl side chains is included in the cavity of the capsule (right).

X-ray crystallography. Crystallization of assembly **1a•2d** in DMSO/MeOH provided single crystals suitable for X-ray diffraction studies. In the solid state **1a** and **2d** form an infinite three-dimensional network (Figure 3.9). The unit cell contains, beside **1a** and **2d** in 1:1 ratio, also nine molecules of DMSO, one molecule of water and a region of disordered solvent molecules. Thiacalix[4]arene **2d** adopts a *1,2-alternate* conformation, thus presenting two adjacent sulfonate moieties on each side of the plane. Calix[4]arene **1a** adopts instead a *pinched-cone* conformation in which the two opposite aromatic rings are bent inwards and the other two aromatic rings are forced to bend outwards. A very

complicated structure is formed where hydrogen bonding interactions are formed either between the two building blocks or between one of the building block and solvent molecules. Figure 3.10a depicts one type of interaction where two opposite amidinium groups of **1a** form hydrogen bonds to one of the sulfonate group of the thiacalix[4]arene **2d**. Figure 3.10b shows hydrogen bonds between two adjacent amidinium groups of **1a** and two sulfonate moieties of **2d**. Interestingly, the *1,2-alternate* conformation in **2d** is stabilized by intramolecular hydrogen bonds between the hydroxyl groups and the sulfur atoms of **2d** (Figure 3.10b).

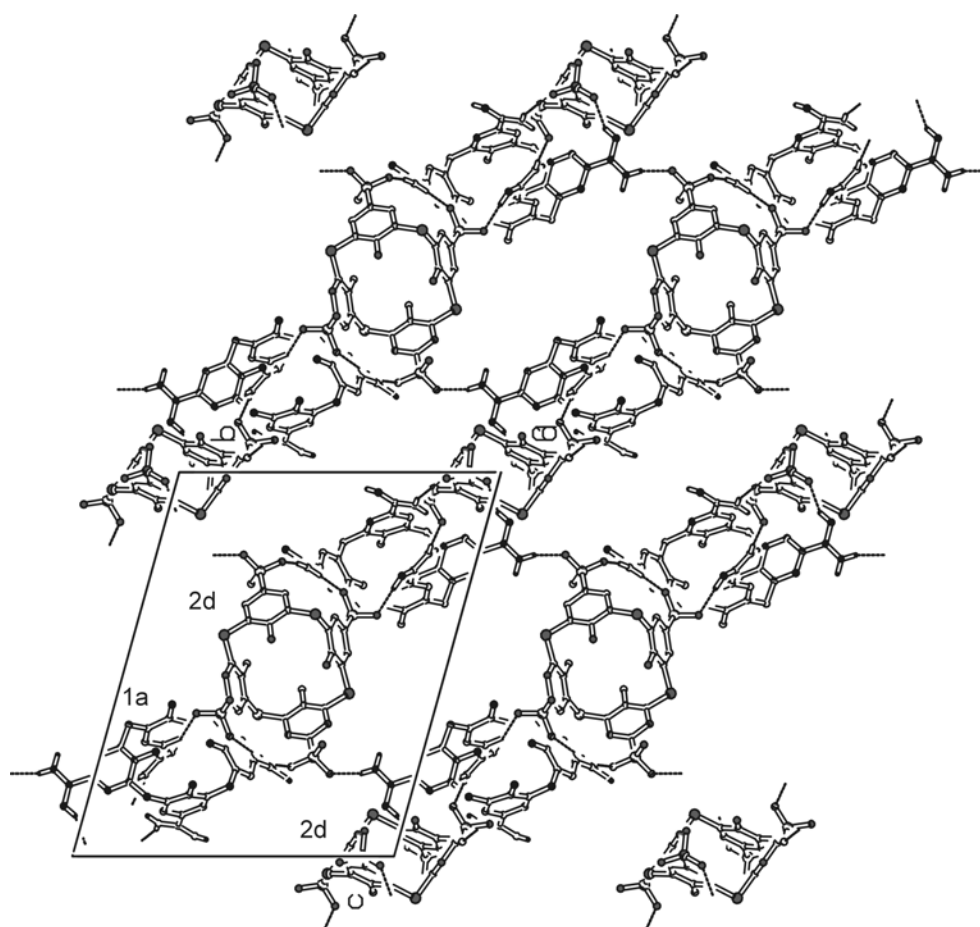
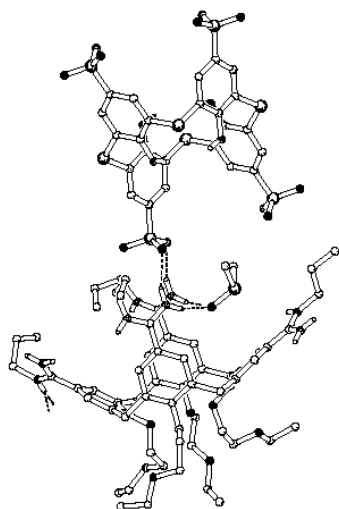


Figure 3.9. Packing diagrams of the three dimensional network viewed along the a axis of **1a•2d**. Solvent molecules, alkyl and alkoxy side chains have been omitted for clarity

a)



b)

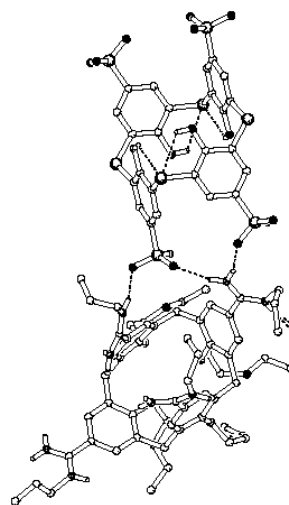


Figure 3.10. Hydrogen bonding interactions between calixarene **1a** and thiacalix[4]arene **2d**.

¹H NMR spectroscopy. As reported for the previous systems, upon addition of **1a** to **2d** in water a precipitate was obtained. ¹H NMR of the solid redissolved in CD₃OD indicates the formation of an equimolar assembly. Upfield shifts in the resonances of the protons of the amidinium chains ($\Delta\delta_{\text{H}\alpha} = 0.46$ ppm, $\Delta\delta_{\text{H}\beta} = 0.45$ ppm, $\Delta\delta_{\text{H}\gamma} = 0.32$ ppm see Table 3.1) and of the aromatic protons ($\Delta\delta_{(1a)} = 0.23$ ppm, $\Delta\delta_{(2d)} = 0.11$ ppm) were observed. Furthermore, analysis of the assembly **1a•2d** by 2D NMR revealed NOE connectivities between the aromatic protons of **2d** and the protons of the propyl amidinium chain of **1a**. In analogy to what was observed for assembly **1a•2a**, this finding would indicate the inclusion of the propyl chain of **1a** in the aromatic zone of **2d**.

According to the X-ray structure, in the solid state compound **2d** in **1a•2d** adopts a *1,2-alternate* conformation. If the same conformation would exist in solution, two singlets for the aromatic protons of **2d** are expected while, for symmetry reasons, one singlet is expected for the *cone* and the *1,3-alternate* conformations. In CD₃OD solution at 25 °C, the ¹H NMR spectrum of **1a•2d** shows a single resonance for the aromatic protons of **2d** which would account for either a symmetrical conformer (as above mentioned either the *cone* or the *1,3-alternate*), or an average among different conformers which are rapidly interconverting (Figure 3.4). Temperature-dependent ¹H NMR spectra of **1a•2d** were

recorded in CD₃OD. At -50 °C a singlet for the aromatic protons was still observed while further decrease in the temperature resulted in the precipitation of the thiacalix[4]arene **2d**. This result indicates that if different conformers are present at 25 °C, at -50 °C the flexibility of **2d** is still too high for the individual conformers to be revealed by NMR spectroscopy.

To study the effect of the concentration on the self-assembly of **1a** and **2d**, ¹H NMR studies in DMSO-*d*₆, where better solubility of the complex is observed, were performed. The ¹H NMR spectrum of a 20 mM solution of **1a•2d** in DMSO-*d*₆ showed no shifts in the propyl chains of the amidinium groups and only small upfield changes for the -NH signals of **1a** (Figure 3.11b).

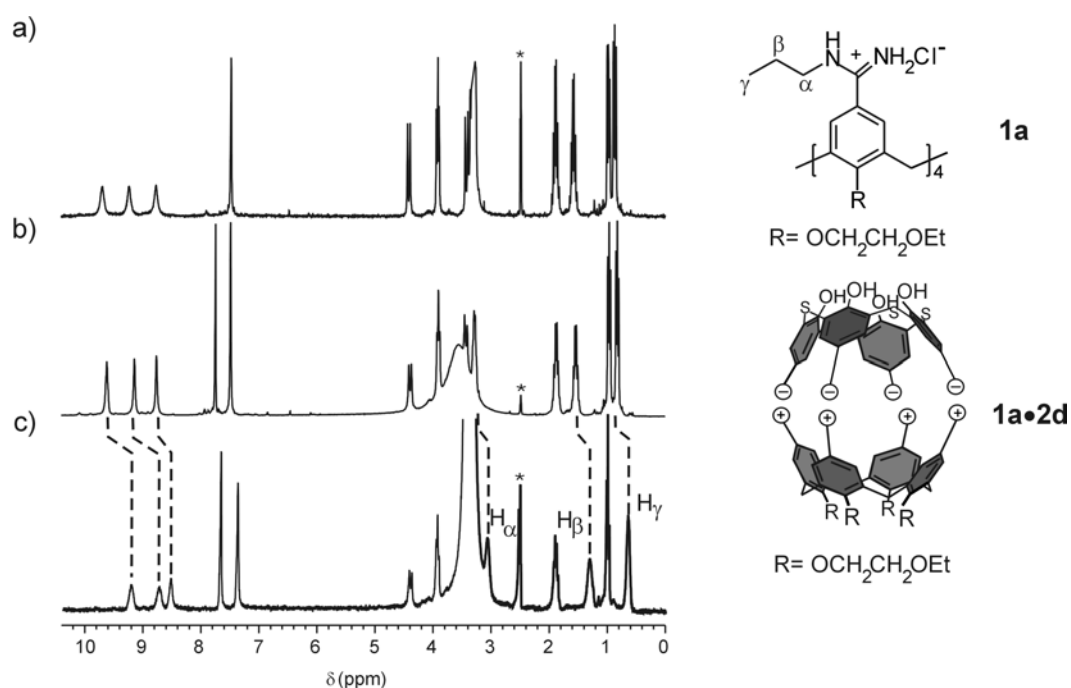


Figure 3.11. ¹H NMR spectra (DMSO-*d*₆, 298 K) of a) **1a**; b) **1a•2d** (c = 20mM), and c) **1a•2d** (c = 1mM). Asterisks indicate solvent signals.

At a much lower concentration of 1 mM, a DMSO-*d*₆ solution of **1a•2d** showed a different spectrum, which is analogous to the one observed in CD₃OD at the same concentration. The signals of the protons of the propyl side chain of **1a** were all upfield shifted (Figure 3.11 and Table 3.1). Furthermore, significant upfield shifts were also observed for the -NH signals of **1a** (upfield shifts, $\Delta\delta = 0.62, 0.64, 0.30$ ppm). These results show that the concentration affects somehow the geometry of the assembly. The

structure obtained in the solid state is likely to exist also in concentrated solutions of the two building blocks while at lower concentration (1 mM) a well-defined complex is most probably formed. Assuming that at 1 mM concentration a 1:1 complex is present in solution, the ^1H NMR does not allow discrimination between the different possible conformations of **2d**.

Mass spectrometry. A 0.5 mM solution of **1a•2d** in MeOH was analyzed by ESI-MS. The spectrum shows a peak at m/z 955.4 corresponding to $[(\mathbf{1a}\cdot\mathbf{2d})+2\text{Na}]^{2+}$. The FAB-MS spectrum shows the presence of a peak at 1865.9 corresponding to the $[(\mathbf{1a}\cdot\mathbf{2d})+\text{H}]^+$. The same results were obtained from the ESI-MS and FAB-MS of a 1 mM and 20 mM solution of **1a•2d** in DMSO. No evidence for high m/z aggregates was observed. In agreement with the results obtained using ESI-MS and FAB-MS, the MALDI-TOF spectrum of a 20 mM solution of **1a•2d** in DMSO shows only the presence of the expected 1:1 complex.

ITC. As in the case of assembly **1a•2a**, ITC measurements were carried out in MeOH/H₂O ($x_{\text{water}} = 0.4$) in the presence of BuN₄ClO₄ as background electrolyte. The data reported in Table 3.1 show that the formation of capsule **1a•2d** is an endothermic and entropy driven process. Since the interaction between sulfonate and amidinium groups should be similar for calix[4]arene **2a** and thiacalix[4]arene **2d**, the more positive values observed for both ΔH° and ΔS° must be the result of a higher degree of solvation of the larger **2d**.

The studies reported indicate that the flexible thiacalix[4]arene **2d** can reversibly self-assemble to give a well-defined receptor cavity **1a•2d** where one of the possible conformations is blocked.⁶⁴

Although based on solution studies it is not possible to reach a conclusion whether **2d** in the complex **1a•2d** adopts a *cone* or a *1,3-alternate* conformation, the ^1H NMR upfield shifts and NOE connectivities observed for the protons of the alkyl side chain of **1a** upon complex formation, which are similar to the ones found for the analogous assembly **1a•2a**, would account for a molecular capsule where the thiacalix[4]arene is in the *cone* conformation (Figure 3.8).⁶⁵

In addition, density functional theory calculations for the structure and conformational equilibrium of thiacalix[4]arene⁶⁶ have shown that the most stable conformer of thiacalix[4]arene is the *cone* which is stabilized by a cyclic array of hydrogen bonding at the lower rim, thus validating the structure proposed in Figure 3.8.

3.3 Conclusions

The results presented in this chapter demonstrate that multiple ionic interactions represent a valid tool for the synthesis of molecular containers in polar solvents.

Evidence for the formation of the 1:1 calix[4]arene-based molecular capsules **1•2a-d** was provided by a combination of different techniques like ¹H NMR, ESI-MS and ITC. The strength of the ionic interactions allows the molecular complexes to form in a highly polar solvent (MeOH/H₂O) and in the presence of a high excess of electrolytes (Bu₄NClO₄ and borate buffer).

The concept for the design of molecular capsules based on preorganized calix[4]arene scaffolds functionalized with oppositely charged groups introduced in this chapter will be further elaborated in the following chapters.

3.4 Experimental section

3.4.1 General information and instrumentation

The reagents used were purchased from Aldrich or Acros Chimica and used without further purification. All the reactions were performed under nitrogen atmosphere. Analytical thin layer chromatography was performed using Merck 60 F₂₅₄ silica gel plates. Column chromatography was carried out on Merck silica gel 60 (230-400 mesh) and reverse phase chromatography on Silica RP-18. Ion exchange chromatography was carried out on DOWEX 1-X8, 50-100 mesh, Cl-form. ¹H and ¹³C NMR spectra were recorded on a Varian Unity INOVA (300 MHz) or a Varian Unity 400 WB NMR spectrometer. ¹H NMR chemical shift values (300 MHz) are reported as δ in ppm using the residual solvent signal as an internal standard (CHD₂OD, δ = 3.30, DMSO-*d*₆, δ = 2.49). ¹³C NMR chemical shift values (100 MHz) are reported as δ in ppm using the residual solvent signal as an internal standard (CD₃OD, δ = 49.0, DMSO-*d*₆, δ = 39.7). Infrared spectra were recorded on a FT-IR Perkin Elmer Spectrum BX spectrometer and only characteristic

absorptions are reported. Fast atom bombardment (FAB) mass spectra were recorded with a Finnigan MAT 90 spectrometer. Electrospray ionization (ESI) mass spectra were recorded on a Micromass LCT time-of-flight (TOF) mass spectrometer. Samples were introduced using a nanospray source. Matrix-Assisted Laser Desorption Ionisation (MALDI) Time-of-Flight (TOF) mass spectra were recorded using a Perkin Elmer/PerSpective Biosystems Voyager-DE-RP MALDI-TOF mass spectrometer. Elemental analyses were carried out using a 1106 Carlo-Erba Strumentazione element analyzer. Compounds **3**⁶⁷, **4**⁶⁸, **5**⁶⁸ and **6**⁶⁹ were synthesized according to literature procedures.

3.4.2 Binding studies

Calorimetric measurements. The titration experiments were carried out using a Microcal VP-ITC microcalorimeter with a cell volume of 1.4115 mL. The formation of the assemblies **1a•2a-d** was studied by adding aliquots of a 1 mM solution of **1a** to a 0.1 mM solution of **2a-d**, in the calorimetric cell, and monitoring the heat change after each addition. Dilution effects were determined in a second experiment by adding the solution of **1a** into the solvent mixture and subtracting this contribution from the raw titration. The final curves were modeled using a 1:1 non-linear regression analysis. The fittings were done using Microcal Origin[®] software. Borate buffer was prepared by dissolving Na₂B₄O₇ × 10 H₂O in MeOH/H₂O (*x*_{water} = 0.4).

3.4.3 Synthesis

5,11,17,23-N-propyltetraamidinium-25,26,27,28-tetrakis(2-ethoxyethoxy)-calix[4]arene, tetrachloride salt (1a)

To a solution of Me₂AlCl (1.0 M in hexane; 20.6 mL, 20.6 mmol) at 0 °C under N₂, propylamine (1.69 mL, 20.6 mmol) in fluorobenzene (5 ml) were added dropwise. The mixture was stirred for 1h at 25 °C and then compound **5** (700 mg, 0.86 mmol) in fluorobenzene (5 mL) were added and the solution left under stirring for 1 hour at room temperature and then at 80 °C for 5 days. The reaction was monitored by TLC (silica, *n*-BuOH/CH₃COOH/H₂O 3:1:1). The mixture was cooled to 0 °C and quenched with ice and MeOH and the suspension filtered through a pad of Hyflo Super Cel[®]. The solid was

washed with CH₃OH and water and the filtrates were treated with an excess of 3N HCl and then concentrated *in vacuo*. The solid residue was submitted to preparative reverse phase chromatography using a step gradient EtOH/H₂O up to 40% (v/v) as the eluent. Ion exchange column chromatography (DOWEX 1-X8, 50-100 mesh, Cl-form) using H₂O as the eluent gave the corresponding chloride salt of **1a** as a white solid in 65% yield. ¹H NMR (CD₃OD): δ (ppm) 7.36 (s, 8H), 4.77 (d, 4H, $J=14.1$), 4.33 (t, 8H, $J=6.0$), 3.88 (t, 8H, $J=6.0$), 3.53 (q, 8H, $J=6.9$), 3.45 (d, 4H, $J=13.8$), 3.33 (t, 8H, $J=7.2$), 1.72 (m, 8H), 1.17 (t, 8H, $J=7.2$), 1.01 (t, 12H, $J=7.2$). ¹³C NMR (CD₃OD): δ (ppm) 162.43, 160.41, 135.05, 127.95, 122.38, 73.60, 68.95, 65.44, 43.60, 30.03, 20.21, 13.72, 9.63. IR (KBr) 2965, 1668, 1623, 1467, 1383, 1224, 998. MS (FAB): m/z 1049.7 [M-4HCl+H]⁺ (M⁺, calcd. 1049.67). Anal. calcd. for C₆₀H₉₂O₈N₈Cl₄·H₂O: C 59.40, H 7.81, N 9.24; found: C 59.27, H 7.76, N 9.13.

5,11,17,23-tetracarboxy-25,26,27,28-tetrakis(2-ethoxyethoxy)calix[4]arene, tetrasodium salt (2b)

tert-Butyllithium (1.7 M in pentane, 11.05 ml, 18.8 mmol) was added to a solution of **4** (2 g, 2.07 mmol) in dry THF (50 mL) under nitrogen at -78 °C. The reaction mixture was stirred at -78 °C for 45 min. After removal of the dewar, CO₂ gas, dried in conc. H₂SO₄, was bubbled through the solution for 1h. The reaction mixture was treated with 6 M HCl (20 mL). The solution was evaporated to dryness, and the solid was dissolved in ethanol (400 mL) and refluxed for 15 min. On gradually cooling down to room temperature a white precipitate appeared, which was filtered off and dried *in vacuo* over P₂O₅. Yield 70 %. ¹H NMR (DMSO-*d*₆): δ (ppm) 0.97 (t, 12 H, $J= 7.29$ Hz), 1.42 (m, 8H), 1.87 (m, 8H), 3.37(d, 4H, $J= 9.0$ Hz), 3.91 (t, 8H, $J= 4.9$ Hz), 4.32 (d, 4H, $J= 8.8$ Hz), 7.32 (s, 8H), 12.34 (s, 4H); ¹³C NMR (DMSO-*d*₆): δ (ppm) 14.18, 19.14, 30.37, 32.11, 75.11, 124.97, 130.01, 134.97, 160.21, 167.13. MS (FD): MS (FAB): m/z 886.8 [M-H]⁻ (M⁻, calcd. 887.3). Anal. calcd. for C₄₈H₅₆O₁₂: C 69.88, H 6.84; found C 70.13, H 6.83.

5,11,17,23-tetrakisphosphonomethyl-25,26,27,28-tetrakis(2-ethoxyethoxy)calix[4]arene (2c)

Compound **6** (200mg, 0.22mmol) was refluxed in triethylphosphite (3mL) for 24 h. After cooling unreacted triethyl phosphite was distilled under reduced pressure and the

residue dried under vacuum. Bromotrimethylsilane (TMSBr) (0.78 mL, 5.97 mmol) was added under nitrogen and the solution stirred overnight at room temperature. TMSBr was removed under vacuum. Methanol (10 mL) was added and the solvent was removed under reduced pressure. Addition of water gave a white precipitate that was filtered, washed with water and dried over P₂O₅. Yield: 54%. ¹H NMR (CD₃OD): δ(ppm) 6.65 (s, 8H), 4.49 (d, 4H, *J*=13.2), 4.07 (t, 8H, *J*=5.4), 3.88 (t, 8H, *J*=5.4), 3.57 (q, 8H, *J*=6.9), 3.1 (d, 4H, *J*=13.2), 2.8 (d, 2H, *J*=21.3) 1.21 (t, 12H, *J*=6.9). ¹³C NMR (CD₃OD): δ(ppm) 166.53, 162.80, 137.09, 129.80, 122.60, 75.44, 70.72, 67.17, 31.68, 15.39. IR (KBr) 3366, 1471, 1056, 976. MS (FD): *m/z* = 1088.32 [M+H]⁺ (M⁺, calcd. 1088.67).

3.5 References and notes

1. Cram, D. J.; Cram, J. M. *Container Molecules and Their Guests*; Royal Society of Chemistry: Cambridge, 1994.
2. Makeiff, D. A.; Pope, D. J.; Sherman, J. C. *J. Am. Chem. Soc.* **2000**, *122*, 1337-1342.
3. MacGillivray, L. R.; Atwood, J. L. *Angew. Chem. Int. Ed.* **1999**, *38*, 1018-1033.
4. Chapman, R.; Sherman, J. C. *J. Am. Chem. Soc.* **1995**, *117*, 9081-9082.
5. Nakamura, K.; Sheu, C.; Keating, A. E.; Houk, K. N. *J. Am. Chem. Soc.* **1997**, *119*, 4321-4322.
6. Warmuth, R.; Yoon, J. *Acc. Chem. Res.* **2001**, *34*, 95-105.
7. Jasat, A.; Sherman, J. C. *Chem. Rev.* **1999**, *99*, 931-965.
8. Rebek, J. Jr. *Acc. Chem. Res.* **1999**, *32*, 278-286.
9. Rebek, J. Jr. *Chem. Commun.* **2000**, 637-643.
10. O'Leary, B. M.; Szabo, T.; Svenstrup, N.; Schalley, C. A.; Lützen, A.; Schöpfer, M.; Rebek, J. Jr. *J. Am. Chem. Soc.* **2001**, *123*, 11519-11533.
11. Meissner, R.; Rebek, J. Jr.; de Mendoza, J. *Science* **1995**, *270*, 1485-1488.
12. Mogck, O.; Pons, M.; Böhmer, V.; Vogt, W. *J. Am. Chem. Soc.* **1997**, *119*, 5706-

5712.

13. Rincon, A. M.; Prados, P.; de Mendoza, J. *J. Am. Chem. Soc.* **2001**, *123*, 3493-3498.
14. Vysotsky, M. O.; Böhmer, V. *Org. Lett.* **2000**, *2*, 3571-3574.
15. Vysotsky, M. O.; Thondorf, I.; Böhmer, V. *Angew. Chem. Int. Ed.* **2000**, *39*, 1264-1267.
16. Branda, N.; Grotzfeld, R. M.; Valdes, C.; Rebek, J. Jr. *J. Am. Chem. Soc.* **1995**, *117*, 85-88.
17. Körner, S. K.; Tucci, F. C.; Rudkevich, D. M.; Heinz, T.; Rebek, J. Jr. *Chem. Eur. J.* **2000**, *6*, 187-195.
18. Heins, T.; Rudkevich, D. M.; Rebek, J. Jr. *Nature* **1998**, *394*, 764-766.
19. Chapman, R. G.; Olovsson, G.; Trotter, J.; Sherman, J. C. *J. Am. Chem. Soc.* **1998**, *120*, 6252-6260.
20. Vysotsky, M. O.; Pop, A.; Broda, F.; Thondorf, I.; Böhmer, V. *Chem. Eur. J.* **2001**, *7*, 4403-4410.
21. Kobayashi, K.; Shirasaka, T.; Yamaguchi, K.; Sakamoto, S.; Horn, E.; Furukawa, N. *Chem. Commun.* **2000**, 41-42.
22. González, J. J.; Ferdani, R.; Albertini, E.; Blasco, J. M.; Arduini, A.; Pochini, A.; Prados, P.; de Mendoza, J. *Chem. Eur. J.* **2000**, *6*, 73-80.
23. van Wageningen, A. M. A.; Timmerman, P.; van Duynhoven, J. P. M.; Verboom, W.; van Veggel, F. C. J. M.; Reinhoudt, D. N. *Chem. Eur. J.* **1997**, *3*, 639-654.
24. MacGillivray, L. R.; Atwood, J. L. *Nature* **1997**, *389*, 469-472.
25. Atwood, L.; Barbour, L. J.; Jerga, A. *Chem. Commun.* **2001**, 2376-2377.
26. Shivanyuk, A.; Rebek, J. Jr. *Chem. Commun.* **2001**, 2374-2375.
27. Vysotsky, M. O.; Thondorf, I.; Böhmer, V. *Chem. Commun.* **2001**, 1890-1891.

28. Takeda, N.; Umemoto, K.; Yamaguchi, K.; Fujita, M. *Nature* **1999**, *398*, 794-799.
29. Zhong, Z.; Ikeda, H.; Ayabe, M.; Shinkai, S.; Sakamoto, S.; Yamaguchi, K. *J. Org. Chem.* **2001**, *66*, 1002-1008.
30. Chand, D. K.; Biradha, K.; Fujita, M. *Chem. Commun.* **2001**, 1652-1653.
31. Park, S. J.; In-Hong, J. *Chem. Commun.* **2001**, 1554-1555.
32. Umemoto, K.; Tsukui, H.; Kusukawa, T.; Biradha, K.; Fujita, M. *Angew. Chem. Int. Ed.* **2001**, *40*, 2620-2622.
33. Ikeda, A.; Udzu, H.; Zhong, Z.; Shinkai, S.; Sakamoto, S.; Yamaguchi, K. *J. Am. Chem. Soc.* **2001**, *123*, 3872-3877.
34. Dalcanale, E.; Jacopozzi, P. *Angew. Chem. Int. Ed. Engl.* **1997**, *36*, 613-615.
35. Fochi, F.; Wegelius, E.; Rissanen, K.; Cozzini, P.; Marastoni, E.; Fisticaro, E.; Mannini, P.; Fokkens, R.; Dalcanale, E. *J. Am. Chem. Soc.* **2001**, *123*, 7539-7552.
36. Fujita, M.; Umemoto, K.; Yoshizawa, M.; Fujita, N.; Kusukawa, T.; Biradha, K. *Chem. Commun.* **2001**, 509-518.
37. Fujita, M.; Nagao, S.; Iida, M.; Ogata, K.; Ogura, K. *J. Am. Chem. Soc.* **1993**, *115*, 1574-1576.
38. Fox, O. D.; Dalley, N. K.; Harrison, R. G. *Angew. Chem. Int. Ed.* **1998**, *120*, 7111-7112.
39. Fox, O. D.; Leung, J. F. Y.; Hunter, J. M.; Dalley, N. K.; Harrison, R. G. *Inorg. Chem.* **2000**, *39*, 783-790.
40. Bok Lee, S.; Hong, J.-I. *Tetrahedron Lett.* **1998**, *39*, 4317-4320.
41. Fujita, M.; Oguro, D.; Miyazawa, M.; Oka, I.; Yamaguchi, K.; Ogura, K. *Nature* **1995**, *378*, 469-471.
42. Lücking, U.; Chen, J.; Rudkevich, D. M.; Rebek, J. Jr. *J. Am. Chem. Soc.* **2001**, *123*, 9925-9934.

43. Starnes, S. D.; Rudkevich, D. M.; Rebek, J. Jr. *J. Am. Chem. Soc.* **2001**, *123*, 4659-4669.
44. Bok Lee, S.; Hong, J. H. *Tetrahedron Lett.* **1996**, *37*, 8501-8504.
45. Hamilin, B.; Jullien, L.; Derouet, C.; Herve' du Penhoat, C.; Berthault, P. *J. Am. Chem. Soc.* **1998**, *120*, 8438-8447.
46. Grawe, T.; Schrader, T.; Gurrath, M.; Kraft, A.; Osterod, F. *Org. Lett.* **2000**, *2*, 29-32.
47. Grawe, T.; Schrader, T.; Gurrath, M.; Kraft, A.; Osterod, F. *J. Phys. Org. Chem.* **2000**, *13*, 670-673.
48. Kim, H.-J.; Sakamoto, S.; Yamaguchi, K.; Hong, J.-I. *Org. Lett.* **2003**, *5*, 1051-1054.
49. Fiammengo, R.; Timmerman, P.; de Jong, F.; Reinhoudt, D. N. *Chem. Commun.* **2000**, 2313-2314.
50. Zadmard, R.; Schrader, T.; Grawe, T.; Kraft, A. *Org. Lett.* **2002**, *4*, 1687-1690.
51. Zadmard, R.; Junkers, M.; Schrader, T.; Grawe, T.; Kraft, A. *J. Org. Chem.* **2003**, *68*, 6511-6521.
52. Harvey, P. D. *Coordin. Chem. Rev.* **2002**, *233*, 289-309.
53. Garipati, R. S. *Tetrahedron Lett.* **1990**, *31*, 1969-1972.
54. Sebo, L.; Diederich, F. *Helv. Chim. Acta* **2000**, *83*, 93-113.
55. Fiammengo, R.; Timmerman, P.; Huskens, J.; Versluis, K.; Heck, A. J. R.; Reinhoudt, D. N. *Tetrahedron* **2002**, *58*, 757-764.
56. Matsumiya, H.; Terazono, Y.; Iki, N.; Miyano, S. *J. Chem. Soc. Perkin., Trans. 2* **2002**, 1166-1172.
57. Berger, M.; Schmidtchen, F. P. *Angew. Chem. Int. Ed.* **1998**, *37*, 2694-2696.
58. Linton, B.; Hamilton, A. D. *Tetrahedron* **1999**, *19*, 6027-6038.

59. Sebo, L.; Schweizer, B.; Diederich, F. *Helv. Chim. Acta* **2000**, *83*, 80-92.
60. Salvatella, X.; Peczuh, M. W. G. M.; Jain, R. K.; Sanchez-Quesada, J.; de Mendoza, J.; Hamilton, A. D.; Giralt, E. *Chem. Commun.* **2000**, 1399-1400.
61. Hauser, S. L.; Johanson, E. W.; Green, H. P.; Smith, P. J. *Org. Lett.* **2000**, *2*, 3575-3578.
62. Arena, G.; Casnati, A.; Mirone, L.; Sciotto, D.; Ungaro, R. *Tetrahedron Lett.* **1997**, *38*, 1999-2002.
63. Berger, M.; Schmidtchen, F. P. *J. Am. Chem. Soc.* **1999**, *121*, 9986-9993.
64. Castellano, R. K.; Rudkevich, D. M.; Rebek, J. Jr. *J. Am. Chem. Soc.* **1996**, *118*, 10002-10003.
65. Arduini, A.; Domiani, L.; Ogliosi, L.; Pochini, A.; Secchi, A.; Ungaro, R. *J. Org. Chem.* **1997**, *62*, 7866-7868.
66. Bernardino, R. J.; Costa-Cabral, B. J. *J. Mol. Struct. (Theochem)* **2001**, *549*, 253-260.
67. Arduini, A.; Casnati, A.; Fabbi, M.; Minari, P.; Pochini, A.; Sicuri, A. R.; Ungaro, R. *Supramol. Chem.* **1993**, *1*, 235-246.
68. Pinkhassik, E.; Sidorov, V.; Stibor, I. *J. Org. Chem.* **1998**, *63*, 9644-9651.
69. Nagasaki, T.; Sisido, K.; Arimura, T.; Shinkai, S. *Tetrahedron* **1992**, *48*, 797-804.

DETAILED STUDY OF THE GEOMETRY AND THE GUEST ENCAPSULATION PROPERTIES OF AN AMIDINIUM- SULFONATE CALIX[4]ARENE BASED CAPSULE IN METHANOL*

*In Chapter 3 it was demonstrated that simple ionic interactions represent an alternative to hydrogen bonds and metal-ligand coordination for the synthesis of noncovalent supramolecular capsules stable in polar organic solvents. Upon formation of assembly **1a•2a** ¹H NMR analysis gave indications for the inclusion of the propyl side chain of the tetraamidinium calix[4]arene **1a** in the capsule's cavity. To study the effect of the side chain length of **1a** on the formation of the molecular capsules, compounds **1b-e** bearing different amidinium substituents were synthesized. ¹H NMR and ITC studies showed that the side-chain length affects both the geometry and the stability of the resulting assemblies **1x•2a**. Molecular modeling and structural analysis by ¹H NMR spectroscopy provided a strong indication for the inclusion of the short side amidinium substituents (i.e. propyl or isopropyl) in the cavity of the capsule. Moreover, the X-ray structure of **1a•2a** confirmed the geometry proposed on the basis of solution studies. ¹H NMR, ITC, and ESI-MS were used to prove the encapsulation of tetramethylammonium, acetylcholine, and N-methylquinuclidinium cations in **1b•2a** in methanol solution.*

* Part of this chapter has been published in: Corbellini, F.; Fiammengo, R.; Timmerman, P.; Crego-Calama, M.; Versluis, K.; Heck, A. J. R.; Luyten, I.; Reinhoudt, D. N. *J. Am. Chem. Soc.* **2002**, *124*, 6569-6575.

4.1 Introduction

As described in Chapter 2, in the last decades the efforts in host-guest chemistry have focused on creating numerous examples of structurally defined container-like molecules held together by noncovalent interactions. A common feature of these three-dimensional dynamic structures is the presence of a well-defined cavity that can accommodate one or more guest molecules or ions.^{1,2}

The guest encapsulation phenomena are dictated by factors like size, shape and chemical surface complementarity. In the absence of additional intermolecular forces, recognition through encapsulation is determined by the host and guest volumes. Rebek established an empirical rule according to which single guests in solution fill typically 55% of the capsule's space.³ Nevertheless, when host and guest molecules are provided with additional functionalities, the 55% rule is not valid and the encapsulation is dependent on the nature of the intermolecular forces engaged in the binding process.

The possibility to constrain “molecule(s) within a molecule” offered examples of noncovalent supramolecular capsules used as reaction chambers in catalysis,⁴ as sensing devices,⁵ for the isolation of reactive species,⁶ and moreover to create new forms of isomerism.⁷⁻⁹ More interestingly, as a result of the noncovalent bonds that hold these capsules together, guest binding and guest release is a dynamic process, a feature that envisages applications like transport and delivery of guest molecules.

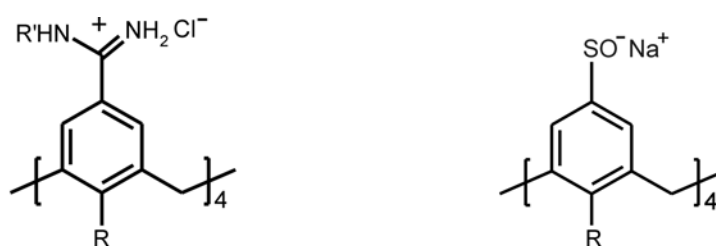
In Chapter 3 the formation of molecular capsules resulting from the self-assembly between either a tetrasulfonate calix[4]arene, a tetracarboxy or tetraphosphonomethyl calix[4]arene and a tetraamidinium calix[4]arene was described. Among these three different types of molecular capsules, the one based on sulfonate-amidinium interactions was determined the most practicable to undertake a detailed study on its geometry and furthermore to investigate the binding properties of these new molecular containers. The choice is essentially motivated by the fact that the tetrasulfonate calix[4]arene **2a** (Chart 4.1) is obtained very easily in good yield.

Moreover, as the formation of the molecular capsules does not depend on the length of the alkyl chains inserted at the bottom rim of the calixarenes, calix[4]arene **1b**, bearing propoxy chains, was preferred over **1a** where the longer ethoxyethoxy chains require more complicated purification (Chart 4.1).

As anticipated from Chapter 3, upon formation of the assemblies **1a•2a** an upfield shift of the proton signals of the propyl side chains of **1a** was observed in the ^1H NMR spectrum. The inclusion of one amidinium alkyl chain was proposed. To prove this hypothesis compounds **1c** and **1d** bearing differently substituted side chains are synthesized (Chart 4.1). In this chapter ^1H NMR studies are presented which show the influence of the amidinium side chain on the geometry of the molecular capsules. In particular, it is reported that while the propyl and isopropyl moieties in **1b** and **1c**, respectively, can be easily accommodated in the interior of the cavity, the longer heptyl chain resides outside the capsule's cavity. These findings are corroborated by X-ray analysis of **1a•2a**. Furthermore, encapsulation of cationic guest molecules like tetramethylammonium (TMA), acetylcholine (ACh) and *N*-methylquinuclidinium cations is reported in this chapter.

Finally, in view of our aim to achieve water soluble molecular capsules, unsubstituted tetraamidinium calix[4]arenes **1f** and **1g**, functionalized at the bottom rim with (poly-)ethylene glycol groups, are prepared. The formation of capsules **1f•2a** and **1g•2a** is studied by ITC in MeOH/H₂O. Preliminary studies with assembly **1g•2a**, having the longer ethylene glycol chains, show that assembly in pure H₂O is also possible.

Chart 4.1



1a	R= OCH ₂ CH ₂ OEt	R'=Pr
1b	R= OPr	R'=Pr
1c	R= OPr	R'=iso-Pr
1d	R= OPr	R'=n-heptyl
1e	R= OPr	R'=H
1f	R= OCH ₂ CH ₂ OEt	R'=H
1g	R= (OCH ₂ CH ₂) ₂ OMe	R'=H

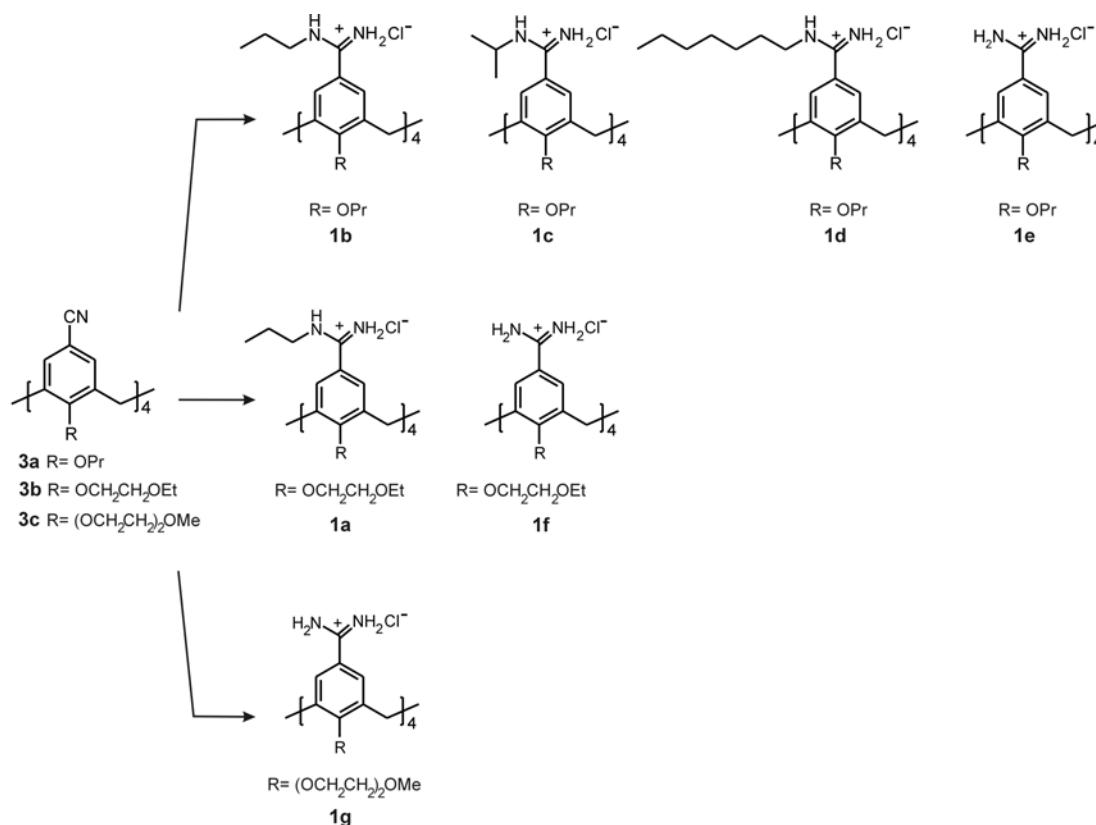
2a R= OCH₂CH₂OEt

4.2 Results and discussion

4.2.1 Synthesis

The syntheses of the calixarenes studied in this chapter are briefly summarized in Scheme 4.1. Calix[4]arenes **1b-d** were synthesized according to the procedure described in Chapter 3 for **1a**^{10,11} while compounds **1e-g** were obtained by reacting the chloroaluminium amide, generated from Me₃Al and ammoniumchloride with the corresponding tetracyano-calix[4]arene **3a-c**¹² in fluorobenzene. The chloride salts of the amidinium compounds were obtained after reverse phase chromatography and ion exchange chromatography in 40 to 60% yields. Compound **2a** was obtained as described in Chapter 3.

Scheme 4.1



Compounds **1a-g** and **2a** are soluble in water and methanol. ¹H NMR spectra in CD₃OD show sharp signals indicating no aggregation in solution. Furthermore, the spectra clearly revealed the C_{4v}-symmetry common to tetrasubstituted *cone* calix[4]arenes.

4.2.2 ^1H NMR studies on the formation of the molecular capsule **1b•2a**

As reported in Chapter 3 the upfield shifts for H_α , H_β and H_γ observed upon formation of the capsule **1a•2a** (see Figure 3.5) suggests that at least one of the propyl side chains is located inside the cavity where the anisotropic environment of the calix[4]arene aromatic rings leads to shielding of the chain protons. A similar behavior was found by Rebek in the dimeric capsule based on resorcinarenes.¹³

Examination of the molecular models (CHARMm 24.0), in which the calix[4]arene units **1b** and **2a** bind with their opposite charges facing each other, confirm that indeed the internal cavity of the complex is sufficiently large to accommodate one or two propyl side chains. However, with three or four propyl groups inside, the assembly becomes severely distorted (Figure 4.1).

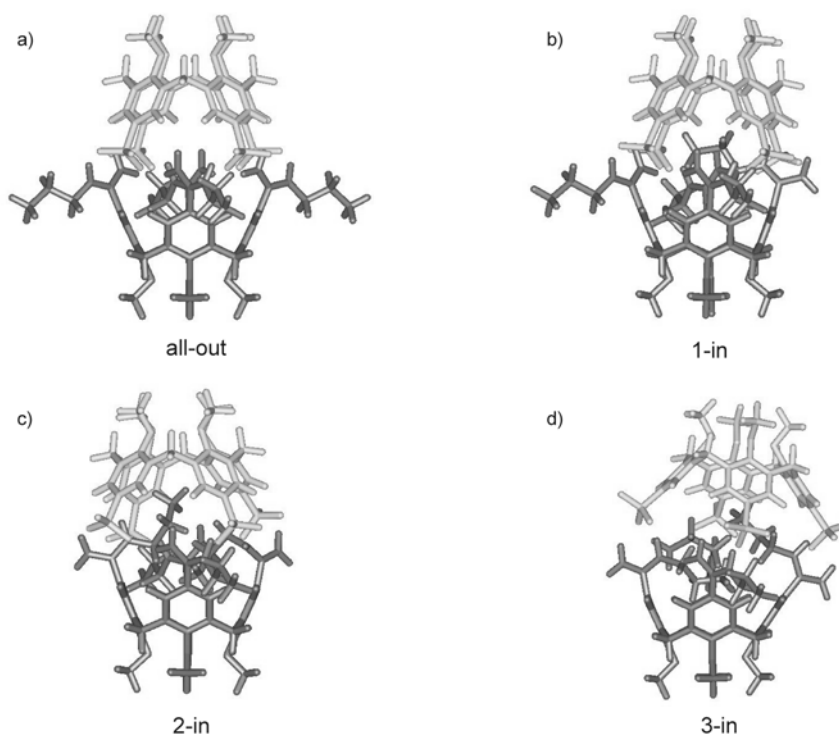


Figure 4.1. Molecular simulations (CHARMm 24.0) of assembly **1b•2a** (a) the alkyl side chains are pointing outside; (b) one or (c) two or (d) three of the alkyl side chains are included in the cavity of the capsule. (The propoxy alkyl chains at the bottom rim are omitted for clarity).

The ^1H NMR spectrum of an equimolar solution of **1b** and **2a** in CD_3OD shows that the protons of the propyl chains of **1b** are all upfield shifted ($\Delta\delta_{\text{H}\alpha} = 0.23$, $\Delta\delta_{\text{H}\beta} = 0.53$, $\Delta\delta_{\text{H}\gamma} = 0.33$) upon formation of the capsule **1b•2a** as a result of the inclusion of the alkyl chain(s) in the cavity of the assembly (Figure 4.2a).

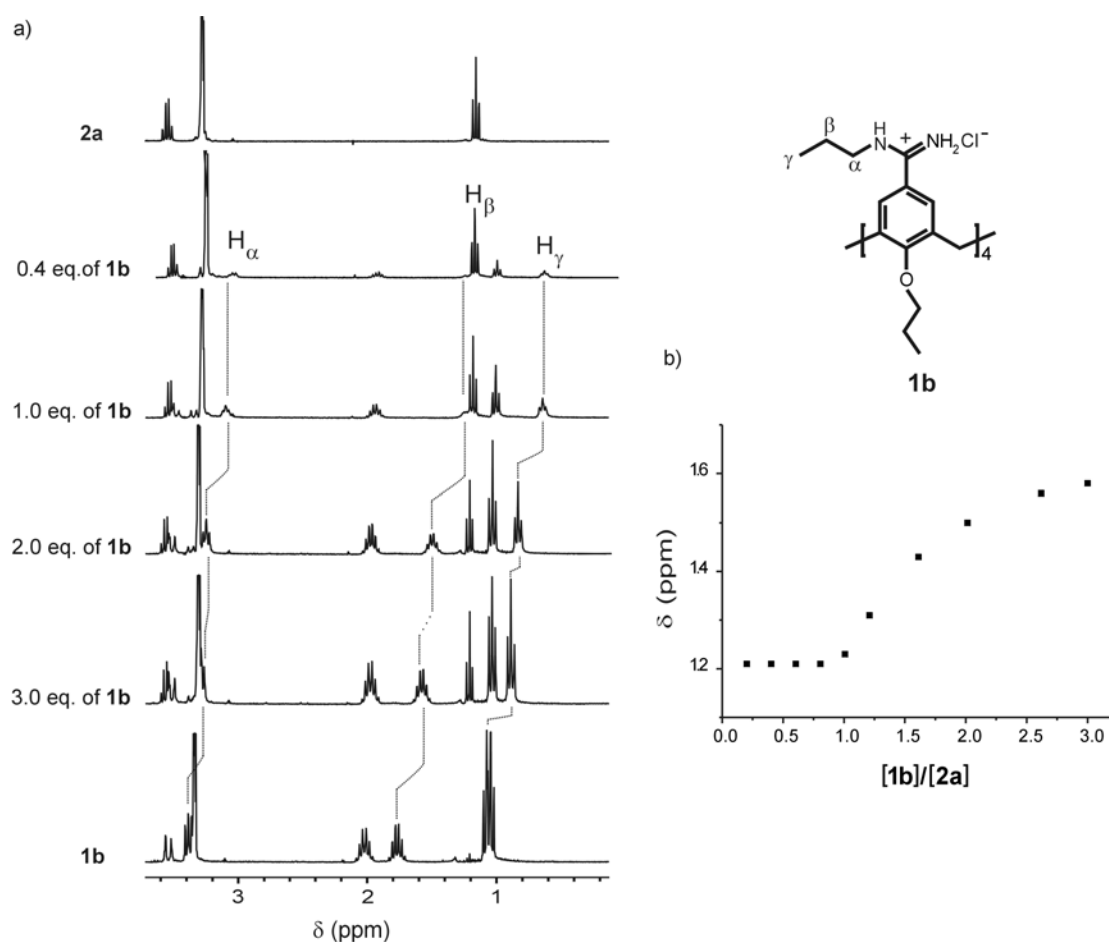


Figure 4.2. (a) ^1H NMR titration of **2a** with **1b** in CD_3OD at 298K. (b) Data points of the upfield shift of the H_β signals of the amidinium chains of **1b**.

Moreover, when D_2O (0-35%) was added to a 1.8 mM solution of **1b**•**2a** in CD_3OD the signals for H_β and H_γ shifted even further upfield ($\Delta\delta_{\text{H}\beta} = 0.07$ ppm, $\Delta\delta_{\text{H}\gamma} = 0.25$ ppm), whereas most of the other proton signals remained at their original positions ($\Delta\delta < 0.05$ ppm). This is in good agreement with the assumption that the cavity inside the capsule **1b**•**2a** provides a hydrophobic environment.

The chemical shift changes for the protons of the propyl side chains were followed by a ^1H NMR titration in CD_3OD (Figure 4.2). For solubility reasons the titration was performed by adding compound **1b** to **2a**. When less than 1 equiv. of **1b** was added the chemical shifts of H_α - H_γ were almost constant and independent of the amount of **1b**, indicating that the calixarene tetraamidinium **1b** is present mainly as the complex **1b**•**2a** and suggesting that the complex is very stable. Beyond the 1:1 ratio, the δ for H_α - H_γ shifts downfield representing time-averaged values for the free

and complexed **1b**. This indicates that the exchange between free and complexed **1b** is fast on the NMR time scale.

A variable temperature (VT) NMR experiment showed that the exchange process is very fast. Even at $-30\text{ }^{\circ}\text{C}$ decoalescence of the signals was not observed. The experimental data were fitted to a 1:1 binding model giving a $K_a \sim 10^6\text{ M}^{-1}$, which is at the limit of what can be determined using NMR techniques.

In addition, 2D NMR studies showed significant NOE connectivities for the H_{α} , H_{β} and H_{γ} protons of the propyl groups of **1b** with the aromatic proton signals of **2a** (Figure 4.3), which can only mean that (part of) the propyl chain is inside the capsule's cavity.

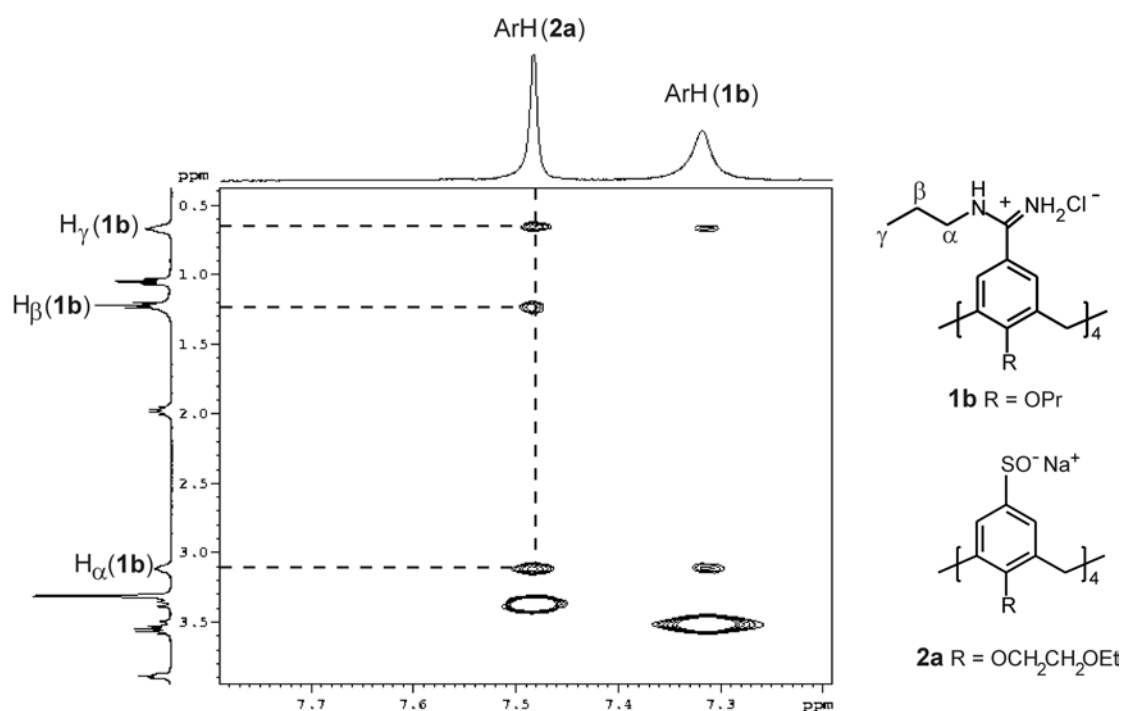


Figure 4.3. Part of the 2D NOESY NMR spectrum of complex **1b•2a** in CD_3OD at 298 K. NOE contacts are observed between the H_{α} , H_{β} and H_{γ} protons of the propyl chains and the aromatic protons of both **1b** and **2a**.

4.2.3 Self-assembly of **1b-e**•**2a**: influence of the amidinium side chain size

¹H NMR spectroscopy. To study the influence of the side chain size on the formation of the capsule, the assembly of **2a** with calix[4]arene tetraamidinium **1c** and **1d** (Chart 4.1) having *N*-isopropyl and *N*-heptyl amidinium substituents respectively was also investigated. The spectrum of **1c**•**2a** in CD₃OD shows strongly upfield shifted and broadened signals for both the H_α and H_β protons ($\Delta\delta_{H\alpha} = 0.17$ ppm and $\Delta\delta_{H\beta} = 0.53$ ppm), indicating that the increased size due to the branched side chain does not hinder encapsulation (Figure 4.4). However, the proton signals of the heptyl side chains in assembly **1d**•**2a** show almost negligible upfield shifts (max shift observed for H_β, $\Delta\delta_{H\beta} = 0.07$ ppm). This leads to the conclusion that the heptyl side chains are too long to be accommodated inside the cavity of the capsule.

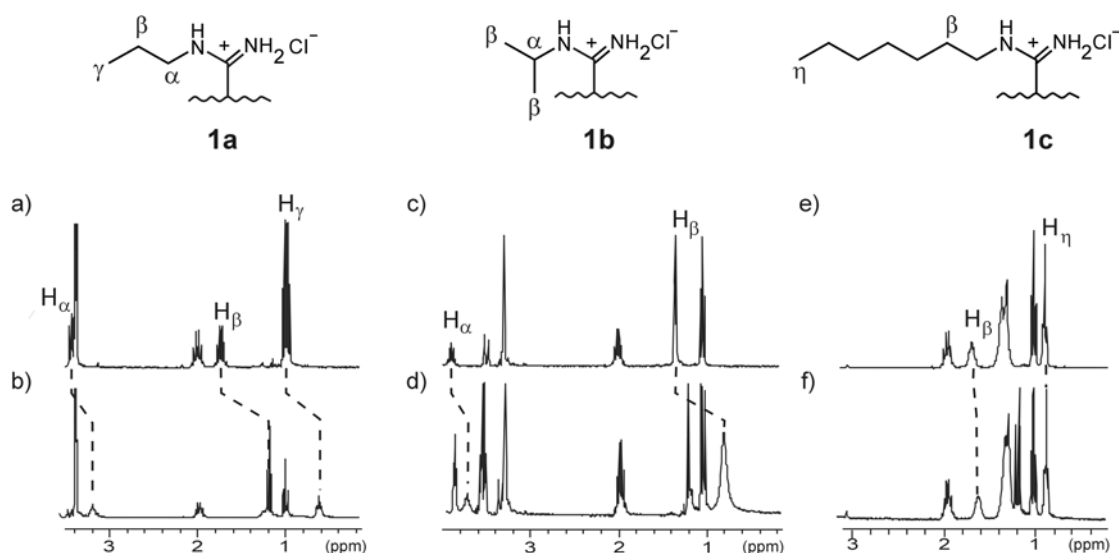


Figure 4.4. Parts of the ¹H NMR spectra (CD₃OD, 298 K) of a) **1b**; b) a 1:1 mixture of **1b** and **2a**; c) **1c**; d) a 1:1 mixture of **1c** and **2a**; e) **1d**, and f) a 1:1 mixture of **1d** and **2a**.

ITC. Isothermal titration calorimetry was utilized to study the thermodynamic of association between **1b-e** and **2a**. Compound **1e**, which lacks substituents on the amidinium groups, was synthesized to investigate the role played by the alkyl chains in the self-assembly formation. All the titrations were carried out by adding aliquots of tetraamidinium calix[4]arenes **1b-e** to a solution of calix[4]arene tetrasulfonate **2a**

at 298 K in MeOH/H₂O ($x_{\text{water}} = 0.4$) in the presence of 1×10^{-2} M of tetrabutylammonium perchlorate (Bu₄NClO₄) as background electrolyte.

In all cases, the titration curves showed an inflection point around 1.0 equivalent of **2a** added, which confirms the formation of a complex with 1:1 stoichiometry. The titration data were fitted to a 1:1 binding model using a non-linear least squares fitting procedure. The corresponding association constants and thermodynamic parameters are listed in Table 4.1. For all the capsules investigated the association constants are in the order of 10^6 M^{-1} with positive ΔH° and ΔS° values.¹⁴⁻¹⁷ The self-assembly of these molecular capsules is thus an entropy driven process. The gain in entropy is the result of the release of highly ordered solvent molecules from the charged groups to the bulk solvent upon complex formation. Within the series, assembly **1e•2a** exhibits the highest positive values for ΔH° and ΔS° . This can be attributed to a more favorable solvation of the non-substituted amidinium groups of **1e**. More interestingly, increasing the length of the alkyl side chains from propyl to heptyl does not have a dramatic effect on the thermodynamic parameters for capsule formation (see Table 4.1) indicating that self-assembly is essentially driven by the ionic interactions between the two building blocks.

Table 4.1. Association constants and thermodynamic parameters for the formation of assemblies **1b•2a** as determined by ITC in MeOH/H₂O ($x_{\text{water}} = 0.4$) at 298 K, background electrolyte: 1×10^{-2} M Bu₄NClO₄.

Assembly	$K_a \text{ (M}^{-1}\text{)}$	$\Delta H^\circ \text{ (kJ mol}^{-1}\text{)}$	$\Delta S^\circ \text{ (J K}^{-1} \text{ mol}^{-1}\text{)}$
1b•2a	$(8.5 \pm 1.4) \times 10^6$	14.1 ± 0.1	180 ± 2
1b•2a ^{a)}	$(2.1 \pm 0.5) \times 10^5$	11.6 ± 0.5	141 ± 3
1c•2a	$(6.4 \pm 1.7) \times 10^6$	13.7 ± 0.2	176 ± 2
1d•2a	$(1.1 \pm 0.1) \times 10^6$	17.9 ± 0.1	176 ± 1
1e•2a	$(1.9 \pm 0.3) \times 10^6$	33.3 ± 0.3	231 ± 2

^{a)} Background electrolyte: 1×10^{-2} M tetramethylammonium chloride (TMACl). See section 4.2.5 for results.

4.2.4 X-ray crystal structure of 1a•2a.

The X-ray structure of **1a•2a** provides direct evidence for the formation of the calixarenes' ionic assemblies in the solid state. Furthermore, it also proves that only one of the propyl side chains of **2a** is included inside the cavity of the capsule pointing towards the aromatic walls of the tetrasulfonate calix[4]arene (Figure 4.5).

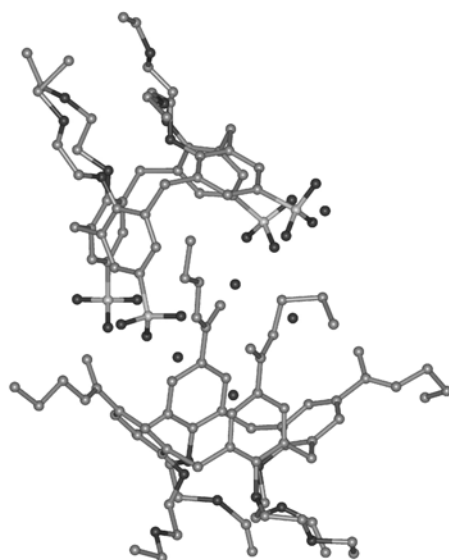


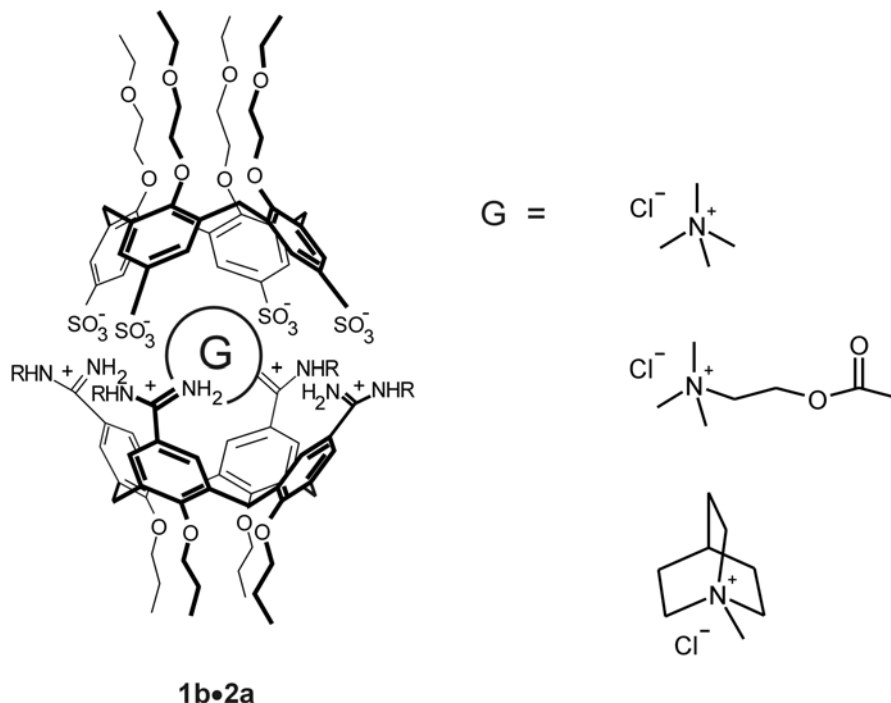
Figure 4.5. X-ray structure of the molecular capsule **1a•2a**.

4.2.5 Guest encapsulation studies with capsule 1b•2a

Due to the drive to understand the complexation of acetylcholine and related biomolecules to their natural receptors, priority has been given to the study of quaternary ammonium cations binding to artificial receptors. Studies have shown that these ions can bind to the face of an aromatic structure through cation- π interactions,¹⁸ a noncovalent force, as occurs in a variety of proteins that bind cationic ligands or substrates. A large number of molecular hosts¹⁹⁻²⁴ containing aromatic units have been synthesized and investigated in the recognition of organic ammonium cations either in polar or apolar solution, and among these, calixarenes have been used as receptors for quaternary ammonium ions.²⁵⁻²⁸ These cations are also suitable guest molecules for hydrogen bonded calixarene capsules²⁹ and coordination cages.^{30,31}

Thus the affinity of capsule **1b•2a** for different tetrammonium cations, including the biological interesting acetylcholine, was tested (Chart 4.2).

Chart 4.2



The encapsulation properties were primarily investigated by ¹H NMR spectroscopy. The included side chain in the capsule's cavity was used as a probe to detect guest encapsulation. According to the model reported in Figure 4.6 the inclusion of a suitable guest molecule should result in the extrusion of the alkyl chain from the cavity.

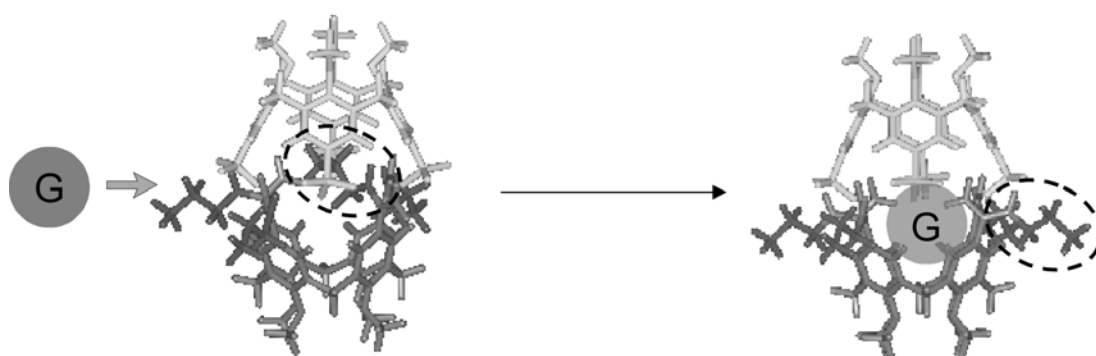


Figure 4.6. Schematic representation of the guest encapsulation process and extrusion of the side chain.

Addition of an excess (=15 equiv.) of tetramethylammonium chloride (TMACl) to the capsule **1b•2a** in CD₃OD (1.0 mM) causes a significant downfield shift of the proton signals of the *N*-propyl amidinium side chains ($\Delta\delta_{\text{H}\alpha} = 0.23$ ppm, $\Delta\delta_{\text{H}\beta} = 0.31$ ppm, $\Delta\delta_{\text{H}\gamma} = 0.19$ ppm) (Figure 4.7). This finding accounts for the extrusion of the alkyl chains from the cavity as a consequence of a more favorable inclusion of TMA. Addition of an excess of TMABr or TMAI (=15 equiv.) to **1b•2a** resulted in analogous chemical shift changes observed upon addition of TMACl, thus suggesting that the encapsulated species is most probably only the cation.

A control experiment using tetrabutylammonium chloride (TBACl), a molecule too bulky to be accommodated inside the cavity, showed no changes in the chemical shift of the chain proton signals.

The TMA resonance itself hardly shifts upon complexation because it is an averaged signal of the free and complexed guest molecule. As the complex is not very strong it can be observed only with a large excess of guest present, which means that the averaged signal does not shift much. However, in a concentrated (10 mM) solution of **1b•2a** in CD₃OD containing 1.0 equiv. of TMACl the TMA resonance is shifted upfield by 0.08 ppm. Fitting of the ¹H NMR titration data for TMACl to a 1:1 binding model gave a $K_a = 170 \pm 30 \text{ M}^{-1}$ in CD₃OD (Figure 4.7, Table 4.2).

Complexation of TMACl was also observed in pure water. However, in this case it was not possible to measure complexation directly in solution, because of the inherently low solubility of complex **1b•2a** in water. Therefore, 8 mg of solid **1b•2a** was suspended in 1.5 mL of a 1.5 M aqueous solution of TMACl and allowed to equilibrate for one hour. Then, the solid was filtered and extensively washed with water. NMR analysis of the solid in CD₃OD showed the presence of 50-70% mol. eq. of TMACl, which strongly supports encapsulation. A control experiment with TBACl, which is too big to fit inside the cavity, did not show any of the ammonium salt present.

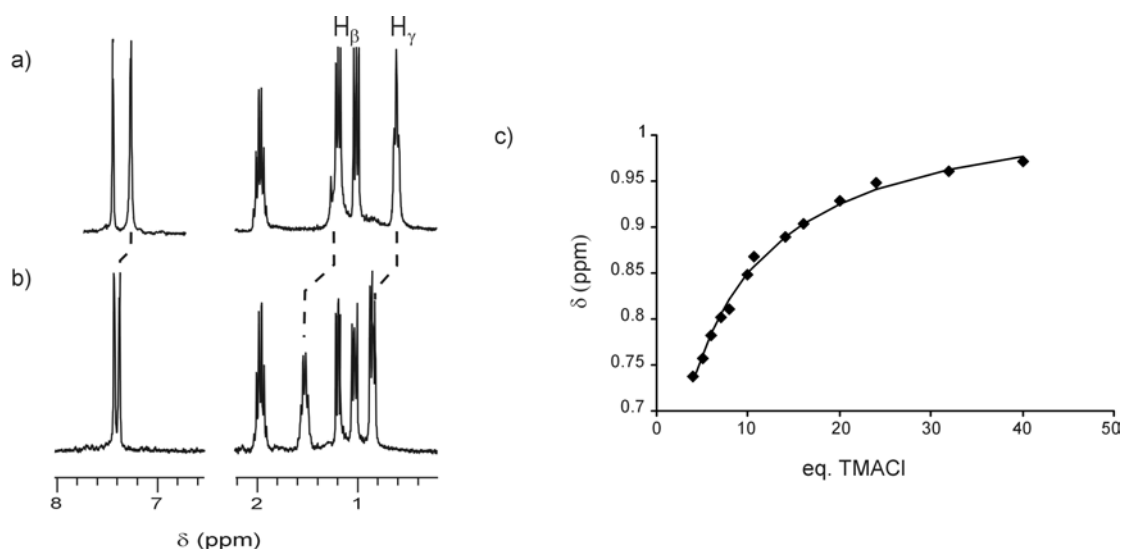
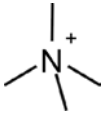
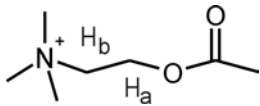
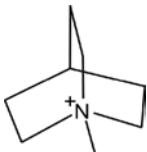


Figure 4.7. Different regions of the ¹H NMR spectra (CD₃OD, 298 K) of a) **1b•2a**; b) **1b•2a** in the presence of 15 equiv. of TMACl, and c) NMR titration curve for the complexation of TMA with **1b•2a** in CD₃OD at 298 K. Data points represent the methyl proton signals (H_γ) of the amidinium chains that shift upon addition of the guest. The line is the best-fit curve calculated by non-linear regression of the titration data. (For assignment of H_β and H_γ see Figure 4.3).

Table 4.2. Binding constants for complexes of **1b•2a** and guest molecules as determined by ¹H NMR spectroscopy, and guest chemical shift changes for the *N*-methyl protons, measured in CD₃OD at 298 K.

Guest	K_a (M ⁻¹)	$\Delta\delta$ (ppm) N ⁺ -CH ₃ ^(a)
	170 ± 30	0.08
	37 ± 7	0.15
	24 ± 4	0.12

^{a)} Measured adding 1 eq. of guest to a 10 mM solution of **1b•2a**.

To further prove encapsulation of the TMA cation, calorimetric experiments were carried out. The calorimetric titration of **2a** with **1b** in MeOH/H₂O ($x_{\text{water}} = 0.4$) using TMACl as background electrolyte (1×10^{-2} M) gives an experimental curve for the

formation of the capsule very similar to that obtained using Bu_4NClO_4 (Table 4.1 and Figure 4.8).

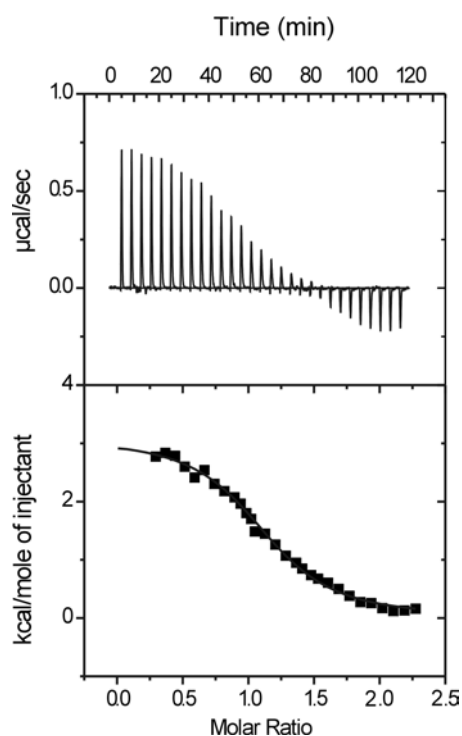


Figure 4.8. Calorimetric titration of **2a** with **1b** in MeOH/H₂O ($x_{\text{water}} = 0.4$) at 298 K in presence of TMACl, $I = 0.01$ M; a) data of heat evolution with injection of **1b**, and b) resulting binding curve and best fit curve.

This result suggests that the presence of TMA chloride does not interfere with the formation of capsule **1b•2a**. Moreover, since it is known from literature that calix[4]arene tetrasulfonate shows binding affinity towards ammonium salts in aqueous solution,³²⁻³⁵ a microcalorimetric titration of **2a** (1×10^{-4} M) with TMACl (1×10^{-2} M) was performed. No heat effect was observed at these concentrations, which allow us to conclude that the experimental curve we observed during the titration is indeed due to the formation of the assembly **1b•2a** and not to the formation of the complex **2a** with TMA ion.

Inclusion of the TMA cation was also confirmed by ESI-MS, clearly showing signals at m/z 1018.32 and 1029.82 corresponding to the $[(\mathbf{1b}\cdot\mathbf{2a})+\text{TMA}+\text{H}]^{2+}$ and the $[(\mathbf{1b}\cdot\mathbf{2a})+\text{TMA}+\text{Na}]^{2+}$ complexes.

The encapsulation of acetylcholine (ACh), an important neurotransmitter, was also studied. Addition of 15 equiv. of ACh chloride also causes significant downfield shifts of the *N*-propyl amidinium protons ($\Delta\delta_{\text{H}_\alpha} = 0.38$ ppm, $\Delta\delta_{\text{H}_\gamma} = 0.24$ ppm). Fitting

of the ^1H NMR data to a 1:1 binding model gave a $K_a = 37 \pm 7 \text{ M}^{-1}$ in CD_3OD (Table 4.2). Also in this case upfield shifts for the ACh resonances ($\Delta\delta = 0.15 \text{ ppm}$ for the *N*-methyl protons, $\Delta\delta = 0.07 \text{ ppm}$ for the H_a protons, $\Delta\delta = 0.13 \text{ ppm}$ for the H_b and $\Delta\delta = 0.07 \text{ ppm}$ for the acetyl protons; see Table 4.2 for assignment of H_a and H_b) were observed in a 10mM solution of **1b•2a** in CD_3OD containing 1.0 equiv. of ACh chloride..

Finally, the complexation of the *N*-methylquinuclidinium ion, which is known to be a suitable guest for molecular capsules based on calix[4]arenes,³⁶ was investigated by ^1H NMR spectroscopy. Similarly to what was observed with the previous guest molecules, addition of 1.0 equiv. of methylquinuclidinium chloride to a 10 mM solution of **1b•2a** in CD_3OD caused an upfield shift of all the guest proton signals, with the largest shift (0.12 ppm) observed for the *N*-methyl protons. The ^1H NMR titration produced a curve, which was successfully fitted to a 1:1 binding model giving an association constant K_a of $24 \pm 14 \text{ M}^{-1}$ (Table 4.2).

4.2.6 Towards water soluble molecular capsules

Tetraamidinium calix[4]arene **1f** and **1g**, substituted with ethylene glycol chains at the bottom rim (Chart 4.1), were expected to be more water-soluble. ITC experiments were performed in $\text{MeOH}/\text{H}_2\text{O}$ ($x_{\text{water}} = 0.4$) and compared with the results obtained for a similar compound (**1e**) (Table 4.3). The presence of different alkyl chains inserted at the bottom rim of the calix[4]arene does not influence the thermodynamic parameters, indicating that the main driving force for the assembly formation is the desolvation of the charged groups located at the upper rims and the subsequent formation of ionic interactions.

For assembly **1g•2a** a titration in H_2O was possible. As expected going from a $\text{MeOH}/\text{H}_2\text{O}$ mixture to pure H_2O , a modest drop in the association constant ($K_a \sim 2.1 \times 10^6 \text{ M}^{-1}$ vs $K_a \sim 4.1 \times 10^5 \text{ M}^{-1}$) is observed. The association process in pure H_2O remains entropy driven and is accompanied by a less favorable value for ΔS° and a more favorable value for ΔH° . This can be rationalized with a different solvation of the building blocks in H_2O vs $\text{MeOH}/\text{H}_2\text{O}$. The less positive values for both ΔS° and ΔH° indicate that in H_2O a fewer number of solvent molecules are released from the

building blocks than in MeOH/H₂O, therefore the enthalpic penalty paid to disrupt the solvation shell is smaller.³⁷

Table 4.3. Association constants and thermodynamic parameters for formation of assemblies **1e-g•2a** as determined by ITC measured in MeOH/H₂O ($x_{\text{water}} = 0.4$) at 298 K, background electrolyte: 1×10^{-2} M in Bu₄NClO₄.

Assembly	K_a (M ⁻¹)	ΔH° (kJ mol ⁻¹)	ΔS° (J K ⁻¹ mol ⁻¹)
1e•2a	$(1.9 \pm 0.3) \times 10^6$	33.3 ± 0.3	231 ± 2
1f•2a	$(6.9 \pm 1.3) \times 10^6$	23.6 ± 0.2	210 ± 2
1g•2a	$(2.1 \pm 0.3) \times 10^6$	27.6 ± 0.2	214 ± 1
	$(4.1 \pm 0.5) \times 10^5$ ^(a)	6.6 ± 0.1	130 ± 1

^a measured in H₂O, background electrolyte: 0.5×10^{-2} M Bu₄NClO₄.

4.3 Conclusions

The results reported in this chapter showed evidence for the formation of 1:1 calix[4]arene-based molecular capsules **1•2a** in MeOH and MeOH/H₂O solutions. NMR studies have demonstrated that the geometry of the molecular capsules is affected by the length of the amidinium side chains of **1**. While the short alkyl side chains, such as propyl or iso-propyl of **1b** and **1c**, respectively, are accommodated in the capsule's cavity upon assembly formation, the longer heptyl substituents of **1d** are most probably residing outside the capsule.

X-ray analysis has shown that capsule **1a•2a** possesses an internal cavity that indeed accommodates one of the **1a** propyl chains. The inclusion of the propyl chain was found to be a useful tool to study the encapsulation of quaternary ammonium cations like TMA, ACh, and *N*-methylquinuclidinium in MeOH.

Moreover, it was also shown that the introduction of small modifications on the building blocks (i.e. ethereal chains at the lower rim of **1**) allows solubility of the molecular capsule in H₂O, thus opening the possibility to use such systems for

purposes like drug storage or delivery. Nevertheless, increased water solubility is necessary to achieve these ultimate objectives (see Chapter 5).

4.4 Experimental section

4.4.1 General information and instrumentation

The reagents used were purchased from Aldrich or Acros Chimica and used without further purification. All the reactions were performed under nitrogen atmosphere. Analytical thin layer chromatography was performed using Merck 60 F₂₅₄ silica gel plates. Column chromatography was carried out on Merck silica gel 60 (230-400 mesh) and reverse phase chromatography on Silica RP-18. Ion exchange chromatography was carried out on DOWEX 1-X8, 50-100 mesh, Cl-form. ¹H and ¹³C NMR spectra were recorded on a Varian Unity INOVA (300 MHz) or a Varian Unity 400 WB NMR spectrometer. ¹H NMR chemical shift values (300 MHz) are reported as δ in ppm using the residual solvent signal as an internal standard (CHD₂OD, δ = 3.30, DMSO-d₆, δ = 2.49). ¹³C NMR chemical shift values (100 MHz) are reported as δ in ppm using the residual solvent signal as an internal standard (CD₃OD, δ = 49.0, DMSO, δ = 39.7). Infrared spectra were recorded on a FT-IR Perkin Elmer Spectrum BX spectrometer and only characteristic absorptions are reported. Fast atom bombardment (FAB) mass spectra were recorded with a Finnigan MAT 90 spectrometer. Electrospray ionization (ESI) mass spectra were recorded on a Micromass LCT time-of-flight (TOF) mass spectrometer. Samples were introduced using a nanospray source. Elemental analyses were carried out using a 1106 Carlo-Erba Strumentazione element analyzer.

4.4.2 Binding studies

Calorimetric measurements. The titration experiments were carried out using a Microcal VP-ITC microcalorimeter with a cell volume of 1.4115 mL. The formation of the assemblies **1x•2a** has been studied adding aliquots of **1x** to **2a** in the calorimetric cell, and monitoring the heat change after each addition. Dilution effects were determined in a second experiment by adding the solution of **1x** into the solvent mixture and subtracting this contribution from the raw titration. The final curves were

modeled using a 1:1 non-linear regression analysis. The fittings were done using Microcal Origin[®] software.

¹H NMR titration of 2a with 1b. The ¹H NMR titration was recorded in CD₃OD at 298 K. A set of 10 titration samples was prepared. In all samples, the concentration of **2a** was kept constant (1×10^{-3} mol/L) whereas the concentration of **1b** was varied from 0 to 3×10^{-3} mol/L. The chemical shifts relative to the protons of the amidinium chains of **1b** were followed and fitted to a 1:1 binding model using Origin[®].

Encapsulation studies: determination of association by ¹H NMR titration. All the ¹H NMR titrations were recorded in CD₃OD at 298 K. To 0.6 mL of a 1 mM solution of capsule **1b•2a**, increasing amounts of a 0.1-0.3 M solution of guest (from 0-40 eq) were added with a maximum volume change of 10%. Dilution experiments showed that the spectrum of **1b•2a** is concentration independent. Addition of CD₃OD up to 10% in volume to 0.6 mL of a 1mM solution of capsule **1b•2a** does not change its NMR spectrum. In the case of *N*-methyluiclidinium chloride, the final K_a value is an average of the values obtained in the evaluation of three individual proton signals. The experimental points were fitted to a 1:1 binding model using Scientist[®].

Encapsulation studies: precipitation experiment. In a typical precipitation experiment, to a 1.5 mL solution of TMA chloride at 1.5 M in water, 8 mg of **1b•2a** was added. The suspension was stirred at room temperature for one hour then filtered and washed extensively with water. The white solid was redissolved in MeOH. The solvent was removed and the residue redissolved in CD₃OD. The experiment was repeated several times and good reproducibility was observed.

4.4.3 Experimental details of the X-ray structure determination

Single crystals of the molecular capsule **1a•2a** were prepared by the vapor diffusion method with hanging-drops at 18 °C using Linbro multi-well tissue plates as containers of reservoir solutions. Drops formed by mixing 3 μ l of a capsule solution (8.0 mM in DMSO) with 3 μ l of a water solution containing DMSO were set to equilibrate against 1 ml of this water solution (reservoir). Crystals suitable for X-ray diffraction experiments were obtained with water solution containing DMSO in the

range 40% - 60% v/v. Preliminary in-house diffraction experiments, using a X-ray conventional source with crystals frozen to 100 K, permitted only the determination of the unit cell parameters (maximum resolution limit 2.5 Å). Therefore, the data collection was performed using synchrotron radiation (XRD1 diffraction beam-line of Elettra, Trieste) with monochromatic X-ray beam (wavelength, 1.000 Å), crystal to detector (MARCCD) distance of 40 mm and oscillation angle of 3.0°. The colorless crystal used in this diffraction experiment (dimensions 0.4x0.4x0.3 mm) was obtained with 55% v/v DMSO. The crystal dipped in its cryoprotected mother liquor was mounted in loop and frozen to 100 K with N₂. The diffraction data were indexed and integrated using MOSFLM and scaled with SCALA (Collaborative Computational Project, Number 4, 1994). Analysis of the diffraction pattern and of the systematic absences allowed the assignment of capsule crystals to the monoclinic spacegroup *P*2₁/*c*. The structure of the capsule was solved by direct methods (SHELXS-97) and anisotropic refined (H atoms at the calculated positions) with bond length and angle restraints by full-matrix least-squares methods on F² (SHELXL-97). By inspection of Fourier difference maps, some oxygen and carbon atoms of the terminal ether groups were found disordered over two orientations with occupancy factors of 0.5. Six water molecules were found in the asymmetric unit.

4.4.4 Synthesis

Compounds **3a-c** were synthesized according to literature procedures.³⁸

5,11,17,23-(*N*-propyltetraamidinium)-25,26,27,28-tetrakis(propoxy) calix[4]arene, tetrachloride salt (1b)

To a solution of Et₂AlCl in hexane (1.0 M, 11.7 mL, 11.7 mmol) at 0 °C was added dropwise propylamine (0.96 mL, 11.7 mmol) in fluorobenzene (5 mL) and the mixture was stirred for 1h at 0 °C. Then, a solution of tetracyanocalix[4]arene **3a** (350 mg, 0.5 mmol) in fluorobenzene (5 mL) was added and stirred for 1h at room temperature and then 5 days at 80 °C. The reaction was monitored by TLC (silica gel, *n*-butanol/CH₃COOH/H₂O 3:1:1). The mixture was cooled to 0 °C and quenched with ice and CH₃COOH and the resulting suspension was filtered through a pad of Hyflo Super Cel[®]. The pad was washed with CH₃OH and H₂O, then the filtrates were concentrated *in vacuo*, the residue was treated with an excess of 3N HCl and then

concentrated *in vacuo*. The residue was purified by reverse phase chromatography using a step gradient from H₂O (100%) to EtOH/H₂O (50%, v/v). The tetrachloride salt of **1b** was obtained as a white solid after ion exchange chromatography, using H₂O as eluent, in 47% yield. ¹H NMR (CD₃OD): δ (ppm) 7.34 (s, 8H), 4.60 (d, 4H, $J=13.5$), 4.04 (t, 8H, $J=7.2$), 3.50 (d, 4H, $J=13.5$), 3.35 (t, 8H, $J=7.5$), 1.98 (m, 8H), 1.73 (m, 8H), 1.02 (2t, 24H). ¹³C NMR (CD₃OD): δ (ppm) 164.19, 162.35, 136.88, 129.99, 124.04, 78.75, 45.53, 31.89, 24.36, 22.16, 11.59, 10.61. IR (KBr) 3101, 2965, 2935, 2877, 1668, 1623, 1467, 1383, 1224, 998, 732. MS (FAB): m/z 929.71 ([M-4HCl+H]⁺, calcd. 929.63). Anal. calcd. for C₅₆H₈₄O₄N₈Cl₄: C 62.56, H 7.87, N 10.42; found: C 63.02, H 7.45, N, 10.68.

5,11,17,23-(N-isopropyltetraamidinium)-25,26,27,28-tetrakis(propoxy) calix[4]arene, tetrachloride salt (1c)

To a solution of Me₂AlCl in hexane (1.0 M, 22.1 mL, 22.1 mmol) at 0 °C, isopropylamine (1.89 mL, 22.1 mmol) in 1,2-dichlorobenzene (5 mL) was added dropwise and the mixture was stirred for 1h at 0 °C. Then a solution of tetracyanocalix[4]arene **3a** (300 mg, 0.369 mmol) in 1,2-dichlorobenzene (5 mL) was added and the reacting mixture stirred for 1h at room temperature and then for 5 days at 80 °C. The reaction was monitored by TLC (silica gel, *n*-butanol/CH₃COOH/H₂O 3:1:1). The mixture was cooled to 0 °C and quenched with ice and CH₃OH and the resulting suspension was filtered through a pad of Hyflo Super Cel[®]. The pad was washed with CH₃OH and H₂O and the filtrates were concentrated *in vacuo*, the residue was treated with an excess of 3N HCl and then concentrated *in vacuo*. The crude product was stirred in ether overnight. The solid residue was submitted to a preparative reverse phase chromatography using a step gradient from H₂O (100%) to EtOH/H₂O (30% v/v). The chloride salt of **1c** was obtained as a white solid after ion exchange column, using H₂O as eluent, in 45% yield. ¹H NMR (CD₃OD): δ (ppm) 7.36 (s, 8H), 4.61 (d, 4H, $J=13.2$), 4.04 (t, 8H, $J=7.2$), 3.90 (sept, 4H, $J=6.3$), 3.50 (d, 4H, $J=13.5$), 2.00 (sex, 8H, $J=7.2$), 1.35 (d, 24H, $J=6.0$), 1.03 (t, 12H, $J=7.8$). ¹³C NMR (CD₃OD): δ (ppm) 163.64, 162.09, 136.60, 130.22, 124.68, 78.73, 46.98, 31.91, 24.34, 21.66, 10.59. IR (KBr) 3066, 2938, 2957, 2855, 1666, 1621, 1464, 1386, 1225, 1126, 997, 733. MS (FAB): m/z 934.20 ([M-4HCl+H]⁺, calcd. 933.67). Anal. calcd.

for C₅₆H₈₄O₄N₈Cl₄·1.5NaCl: C, 57.84; H, 7.28; N, 9.64; found: C, 57.61; H, 7.56; N, 9.19.

5,11,17,23-(N-heptyltetraamidinium)-25,26,27,28-tetrakis(propoxy) calix[4]arene, tetrachloride salt (1d)

To a solution of Et₂AlCl in hexane (1.0 M, 10.4 mL, 10.4 mmol) at 0 °C was added dropwise heptylamine (1.56 mL, 10.4 mmol) in fluorobenzene (5 mL) and the mixture was stirred for 1h at 0 °C. Then, a solution of tetracyanocalix[4]arene **3a** (300 mg, 0.43 mmol) in fluorobenzene (5 mL) was added and the reaction mixture was stirred for 1h at room temperature and then for 3 days at 80° C. The reaction was monitored by TLC (silica gel *n*-butanol/CH₃COOH/H₂O 6:0.5:0.5). The mixture was cooled to 0 °C and quenched with ice and CH₃OH and the resulting suspension was filtered through a pad of Hyflo Super Cel[®]. The pad was washed with CH₃OH and H₂O, then the filtrates were concentrated *in vacuo* and the residue was treated with an excess of HCl 3M and then concentrated *in vacuo*. The solid residue was triturated in H₂O at 25°C for 8h. The corresponding chloride salt of **1d** was obtained as a white solid after ion exchange column using H₂O as eluent in 20% yield. ¹H NMR (CD₃OD): δ(ppm) 7.34 (s, 8H), 4.59 (d, 4H, J 13.5), 4.03 (t, 8H, J=7.2), 3.48 (d, 4H, J=13.5), 3.36 (t, 8H, J=7.5), 1.97 (sex, 8H, J=7.5), 1.71 (br m, 8H), 1.33 (br m, 32H), 1.03 (t, 12H, J=7.5), 0.93-0.89 (t, 12H). ¹³C NMR (CD₃OD): δ(ppm) 164.31, 162.30, 136.85, 130.00, 124.24, 78.76, 44.12, 32.92, 31.94, 30.10, 28.84, 27.95, 24.36, 23.68, 14.43, 10.60. IR (KBr) 3066, 2928, 2958, 2856, 1666, 1622, 1581, 1467, 1381, 1224, 999, 730. MS (FAB): *m/z* 936.6 ([M-4HCl+H]⁺, calcd.: 936.5). Anal. calcd. for C₇₂H₁₁₆N₈O₄Cl₄ 1 NaCl: C 63.80, H 8.80, N 8.14; found: C, 63.68; H, 8.61; N, 8.25.

General Procedure for the preparation of 5,11,17,23-(N-tetraamidinium)-calix[4]arenes 1e, 1f, 1g tetrachloride salts.

To a suspension of NH₄Cl (357.31 mg, 6.68 mmol) in dichloroethane (5 mL) at 0 °C, (CH₃)₃Al (2M in toluene, 3.34mL, 6.68 mmol) was slowly added and the mixture was stirred for 1h at 0 °C. Then a solution of the appropriate tetracyanocalix[4]arene (200 mg, 0.288 mmol) in dichloroethane (3 mL) was added and stirred for 1h at room temperature and then for 5 days at 80 °C. The reaction was monitored by TLC (silica gel *n*-butanol/CH₃COOH/H₂O 3:1:1). The mixture was cooled to 0 °C, and quenched

with ice and CH₃OH and the resulting suspension was filtered through a pad of Hyflo Super Cel[®]. The pad was washed with CH₃OH and H₂O, then the filtrates were concentrated *in vacuo*, the residue was treated with an excess of 3N HCl and then concentrated *in vacuo*.

5,11,17,23-(*N*-tetraamidinium)-25,26,27,28-tetrakis(propoxy)calix[4]arene, tetrachloride salt (1e)

The solid residue was purified by column chromatography (silica gel; *n*-butanol/H₂O/CH₃COOH 6:1:1). The tetrachloride salt of **1e** was obtained as a white solid after ion exchange column using H₂O as eluent in 63% yield. ¹H NMR (CD₃OD): δ (ppm) 7.44 (s, 8H), 4.60 (d, 4H, $J=13.8$), 4.04 (t, 8H, $J=7.2$), 3.52 (d, 4H, $J=13.8$), 1.97 (sex, 8H, $J=7.2$), 1.04 (t, 8H, $J=7.5$). ¹³C NMR (CD₃OD): δ (ppm) 166.78, 163.18, 137.32, 130.26, 122.73, 78.94, 32.02, 24.55, 10.74. IR (KBr) 3140, 2961, 2875, 1674, 1652, 1605, 1455, 1273, 1144, 997. MS (FAB): m/z 761.3 ([M-4HCl+H]⁺, calcd. 761.4). Anal. calcd. for C₄₄H₆₀O₄N₈Cl₄·5NaCl: C 44.08, H 5.04, N 9.35; found: C, 44.41; H, 6.10; N, 9.21.

5,11,17,23-(*N*-tetraamidinium)-25,26,27,28-tetrakis(ethoxyethoxy)calix[4]arene, tetrachloride salt (1f)

The solid residue was purified via reverse phase column chromatography (RP=8, water:ethanol = 7:3). The tetrachloride salt of **1f** was obtained as a white solid after ion exchange column using H₂O as eluent in 55% yield. ¹H NMR (CD₃OD): δ (ppm) 7.46 (s, 8H), 4.77 (d, 4H, $J=14.0$), 4.32 (t, 8H, $J=3.9$), 3.87 (t, 8H, $J=3.9$), 3.53 (q, 8H, $J=6.9$), 3.49 (d, 4H, $J=13.8$), 1.17 (t, 12H, $J=6.9$). ¹³C NMR (CD₃OD): δ (ppm) 156.47, 136.00, 131.03, 127.68, 74.54, 71.08, 67.48, 35.98, 34.20, 31.67, 15.72. IR (KBr) 3116, 1673, 1455, 1275, 1119, 1045, 900. MS (FAB): m/z 881.4 ([M-4HCl+H]⁺, calcd. 881.5). Anal. calcd. for C₄₈H₆₈O₈N₈Cl₄·2NaCl: C 50.40, H 5.99, N 9.80; found: C, 50.58; H, 6.10; N, 9.21.

5,11,17,23-(*N*-tetraamidinium)-25,26,27,28-tetrakis(ethoxyethoxymethylether)calix[4]arene tetrachloride salt (1g)

The solid residue was purified via reverse phase column chromatography (RP 8, 40-63 μ m; water:ethanol=9:1). The tetrachloride salt of **1g** was obtained as a white

solid after ion exchange column using H₂O as eluent in 60% yield. ¹H NMR (DMSO): δ (ppm) 9.21 and 8.79 (2s, 16H), 7.59 (s, 8H), 4.55 (d, 4H, $J=13.4$), 4.18 (t, 8H, $J=4.4$) 3.82 (t, 8H, $J=4.5$), 3.55 (dd, 8H, $J=5.8, 3.6$), 3.42 (dd, 8H, $J=5.7, 3.6$) 3.37 (d, 4H, $J=13.3$), 3.21 (s, 4H). ¹³C NMR (DMSO): δ (ppm) 164.1, 160.8, 135.0, 129.0, 121.1, 73.9, 71.4, 69.8, 69.6, 58.2, 30.2. IR (KBr) 3265, 3117, 2927, 2879, 1676, 1605, 1458, 1105 cm⁻¹. MS (FAB): m/z 1001.7 ([M-4HCl+H]⁺, calcd. 1001.5). Anal. calcd. for C₅₂H₇₆O₁₂N₈Cl₄: C 54.45, H 6.68, N 9.77; found: C, 51.86; H, 6.43; N, 9.00.

4.5 References and notes

1. Lehn, J.-M. *Supramolecular Chemistry: Concepts and Perspectives*; VCH: Weinheim, 1995.
2. Hof, F.; Craig, S. L.; Nuckolls, C.; Rebek, J. Jr. *Angew. Chem. Int. Ed.* **2002**, *41*, 1488-1508.
3. Mecozzi, S.; Rebek, J. Jr. *Chem. Eur. J.* **1998**, *4*, 1016-1022.
4. Kang, J.; Rebek, J. Jr. *Nature* **1997**, *385*, 50-52.
5. Castellano, R. S.; Craig, S. L.; Nuckolls, C.; Rebek, J. Jr. *J. Am. Chem. Soc.* **2000**, *122*, 7876-7882.
6. Ziegler, M.; Brumaghin, J. L.; Raymond, K. N. *Angew. Chem. Int. Ed.* **2000**, *39*, 4119-4121.
7. Chapmann, R. G.; Sherman, J. C. *J. Am. Chem. Soc.* **1995**, *117*, 9081-9082.
8. Shivanyuk, A.; Rebek, J. Jr. *Angew. Chem. Int. Ed.* **2003**, *42*, 684-686.
9. Shivanyuk, A.; Rebek, J. Jr. *J. Am. Chem. Soc.* **2002**, *124*, 12074-12075.
10. Garipati, R. S. *Tetrahedron Lett.* **1990**, *31*, 1969-1972.
11. Sebo, L.; Diederich, F. *Helv. Chim. Acta* **2000**, *83*, 93-113.
12. Pinkhassik, E.; Sidorov, V.; Stibor, I. *J. Org. Chem.* **1998**, *63*, 9644-9651.

13. Shihong, M.; Rudkevich, D. M.; Rebek, J. Jr. *J. Am. Chem. Soc.* **1998**, *120*, 4977-4981.
14. Berger, M.; Schmidtchen, F. P. *Angew. Chem. Int. Ed.* **1998**, *37*, 2694-2696.
15. Linton, B.; Hamilton, A. D. *Tetrahedron* **1999**, *19*, 6027-6038.
16. Sebo, L.; Schweizer, B.; Diederich, F. *Helv. Chim. Acta* **2000**, *83*, 80-92.
17. Salvatella, X.; Peczu, M. W. G. M.; Jain, R. K.; Sanchez-Quesada, J.; de Mendoza, J.; Hamilton, A. D.; Giralt, E. *Chem. Commun.* **2000**, 1399-1400.
18. Ma, J. C.; Dougherty, D. A. *Chem. Rev.* **1997**, *97*, 1303-1324.
19. Dhaenens, M.; Lacombe, L.; Lehn, J.-M.; Vigneron, J.-P. *Chem. Commun.* **1984**, 1097-1099.
20. Meric, R.; Vigneron, J.-P.; Lehn, J.-M. *Chem. Commun.* **1993**, 129-131.
21. Araki, K.; Shimizu, H.; Shinkai, S. *Chem. Lett.* **1993**, 205-208.
22. Murayama, K.; Aoki, K. *Chem. Commun.* **1997**, 119-120.
23. Garel, L.; Lozach, B.; Dutasta, J.-P.; Collet, R. *J. Am. Chem. Soc.* **1993**, *115*, 11652-11653.
24. Kubik, S. *J. Am. Chem. Soc.* **1999**, *121*, 5846-5855.
25. Nakamura, R.; Ikeda, A.; Sarson, L. D.; Shinkai, S. *Supramol. Chem.* **1998**, *9*, 25-29.
26. Arena, G.; Casnati, A.; Contino, A.; Lombardo, G. G. *Chem. Eur. J.* **1999**, *5*, 738-744.
27. Arena, G.; Contino, A.; Fujimoto, T.; Sciotto, D.; Aoyama, Y. *Supramol. Chem.* **1999**, *10*, 279-288.
28. Arduini, A.; Pochini, A.; Secchi, A. *Eur. J. Org. Chem.* **2000**, *12*, 2325-2334.
29. Schalley, C. A.; Castellano, M. S.; Rudkevich, D. M.; Siuzdak, G.; Rebek, J. Jr.

- J. Am. Chem. Soc.* **1999**, *121*, 4568-4579.
30. Ziegler, M.; Brumaghin, J. L.; Raymond, K. N. *Angew. Chem. Int. Ed.* **2000**, *39*, 4119-4121.
31. Bourgeois, J.-P.; Fujita, M.; Kawano, M.; Sakamoto, S.; Yamaguchi, K. *J. Am. Chem. Soc.* **2003**, *125*, 9260-9261.
32. Arena, G.; Casnati, A.; Mirone, L.; Sciotto, D.; Ungaro, R. *Tetrahedron Lett.* **1997**, *38*, 1999-2002.
33. Arena, G.; Casnati, A.; Contino, A.; Gulino, F. G.; Sciotto, D.; Ungaro, R. *J. Chem. Soc., Perkin Trans. 2* **2000**, 419-423.
34. Arena, G.; Casnati, A.; Contino, A.; Lombardo, G. G.; Sciotto, D.; Ungaro, R. *Chem. Eur. J.* **1999**, *5*, 738-744.
35. Bonal, C.; Israeli, Y.; Morel, J.-P.; Morel-Desrosiers, N. *J. Chem. Soc., Perkin Trans. 2* **2001**, 1075-1078.
36. Cho, Y. C.; Rudkevich, D. M.; Rebek, J. Jr. *J. Am. Chem. Soc.* **2000**, *122*, 9868-9869.
37. Gohlke, H.; Klebe, G. *Angew. Chem. Int. Ed.* **2002**, *41*, 2644-2676.
38. Pinkhassik, E.; Sidorov, V.; Stibor, I. *J. Org. Chem.* **1998**, *63*, 9644-9651.

WATER-SOLUBLE MOLECULAR CAPSULES: SYNTHESIS AND BINDING PROPERTIES*

*In the previous chapters the formation of molecular capsules in polar organic solvents has been discussed. This chapter will report on molecular capsules (**1•2**) that are made soluble in neat water by introducing amino acidic moieties at the upper rim of one of the building blocks. Guest encapsulation studies have shown that capsule **1a•2a** is an effective host for both charged (*N*-methylquinuclidinium cation) and neutral molecules (6-amino-2-methylquinoline) in water.*

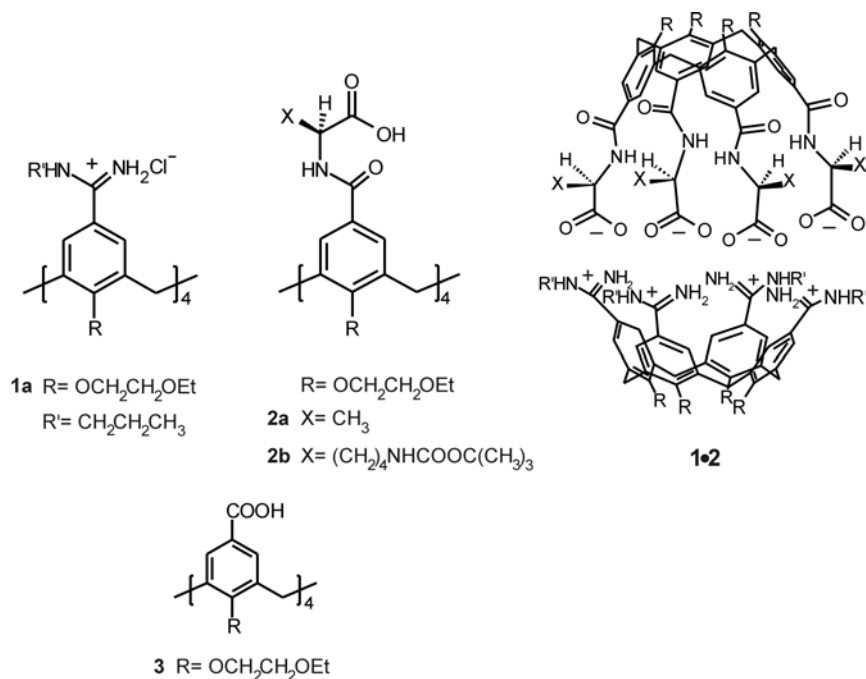
* Part of this chapter has been published in: Corbellini, F.; Fiammengo, R.; Timmerman, P.; Crego-Calama, M.; Versluis, K.; Heck, A. J. R.; Luyten, I.; Reinhoudt, D. N. *J. Am. Chem. Soc.* **2002**, *124*, 6569-6575.

5.1 Introduction

Natural processes take place in aqueous medium, therefore water solubility represents a desirable requirement for applications of molecular capsules for medical purposes (like storage of molecules and drug delivery) or biological model studies (for example the mimicry of the catalytic efficiency of enzymes).¹ So far water solubility has been achieved for molecular capsules based on metal-ligand coordination.^{2,3} Among others, Fujita's cage complexes are formed by the assembly of planar organic components and metal ions and they are able to reversibly bind or stabilize guest molecules and accelerate reactions in water.⁴⁻⁹ Nevertheless, the rigidity provided by the metal-ligand coordination in some cases disables the encapsulation of guest molecules.¹⁰ Simple ionic interactions provide a powerful tool for building molecular capsules in polar solvents.^{9,11-15} In Chapter 4 the formation of a stable molecular capsule based on ionic interactions between a tetrasulfonate and a tetraamidinium calix[4]arene was reported (see Figure 4.5, Chapter 4). The 1:1 complex was found to be soluble in methanol and in mixtures of methanol/water (up to 40% of water) while a precipitate was observed upon increasing the percentage of water. Water solubility has been achieved upon introduction of long ethylene glycol chains at the bottom rim of one of the calix[4]arenes (assembly **1g•2a** in Chart 4.1, Chapter 4). Nevertheless, concentrations higher than 0.2 mM could not be reached for this assembly in water.

In this chapter the synthesis of the first water soluble (up to millimolar concentrations) molecular capsules based on ionic interactions is reported. The design resembles the molecular capsule reported in Chapter 4. Here, one of the components is modified by the introduction of amino acidic moieties to accomplish water solubility. The formation of assemblies **1a•2** (Chart 5.1) is the result of the electrostatic interactions between the positively charged calix[4]arene **1a** and the negatively charged calix[4]arenes **2a** or **2b**, functionalized at the upper rim with L-alanine and L-lysine units, respectively. The amino functionality of the lateral chain of the lysine residues is protected with t-butoxycarbonyl (t-Boc) group. The amino acids are *N*-linked to the calix[4]arene scaffold and the carboxylic acid groups of **2a** and **2b** provide the anionic counterparts to the positively charged amidinium groups of **1a**.

Chart 5.1



The self-assembly of the molecular capsules **1a•2a** and **1a•2b** from the calix[4]arene building blocks was studied by ¹H NMR, ESI mass spectrometry (ESI-MS) and ITC.

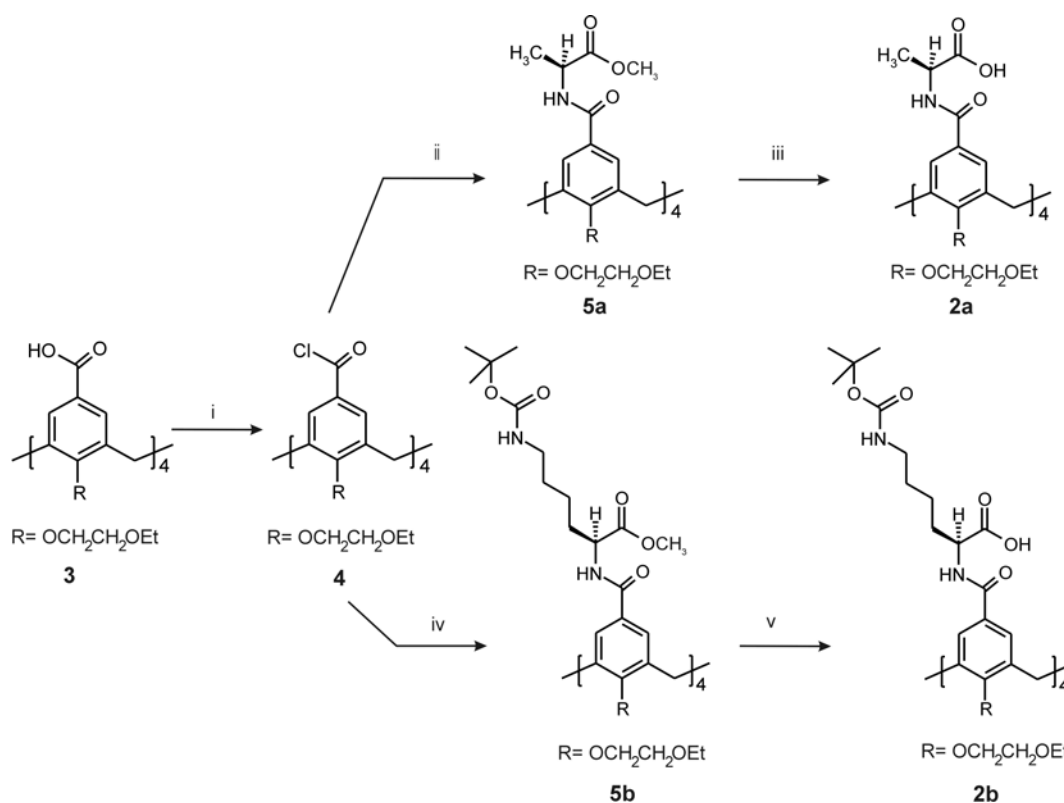
For comparative purposes the formation of the molecular capsule **1a•3** was also investigated. The thermodynamic data determined by ITC allowed estimation of how the size of the amino acidic side chains in **2a** and **2b**, and moreover the distance of the carboxylate groups from the calix[4]arene scaffold, affects the self-assembly formation.

Furthermore, this chapter describes the encapsulation properties of the molecular capsule **1a•2a**. The encapsulation of tetramethylammonium (TMA), acetylcholine (ACh) and *N*-methylquinuclidinium (NMQ), was primarily investigated. Evidence for the inclusion of the NMQ cation was provided by ¹H NMR and mass spectrometry while no indication for the encapsulation of TMA and ACh cations was observed. As previously reported by our group, a computational method, (docking), has been successfully applied to identify potential binders for a synthetic host.¹⁶ The same approach is used here for the identification of possible guest molecules for the capsule **1a•2a**. A docking study was performed with **1a•2a** and different guests. The actual binding properties of the selected guest molecules were subsequently tested by ¹H NMR spectroscopy.

5.2 Results and discussion

5.2.1 Synthesis

Compounds **2a** and **2b** were synthesized starting from calix[4]arene **3** (for the synthesis of **3** see Chapter 3, Scheme 3.1). After the formation of the corresponding tetra-acyl chloride derivative **4**, L-alanine methyl ester hydrochloride and L-lysine(t-Boc)-methyl ester hydrochloride were added to a CH₂Cl₂ solution of **4** affording the corresponding calix[4]arene tetraesters **5a** and **5b**. Hydrolysis using LiOH provided **2a** and **2b** (Scheme 5.1) which were fully characterized by NMR, ESI-MS and elemental analysis. The ¹H NMR spectra of both compounds in D₂O ([**2**] = 2 mM) display a well-resolved pattern indicating that under these conditions aggregation is not likely to happen. Moreover, no changes in the ¹H NMR spectrum were discernible upon dilution of concentrated solution of **2a** and **2b** in D₂O thus confirming their monomeric structure.



Scheme 5.1. (i) SOCl₂, CCl₄/DMF 50°C; (ii) L-alanine methyl ester, DMAP, Et₃N, dry CH₂Cl₂, rt; (iii) LiOH/H₂O/MeOH, THF, rt; (iv) L-lysine(t-Boc) methyl ester, DMAP, Et₃N, dry CH₂Cl₂ rt; (v) LiOH/H₂O/MeOH, THF, rt.

5.2.2 Characterization of the molecular capsules **1a•2a-b**

¹H NMR spectroscopy. Building blocks **1a** and **2** are readily soluble in H₂O and, remarkably, the 1:1 mixture of **1a** and **2** was also completely soluble in H₂O buffered at pH 9.2 (borate buffer). In the case of assembly **1a•2a** the ¹H NMR spectrum of the 1:1 mixture in buffered D₂O shows upfield shifts ($\Delta\delta_{\text{Ha}} = 0.22$ ppm, $\Delta\delta_{\text{Hb}} = 0.20$ ppm, $\Delta\delta_{\text{Hc}} = 0.25$ ppm) for the protons of the propyl amidinium chains of **1a** (Figure 5.1).

In analogy with what was observed for the previous tetrasulfonate-tetraamidinium capsule (see Figure 4.2, Chapter 4) this behavior can be attributed to the shielding provided by the aromatic walls of the calix[4]arene upon inclusion of the propyl side chain in the cavity of the capsule **1a•2a**. Additionally, there is a significant broadening of the propyl signals, most probably as the result of the hindered rotation around the propyl C-N bond. In contrast the signal of the aromatic protons of **2a** undergoes a downfield shift and sharpens upon formation of the complex (data not shown). An upfield shift is also observed for the α proton and the side chain protons of the alanine substituents of calix[4]arene **2a** ($\Delta\delta_{\text{H}\alpha} = 0.12$ ppm, $\Delta\delta_{\text{H}\beta} = 0.08$ ppm).

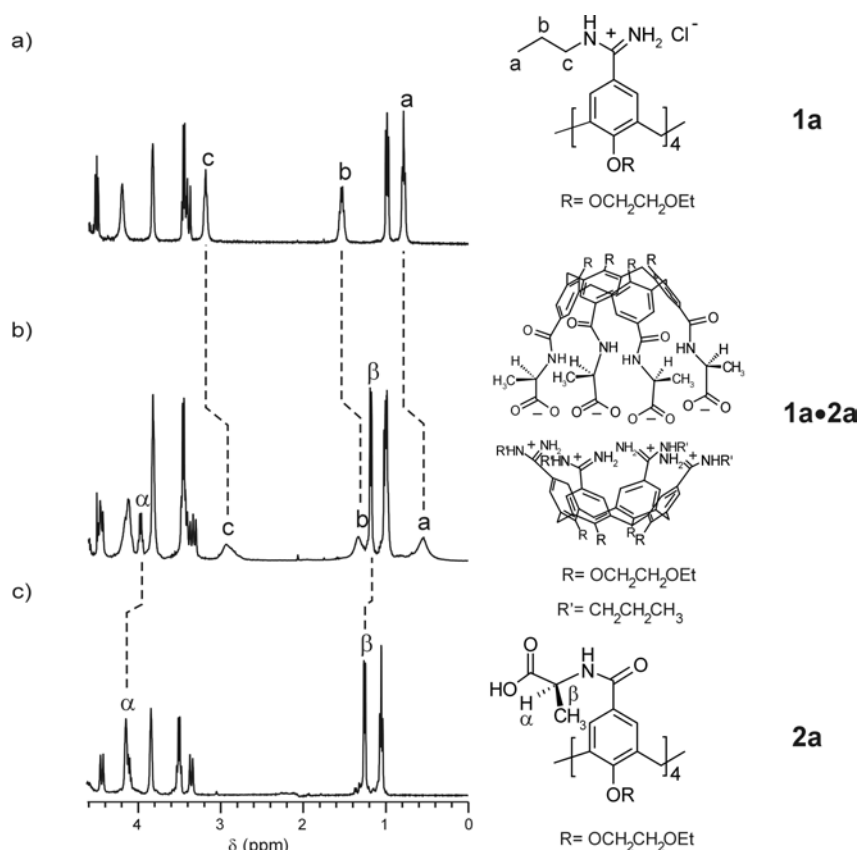


Figure 5.1. Portion of the ¹H NMR spectra (Na₂B₄O₇ × 10 H₂O, D₂O, 298 K) for a) **1a**; b) **1a•2a**; c) **2a**.

An equimolar solution of **1a** and **2b** in buffered D₂O provided a more complicated ¹H NMR spectrum. A general broadening of the signals is also observed and analogously to the assembly **1a•2a**, upfield shifts of the protons of the propyl chains are evident. A more resolved spectrum was obtained in CD₃OH/H₂O (*x*_{water} = 0.4) in the presence of borate buffer (Figure 5.2). Upfield shifts accompanied by broadening are observed for the protons of the propyl chains of **1a** ($\Delta\delta_{\text{Ha}} = 0.09$ ppm, $\Delta\delta_{\text{Hb}} = 0.08$ ppm, $\Delta\delta_{\text{Hc}} = 0.15$ ppm). An upfield shift ($\Delta\delta = 0.11$ ppm) of the signal of the aromatic protons of **1a** is also observed while small downfield shift changes are detectable for the protons of the methylene bridge of **1a**. The rest of the signals of **1a** do not undergo any significant changes ($\Delta\delta_{\text{H}\alpha} \leq 0.02$ ppm).

The signal of the aromatic protons H_g of **2b** (Figure 5.2) also experiences a small upfield shift ($\Delta\delta_{\text{Hg}} = 0.09$ ppm). Interestingly, the protons NH_h, H_e and H_f (Figure 5.2) corresponding to the amide bond, the α proton, and the proton of the first CH₂ of the lateral chains of the lysine, respectively, are all upfield shifted ($\Delta\delta_{\text{Hh}} = 0.21$ ppm, $\Delta\delta_{\text{He}} = 0.12$ ppm, $\Delta\delta_{\text{Hf}} = 0.06$ ppm), probably as a consequence of their proximity to the carboxylic groups involved in ionic interactions with the oppositely charged amidinium groups of **1a**. No changes were observed for the rest of the protons of the side chains. This finding indicates that the side chains of **2b** are most probably outside the capsule cavity.

Addition of an excess of either calix[4]arenes **1a** or **2a-b** to the 1:1 mixture of the components resulted in averaged signals for the free and complexed components indicating that the assembly formation is fast on the NMR time scale.

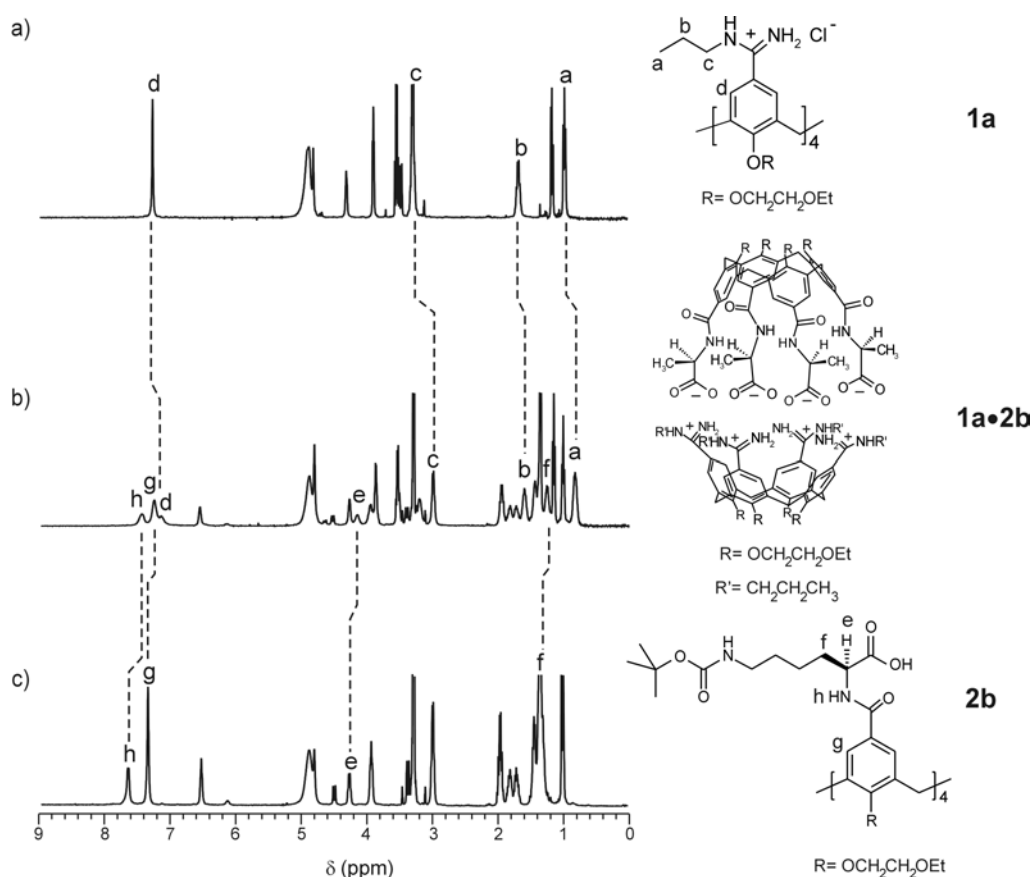


Figure 5.2. ^1H NMR spectra (borate buffer, $\text{CD}_3\text{OH}/\text{H}_2\text{O}$ ($x_{\text{water}} = 0.4$), 298 K) for a) **1a**; b) **1a•2b**; c) **2b**.

ESI mass spectrometry. Additional evidence for the proposed self-assembly motif came from ESI-MS. The spectrum of an equimolar mixture of **1a** and **2a** ($c = 0.1$ mM) in buffered H_2O shows a peak at m/z 1134 corresponding to the capsule $[(\mathbf{1a}\cdot\mathbf{2a})+2\text{Na}]^{2+}$ together with two other major peaks, one at m/z 1049 and the other at m/z 620 corresponding to $[(\mathbf{1a}-4\text{HCl})+\text{H}]^+$ and $[(\mathbf{2a}-\text{H}+\text{Na})+2\text{Na}]^{2+}$ respectively. Analogously, the ESI-MS spectrum of a 0.1 mM solution of the assembly **1a•2b** in buffered H_2O shows a doubly charged peak at m/z 1681 corresponding to the capsule $[(\mathbf{1a}\cdot\mathbf{2b})+2\text{Na}]^{2+}$ together with other two relatively intense signals, at m/z 1049 and at m/z 516 corresponding to $[(\mathbf{1a}-4\text{HCl})+\text{H}]^+$ and $[(\mathbf{1a}-4\text{HCl})+2\text{H}]^{2+}$ respectively.

ITC. The thermodynamic parameters for the self-assembly of the molecular capsules **1a•2a-b** were studied using ITC. To evaluate the effect that the side chains of **2a** and **2b** and the distance of the carboxylate groups from the calix[4]arene scaffold play in the assembly formation, self-assembly of **1a•3** was also investigated.

Titration experiments were carried out in MeOH/H₂O ($x_{\text{water}} = 0.4$) and in pure H₂O containing in both cases borate buffer (pH = 9.2, $I = 0.03$ M).

In MeOH/H₂O solution the formation of a 1:1 complex was observed for all the assemblies with association constants, K_a in the order of 10^5 M⁻¹ (Table 5.1 and Figure 5.3).

Analysis of the thermodynamic parameters shows negative values for both ΔH° and ΔS° that account for an exothermic, enthalpy driven association process. The gain in enthalpy is the result of the formation of four ionic interactions upon self-assembly of the molecular capsules. This favorable contribution overrides the cost in energy needed for the desolvation of the charged groups prior to the self-assembly process. The large unfavorable entropy change reflects instead a loss of degrees of freedom associated with self-assembly formation, thus indicating that the conformational restrictions and/or reorganization upon capsule formation are of importance.¹⁷

The formation of the complex **1a•3** is accompanied by a lower loss of entropy ($\Delta S^\circ = -66$ J K⁻¹mol⁻¹). In compound **3**, the carboxylate moieties are directly attached to the calix[4]arene scaffold allowing more preorganization than in **2a** and **2b**. Assembly **1a•2b** shows the largest negative value for ΔS° ($= -140$ J K⁻¹mol⁻¹) in MeOH/H₂O, indicative of a higher loss of entropy upon complex formation. Calix[4]arene **2b** is indeed less preorganized than **3** and **2a**, due to the long side chain of the lysine moieties, thus explaining the higher penalty in entropy paid for the formation of the molecular capsule **1a•2b**.

On the other hand, the small differences between the association constants determined for **1a•2a** and **1a•2b** ($\Delta \text{Log}K_a = 0.19$) suggest that under these conditions the binding strength is independent of the nature of the amino acidic moieties at the upper rim of the calix[4]arene scaffold. Moreover, comparison with assembly **1a•3** indicates that the strength of the binding is not affected by the structural differences of the anionic building components of the capsule: only a small decrease in association constant in the order $K_{a1a•3} > K_{a1a•2a} > K_{a1a•2b}$ is observed ($\Delta \text{Log}K_{a(1a•3-1a•2b)} = 0.37$).

In pure water differences in the thermodynamic of binding were determined for the formation of complexes **1a•2a-b** and **1a•3**. In general, when compared to the self-assembly in MeOH/H₂O, much less favorable values for ΔH° but more favorable (positive) values for ΔS° are observed. As depicted in Figure 5.3, the resulting

titration curves for the self-assembly of **1a•3** and **1a•2a** account for an exothermic process; while the binding curve for **1a•2b** is indicative of an endothermic binding event (*vide infra*).

A slight decrease in the association constant for both **1a•3** and **1a•2a** was found in H₂O vs MeOH/H₂O solution. This can be qualitatively explained considering the higher dielectric constant (ϵ) of the H₂O compared to MeOH/H₂O solution. The shielding of the electrostatic interactions depends in fact on the ϵ of the surrounding medium. The Coulombic interaction energy is proportional to ϵ^{-1} , i.e. higher ϵ results in a weaker binding.

The thermodynamic parameters indicate that the formation of **1a•3** and **1a•2a** in water is enthalpically favored. The formation of capsule **1a•2b** is instead more strongly entropically driven. The nature of the carboxylate-amidinium interactions should be similar for assemblies **1a•3**, **1a•2a** and **1a•2b**, thus the different behavior was rationalized considering the different length of the side chain of the amino acidic residues.¹⁸⁻¹⁹ Similar changes in thermodynamic of binding due to side chain lengths, have been observed by Hamilton²⁰ in the molecular recognition of tetraanionic peptides.

It is not unlikely that the flexibility of the lysine lateral chains could allow additional (intra- and/or intermolecular) interactions in solution. Most probably, prior to self assembling the functional groups of **2b** are involved in hydrogen bonding to surrounding water molecules and/or with neighboring amino acidic groups. In this respect, a study²¹ confirmed that there are only a low percentage of “buried” nitrogen or oxygen atoms of amide bonds in proteins that do not form hydrogen bonds with either the solvent or other amino acid residues. The complex formation involves the rupture of strong hydrogen bonds at the hydrocarbon/water interface and the release of highly structured water molecules. The water shell structure becomes more disordered explaining the large positive contribution of the entropy term ($\Delta S^\circ = 370 \text{ J K}^{-1} \text{ mol}^{-1}$). The large positive ΔH° value ($\Delta H^\circ = 74.7 \text{ kJ mol}^{-1}$) is most probably a reflection of the energy needed to set the solvent molecules free upon assembly formation.

Table 5.1. Association constants and thermodynamic parameters for the formation of assemblies **1a•3** and **1a•2** as determined by ITC at 298 K. [**1a**] = 1 mM, [**2a**], [**2b**], [**3**] = 0.1 mM.

Assembly	K_a (M^{-1})	ΔH° ($kJ\ mol^{-1}$)	ΔS° ($J\ K^{-1}\ mol^{-1}$)
1a•3 ^(a)	$(1.8 \pm 0.1) \times 10^5$	-49.7 ± 0.2	-66 ± 2
1a•3 ^(b)	$(1.5 \pm 0.7) \times 10^5$	-8.9 ± 0.2	69 ± 1
1a•2a ^(a)	$(1.4 \pm 0.2) \times 10^5$	-58.5 ± 0.4	-98 ± 1
1a•2a ^(b)	$(2.3 \pm 0.7) \times 10^4$	-12.3 ± 0.2	43 ± 2
1a•2b ^(a)	$(0.9 \pm 0.1) \times 10^5$	-69.9 ± 0.3	-140 ± 1
1a•2b ^(b)	$(1.7 \pm 0.1) \times 10^6$	74.7 ± 0.4	370 ± 2

a) MeOH/H₂O ($x_{\text{water}} = 0.4$), borate buffer, $I = 0.03\ M$, pH = 9.2; b) H₂O, borate buffer, $I = 0.03\ M$, pH = 9.2.

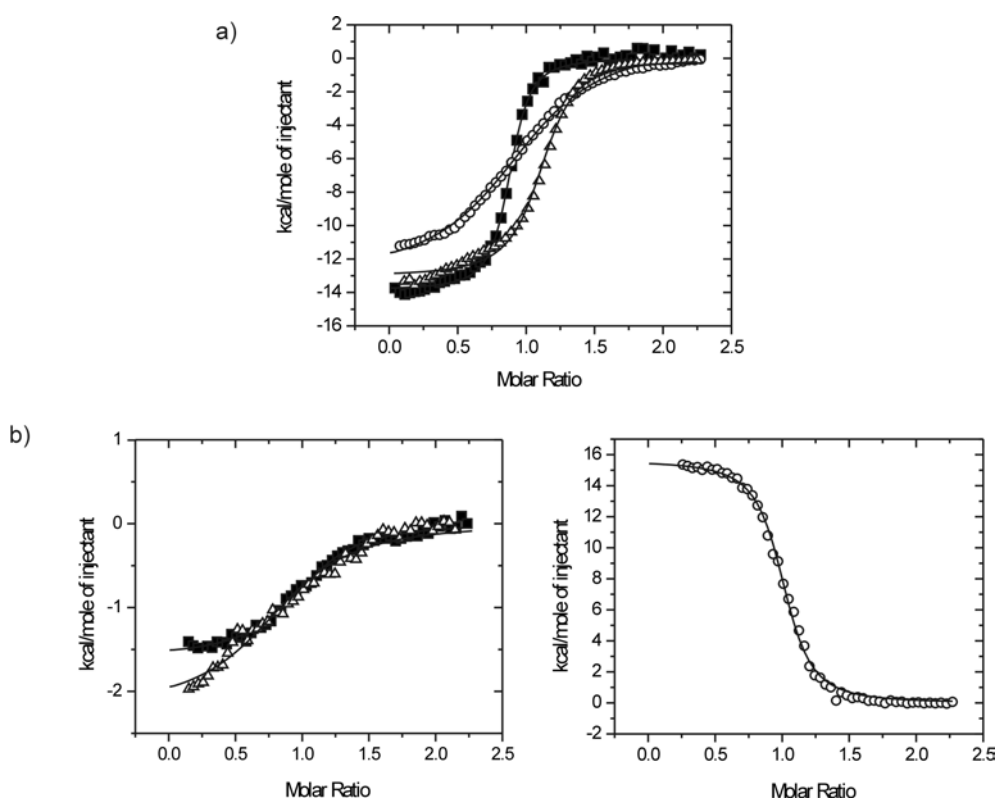


Figure 5.3. ITC binding curves for capsule formation in a) MeOH/H₂O ($x_{\text{water}} = 0.4$) at 298 K, borate buffer, $I = 0.03\ M$, pH = 9.2; b) H₂O at 298 K, borate buffer, $I = 0.03\ M$, pH = 9.2. ■ = **1a•3**, △ = **1a•2a**, ○ = **1a•2b**.

5.2.3 Guest encapsulation in 1a•2a

5.2.3.1 Charged guest: *N*-methylquinuclidinium

Molecular mechanics calculations showed that the *N*-methylquinuclidinium (NMQ) cation (Figure 5.4) exhibits a good fit for encapsulation in the assembly **1a•2a**. ^1H NMR experiments were performed in $\text{D}_2\text{O}/\text{Na}_2\text{B}_4\text{O}_7 \times 10 \text{ H}_2\text{O}$ and the propyl side chain of **1a**, was used as a probe to detect guest encapsulation (Figure 5.4).

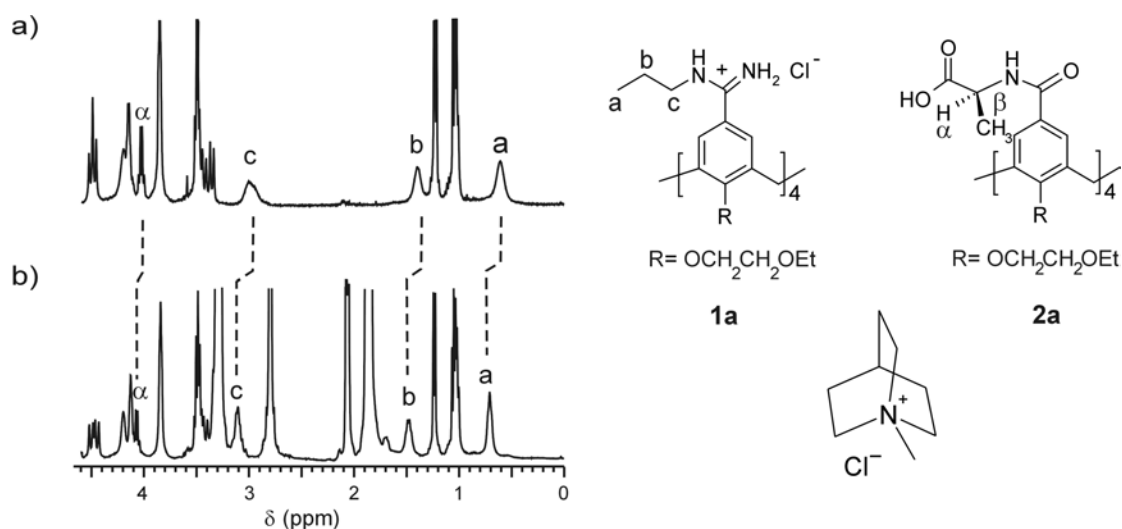


Figure 5.4. Portion of the ^1H NMR spectra ($\text{Na}_2\text{B}_4\text{O}_7 \times 10 \text{ H}_2\text{O}$, D_2O , 298 K) for a) **1a•2a**; b) **1a•2a** + 30 eq. of NMQ chloride.

Changes in the chemical shifts of the signals of the protons of the amidinium side chains ($\Delta\delta_{\text{Ha}} = 0.17$ ppm, $\Delta\delta_{\text{Hb}} = 0.15$ ppm, $\Delta\delta_{\text{Hc}} = 0.17$ ppm) were observed upon addition of 30 eq. of *N*-methylquinuclidinium chloride to a 1.2 mM solution of **1a•2a** (Figure 5.4). A slight downfield shift was also observed for the α proton of compound **2a**. The chemical shifts of the other protons, including the one of the guest, did not show significant changes. The fact that there is only one set of resonances of the guest indicates that the encapsulation is a fast process on the NMR time scale. Therefore, the chemical shifts are simply averaged signals between free and complexed NMQ. A ^1H NMR titration was performed by adding increasing amounts of NMQ chloride to a solution of **1a•2a** giving an association constant $K_a = 36 \pm 12 \text{ M}^{-1}$.

An experiment to detect chemical shift changes in the guest by adding increasing amounts of the capsule to a $1 \times 10^{-4} \text{ M}$ solution of the guest in $\text{D}_2\text{O}/\text{Na}_2\text{B}_4\text{O}_7 \times 10$

H₂O was also performed. Due to solubility reasons only an excess of 10 eq. of the capsule could be reached which did not result in significant changes in the guest's resonances ($\Delta\delta = 0.005$ ppm).

Interestingly, addition of an excess (up to 100 eq.) of acetylcholine (Ach) and tetramethylammonium (TMA) chloride to a solution of **1a•2a** did not show any indication for guest-encapsulation. Presumably, even if these cations possess the appropriate shape they do not have the right volume to fit into the capsule's cavity. As reported by Rebek, binding of molecules in the cavity of a molecular capsule in solution can be expected when the packing coefficient (PC), i.e. the ratio of the guest volume to the host volume is around 0.55.²² Most probably the PCs for ACh and TMA are too low for encapsulation to occur.

A calorimetric titration of **1a** with **2a** in presence of a large excess (60 eq.) of NMQ chloride was performed. The experimental data were consistent with a 1:1 binding mode with an association constant K_a on the same order of magnitude as the one found in absence of the salt which rules out the possibility that the NMQ, being a charged guest, dissociates the capsule.

The encapsulation of the NMQ cation was also supported by mass spectrometry. The ESI-MS spectrum of an aqueous solution of **1a•2a** containing 30 equiv. of NMQ chloride shows signals at m/z of 2222.6 and 2347.7 corresponding to $[(\mathbf{1a}\cdot\mathbf{2a})+\text{H}]^+$ and $[(\mathbf{1a}\cdot\mathbf{2a})+\text{NMQ}]^+$, respectively (Figure 5.5). Analogous results were obtained using FAB mass spectrometry (FAB-MS). Signals at m/z 2222.6 and 2244.4 corresponding to $[(\mathbf{1a}\cdot\mathbf{2a})+\text{H}]^+$ and $[(\mathbf{1a}\cdot\mathbf{2a})+\text{Na}]^+$ respectively, and m/z 2347.7 and 2369.7 corresponding to $[(\mathbf{1a}\cdot\mathbf{2a})+\text{NMQ}]^+$ and $[(\mathbf{1a}\cdot\mathbf{2a}-\text{H}+\text{Na})+\text{NMQ}]^+$, respectively, were observed. An additional experiment with FAB-MS was performed: the addition of a small amount of K₂CO₃ resulted in a shift of the peaks of 16 m.u. which confirms the molecular weight of the complexes.

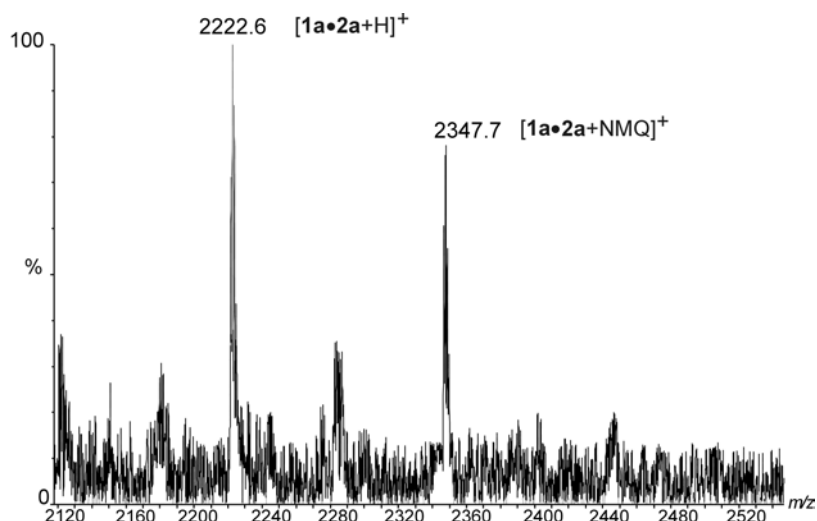


Figure 5.5. Portion of the ESI-MS spectrum ($D_2O/Na_2B_4O_7 \times 10 H_2O$) of **1a•2a** + 30 eq. of NMQ chloride.

5.2.3.2 Neutral molecules: docking study

In order to identify guest molecules for the molecular capsule **1a•2a**, a computational method (docking) was utilized which allowed a rapid screening of molecular databases, thus providing a number of potential guests. Docking techniques are often used in medicinal chemistry to identify new leads or to suggest possible binding modes of known guests.²³⁻²⁵ Applications involving the screening of molecular databases requires a simplified representation of the binding pocket of a protein or receptor from a crystal structure by, for instance, a number of spheres or interaction site points. Subsequently, a large number of potential substrates are fitted into this binding site model and the docking algorithm decides whether the interaction energy of each guest in the binding site is favorable or unfavorable.

In the absence of an X-ray crystal structure, a molecular modeling study provided the conformation of the molecular capsule **1a•2a** which was used for docking of the available chemicals database (ACD) (Figure 5.6).

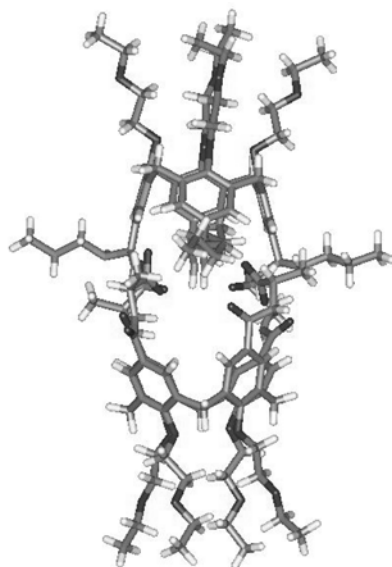


Figure 5.6. Conformation of the molecular capsule **1a•2a** used for docking study. The propyl chains of **1a** are pointing outside the capsule's cavity.

Docking into the molecular capsule **1a•2a** was a challenging exercise due to the small size/volume and the extremely charged nature of the assembly. From the ACD database we picked the molecules having molecular weights lower than 250. After filtering out molecules having reactive functionalities, a database of 27999 compounds was obtained. A further selection was made retaining only those molecules possessing a 0 or 1 charge. This yielded a database containing 22818 molecules for docking. Two different scoring functions were used for docking of the selected ACD molecules to **1a•2a**. The “energy scoring”, which applies a grid-based representation of the AMBER force field, provided a large number of neutral molecules having hydrogen bond donor groups (-OH and/or -NH) for the interaction with the oxygen of the ethylene glycol chains located at the lower rim of the components of the capsule **1a•2a**. Most of the molecules had also polar groups that could interact with the belt of carboxylate-amidinium moieties. The “chemical scoring” function provided instead quite hydrophobic molecules with some polar functionalities that could interact with the charges that held the capsule together. Based on cost and commercial availability a restricted number of guest molecules were selected for experimental screening.

To obtain a rapid indication as to whether a guest binds or not, ^1H NMR experiments were performed. Guest encapsulation was primarily studied by ^1H NMR, adding first one equivalent followed by an excess of the pure substances to a solution of the preformed molecular capsule **1a•2a** in $\text{D}_2\text{O}/\text{Na}_2\text{B}_4\text{O}_7 \times 10 \text{ H}_2\text{O}$.

Unfortunately, most of the guest molecules provided by the docking studies are very insoluble in $\text{D}_2\text{O}/\text{Na}_2\text{B}_4\text{O}_7 \times 10 \text{ H}_2\text{O}$ and their addition to the host solution resulted in precipitation. A further limitation was due to the fact that **1a** undergoes hydrolysis over time or with heat. Therefore, no heating was allowed for dissolution of the guest molecules and their encapsulation, limiting the amount of studies that could be performed.

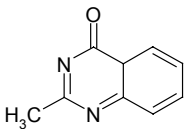
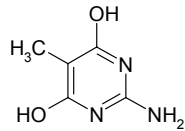
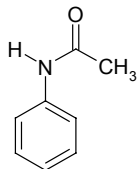
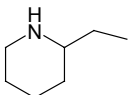
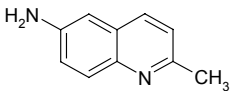
The addition of an excess (varying from 25 to 30 eq.) of the compounds listed in Table 5.2 to a solution of **1a•2a** shifted the signals for the protons of the propyl side chains of **1a** downfield.²⁶ This was considered as an indication for guest encapsulation.

The addition of 1 eq. of 2-methyl-4-quinazolinone (**6**) to a 0.5 mM solution of **1a•2a** resulted in small downfield shifts for all the resonances of the guest ($\Delta\delta_{\text{max}} = 0.07$ ppm) while the signals of the protons of the propyl side chains did not move. When a large excess of **4** was added, downfield shifts for the protons of the propyl chain were observed (Table 5.2) while the guest's signals moved upfield ($\Delta\delta_{\text{max}} = -0.01$ ppm) towards the values for the free guest. The addition of 1 eq. of **7**, **8** or **9** to a 0.5 mM solution of **1a•2a** did not cause any changes either in the guests or in the host. Nevertheless, when a large excess of these guests was added, downfield shifts for the protons of the propyl chains of **1a** were observed (Table 5.2) while the guest's signals did not experience any shifts.

For all of the guest molecules mentioned above, small but reproducible changes were also observed for the methylene protons, the α and the CH_3 protons of the alanine moieties of **2a** ($\Delta\delta \leq 0.05$ ppm). Moreover, for guest **9** additional sharpening of the aromatic protons was observed.

ITC calorimetry was used to attempt the determination of the binding constants for the encapsulation. However, for solubility reasons the association constants could not be determined experimentally. (Titrations of 1 mM solutions of **1a•2a** with 10 mM of the guest molecules in H_2O /borate produced either not enough heat or a heat contribution which was much lower than the heat of dilution).

Table 5.2. ^1H NMR chemical shift changes (downfield) for the protons of the propyl side chains of **1a** upon addition of an excess (25-30 eq.) of guest molecules to the capsule **1a•2a**. ($\text{Na}_2\text{B}_4\text{O}_7 \times 10 \text{H}_2\text{O}$, D_2O , 298 K). (For assignment of H_a , H_b and H_c see Figure 5.1).

Guest	$\Delta\delta_{\text{Ha}}$	$\Delta\delta_{\text{Hb}}$	$\Delta\delta_{\text{Hc}}$
 6 2-methyl-4-quinazolinone	0.13	0.06	0.1
 7 2-amino-4,6-dihydroxy-5-methyl pyrimidine	0.09	0.08	0.07
 8 acetanilide	0.13	0.05	0.07
 9 ethylpiperidine	-	-	0.04
 10 6-amino-2-methylquinoline	0.03	0.03	0.02

¹H NMR studies on the encapsulation of 6-amino-2-methylquinoline

Interestingly, upon addition of an excess of 6-amino-2-methylquinoline (**10**) to a 0.5 mM solution of **1a•2a** significant upfield shifts of the resonances of the guest were observed, accompanied by small downfield shifts for the protons of the propyl chains of **1a** (Table 5.3).

According to the docking studies the guest is expected to be included into the capsule with its -NH₂ group pointing towards the first oxygen of one of the ethylene glycol chains located at the lower rim of the calix[4]arene. In this way the protons of the aniline ring of the guest would be residing in the core of the calix[4]arene and therefore experience the shielding provided by the aromatic rings of the aromatic scaffold.

Additionally, ¹H NMR experiments were carried out to assess whether the upfield shifts observed for the resonances of the guest were generated from the binding to one of the calix[4]arene components or indeed to inclusion in the capsule's cavity. Addition of 1 eq. of **2a** to a 1 mM solution of **10** in D₂O/Na₂B₄O₇ × 10 H₂O caused an upfield shift for the protons of the guest, (Figure 5.7 and Table 5.3) accompanied by an upfield shift change for the α proton of the alanine moieties. These results indicate that there is an interaction between the guest and **2a**, most likely an inclusion complex of the aniline ring of the guest into the core of the calix[4]arene as suggested by the strongest upfield shifts experienced by the protons H_i, H_l, H_m. (On the contrary, the addition of 1 eq. of **1a** to a 1 mM solution of the same guest led only to slight upfield shifts of the guest's resonances). The subsequent addition of 1 eq. of the tetraamidinium calix[4]arene **1a** caused a downfield shift of the resonances of the guest towards the position of the free guest (Figure 5.7) while the tetraamidinium calix[4]arene **1a** shows the characteristic upfield shifted signals for the protons of the propyl side chains indicative for capsule formation. The partial downfield shift experienced by the guest's resonances can be ascribed either to a partial dissociation of the complex **10•2a** upon addition of **1a** and subsequent formation of the capsule **1a•2a** (which results in an increase in the amount of guest free in solution), or simply to a rearrangement of the guest inside the cavity of **2a** upon formation of the complex **1a•10•2a** (Scheme 5.2).

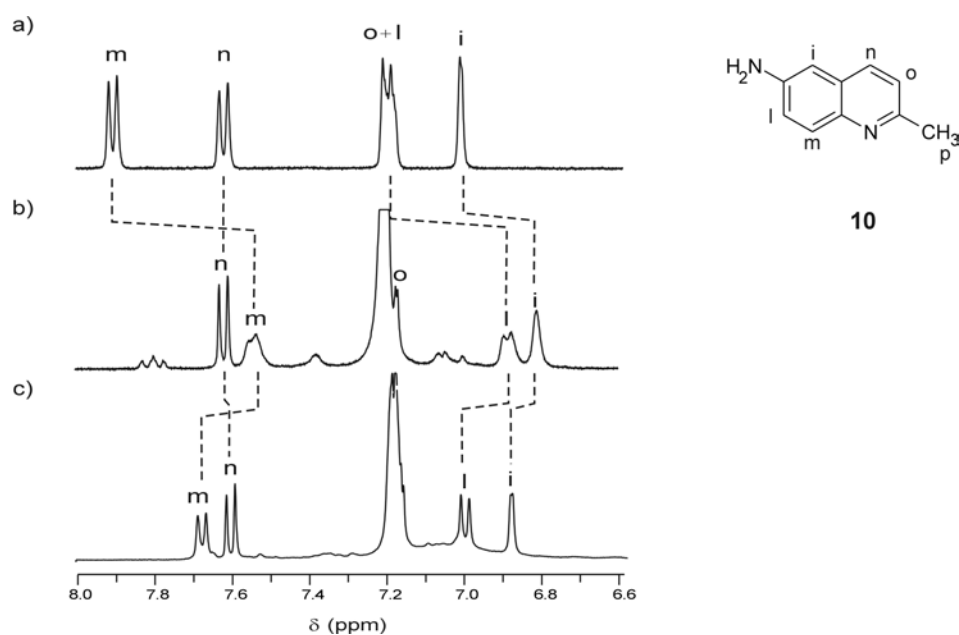
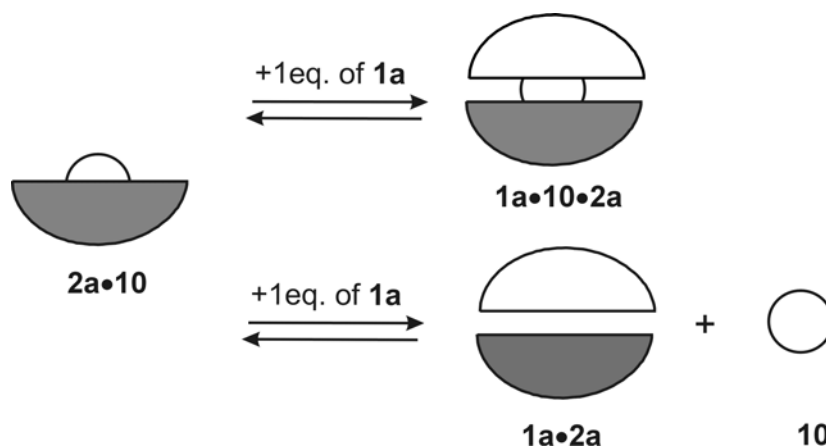


Figure 5.7. Portion of the ¹H NMR spectra (Na₂B₄O₇ × 10 H₂O, D₂O, 298 K) of a) 6-amino-2-methylquinoline **10**; b) **10** + 1 eq. **2a**; c) **10** + 1 eq. **2a** + 1 eq. **1a**.

Table 5.3. ¹H NMR chemical shift changes for the protons of 6-amino-2-methylquinoline (**8**) for the binding to the tetraalanine calix[4]arene **2a** and to the capsule **1a•2a** (Na₂B₄O₇ × 10 H₂O, D₂O, 298 K). (For assignment of the protons see Figure 5.7).

	10	10 + 1eq. 2a	10 + 1eq. 1a•2a
	δ _{free} (ppm)	Δδ (ppm) = δ - δ _{free}	Δδ (ppm) = δ - δ _{2a}
H _i	7.04	0.24	-0.16
H _l	7.23	0.35	-0.25
H _m	7.94	0.32	-0.21
H _n	7.68	0.12	-0.1
H _o	7.22	0.04	-
H _p	2.51	0.085	-0.054



Scheme 5.2. Schematic representation of the two possible complexes formed upon addition of 1 eq of **1a** to a solution of **2a•10**.

As a control experiment, an excess of calix[4]arene **1a** was added to the 1:1 solution of **1a•2a** and **10**. Small additional upfield shifts in the resonances of the protons of the guest were observed upon addition of **1a**. Nevertheless, if the guest was expelled from the cavity all the guest signals should have had the chemical shifts of the free guest. The fact that the upfield shifts have been retained at least in part even in the presence of an excess of tetraamidinum calix[4]arene **1a** is a good indication that the guest is held inside the capsule cavity.

A ^1H NMR titration was performed by adding increasing amounts of capsule **1a•2a** to a solution of **10** in $\text{D}_2\text{O}/\text{Na}_2\text{B}_4\text{O}_7 \times 10 \text{ H}_2\text{O}$. The titration caused small but reproducible changes in the resonances of the guest.²⁷ The corresponding isotherm could be fitted to a 1:1 model producing a binding constant K_a of $2 \times 10^3 \text{ M}^{-1}$ (Figure 5.8).

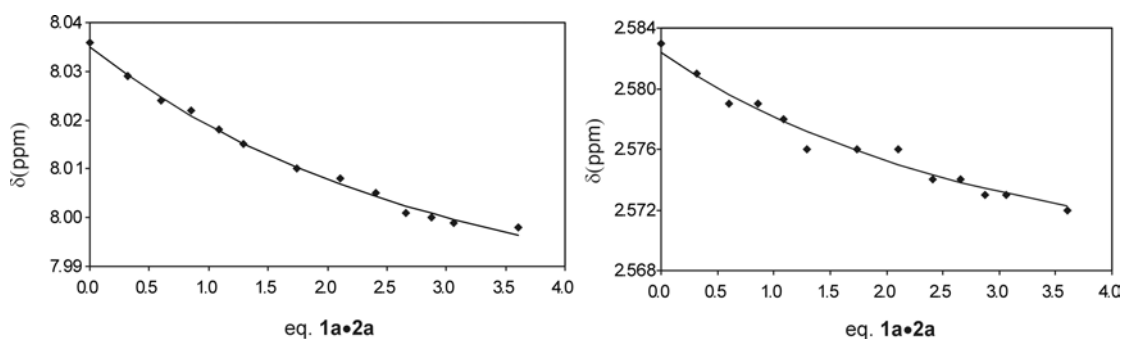


Figure 5.8. Chemical shift changes for protons H_m (left) and H_p (right) experienced by the 6-amino-2-methylquinoline (**10**) upon addition of increasing amount of **1a•2a**. The line represents the fit to a 1:1 binding model.

5.3 Conclusions

The results reported in this chapter demonstrate that water soluble molecular capsules are easily obtained upon introduction of amino acidic groups at the upper rim of one of the calix[4]arene components. The strength of the ionic interactions allows the formation of stable molecular assemblies in pure water with association constants $K_a \sim 10^5 \text{ M}^{-1}$.

ITC studies have shown that although the association constants for the assembly of the molecular capsules **1a•2a** and **1a•2b** in water are similar, the side chain length of the different amino acidic moieties strongly influences the thermodynamic parameters of binding.

The encapsulation properties of the molecular capsule **1a•2a** in water have been also investigated. As demonstrated, docking against **1a•2a** allowed the identification of several guest molecules that bind to the capsule.

The ability of **1a•2a** to encapsulate guest molecules in water could open new ways for the use of supramolecular structures as molecular receptors or drug delivery systems in physiological media. For example, in the lower pH of the tumor environment and the even lower pH of tumor cell endosomes following endocytosis, an anionic calixarene could be protonated and thereby open the ionic capsule and release the encapsulated anticancer drug, increasing the selectivity of drug action against tumors and decreasing the side effects.

5.4 Experimental section

5.4.1 General information and instrumentation

The reagents used were purchased from Aldrich or Acros Chimica and used without further purification. All the reactions were performed under nitrogen atmosphere. Analytical thin layer chromatography was performed using Merk 60 F₂₅₄ silica gel plates. ¹H and ¹³C NMR spectra were recorded on a Varian Unity INOVA (300 MHz) or a Varian Unity 400 WB NMR spectrometer. ¹H NMR chemical shift values (300 MHz) are reported as δ in ppm using the residual solvent signal as an internal standard (CHD₂OD, δ = 3.30, HDO, δ = 4.67). ¹³C NMR chemical shift values (100 MHz) are reported as δ in ppm using the residual solvent signal as an

internal standard (CD_3OD , $\delta = 49.0$). Infrared spectra were recorded on a FT-IR Perkin Elmer Spectrum BX spectrometer and only characteristic absorptions are reported. Fast atom bombardment (FAB) mass spectra were recorded with a Finnigan MAT 90 spectrometer. Electrospray ionization (ESI) mass spectra were recorded on a Micromass LCT time-of-flight (TOF) mass spectrometer. Samples were introduced using a nanospray source. Elemental analyses were carried out using a 1106 Carlo-Erba Strumentazione element analyzer. Compound **3** was synthesized according to literature procedures.²⁸

5.4.2 Binding studies

Calorimetric measurements. The titration experiments were carried out using a Microcal VP-ITC microcalorimeter with a cell volume of 1.4115 mL. The formation of the assemblies **1a•2a-b** and **1a•3** have been studied adding aliquots of a 1 mM solution of **1a** to a 0.1 mM solution of **2a-b** or **3**, in the calorimetric cell, and monitoring the heat change after each addition. Dilution effects were determined in a second experiment by adding the same 1 mM solution of **1a** into the solvent and subtracting this contribution from the raw titrations to produce the final binding curves. The association constants were determined by applying a 1:1 binding model using Microcal Origin[®].

¹H NMR spectroscopy. The titrations were performed in a 10 mM solution of $\text{Na}_2\text{B}_4\text{O}_7 \times 10 \text{ H}_2\text{O}$ in D_2O . A solution containing 1 mM of **1a•2a** and 200 mM of *N*-methylquinuclidinium chloride was added in numerous aliquots to a 1 mM solution of **1a•2a**, and the observed chemical shift was recorded after each addition.

In the case of 6-amino-2-methylchinoline (**10**) titrations were carried out by adding increasing amounts of a solution containing 0.3 mM of **1a•2a** and 1.0 mM of 6-amino-2-methylchinoline (**10**) to a 0.3 mM solution of **1a•2a** and following the chemical shift changes of **10**. The binding of **10** to **1a** and **2a** was evaluated in separate titrations. The association constants were calculated by fitting the experimental spectral changes to a 1:1 binding model.

5.4.3 Docking

The molecular capsule **1a•2a** with *N*-methylquinuclidinium as a guest, (the most bulky known ligand to create the maximum cavity inside the host), was carried out with Quanta97,²⁹ and minimized with CHARMM.³⁰⁻³² The minimized structure was used for docking with DOCK 4.0.³³ The minimized *N*-methylquinuclidinium coordinates were used as spheres to match with heavy atoms of ligands from the ACD. From the ACD database the molecules having molecular weights lower than 250 were picked. After filtering out molecules having reactive functionalities a database of 27999 compounds was obtained. The selection was further refined, retaining only those molecules possessing a 0 or 1 charge.

This yielded a database containing 22818 molecules for docking. All ACD compounds were docked in a single CORINA³⁴ generated conformation with Gasteiger-Marsili³⁵ charges. Scoring of the interactions with the host was done using two different scoring functions: a gridded version of the AMBER³⁶ force field intermolecular energy and a scoring function called “chemical scoring”. The 250 best docking results for the host were visually inspected with VIDA.

5.4.4 Synthesis

5,11,17,23-(carbonyl-*N*-L-alanine)-25,26,27,28-tetrakis(2-ethoxyethoxy) calix[4]arene (2a)

Compound **3** (340 mg, 0.38 mmol) was dissolved in CCl₄ (1mL) and 1 drop of DMF under N₂. SOCl₂ (0.15 mL, 2.10 mmol) was added to the solution at 0 °C and stirred for 2h at 50 °C. The solvent was removed under vacuum to afford compound **4** which, without further purification was dissolved in dry CH₂Cl₂ (5 mL) and added to a mixture of H-L-Ala-OMe·HCl (222 mg, 1.59 mmol, 4.4 eq.), DMAP (17.7 mg, 0.145 mmol, 0.4eq.) and Et₃N (0.47 mL, 3.4 mg, 9.4 eq.) in dry CH₂Cl₂ (10 mL). The reaction mixture was stirred under N₂ for 24 hours at 25 °C. The reaction course was followed by TLC (silica gel, CH₂Cl₂/acetone 5:1). The reaction mixture was diluted with ethyl acetate and washed with citric acid (0.5 M), NaHCO₃ and brine. The solvent was then removed under vacuum and compound **5a** purified by column chromatography using toluene/ethanol (95:5) as the eluent. **5a** (200 mg, 0.16 mmol, 1eq.) was dissolved in a 3:1:1 solution of MeOH/H₂O/THF (7 mL) and added to a 3:1

MeOH/H₂O (4 mL) solution of LiOH (76.6 mg, 3.2 mmol). The reaction was stirred for 24 hours at 25 °C. The solvent was then removed under vacuum. Upon re-dissolution in H₂O and addition of 1N HCl compound **2a** was obtained as a white precipitate. Yield: 54%. ¹H NMR (300 MHz, CD₃OD) δ 7.38 (s, 4H), 7.35 (s, 4H), 4.68 (d, 4H, *J*=13.2), 4.33 (q, 4H, *J*=7.5), 4.26 (t, 8H, *J*=4.8), 3.90 (t, 8H, *J*=4.8), 3.55 (q, 8H, *J*=7.2), 3.33 (d, 4H, *J*=13.2), 1.45 (d, 12H, *J*=7.2), 1.21 (t, 12H, *J*=7.2). ¹³C NMR (300 MHz, CD₃OD) δ 170.63, 163.41, 154.51, 130.26, 130.10, 123.57, 123.07, 69.0, 64.98, 61.84, 26.35, 25.10, 12.67, 10.58. IR (KBr) 3365, 2977, 1732, 1621, 1538, 1456, 1209, 1120. MS (ESI-MS): *m/z* 1194.5 ([M+Na]⁺, calcd. 1194.3). Anal. calcd. for C₆₀H₇₆N₄O₂₀: C 61.42, H 6.53, N 4.75; found: C 62.07, H 6.83, N 4.21.

5,11,17,23-(carbonyl-*N*^t-Boc-L-lysine)-25,26,27,28-tetrakis(2-ethoxyethoxy) calix[4]arene (2b)

Compound **3** (340 mg, 0.38 mmol) was dissolved in CCl₄ (1mL) and 1 drop of DMF under N₂. SOCl₂ (0.15 mL, 2.10 mmol) was added to the solution at 0 °C and stirred for 2h at 50 °C. The solvent was removed under vacuum to afford compound **4** which, without further purification was dissolved in dry CH₂Cl₂ (5 mL) and added to a mixture of H-L-Lys(t-Boc)-OMe·HCl (490 mg, 1.82 mmol, 4.4 eq.), DMAP (20.28 mg, 0.166 mmol, 0.4eq.) and Et₃N (0.5 mL, 3.65 mmol, 9.4 eq.) in dry CH₂Cl₂ (10 mL). The reaction mixture was stirred under N₂ for 24 hours at 25 °C. The reaction course was followed by TLC (silica gel, CH₂Cl₂/acetone 5:1). The reaction mixture was diluted with ethyl acetate and washed with citric acid (0.5 M), with NaHCO₃ and with brine. The solvent was then removed under vacuum to afford compound **5b** which was purified by column chromatography using toluene/ethanol (90:1) as the eluent. Compound **5b** (200 mg, 0.16 mmol, 1eq.) was dissolved in a 3:1:1 solution of MeOH/H₂O/THF (7 mL) and added to a 3:1 MeOH/H₂O (4 mL) solution of LiOH (76.6 mg, 3.2 mmol). The reaction was stirred for 24 hours at 25 °C. The solvent was then removed under vacuum. Upon re-dissolution in H₂O and addition of 1N HCl compound **2b** was formed as a white precipitate. Yield: 45%. ¹H NMR (400 MHz, CD₃OD) δ 7.38 (s, 4H), 7.36 (s, 4H), 4.69 (d, 4H, *J*=10.6), 4.42 (t, 4H, *J*=7.2), 4.26 (t, 8H, *J*=6.8), 3.91 (t, 8H, *J*=6.8), 3.56 (q, 8H, *J*=9.2), 3.35 (d, 4H, *J*=10.2), 3.04 (t, *J*=8.8) 1.84 (m, 8H), 1.48 (m, 16H) 1.40(m+s, 16H+36H), 1.20 (t, 12H, *J*=9.6). ¹³C

NMR (CD₃OD, CDCl₃) δ 176.01, 170.05, 160.61, 158.46, 136.13, 129.59, 129.14, 79.82, 75.02, 71.00, 67.40, 54.42, 41.22, 32.15, 30.64, 28.84, 24.58, 15.72. IR (KBr) 3365, 2977, 1732, 1621, 1538, 1456, 1209, 1120. MS (ESI-MS): m/z 1824.5 ([M+Na]⁺, calcd. 1823.9). Anal. calcd. for C₉₂H₁₃₆N₈O₂₈: C 61.32, H 7.61, N 6.22; found: C 60.64, H 7.39, N 6.47.

5.5 References and notes

1. Hof, F.; Craig, S. L.; Nuckolls, C.; Rebek, J. Jr. *Angew. Chem. Int. Ed.* **2002**, *41*, 1488-1508.
2. Caulder, D. L.; Brückner, C.; Powers, R. E.; Köning, S.; Parac, T. N.; Leary, J. A.; Raymond, K. N. *J. Am. Chem. Soc.* **2001**, *123*, 8923-8938.
3. Caulder, D. L.; Powers, R. E.; Parac, T. N.; Raymond, K. N. *Angew. Chem. Int. Ed.* **1998**, *37*, 1840-1843.
4. Kusukawa, T.; Fujita, M. *J. Am. Chem. Soc.* **1999**, *121*, 1397-1398.
5. Fox, O. D.; Dalley, N. K.; Harrison, R. G. *J. Am. Chem. Soc.* **1998**, *120*, 7111-7112.
6. Fox, O. D.; Leung, J. F. Y.; Hunter, J. M.; Dalley, N. K.; Harrison, R. G. *Inorg. Chem.* **2000**, *39*, 783-790.
7. Fujita, M.; Umemoto, K.; Yoshizawa, M.; Fujita, N.; Kusukawa, T.; Biradha, K. *Chem. Commun.* **2001**, 509-518.
8. Umemoto, K.; Tsukui, H.; Kusukawa, T.; Biradha, K.; Fujita, M. *Angew. Chem. Int. Ed.* **2001**, *40*, 2620-2622.
9. Lee, S. B.; Hong, J.-I. *Tetrahedron Lett.* **1998**, *39*, 4317-4320.
10. Takeda, N.; Umemoto, K.; Yamaguchi, K.; Fujita, M. *Nature* **1999**, *398*, 794-799.
11. Fiammengo, R.; Timmerman, P.; de Jong, F.; Reinhoudt, D. N. *Chem. Commun.* **2000**, 2313-2314.

12. Grawe, T.; Schrader, T.; Gurrath, M.; Kraft, A.; Osterod, F. *J. Phys. Org. Chem.* **2000**, *13*, 670-673.
13. Hamilin, B.; Jullien, L.; Derouet, C.; Herve' du Penhoat, C.; Berthault, P. *J. Am. Chem. Soc.* **1998**, *120*, 8438-8447.
14. Zadnard, R.; Schrader, T.; Grawe, T.; Kraft, A. *Org.Lett.* **2002**, *4*, 1687-1690.
15. Grawe, T.; Schrader, T.; Gurrath, M.; Kraft, A.; Osterod, F. *Org. Lett.* **2000**, *2*, 29-32.
16. de Jong, M. R.; Knegt, R. M. A.; Grootenhuis, P. D. J.; Huskens, J.; Reinhoudt, D. N. *Angew. Chem. Int. Ed.* **2002**, *41*, 1004-1008.
17. Fiammengo, R.; Crego-Calama, M.; Timmerman, P.; Reinhoudt, D. N. *Chem. Eur. J.* **2003**, *9*, 784-792.
18. Gohlke, H.; Klebe, G. *Angew. Chem. Int. Ed.* **2002**, *41*, 2644-2676.
19. Calderone, C. T.; Williams, D. H. *J. Am. Chem. Soc.* **2001**, *123*, 6262-6267.
20. Salvatella, X.; Pecuh, M. W. G. M.; Jain, R. K.; Sanchez-Quesada, J.; de Mendoza, J.; Hamilton, A. D.; Giralt, E. *Chem. Commun.* **2000**, 1399-1400.
21. McDonald, I. K.; Thornton, J. M. *J. Mol. Biol.* **1994**, *238*, 777-793.
22. Mecozzi, S.; Rebek, J. Jr. *Chem. Eur. J.* **1998**, *4*, 1016-1022.
23. Kuntz, D. *Science* **1992**, *257*, 1078-1082.
24. Walters, P. A.; Stahl, M. T.; Murko, M. A. *Drug Discov. & Develop.* **1998**, *1*, 16-27.
25. Kubinyi, H. *Curr. Opin. Drug Discov. & Develop.* **1998**, *3*, 160-178.
26. No changes were observed upon addition of either 1 eq. or an excess of the following compounds: 1,1-diethylpropargilamine, 2,5-dichlorothiophene, 2,6-dihydroxynaphtalene, 2-methylbenzofuran, norbornane, pyridine, *p*-xylene, 1,4-diiodobenzene, ethylpropionate.

27. Under the same experimental conditions, no binding isotherms could be obtained for the titrations of **10** with **1a** or **2a**.
28. Larsen, M.; Jørgensen, M. *J. Org. Chem.* **1996**, *61*, 6651-6655.
29. Quanta was bought from Molecular Simulations Inc., B. M. U.
30. Brooks, B. R.; Brucoleri, R. E.; Olafsen, B. D.; States, D. J.; Swaminathan, S.; Karplus, M. *Comput. Chem.* **1983**, *4*, 187-217.
31. Momany, F. A.; Klimkowski, V. J.; Schäfer, L. *J. Comput. Chem.* **1990**, *11*, 654-662.
32. Momany, F. A.; Rone, R.; Kunz, H.; Frey, R. F.; Newton, S. Q.; Schäfer, L. *J. Mol. Structure* **1993**, *286*, 1-18.
33. Ewing, T. J. A.; Kuntz, I. D. *J. Comput. Chem.* **1997**, *18*, 1175-1189.
34. Sadowski, J.; Gasteiger, J.; Klebe, G. J. *Chem. Inf. Comput. Sci.* **1994**, *34*, 1000-1008.
35. Gasteiger, J.; Marsili, M. *Tetrahedron* **1980**, *36*, 3219-3288.
36. Weiner, S. J.; Kollman, P. A.; Nguyen, D. T.; Case, D. A. *J. Comput. Chem.* **1986**, *7*, 230-252.

SELF-ASSEMBLY OF MULTICOMPONENT SUPRAMOLECULAR STRUCTURES THROUGH IONIC INTERACTIONS

*In this chapter, the formation of a multicomponent molecular capsule $1_2 \bullet 2_4$ is described. The design principle for this complex envisages the self-assembly, through eight ionic interactions, of six independent units: two tetrasulfonate calix[4]arenes (**1**) and four bisbenzamidine spacers (**2**). ESI and FAB mass spectrometry suggest the self-association of the components into the $1_2 \bullet 2_4$ complex together with other aggregates having 1:1 and 1:2 stoichiometries. In solution, the formation of the products with different stoichiometries depends on the solvent used in the experiments. The self association of the monomeric units into the $1 \bullet 2$ complex is favored in water while in methanol the coexistence of $1 \bullet 2$ and $1_n \bullet 2_{2n}$ complexes is most likely as indicated by ^1H NMR titrations, Job's plot analysis and isothermal titration calorimetry (ITC). X-ray crystallography shows that in the solid state the ternary complex $1 \bullet 2_2$ is formed.*

6.1 Introduction

Supramolecular chemistry is a well-implemented discipline for the synthesis of macroscopic multicomponent complexes *via* noncovalent interactions.¹⁻⁴ The self-assembly of independent monomeric units into bigger architectures requires that the single components possess the information to recognize and interact with other complementary molecules. Moreover, preorganization of the single components is desirable to minimize the loss of entropy due to intermolecular association. Among supramolecular systems, molecular capsules have been created from the self-assembly of opportunely functionalized building blocks that can assemble and disassemble under certain conditions. Generally, multicomponent capsules require the presence of a guest molecule to assemble in solution, and sometimes they only form in the solid state.⁵⁻¹⁰

Besides the strong and highly directional metal-ligand interactions employed in the synthesis of cages of different sizes, stoichiometries and symmetries,¹¹⁻²³ multicomponent capsules have been reported making use of the weaker but still highly directional hydrogen bond interactions.²⁴⁻²⁹ One example is the molecular capsule reported by Kobayashi et al³⁰ (Figure 6.1) based on the assembly of six components, two cavitands as concave units and four 2-aminopyrimidine as linker units *via* 16 hydrogen bonds. In the solid state two molecules of nitrobenzene occupy the capsule's cavity.

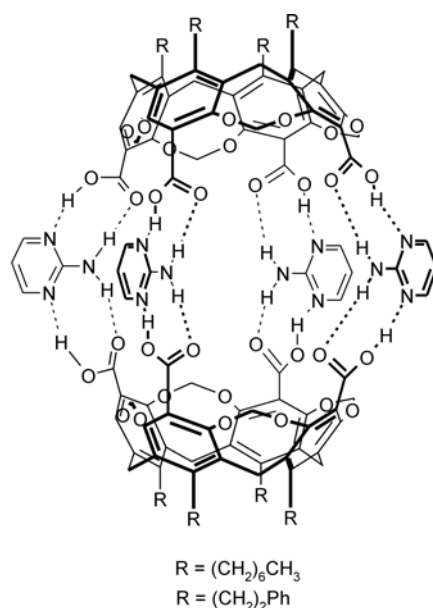


Figure 6.1. Molecular capsule resulting from the assembly of two tetracarboxylic cavitand and four 2-aminopyrimidine units *via* 16 hydrogen bonds.

Nevertheless, to the best of our knowledge, ionic interactions have not yet been employed for this purpose. The lack of directionality seems to prevent the use of this very strong interaction as a general tool for the construction of multicomponent containers and to limit its use to simpler assemblies i.e. the bimolecular capsules reported in the previous chapters.

This chapter reports the studies on the formation of a multicomponent molecular capsule resulting from the self-assembly of two tetrasulfonate calix[4]arenes **1** and four bisbenzamidinium spacers **2** based on ionic interactions. This assembly, schematically depicted in Chart 6.1, would represent an extension of the bimolecular capsules described in previous chapters. The positively charged amidinium groups of **2** are designed to bridge the two calix[4]arenes through complementary electrostatic interactions thus providing a wide internal cavity for the encapsulation of bigger guest molecules.

Besides the self-assembly of the molecular capsule $1_2 \bullet 2_4$, complexes having different stoichiometries are also formed in solution. The solvent polarity has a pronounced effect on the equilibria present in solution as it can be deduced from the different self-assembly behavior of **1** and **2** in methanol and in water.³¹

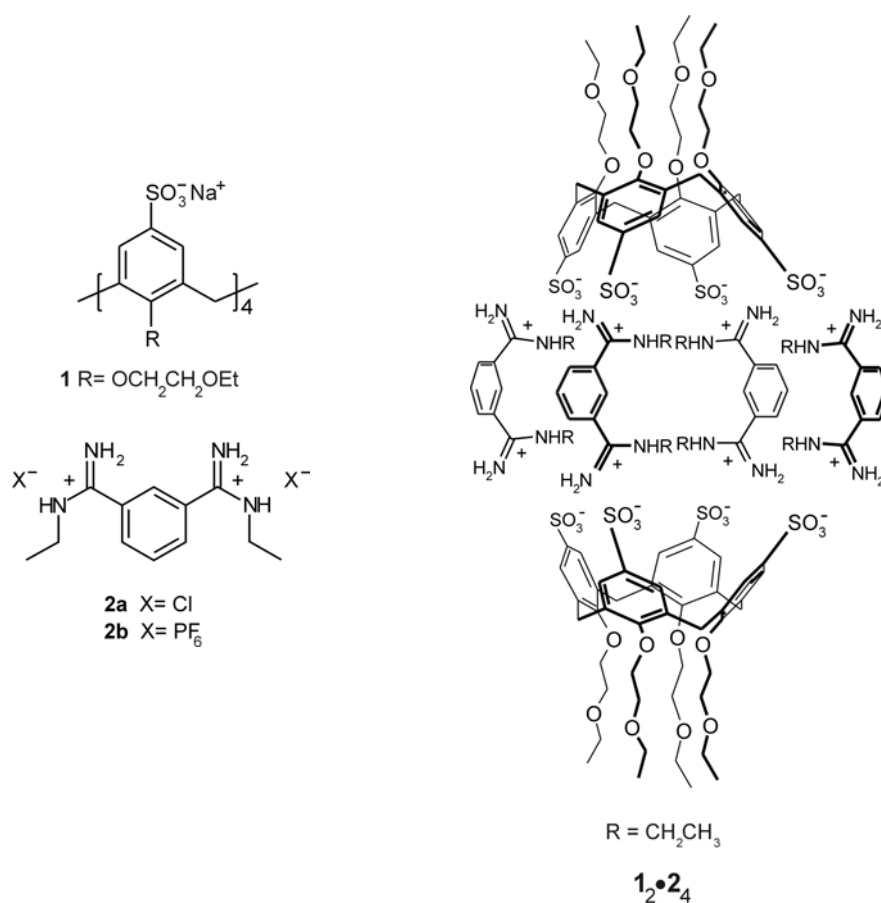
6.2 Results and discussion

6.2.1 Synthesis of the building blocks

Tetrasulfonate calixarene **1** was prepared according to a literature procedure.³² The synthesis of **2a** (Chart 6.1) was achieved by reaction of alkylchloroaluminium amide, generated from Me_3Al and ethylammonium chloride, with 1,3-dicyanobenzene for four days at 80 °C. The chloride salt was obtained after reverse phase chromatography and ion exchange chromatography in 40% yield. The hexafluorophosphate salt **2b** was obtained in quantitative yield as a white precipitate upon addition of an aqueous saturated solution of NH_4PF_6 to the corresponding chloride salt **2a**. Amidinium substituted calixarene **2** was synthesized with two different counterions, chloride and hexafluorophosphate, to assess their potential role in the self-assembly process.³³⁻³⁵

All the compounds have been characterized by ^1H NMR, ^{13}C NMR spectroscopy, and FAB mass spectrometry.

Chart 6.1



6.2.2 Assembling studies in aqueous solution

The formation of the molecular assembly $1_2 \bullet 2_4$ was first studied by ^1H NMR in D_2O at 298 K. The ^1H NMR spectrum of a 1:2 mixture (1 mM) of **1** and **2a** shows a simple pattern containing one set of signals. The up- and downfield chemical shifts of the signals of the two building blocks gave a strong indication that a discrete assembly was formed (Figure 6.2).

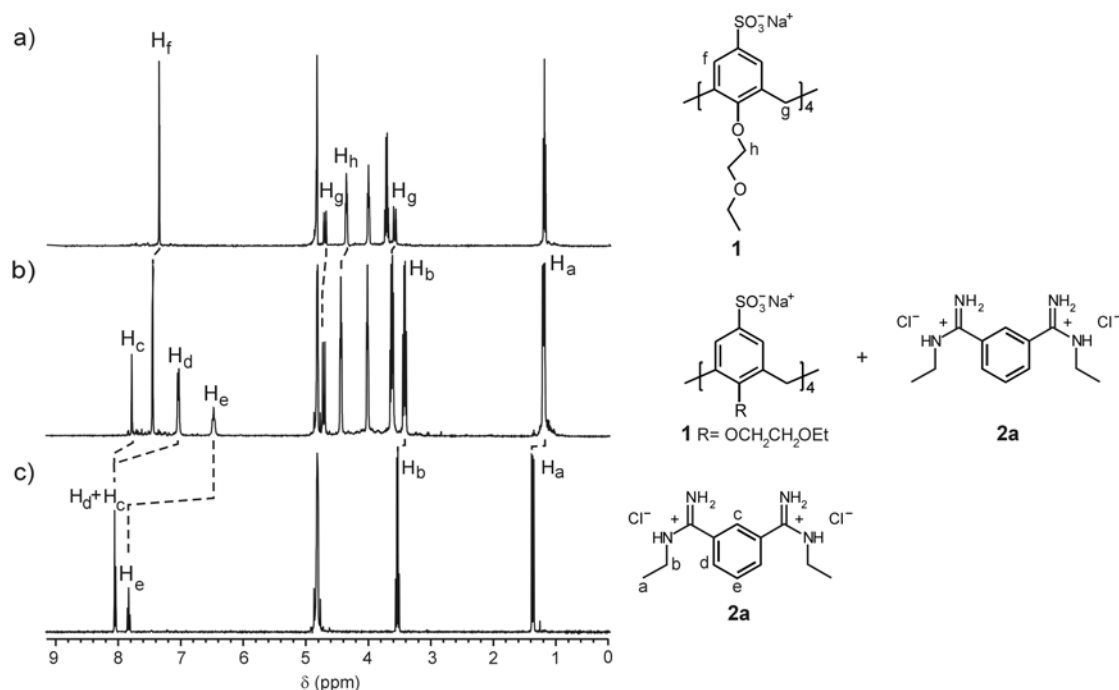


Figure 6.2. ^1H NMR spectra of a) **1**; b) **1•2a**; c) **2a** in D_2O at 298K.

The proton signals of **2a** in the solution mixtures are all upfield shifted (Figure 6.2b) compared to the spectrum of the free component (Figure 6.2c). The largest chemical shift changes were observed for the ^1H NMR signals corresponding to the aromatic protons of **2a** ($\Delta\delta_{\text{Hc}} = 0.27$ ppm, $\Delta\delta_{\text{Hd}} = 0.99$ ppm, $\Delta\delta_{\text{He}} = 1.35$ ppm) while the protons of the ethyl chains experience smaller upfield shifts ($\Delta\delta_{\text{Ha}} = 0.17$ ppm, $\Delta\delta_{\text{Hb}} = 0.10$ ppm). On the contrary, most of the proton signals of **1** in the solution mixture are downfield shifted ($\Delta\delta_{\text{Hf}} = 0.06$ ppm, $\Delta\delta_{\text{Hh}} = 0.09$ ppm, $\Delta\delta_{\text{Hg}} = 0.1$ ppm).

Upon addition of an excess of **2a** the chemical shifts of **2a** moved progressively downfield towards time-averaged values for the free and complexed **2a**, indicating that the self-assembly process is fast on the NMR time scale.

A 4 mM aqueous solution of **1** and **2a** in a 1:2 ratio was analyzed by ESI-TOF mass spectrometry. The spectrum showed a signal at 1251.3 as base peak (100%) corresponding to the complex $[(\mathbf{1}\cdot\mathbf{2a}+2\text{H})+\text{H}]^+$ and a minor signal (20%) at 1469.4 corresponding to $[(\mathbf{1}\cdot\mathbf{2a}_2)+\text{H}]^+$. Small signals at 1481.4, 2939.8, 2721.7, 2502.7, 2306.4 corresponding to $[(\mathbf{1}_2\cdot\mathbf{2a}_4)+2\text{H}]^{2+}$, $[(\mathbf{1}_2\cdot\mathbf{2a}_4)+\text{H}]^+$, $[(\mathbf{1}_2\cdot\mathbf{2a}_3+2\text{H})+\text{H}]^+$, $[(\mathbf{1}_2\cdot\mathbf{2a}_2+4\text{H})+\text{H}]^+$, $[(\mathbf{1}_2\cdot\mathbf{2a}+6\text{H})+\text{Na}]^+$ were also present.³⁶

The continuous variation method (Job's plot) was used to verify the stoichiometry of the complex in solution (Figure 6.3). ^1H NMR spectra of 1 mM solutions containing different molar fractions of **1** and **2a** in D_2O were recorded. The plots of the resonances of the aliphatic and aromatic protons of **2a** versus the molar fraction of **2a** display a clear maximum at 0.5 confirming the formation of a 1:1 complex.³⁷ The Job's plots for the assembly of **2b** with **1** are very similar to that of **2a** with **1**, with nearly identical chemical shifts for the ^1H NMR resonances of the bisbenzamidinium spacer **2b**. This finding indicates that different counterions do not influence the stoichiometry of the assembly.

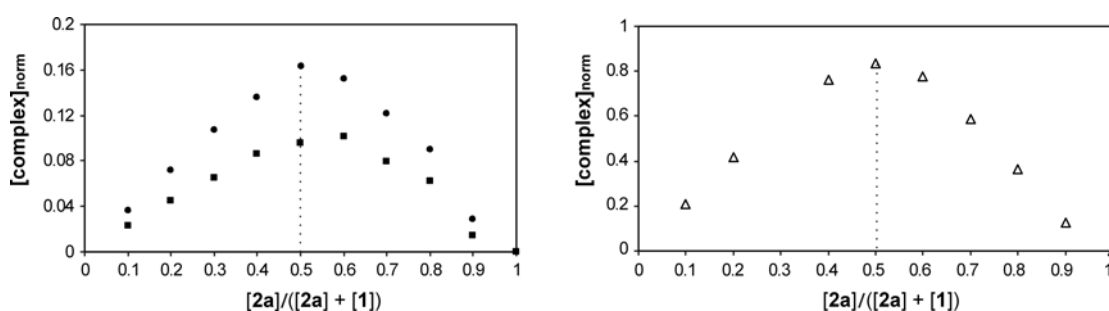


Figure 6.3. Job's plots of the ^1H NMR titration data for solutions of **1** and **2a** at a total concentration of 1 mM in D_2O at 298K. The aliphatic ($\bullet = \text{H}_a$ and $\blacksquare = \text{H}_b$) and one of the aromatic ($\Delta = \text{H}_d$) signals of **2a** are reported. (For proton assignment, see Figure 6.2).

A ^1H NMR titration in D_2O was performed by adding **2a** (17 mM) to **1** (3 mM) and following the chemical shift changes for **2a**. Addition of increasing amounts of the bisbenzamidinium **2a** resulted in a progressive downfield shift of the proton NMR signals of **2a**. A general broadening in the resonances of the aromatic protons of **2a** was also observed. Dilution experiments for **2a** showed that its ^1H NMR resonances are constant from 20 mM to 1 mM meaning that no aggregates are formed over the investigated concentration range. The ^1H NMR titration data were successfully fitted to a 1:1 binding model giving an association constant $K_a \sim 10^4 \text{ M}^{-1}$ (Figure 6.4). Analogous chemical shift changes for **2a** were obtained from the reverse titration performed by adding **1** to **2a**.

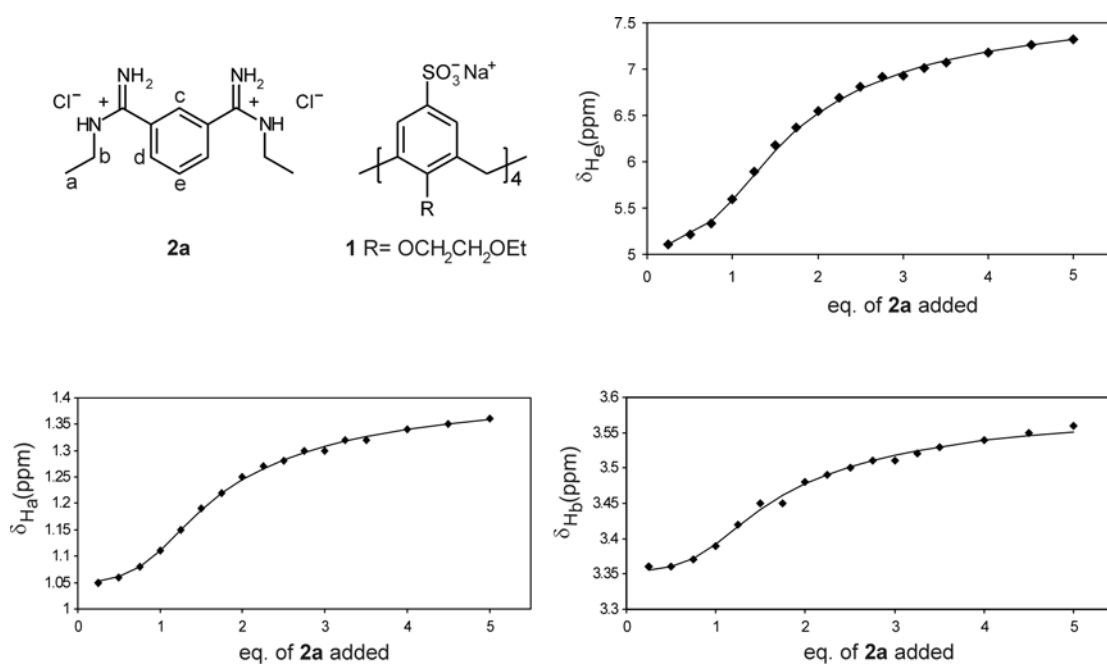


Figure 6.4. Binding isotherms derived from the ^1H NMR titration of **1** (3 mM) with **2a** (17 mM) in D_2O at 298 K.

The significant chemical shift changes observed for the resonances of the aromatic protons (H_c , H_d , H_e) indicate a binding mode where one molecule of **2a** is in close proximity to the aromatic region of the calix[4]arene **1**. The large upfield shift observed for the proton H_e ($\Delta\delta_{\text{H}_e} = 2.67$ ppm) of **2a** strongly suggests that this proton is located inside the cone of the calix[4]arene **1** while the charged amidinium groups are forming ionic interactions with the opposite charged groups located at the upper rim of **1**. Therefore, the geometry of the complex reported in Figure 6.5a is more probable than the one depicted in Figure 6.5b where the aromatic part of **2a** is outside of the calix[4]arene cone.

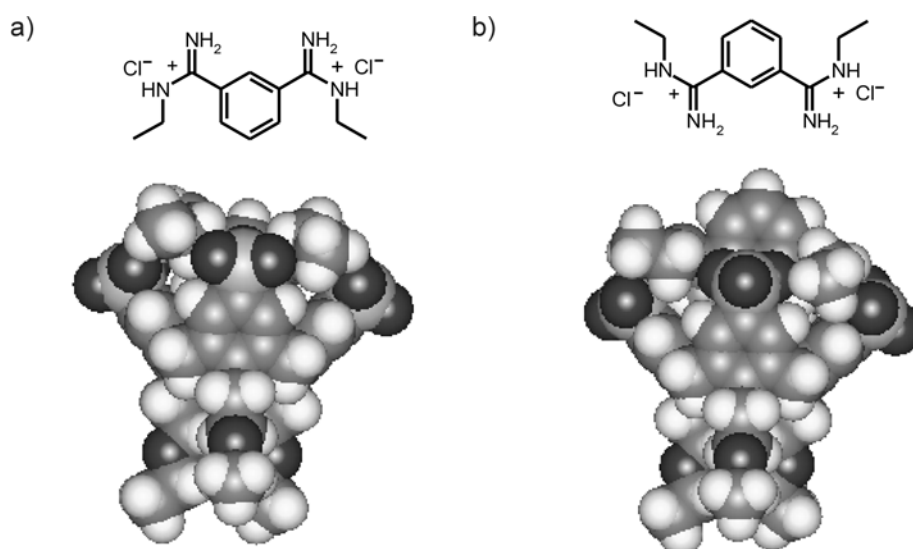


Figure 6.5. Molecular simulation (CHARMm 24.0) of the two possible ways of binding of **2a** to **1**.

The binding of **2a** to **1** in water was further studied by isothermal titration calorimetry (ITC). The inflection point of the resulting binding isotherm (Figure 6.6) indicates the formation of a complex having 1:1 stoichiometry.

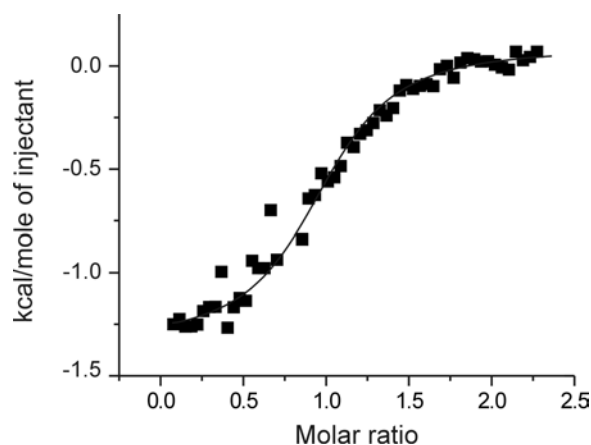


Figure 6.6. Heat evolved per injection as a function of $[2a]/[1]$ ratio as observed for the microcalorimetric titration of **1** (0.1 mM) with **2a** (1 mM) in H_2O at 298 K. Line: fit to a 1:1 binding model.

Analysis of the thermodynamic data shows that the self-assembly process is accompanied by a favorable entropy and a small favorable enthalpy change ($\Delta S^\circ = 61 \text{ JK}^{-1}\text{mol}^{-1}$ and $\Delta H^\circ = -7.9 \text{ kJ mol}^{-1}$) accounting for a binding driven by the classical hydrophobic effect.³⁸ The positive value for ΔS° reflects the gain in entropy

associated with the release of organized solvent molecules from the building blocks. Both **1** and **2a** are expected to be well solvated in aqueous media; upon binding the solvent spheres are disrupted and organized water molecules are released into the bulk solvent. The favorable enthalpy change is most probably the result of the formation of electrostatic and hydrophobic interactions. The data obtained from the titration were fitted to a 1:1 binding model giving an association constant $K_a \sim 10^4 \text{ M}^{-1}$ which coincides with the K_a determined by ^1H NMR.

Although mass spectrometry suggests the presence of multiple complexes, ^1H NMR and ITC studies strongly indicate that the complex **1•2a** is by far the predominant species formed in aqueous solution. Thus, complexes having higher stoichiometries contribute only marginally to the total composition of the solution.

6.2.3 Assembling studies in methanol

The formation of the 1:1 complex between **1** and **2a** in aqueous solution reported in the previous section was attributed to the cooperative formation of electrostatic and hydrophobic interactions.³⁹ The hydrophobic interactions responsible for the inclusion of **2a** in the cavity of **1** could be reduced by studying the assembly in a less polar solvent like methanol, where the assembly of the molecular capsule **1₂•2₄** should be favored.

The addition of ~ 2 eq. of **2a** to a 4 mM solution of **1** in methanol led to a white precipitate in the solution despite the fact that compounds **2a** and **1** are very well soluble in methanol. The solid was redissolved in $\text{DMSO-}d_6$ and the solution analyzed by ^1H NMR spectroscopy. The integrals of the signals in the spectrum confirmed the 1n:2n stoichiometry of the complex (Figure 6.7). Significant upfield chemical shift changes were observed for the aromatic protons ($\Delta\delta_{\text{Hc}} = 0.41$ ppm, $\Delta\delta_{\text{Hd}} = 0.40$ ppm, $\Delta\delta_{\text{He}} = 0.55$ ppm) and the aliphatic protons of **2a** ($\Delta\delta_{\text{Ha}} = 0.59$ ppm, $\Delta\delta_{\text{Hb}} = 0.37$ ppm). Furthermore, the NH proton signals of **2a** were also significantly upfield shifted ($\Delta\delta = 0.58, 0.51$ and 0.28 ppm) in comparison with the ones of the free **2a**. Small downfield shifts were observed for the protons of **1** ($\Delta\delta_{\text{Hf}} = 0.12$ ppm, $\Delta\delta_{\text{Hg}} = 0.06$ ppm, $\Delta\delta_{\text{Hh}} = 0.03$ ppm).

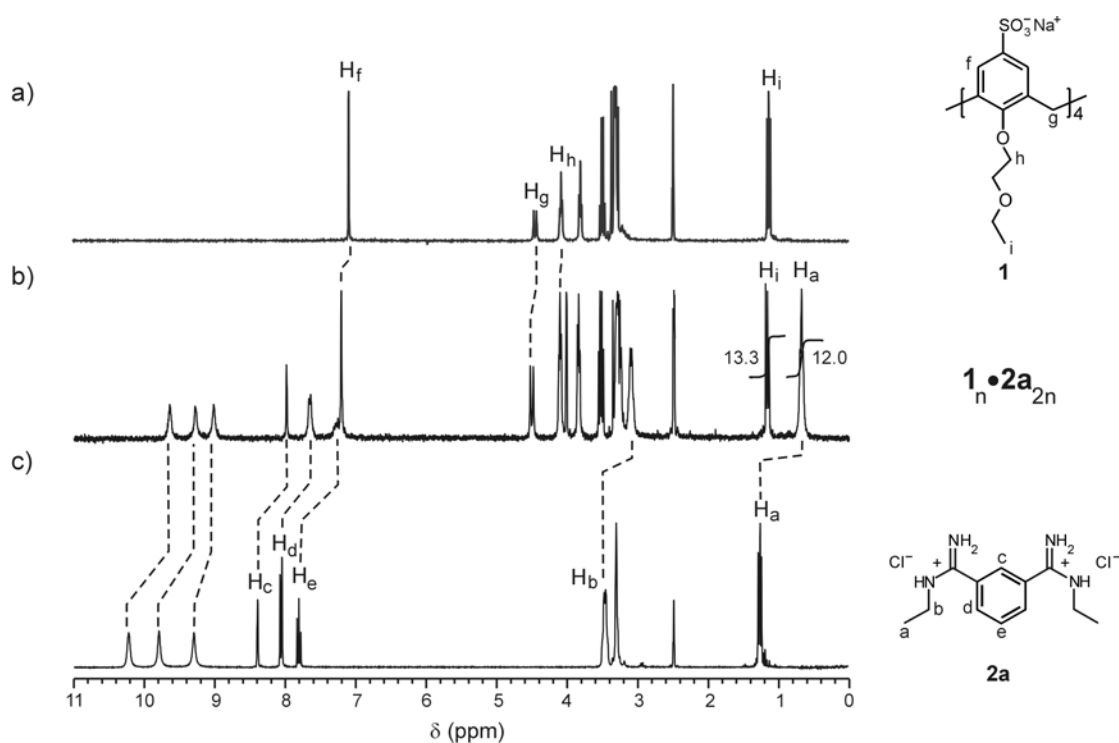


Figure 6.7. ^1H NMR spectra of a) **1**; b) $\mathbf{1} \cdot \mathbf{2a}_{2n}$ complex obtained from precipitation from methanol; c) **2a** in $\text{DMSO-}d_6$ at 298 K.

The precipitate was analyzed by FAB mass spectrometry (Figure 6.8) and the data are given in Table 6.1.

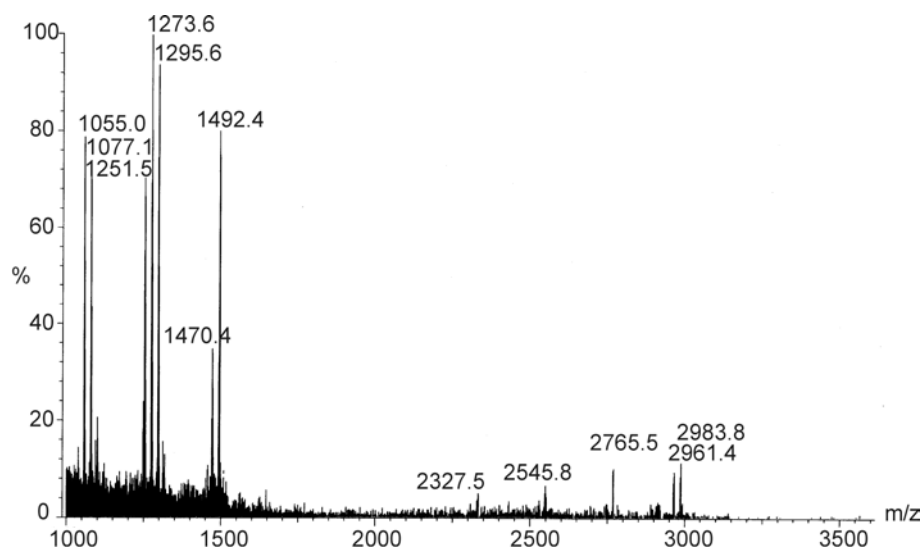


Figure 6.8. FAB mass spectrum of the 1:2 mixture of **1** and **2a**.

The FAB mass spectrum of the solid clearly shows signals at mass-to-charge ratio (m/z) of 2961.4 and 2983.8 corresponding to the $[(\mathbf{1}_2 \cdot \mathbf{2a}_4) + \text{Na}]^+$ and $[(\mathbf{1}_2 \cdot \mathbf{2a}_4 - \text{H} + \text{Na}) + \text{Na}]^+$ complexes, respectively. Importantly, peaks for the species resulting

from the loss of one, two and three bisbenzamidinium spacers **2a** with m/z of 2765.5, 2545.8, 2327.5, respectively, are also present (for the assignment of the molecular ions see Table 6.1). The absence of any higher-mass aggregates rules out the possibility that the peaks for **1₂•2a₄** are the result of fragmentation of higher stoichiometry aggregates. Peaks corresponding to the **1•2a** and **1•2a₂** complexes at a m/z of 1295.6 and 1492.4 respectively are also present.⁴⁰ Analysis of different mixtures of **1** and **2b** by FAB mass spectrometry resulted in analogous spectra as the one reported in Figure 6.8. A signal at 3128.9 corresponding to the $[(\mathbf{1}_2\cdot\mathbf{2b}_4+\text{PF}_6\text{Na})+\text{Na}]^+$ complex was present in addition to the peaks found for the **1:2a** mixtures.

Table 6.1. FAB-MS data. The theoretical data refer to the highest isotope line in Da as calculated by Isoform[®] program.³⁶

Complex	Theoretical	Experimental
$[(\mathbf{1}+3\text{H}+\text{Na})+\text{H}]^+$	1055	1055
$[(\mathbf{1}+2\text{H}+2\text{Na})+\text{H}]^+$	1077	1077.1
$[(\mathbf{1}\cdot\mathbf{2a}+2\text{H})+\text{H}]^+$	1251	1251.5
$[(\mathbf{1}\cdot\mathbf{2a}+2\text{H})+\text{Na}]^+$	1273	1273.6
$[(\mathbf{1}\cdot\mathbf{2a}+2\text{Na})+\text{H}]^+$	1295	1295.6
$[(\mathbf{1}\cdot\mathbf{2a}_2)+\text{H}]^+$	1469	1470.4
$[(\mathbf{1}\cdot\mathbf{2a})+\text{Na}]^+$	1491	1492.4
$[(\mathbf{1}_2\cdot\mathbf{2a}+4\text{H}+2\text{Na})+\text{H}]^+$	2328	2327.5
$[(\mathbf{1}_2\cdot\mathbf{2a}_2+2\text{H}+2\text{Na})+\text{H}]^+$	2546	2545.8
$[(\mathbf{1}_2\cdot\mathbf{2a}_3+2\text{Na})+\text{H}]^+$	2765	2765.5
$[(\mathbf{1}_2\cdot\mathbf{2a}_4)+\text{H}]^+$	2939	-
$[(\mathbf{1}_2\cdot\mathbf{2a}_4)+\text{Na}]^+$	2961	2961.4
$[(\mathbf{1}_2\cdot\mathbf{2a}_4-\text{H}+\text{Na})+\text{Na}]^+$	2983	2983.8

The assembly of **1** and **2a** in CD₃OD was studied by Job's method (Figure 6.9). The Job's plot of the chemical shift changes for the resonance of **2a** against its molar fraction show a maximum at around 0.7 suggesting the formation of a complex of relative stoichiometry $1_n \cdot 2a_{2n}$ as the most relevant species in solution.

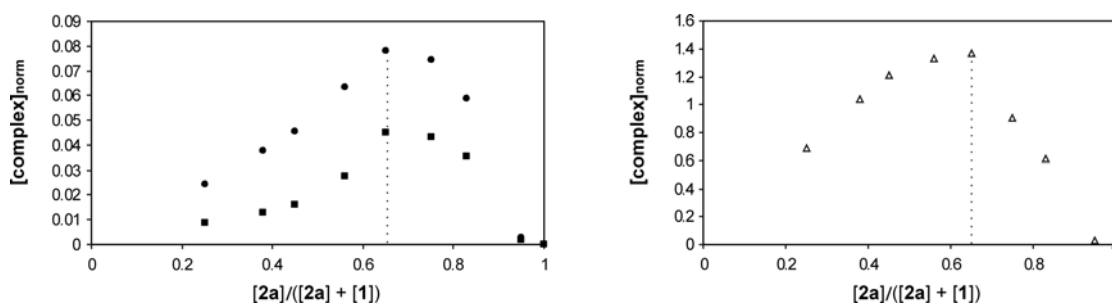


Figure 6.9. Job's plots of the ¹H NMR titration data for solutions of **1** and **2a** of total concentration at a 1 mM in CD₃OD at 298 K. The aliphatic (● = H_a and ■ = H_b) and one of the aromatic (▲ = H_d) signals of **2a** are reported. (For proton assignment, see Figure 6.2).

¹H NMR titrations were performed adding **2a** to **1** and following the chemical shift changes for **2a**. Interestingly and in contrast to that observed in D₂O, different protons of **2a** gave different ¹H NMR titration curves (Figure 6.10). The signals for the protons H_a and H_b of the alkyl chains of **2a** shift first to higher field until the addition of 1 eq. of **2a** and then these proton signals move to lower fields. The aromatic protons instead experience a progressive upfield shift. The unusual chemical shift changes for H_a and H_b would account for the formation of different species in solution. Inoue observed similar behavior for the formation of 1:1 and 1:2 complexes between a guanidinium host and the sulfate anion in acetonitrile.⁴¹ Most probably at the early stage of the titration the **1**•**2a** complex is predominantly formed, which, upon addition of increasing amount of **2a**, is replaced by a complex of type $1_n \cdot 2a_{2n}$.⁴²

The presence of a single set of resonances in the ¹H NMR spectra of different solutions of **1** and **2a** in CD₃OD indicates that at room temperature the components are in rapid exchange on the NMR time scale. To prove the coexistence in solution of at least two different complexes, (most probably the **1**•**2a** and $1_n \cdot 2a_{2n}$ as suggested by mass spectrometry and the NMR, *vide infra*), a variable temperature experiment of a solution of **1** and **2a** in a 1:4 ratio in CD₃OD was performed. Unfortunately, the rapid exchange between the components continues even at low temperatures. Only a

broadening of the ^1H NMR signals was observed upon decreasing the temperature to -80°C .

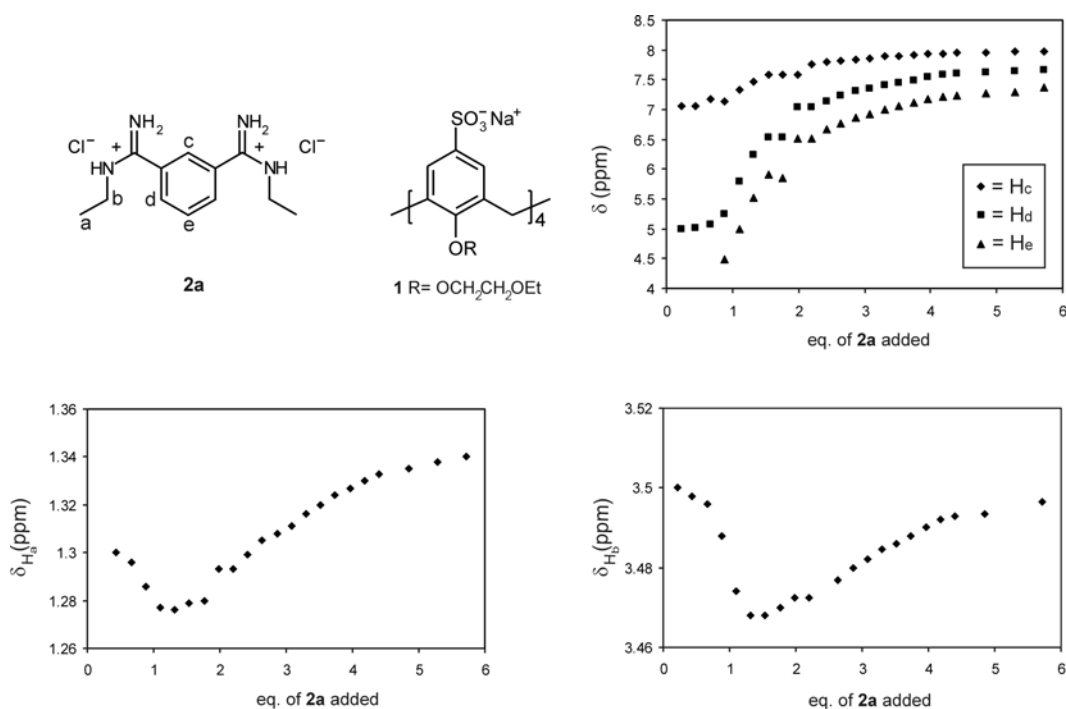
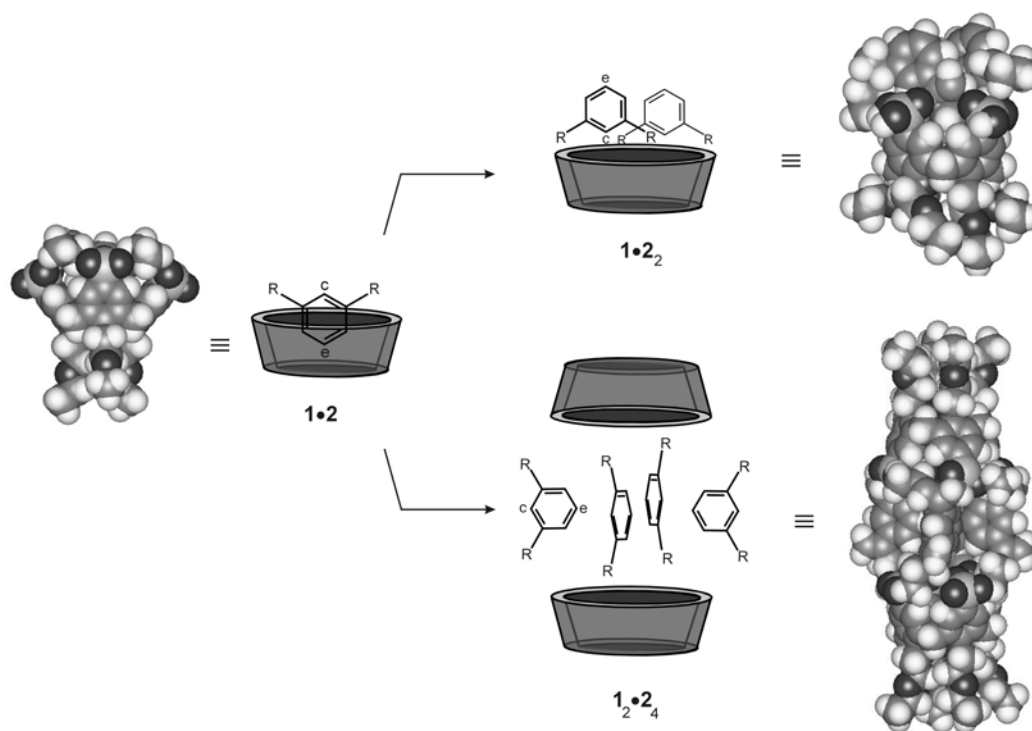


Figure 6.10. ^1H NMR titration data for the addition of **2a** (2 mM) to **1** (0.3 mM) in CD_3OD at 298 K. The chemical shift for the proton H_e could not be followed in the first part of the titration. Most probably the resonance of this proton overlaps with other signals present in the spectrum.

Detailed analysis of the CPK models and of the chemical shift in the NMR spectra confirm the hypothesis that at least two species are formed in solution. At the early stage of the titration (when the **1•2a** complex is formed), the resonances of the aromatic protons of **2a** are all upfield shifted compared to the ones of the free **2a** (not shown). Although the chemical shift changes for H_e of **2a** in the first part of the titration could not be followed, it can be seen that this proton experiences a strong upfield shift ($\Delta\delta_{\text{H}_e} > 3.37$ ppm). A significant shift is also observed for the proton H_d ($\Delta\delta_{\text{H}_d} = 3.07$ ppm), while the signal for H_c suffers a more moderate upfield shift ($\Delta\delta_{\text{H}_c} = 1.15$ ppm). These chemical shifts suggest that at the beginning of the titration the same binding mode proposed for the **1a•2** complex in water predominates. According to this model, **2a** is included in the calixarene cone with the proton H_e pointing inside the cone of the calixarene, while the amidinium groups form ionic interactions with the tetrasulfonate groups of **1** (Chart 6.2).

Chart 6.2



Subsequently, the addition of increasing amounts of **2a** leads progressively to the formation of the 1:2 or 2:4 complex (Chart 6.2). These binding modes require a considerable reorganization of **2a** within the complex. In both cases the aromatic part of **2a** has to leave the calixarene cavity, in agreement with the strong downfield shift observed for the proton H_e upon addition of increasing amounts of **2a** (*vide infra*). Analysis of the ^1H NMR data shows small upfield shifts for the protons H_a and H_b of the alkyl chains of **2a** until the point where 1 eq. of **2a** are added, suggesting that the alkyl chains of **2a** are located in closer proximity to the aromatic ring of the calixarene compared to the **1•2a** complex. Thus, taking all the NMR data into consideration, the formation of the 1:2 complex is only possible if **2a** rearranges in a such a way that the two aromatic rings of **2a** are turned upwards with respect to the calixarene which would confirm the structure obtained by the X-ray analysis (see Figure 6.14).

Nevertheless, a 2:4 binding model cannot be ruled out by the detailed NMR analysis. The CPK models for the 2:4 complex indicate that **2a** can adopt two different orientations in the complex: the aromatic part of **2a** pointing inward or outward with respect to the the interior of the capsule's cavity. In both cases the alkyl

chains of **2a** are located close to the calixarene cone, thus experiencing the ring current shielding effect responsible for the small upfield shifts of H_a and H_b . However, the fact that the ^1H NMR signal for H_c at around 2 eq. is still strongly upfield shifted (even upon addition of 6 eq. of **2a** its original chemical shift is not completely restored), suggests the binding mode where the aromatic rings are turned inward (Chart 6.2). In this binding mode H_c points toward the interior of the cavity, experiencing the strong shielding environment of the surrounding aromatic rings. Moreover, analysis of this model indicates that due to the close proximity of the **2a** units, CH- π interactions between H_c and the aromatic nucleus of the neighboring **2a** are also possible.

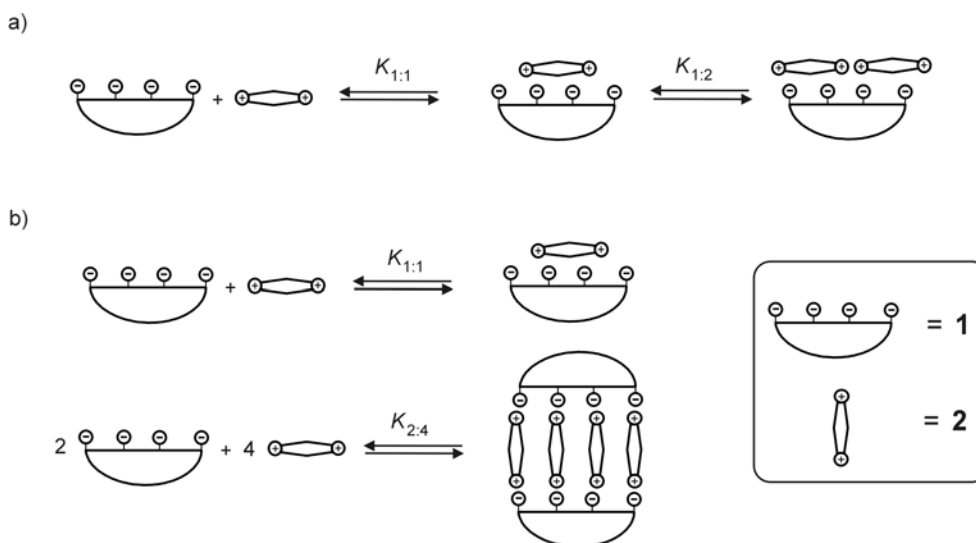
Among the aromatic protons H_c is the one which would be less affected from the rearrangement of **2a** upon formation of either the 1:2 or 2:4 complex from the 1:1 complex. As depicted in Chart 6.2 this proton resides outside the cone of the calix[4]arene in all three complexes, and therefore it would feel a similar intensity of resonance shielding in all cases which is consistent with its smaller chemical shift changes in comparison to the other two aromatic protons.

In conclusion, the shapes of the titration curves for the protons H_a and H_b would reflect the change of chemical environment: in the **1•2a** complex the alkyl chains are likely to reside outside the calix[4]arene cavity, while in the 1:2 or 2:4 complex most probably one of the chains points inside the cone of the calix[4]arene. On the contrary, the aromatic protons experience an opposite change in chemical environment: from the interior of the cavity, where they feel the shielding effect of the calix[4]arene cone they move to a less shielding environment.

Job's plot analysis and ^1H NMR titration of **1** and **2b** led to analogous results as for **2a** meaning that the counterion does not influence the binding behavior in methanol.

The experimental data for the titration of **1** with **2a** were fitted to two binding models, one that accounts for the formation of the 1:1 plus 1:2 complexes and the other accounting for the formation of the 1:1 plus 2:4 complexes (Scheme 6.1). The fitting optimized two binding constants ($K_{1:1}$ and $K_{1:2}$ or $K_{1:1}$ and $K_{2:4}$) and three NMR resonances for each NMR signal of **2a** (free **2a**, $\delta(\mathbf{2a})$; 1:1 complex, $\delta(\mathbf{1\cdot 2a})$; 1:2 or

2:4 complex, $\delta(\mathbf{1}\cdot\mathbf{2a}_2)$ or $\delta(\mathbf{1}_2\cdot\mathbf{2a}_4)$, simultaneously. In both cases a good fit to the experimental data was obtained.



Scheme 6.1. Schematic representation of the equilibria for the a) 1:1 + 1:2 and b) 1:1 + 2:4 binding model.

To determine the absolute stoichiometry of the complex $\mathbf{1}_n\cdot\mathbf{2a}_{2n}$, i.e. to differentiate between the $\mathbf{1}\cdot\mathbf{2a}_2$ and $\mathbf{1}_2\cdot\mathbf{2a}_4$ complexes, ^1H NMR titrations at three different concentrations were carried out. Figure 6.11 shows a representative plot of the change in chemical shifts of two protons of $\mathbf{2a}$ as a function of the $\mathbf{2a}:\mathbf{1}$ ratio. The solid line represents the best curve fitting of these changes in chemical shifts assuming an equilibrium mixture of 1:1 plus 1:2 complexes in solution. Analogous fitting curves were obtained for the equilibrium mixtures of 1:1 plus 2:4. Analysis of the association constants determined for each of the three titrations applying both binding models indicate that while the $K_{1:1}$ maintains more or less constant over the concentration range investigated, $K_{1:2}$ and $K_{2:4}$ change depending on the concentration. The fact that the values for the $K_{2:4}$ undergo smaller changes compared to the $K_{1:2}$ over the concentration range studied suggests a preference for the 1:1 plus 2:4 binding model. From the fits of the experimental data the following stability constants of the complexes were derived: $K_{1:1} \sim 10^5 \text{ M}^{-1}$, $K_{1:2} \sim 10^3 \text{ M}^{-1}$, $K_{2:4} \sim 10^{22} \text{ M}^{-5}$.

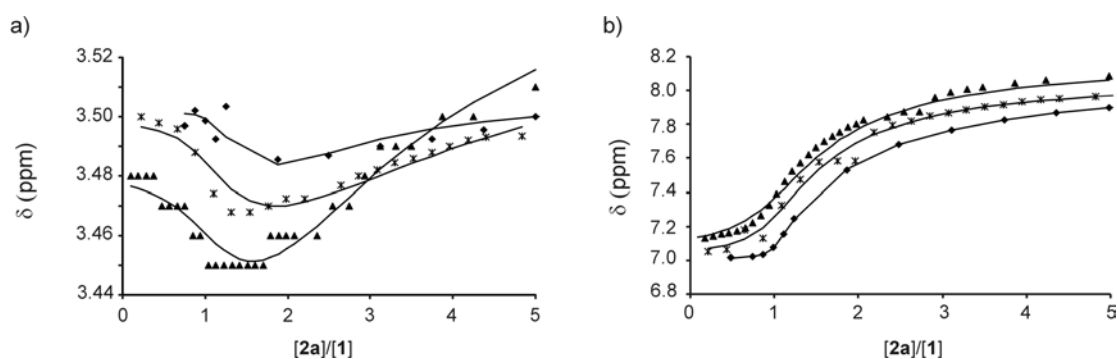


Figure 6.11. Chemical shift changes for a) H_b and b) H_c of **2a** for the ^1H NMR titrations of **2a** to **1** in CD_3OD at 298 K at three different concentrations. (\blacktriangle) $[\mathbf{1}] = 3 \text{ mM}$ and $[\mathbf{2a}] = 17 \text{ mM}$; (\ast) $[\mathbf{1}] = 0.3 \text{ mM}$ and $[\mathbf{2a}] = 2 \text{ mM}$; (\blacklozenge) $[\mathbf{1}] = 0.06 \text{ mM}$ and $[\mathbf{2a}] = 0.4 \text{ mM}$. Lines: fit to the 1:1 + 1:2 binding model. (For proton assignment see Figure 6.2).

The coexistence of multiple binding equilibria in solution was also confirmed by ITC. Figure 6.12 depicts the titration curves for three microcalorimetric experiments performed at various **2a/1** concentrations in MeOH containing Bu_4NClO_4 ($1 \times 10^{-2} \text{ M}$) as a background electrolyte. In each of the three cases the shape of the curves indicate that there are at least two different complexation events in solution. The heat evolution pattern obtained upon injection of **2a** (2 mM) into a solution of **1** (0.1 mM) is indicative of an exothermic event. However, a small additional event at the early stage of the titration is evident. At higher concentrations of **1** and **2a**, first an exothermic binding event, (indicated by a negative slope in the ITC data points), is evident before 1 eq of **2a** is reached, while a second endothermic binding event is visible from the portion of the curve directly after the addition of 1 eq (positive slope in the ITC data points).

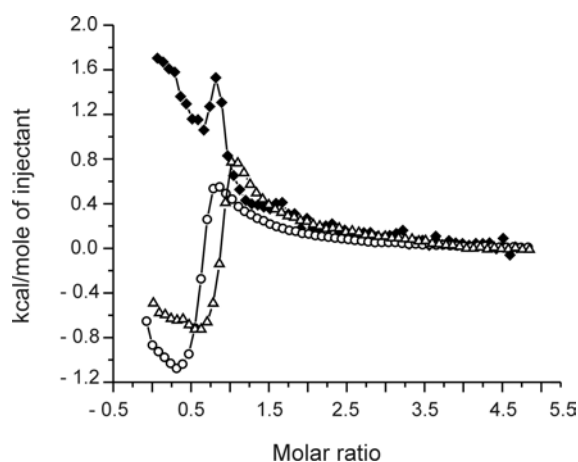


Figure 6.12. Heats evolved per injection as a function of the $[2\mathbf{a}]/[1]$ ratio as observed for the microcalorimetric titrations of $\mathbf{1}$ with $\mathbf{2a}$ in MeOH in presence of Bu_4NClO_4 at 298 K. (\blacklozenge) $[1] = 0.1$ mM, $[2\mathbf{a}] = 2$ mM; (Δ) $[1] = 0.5$ mM, $[2\mathbf{a}] = 10$ mM; (\circ) $[1] = 1$ mM, $[2\mathbf{a}] = 20$ mM.

The presence of two inflection points in the ITC curves would suggest the formation of at least two complexes in solution.⁴³ The first part of the curves could be attributed to the formation of the 1:1 complex which is replaced by the formation of the higher stoichiometry complex(es) (1n:2n) when the concentration of $\mathbf{2a}$ increases. Microcalorimetric dilution experiments were performed by injection of $\mathbf{2a}$ in 1×10^{-2} M Bu_4NClO_4 in MeOH, into the microcalorimetric cell charged with the same background electrolyte solution. While the dilution of the 2 mM solution of $\mathbf{2a}$ gave no indication of aggregation, the dilution curves for the 10 mM and 20 mM solution of $\mathbf{2a}$ showed heat effects that account for self-association. This is not unlikely because compound $\mathbf{2a}$ possesses a phenyl ring and therefore it has the potential to aggregate through the stacking of the aromatic rings.

The presence of multiple binding equilibria, together with the self-association of $\mathbf{2a}$ precluded an accurate curve fitting. However, the ITC studies performed offer qualitative data of the association in MeOH, which, in agreement with the ^1H NMR studies, account for the formation of different complexes.

Solutions of $\mathbf{1}$ and $\mathbf{2a}$ in a 1:2 ratio in MeOH were analyzed also by ESI-TOF mass spectrometry. In Figure 6.13 the spectra measured at two different concentrations are depicted. The spectrum of a 170 μM solution shows ions at m/z of 512.57 and 757.32 corresponding to the $[(\mathbf{1}\cdot\mathbf{2a}_2)+3\text{Na}]^{3+}$ and $[(\mathbf{1}\cdot\mathbf{2a}_2)+2\text{H}]^{2+}$ complexes, together with peaks at 670.25 and 844.40 for the $[(\mathbf{1}\cdot\mathbf{2a})+2\text{H}]^{2+}$,

$[(\mathbf{1}\cdot\mathbf{2a}_3)+2\text{H}]^{2+}$ complexes. Signals at 1002.66, 944.60, 886.51 corresponding to the $[(\mathbf{1}_2\cdot\mathbf{2a}_4)+3\text{Na}]^{3+}$, $[(\mathbf{1}_2\cdot\mathbf{2a}_3)+3\text{Na}]^{3+}$, $[(\mathbf{1}_2\cdot\mathbf{2a}_2)+3\text{Na}]^{3+}$, and $[(\mathbf{1}_2\cdot\mathbf{2a}_4)+3\text{Na}]^{3+}$, respectively, are also present.³⁶ When the same solution was diluted to 30 μM the ESI-TOF mass spectrum showed a similar pattern of signals.⁴⁴ The peaks corresponding to the $\mathbf{1}_2\cdot\mathbf{2a}_4$ complex remained evident and more importantly their relative intensity compared to the major peaks increased. This finding would rule out the possibility that the peaks for the 2:4 complex are the result of dimerization or aggregation of the complexes having lower stoichiometry.

These findings, in agreement with the results obtained by ^1H NMR and ITC, corroborate the hypothesis of the coexistence of the $\mathbf{1}\cdot\mathbf{2a}$, $\mathbf{1}\cdot\mathbf{2a}_2$ and $\mathbf{1}_2\cdot\mathbf{2a}_4$ in solution.

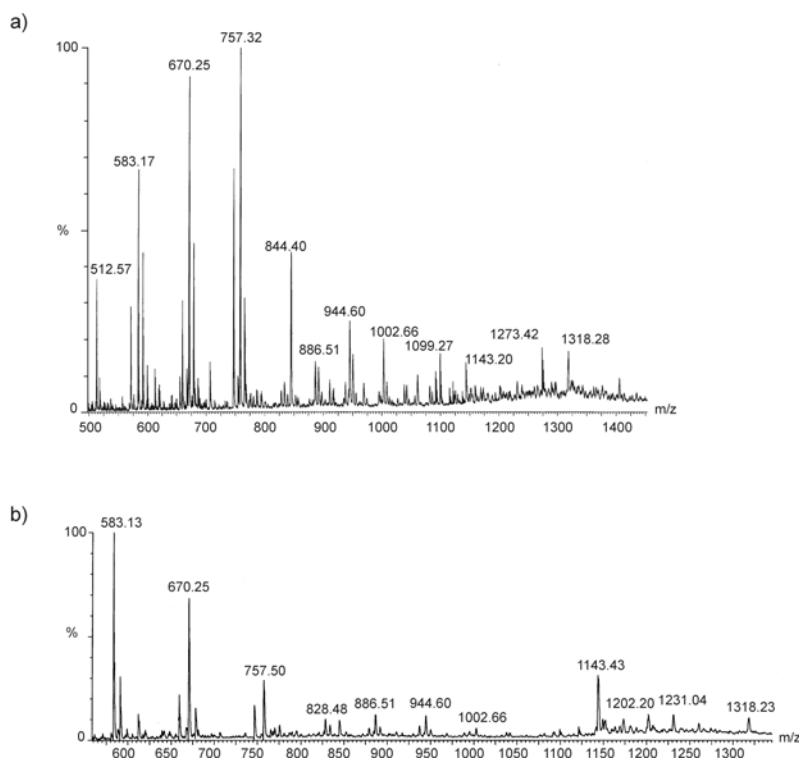


Figure 6.13 ESI-TOF mass spectra of 1:2 solution of **1** and **2a** in MeOH a) 170 μM b) 30 μM .

6.2.4 X-ray crystal structure of $\mathbf{1a}\cdot\mathbf{2a}_2$

Crystals suitable for X-ray analysis were obtained from a solution of **1** and **2a** in CD_3OD . The X-ray structure shows evidence for the formation of a 1:2 molecular assembly between **1** and **2a** (Figure 6.14). The two bisbenzamidinium spacers are assembled along the upper rim of the tetrasulfonate calix[4]arene through ionic

interactions. Interestingly, one of the ethyl side chains of the amidinium groups of **2a** is located inside the calix[4]arene cone. The X-ray structure suggests that the ternary complex **1•2a₂** is held together by a number of noncovalent intermolecular forces, which, besides the ionic interactions between the amidinium and the sulfonate moieties, include CH₃- π interaction between the included ethyl chain of **2a** and the aromatic rings of the calixarene, and π - π interactions between the aromatic rings of **2a**.

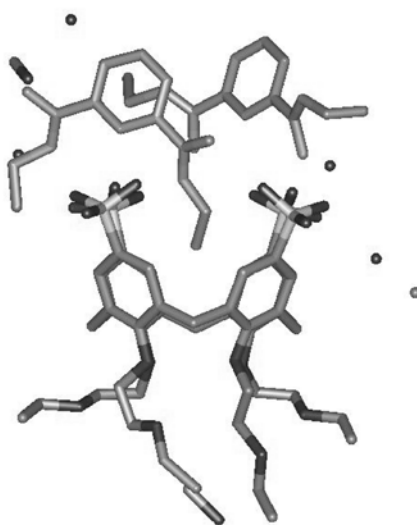


Figure 6.14. X-ray crystal structure of the molecular assembly **1•2a₂**.

6.3 Conclusions

The results reported in this chapter showed that different superstructures are generated from the self-assembly of the bisbenzamidinium **2** and the calix[4]arene **1**. The 1:1 complex is predominantly formed in water, while the formation of higher stoichiometry assemblies is favored in methanol. Most probably in water hydrophobic interactions drive the inclusion of **2** in the cone of the calix[4]arene while in methanol the hydrophobic interactions are weakened and complexes with higher stoichiometry are formed. The effect of the counterion on the self-assembly was also evaluated. The behavior of **2a** and **2b** is essentially identical thus indicating that the counterion does not influence the geometry of binding.

Moreover, solution studies provided indication for the formation of the molecular capsule **1₂•2a₄** in methanol although not as a unique product. The X-ray structure

obtained indicate that in the solid state the building blocks assemble in the **1•2_{a2}** complex

6.4 Experimental section

6.4 General information and instrumentation

The reagents used were purchased from Aldrich or Acros Chimica and used without further purification. All the reactions were performed under nitrogen atmosphere. Analytical thin layer chromatography was performed using Merck 60 F₂₅₄ silica gel plates. ¹H and ¹³C NMR spectra were recorded on a Varian Unity INOVA (300 MHz) or a Varian Unity 400 WB NMR spectrometer. ¹H NMR chemical shift values (300 MHz) are reported as δ in ppm using the residual solvent signal as an internal standard (CHD₂OD, δ = 3.30, HDO, δ = 4.67). ¹³C NMR chemical shift values (100 MHz) are reported as δ in ppm using the residual solvent signal as an internal standard (CD₃OD, δ = 49.0). Infrared spectra were recorded on a FT-IR Perkin Elmer Spectrum BX spectrometer and only characteristic absorptions are reported. Electrospray ionization (ESI) mass spectra were recorded on a Micromass LCT time-of-flight (TOF) mass spectrometer. Samples were introduced using a nanospray source. Fast atom bombardment (FAB) mass spectra were recorded with a Finnigan MAT 90 spectrometer. The consistency of the molecular mass and the stoichiometric formulation were verified by comparison of the isotopic patterns between the observed peaks and the theoretical simulation calculated by “Isoform” program. Elemental analyses were carried out using a 1106 Carlo-Erba Strumentazione element analyzer.

Calorimetric measurements. The titration experiments were carried out using a Microcal VP-ITC microcalorimeter with a cell volume of 1.4115 mL. The formation of the assemblies between **1** and **2** was studied adding aliquots of a solution of **2** in the syringe to a solution of **1**, in the calorimetric cell, and monitoring the heat change after each addition. Dilution effects were determined by a second experiment by adding the same solution of **2** into the solvent and subtracting this contribution from the raw titrations to produce the final binding curves. The association constant for

1•2a was determined by applying a 1:1 binding model using Microsoft Excel[®] software in water.

6.4.2 Binding studies

¹H NMR titrations. The titrations were performed by adding aliquots of a solution of **2** to the solution of **1** in the NMR tube and recording the chemical shifts of **2** after each addition. The effect of dilution was evaluated in separate titrations and it was found that **1** and **2** are concentration independent under the studied conditions. For **1** and **2a** titrations at three different concentrations [**1**] = 3 mM, [**2a**] = 17 mM; [**1**] = 0.3 mM, [**2a**] = 2 mM; [**1**] = 0.06 mM, [**2a**] = 0.4 mM were performed.

Job's plots. A set of 11 NMR tubes was prepared with the total concentration of both components, **1** and **2**, kept constant at 1 mM. The **1:2** ratio was varied in such a way that the molar fraction of **2** ($c_o(\mathbf{2})/(c_o(\mathbf{1})+c_o(\mathbf{2}))$) (c_o = total concentration) increased in intervals of 0.10 and the molar fraction of **1** ($c_o(\mathbf{1})/(c_o(\mathbf{1})+c_o(\mathbf{2}))$) correspondingly decreased.

6.4.3 Synthesis

1,3-*N*-ethylbisbenzamidine chloride (**2a**)

To a suspension of ethylammonium chloride (3.81 g, 46.8 mmol) in dichloroethane (10 mL) at 0 °C and under nitrogen a 2.0 M solution of (CH₃)₃Al in heptane (23.4 mL, 46.8 mmol) was slowly added. The mixture was stirred for 1h at 0 °C and at room temperature for 30 min. Then, dicyanobenzene (500 mg, 3.9 mmol) in dichloroethane (5 mL) were added and the solution stirred for 1h at room temperature and subsequently for 4 days at 80° C. The reaction was monitored by TLC (silica gel, n-butanol/CH₃COOH/H₂O 3:1:1). The mixture was cooled to 0 °C and quenched with ice and CH₃OH and the resulting suspension was filtered through a pad of Hyflo Super Cel[®]. The pad was washed with CH₃OH and H₂O, then the filtrates were concentrated in vacuo, the residue was treated with 3N HCl and then concentrated in vacuo. The residue was recrystallized from ethanol. The tetrachloride salt of **1a** was obtained as a white powder after ion exchange chromatography, using H₂O as eluent, in 40 % yield. ¹H NMR (300 MHz, CD₃OD) δ 8.07 (s, 1H), 8.09 (d, 2H, *J*=5.8), 7.86

(t, 1H, $J=5.7$), 3.57 (q, 4H, $J=5.4$), 1.41 (t, 6H, $J=5.4$). ^{13}C NMR δ 164.31, 133.75, 131.48, 131.29, 129.16, 39.57, 13.11 IR (KBr) 3454, 3383, 3035, 1674, 1627, 1447, 1349, 1129, 812, 702. MS (FAB): m/z 219.0 ($[(\text{M}-2\text{HCl})+\text{H}]^+$, calcd. 219.16). Anal. calcd. for $\text{C}_{12}\text{H}_{20}\text{N}_4\text{Cl}_2\cdot\text{H}_2\text{O}$: C 46.61, H 7.17, N 18.12; found: C 46.65, H 7.10, N 17.42.

1,3-*N*-ethylbisbenzamidinium hexafluorophosphate (2b)

The PF_6^- salt was obtained as a white precipitate upon addition of an aqueous saturated solution of NH_4PF_6 to the corresponding chloride salt dissolved in water.

^1H NMR (300 MHz, CD_3OD) δ 8.07 (s, 1H), 8.09 (d, 2H, $J=5.8$), 7.86 (t, 1H, $J=5.7$), 3.54 (q, 4H, $J=5.4$), 1.40 (t, 6H, $J=5.4$). ^{13}C NMR δ 164.36, 133.67, 131.47, 128.86, 39.54, 12.97. IR (KBr) 3469, 3385, 3042, 1681, 1635, 1610, 1403, 1383, 845, 558. MS (FAB): m/z 219.2 ($[(\text{M}-2\text{HPF}_6)+\text{H}]^+$, calcd. 219.16).

6.5 References and notes

1. Lehn, J.-M. *Chem. Eur. J.* **2000**, *6*, 2097-2102.
2. Lehn, J.-M. *Science* **2002**, *295*, 2400-2403.
3. Prins, L. J.; Reinhoudt, D. N.; Timmerman, P. *Angew. Chem., Int. Ed.* **2001**, *40*, 2382-2426.
4. Caulder, D. L.; Raymond, K. N. *Acc. Chem. Res.* **1999**, *32*, 975-982.
5. Shivanyuk, A.; Rebek, J. Jr. *Chem. Commun.* **2001**, 2424-2425.
6. Shivanyuk, A.; Rebek, J. Jr. *Proc. Natl. Acad. Sci. USA* **2001**, *98*, 7662-7665.
7. MacGillivray, L. R.; Diamante, P. R.; Reid, J. L.; Ripmeester, J. A. *Chem. Commun.* **2000**, 359-360.
8. MacGillivray, L. R.; Holman, K. T.; Atwood, J. L. *J. Supramol. Chem.* **2001**, *1*, 125-130.
9. Atwood, J. L.; Barbour, L. J.; Jerga, A. *J. Supramol. Chem.* **2001**, *1*, 131-134.

10. Cave, G. W. V.; Hardie, M. J.; Roberts, B. A.; Raston, C. L. *Eur. J. Org. Chem.* **2001**, *17*, 3227-3231.
11. Fujita, M.; Umemoto, K.; Yoshizawa, M.; Fujita, N.; Kusukawa, T.; Biradha, K. *Chem. Commun.* **2001**, 509-518.
12. Jacopozzi, P.; Dalcanale, E. *Angew. Chem., Int. Ed.* **1997**, *36*, 613-615.
13. Inomata, T.; Konishi, K. *Chem. Commun.* **2003**, 1282-1283.
14. Caulder, D. L.; Powers, R. E.; Parac, T. N.; Raymond, K. N. *Angew. Chem., Int. Ed.* **1998**, *37*, 1840-1843.
15. Manimaran, B.; Rajendran, T.; Lu, Y.-L.; Lee, G.-H.; Peng, S.-M.; Lu, K.-L. *Eur. J. Inorg. Chem.* **2001**, *3*, 633-636.
16. Sun, S.-S.; Lees, A. J. *Chem. Commun.* **2001**, 103-104.
17. Kuehl, C. J.; Yamamoto, T.; Seidel, S. R.; Stang, P. J. *Org. Lett.* **2002**, *4*, 913-915.
18. Kuehl, C. J.; Kryshenko, Y. K.; Radhakrishnan, U.; Sidel, S. R.; Huang, S. D.; Stang, P. J. *Proc. Nat. Acad. Sci. USA* **2002**, *99*, 4932-4936.
19. Baxter, P. N. W.; Lehn, J.-M.; Baum, G.; Fenske, D. *Chem. Eur. J.* **1999**, *5*, 102-112.
20. Garcia, A. M.; Bassani, D. M.; Lehn, J.-M.; Baum, G.; Fenske, D. *Chem. Eur. J.* **1999**, *5*, 1234-1238.
21. Su, C.-Y.; Cai, Y.-P.; Chen, C.-L.; Smith, M. D.; Kaim, W.; zur Loye, H.-C. *J. Am. Chem. Soc.* **2003**, *125*, 8595-8613.
22. Radhakrishnan, U.; Schweiger, M.; Stang, P. J. *Org. Lett.* **2001**, *3*, 3141-3143.
23. Hiraoka, S.; Shiro, M.; Shionoya, M. *J. Am. Chem. Soc.* **2004**, *126*, 1214-1218.
24. MacGillivray, L. R.; Atwood, J. L. *Nature* **1997**, *389*, 469-472.
25. Baldini, L.; Ballester, P.; Casnati, A.; Gomila, R. M.; Hunter, C. A.; Sansone,

- F.; Ungaro, R. *J. Am. Chem. Soc.* **2003**, *125*, 14181-14189.
26. Atwood, J. L.; Barbour, L. J.; Jerga, A. *Chem. Commun.* **2001**, 2376-2377.
27. Shivanyuk, A.; Rebek, J. Jr. *Chem. Commun.* **2003**, *125*, 3432-3433.
28. Martín, T.; Obst, U.; Rebek, J. Jr. *Science* **1998**, *281*, 1842-1845.
29. Kim, H.-J.; Sakamoto, S.; Yamaguchi, K.; Hong, J.-I. *Org. Lett.* **2003**, *5*, 1051-1054.
30. Kobayashi, K.; Shirasaka, T.; Yamaguchi, K.; Sakamoto, S.; Horn, E.; Furukawa, N. *Chem. Commun.* **2000**, 41-42.
31. A dependence of the stoichiometry of binding from the solvent was observed by Diederich for the binding of dicarboxylates and isophthalates to a positively charged resorcinarene receptor in aqueous solution and in methanol. Ref. Sebo, L.; Diederich, F.; *Helv. Chem. Acta* **2000**, *83*, 93-113.
32. Fiammengo, R.; Timmerman, P.; Huskens, J.; Versluis, K.; Heck, A. J. R.; Reinhoudt, D. N. *Tetrahedron* **2002**, *58*, 757-764.
33. Haj-Zaroubi, M.; Mitze, N. W.; Schmidten, F. P. *Angew. Chem., Int. Ed.* **2002**, *41*, 104-107.
34. Hiraoka, S.; Yi, T.; Shionoya, M. *J. Am. Chem. Soc.* **2002**, *124*, 14510-14511.
35. Kneeland, D. M.; Ariga, K.; Lynch, V. M.; Huang, C.-Y.; Anslyn, E. V. *J. Am. Chem. Soc.* **1993**, *115*, 10042-10055.
36. In the complexes **1** and **2** stand for the charged building blocks, i.e. without Na and Cl counterions.
37. The strong ¹H NMR upfield shift observed for the aromatic proton He of **2a** accounts for the formation of a 1:1 complex where the **2a** is included in the cavity of the calix[4]arene **1**.
38. Meyer, A. E.; Castellano, R. K.; Diederich, F. *Angew. Chem. Int. Ed.* **2003**, *42*, 1210-1250.

39. Examples of charged water-soluble receptors which bind oppositely charged aromatic guests through the cooperative formation of electrostatic and hydrophobic interactions have been reported in the literature. For an example see: Ahn, D.-R.; Kim, T.W.; Hong, J.-I. *Tetrahedron Lett.* **1999**, *40*, 6045-6048.
40. Similar FAB mass spectra were obtained from the analysis of solutions of **1** and **2a** at 1:1, 1:2, and 1:4 ratio.
41. Kobiro, K.; Inoue, Y. *J. Am. Chem. Soc.* **2003**, *125*, 421-427.
42. Analogous but reversed results were obtained when the titration was performed by adding **1** to **2a**, confirming that a change in stoichiometry of the complex is taking place in solution.
43. Linton, B. R.; Goodman, S.; Fan, E.; van Arman, S. A.; Hamilton, A. D. *J. Org. Chem.* **2001**, *66*, 7313-7319.
44. The signal at m/z of 1143.43 corresponds to $[\mathbf{1}+\text{Na}]^+$.

SOLUTION AND SURFACE STUDIES ON THE SELF- ASSEMBLY OF A NONCOVALENT MOLECULAR CAPSULE BASED ON IONIC INTERACTIONS*

In this chapter the self-assembly of a molecular capsule based on ionic interactions between two oppositely charged calix[4]arenes, (1 and 2), on a solid support is reported. Calix[4]arene 2 is functionalized at the lower rim with four adamantyl units which form stable inclusion complexes with the β -cyclodextrins (β -CDs) at self-assembled monolayers (SAMs). The noncovalent anchoring of calix[4]arene 2 on a β -CD SAM allows the investigation of capsule formation at a surface. ^1H NMR and ITC studies were primarily performed to provide evidence for the formation of the equimolar assembly in solution. Subsequently, surface plasmon resonance (SPR) was used to compare the effect of the immobilization of one component on a solid support on the ability of oppositely charged building blocks to form a molecular capsule. The association constant K_a for the capsule formation on the surface is $3.5 \times 10^6 \text{ M}^{-1}$, thus comparing well with a K_a of $7.5 \times 10^5 \text{ M}^{-1}$ determined in solution.

* Corbellini F.; Mulder A.; Sartori A.; Ludden M. J. W.; Casnati A.; Ungaro R.; Huskens J.; Crego-Calama M.; Reinhoudt D. N., manuscript in preparation.

7.1 Introduction

Covalent and noncovalent interactions have been exploited in solution chemistry to direct the assembly of molecules into nanometer-sized supramolecular structures.¹⁻⁶ Considerable efforts have been devoted to the synthesis of molecular containers possessing a confined space for the stabilization of reactive intermediates and for catalysis. Moreover, in view of applications like encapsulation of drugs and/or their active transport/delivery, the design of water compatible, reversible containers is actively investigated.^{7,8}

As reported in Chapter 2, various methodologies have been used to obtain molecular containers *via* noncovalent synthesis, the highest number of examples being provided by molecular capsules and cages based on hydrogen bonding^{9,10} and metal-ligand interactions.¹¹⁻¹⁴ Only recently, and as reported in Chapter 3 and 4, the use of electrostatic interactions has attracted the interest of chemists seeking for an alternative and effective way to arrange independent components into strong, reversible and well-defined molecular architectures.¹⁵⁻²⁰

The increasing ability to control the way in which molecules associate in solution offers the possibility to extend the concepts of supramolecular organization to surfaces.²¹ Self-assembled monolayers (SAMs) on gold have been used to organize monomolecular films of supramolecular systems²² and as platform to control the orientation of molecules in two dimensions through specific interactions.²³⁻²⁸

The self-assembly of supramolecular containers on solid support is so far restricted to very few cases. The confinement of a resorcin[4]arene-based carceplex in a SAM on gold has been reported by our group.^{29,30} Furthermore, the formation of a molecular cage based on metal-ligand coordination has been achieved at a surface, while one of the components was anchored to a gold support.³¹

As presented in Chapter 5, the design of molecular capsules based on electrostatic interactions is effective to drive the self-assembly of two oppositely charged components into a molecular capsule in water.³²

In this chapter, a new strategy to attach self-assembled water-soluble molecular containers at a surface is described. The approach used to investigate the capsule formation at the surface level relies on the immobilization of one component of the molecular capsule on a SAM of β -CD derivatives previously chemisorbed on a gold surface, followed by the self-assembly of the second component at the interface. The

effectiveness of the formation of the molecular capsule on the solid support and in solution is compared.

7.2 Results and Discussion

^1H NMR and ITC were used to study the self-assembly of capsule **1•2** in aqueous solution. The capsule is formed through ionic interactions between oppositely charged building blocks i.e. tetrasulfonate calix[4]arene **1** and tetraguanidinium calix[4]arene **2** (Figure 7.1).

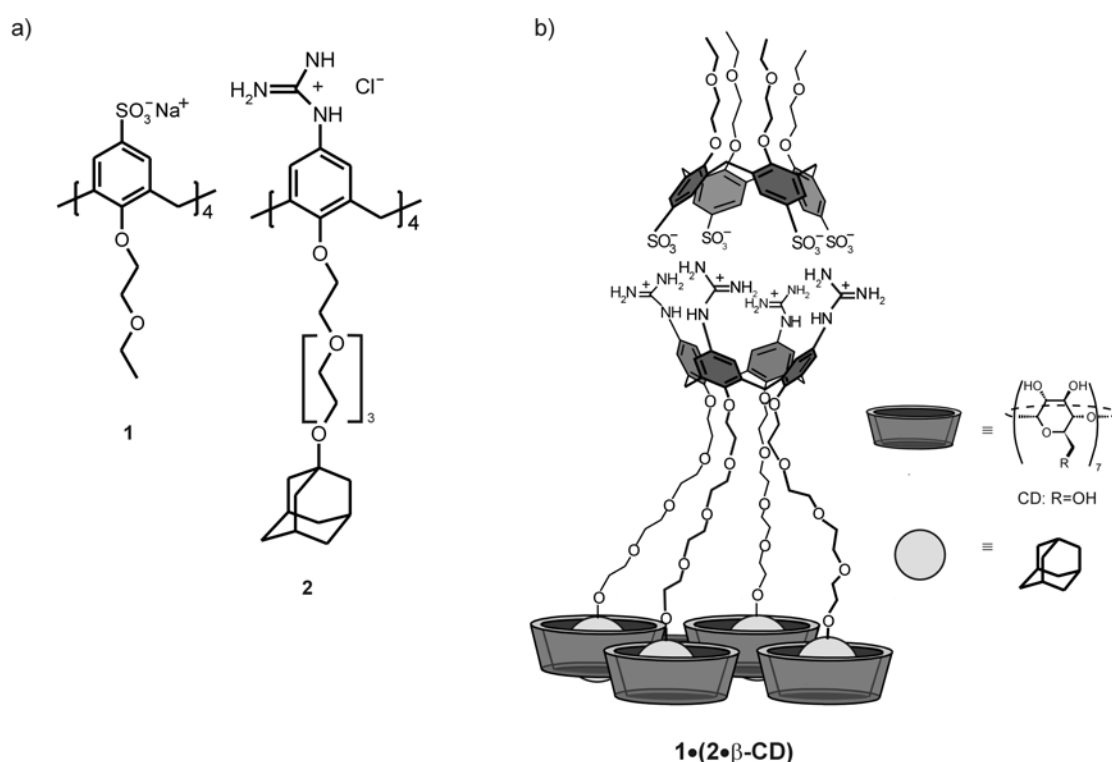


Figure 7.1. a) Molecular building blocks of the capsule **1•2**; b) schematic representation of the molecular capsule **1•(2•β-CD)** in solution.

The strategy used to build the molecular capsule **1•2** at the surface involves the noncovalent positioning of **2** onto a β-CD SAM chemisorbed on a gold surface, followed by the self-assembly of the oppositely charged calix[4]arene **1** as schematically depicted in Figure 7.2. In a previous study it was shown that adamantyl derivatives form strong inclusion complexes with the hydrophobic cavity of the β-CD

both in solution and at the β -CD SAM.³³ In addition, larger organic structures functionalized with adamantyl (Ad) units have been ordered on a β -CD SAM through multiple Ad- β -CD interactions.^{34,35}

Therefore, tetraguanidinium calix[4]arene **2**, functionalized at the lower rim with four adamantyl units, was synthesized. The pendent adamantyl groups are able to form stable inclusion complexes with surface-confined β -CD cavities thus providing a platform for the self-assembly of the tetrasulfonate calix[4]arene **1**. The (poly)ethylene glycol chains space the charged guanidinium groups of **2** from the β -CD cavities. When fixed on a β -CD SAM the cationic moieties of **2** are pointing upwards thus exposing the four positive charges to the outer face of the surface for the self-assembly of the negatively charged component **1** of the capsule (Figure 7.2).

The advantage of using the β -CD SAM as a ‘molecular printboard’ is that isolated single molecules of **2** are kept separated, thus avoiding steric hindrance and/or repulsive forces between the positively charged groups present at the upper rim of the calix[4]arene scaffolds. Furthermore, the stable binding of **2** onto the surface, ensured by the multipoint Ad- β -CD interaction, enables a study of the reversible formation of the molecular capsule **1•2**. In addition, this approach avoids synthetic modifications that the covalent attachment to bare gold would require.

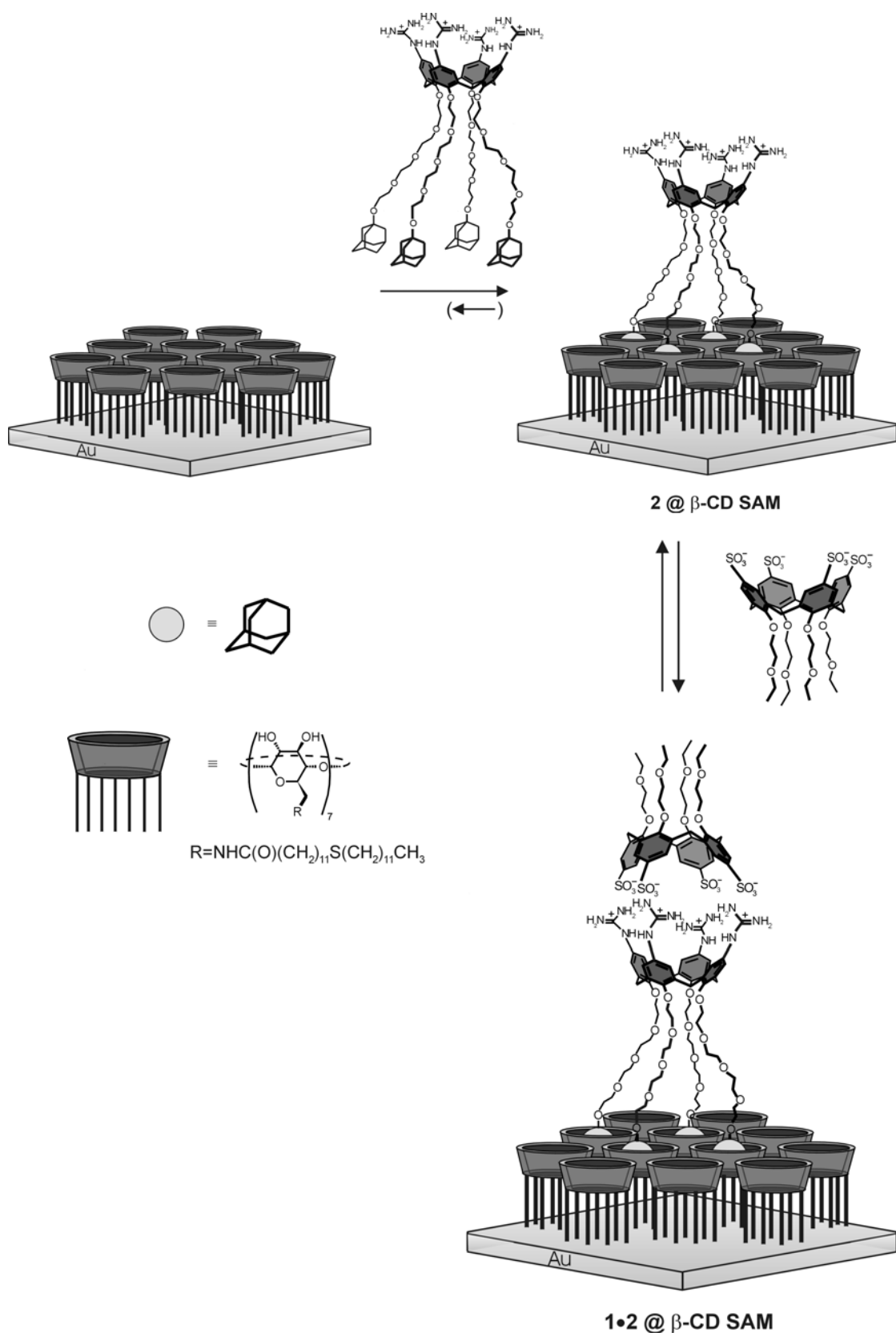
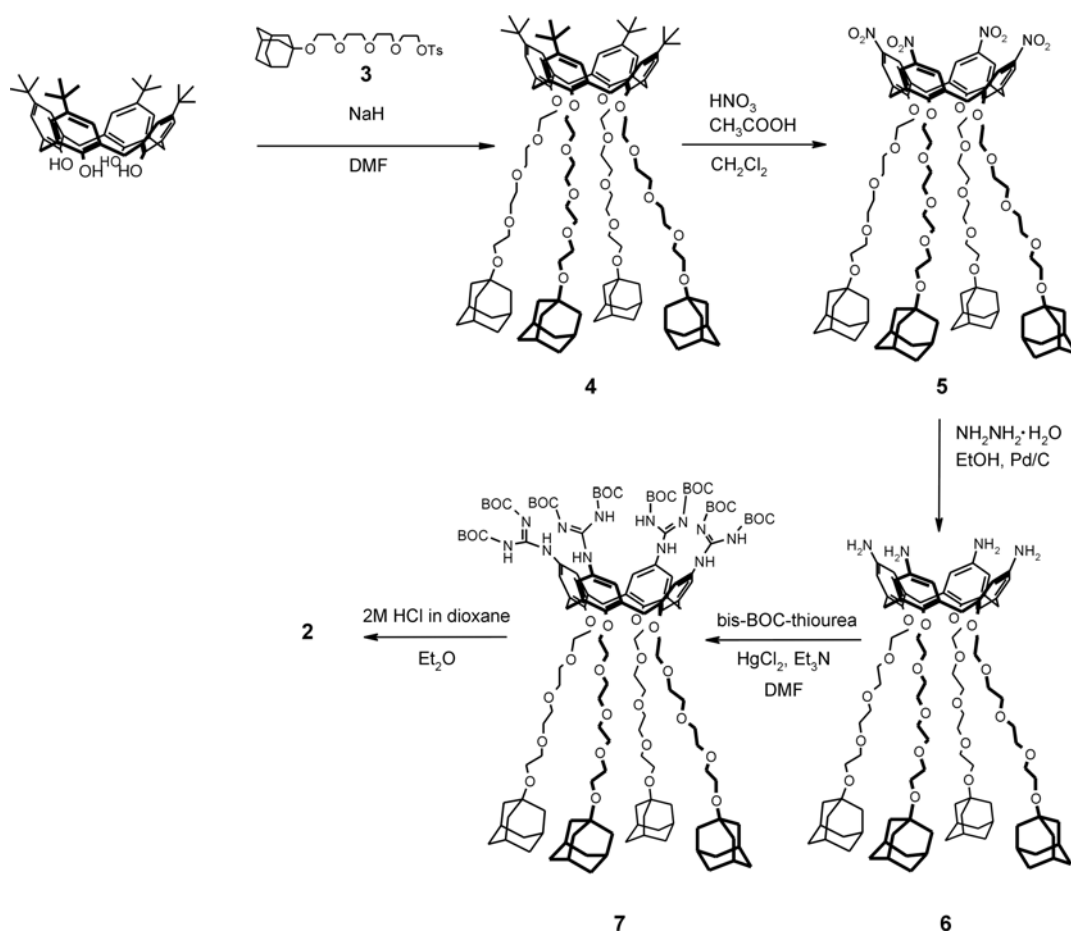


Figure 7.2. Schematic representation of the adsorption of **2** onto a β -CD SAM through the interactions of the adamantyl units with the confined β -CD cavities, and of the self-assembly of the molecular capsule **1•2** at a surface.

7.2.1 Synthesis

Tetrasulfonate calixarene **1** was synthesized according to a literature procedure¹⁹ while compound **2** was prepared as outlined in Scheme 7.1. 1-Adamantyl tetraethylene glycol tosylate **3** was reacted with 5,11,17,23-tetra-*p-tert*-butyl-25,26,27,28-tetrahydroxycalix[4]arene at 80 °C in dry DMF using NaH as a base to give the tetra(adamantyl-tetraethylene glycol)-functionalized calix[4]arene **4**. Substitution of the *tert*-butyl for nitro groups via an ipso-nitration reaction using glacial acetic acid and nitric acid gave tetranitro-calix[4]arene **5**. Low temperature and dry conditions are prerequisites for this reaction in order to prevent elimination of the adamantoxy groups under the strong acidic conditions used. Reduction of the nitro groups using hydrazine monohydrate and Pd/C in absolute ethanol gave the tetraamine calix[4]arene **6** in nearly quantitative yield. Introduction of the BOC-protected guanidinium groups using bis-BOC-thiourea was performed under the conditions reported by the group of Qian³⁶ and led to the formation of **7**. Specific removal of the BOC groups was achieved using 2 N HCl in dioxane, giving the desired product **2** as a tetrachloride salt.



Scheme 7.1. Synthetic route to the tetraguanidinium calix[4]arene **2**.

7.2.2 Formation of the molecular capsule **1•2** in solution

Tetrasulfonate calixarene **1** is soluble in water as a result of the charged groups and of the glycol chains inserted respectively at the upper and at the lower rims of the calix[4]arene scaffold. Tetraguanidinium substituted calixarene **2** possesses charged groups and long ethylene glycol chains that ensure water solubility. Nevertheless, precipitation was observed upon mixing the two components in water. This is a consequence of the neutralization of the charges upon capsule formation and of the presence of the four adamantyl groups which further limit the water solubility of the assembly. A clear aqueous solution was obtained upon addition of β -CD, which forms an inclusion complex with the adamantyl units of **2** thus increasing the solubility of the **1•2** assembly in water (Figure 7.1).

The formation of the molecular capsule **1•2** in 1×10^{-2} M β -CD D₂O was studied by ¹H NMR. The ¹H NMR spectrum of an equimolar solution of **1** and **2** showed up- and downfield shifts for the resonances of the two capsule components indicating that

a well-defined assembly was formed. Formation of undefined aggregates was ruled out as no broadening of the NMR signals was observed (Figure 7.3).

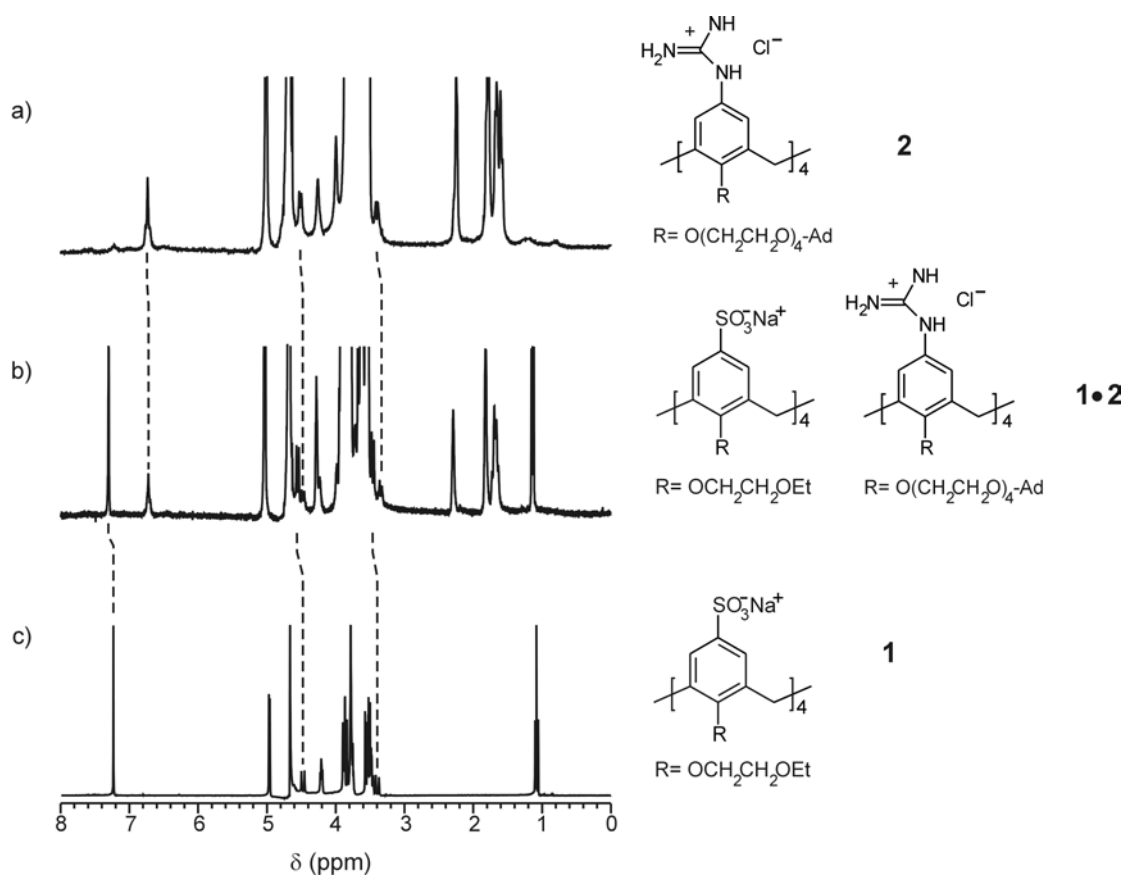


Figure 7.3. ^1H NMR spectra (1×10^{-2} M β -CD in D_2O , 298 K) of a) **2**; b) **1•2**; c) **1**. Ad=adamantyl

Upfield shifts were observed for the signals of the aromatic protons ($\Delta\delta = 0.01$ ppm) and of the methylene bridge hydrogens ($\Delta\delta = 0.04$ and $\Delta\delta = 0.05$ ppm) of the tetraguanidinium calix[4]arene **2** while downfield shifts were observed for the resonance of the aromatic protons of **1** ($\Delta\delta = 0.06$ ppm) and of the protons of the methylene bridge hydrogens ($\Delta\delta = 0.08$ and $\Delta\delta = 0.07$ ppm). Small changes were also detectable for the signals of the ethylene glycol chains of **1** and **2** ($\Delta\delta_{\text{max}} = 0.05$ ppm).

The strength of the capsule formation was studied by Isothermal Titration Calorimetry (ITC) in H_2O containing β -CD (1×10^{-2} M) and KCl (1×10^{-2} M) as a background electrolyte. A 5×10^{-5} M solution of **2** in the calorimetric cell was titrated with a 5×10^{-4} M solution of **1** in the syringe.

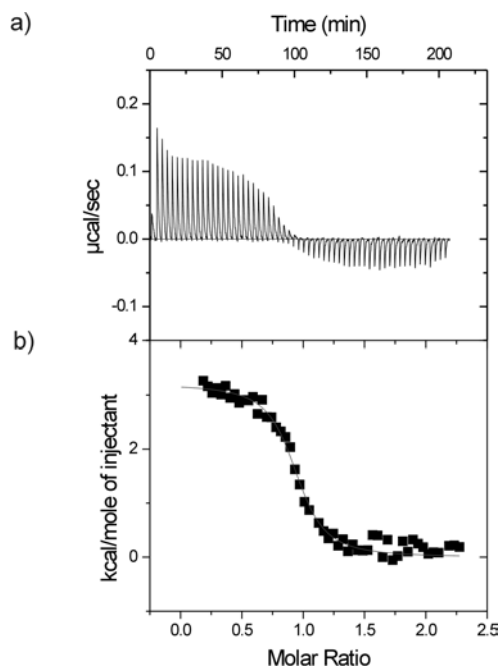


Figure 7.4. Calorimetric titration of **2** (5×10^{-5} M) with **1** (5×10^{-4} M) in H_2O containing $\beta\text{-CD}$ (1×10^{-2} M) and KCl (1×10^{-2} M) at 298 K. a) Data of heat evolution with injection of **1**; b) resulting binding curve markers and best fit line to a 1:1 model.

The resulting enthalpogram (Figure 7.4) is indicative of the formation of a 1:1 assembly as suggested by the presence of an inflection point at a molar ratio of 1. The positive values for both ΔH° ($2.5 \text{ kcal mol}^{-1}$) and $T\Delta S^\circ$ (10 kcal mol^{-1}) account for an endothermic, entropy-driven process. As found for analogous systems^{16,17,20} the formation of molecular capsules based on ionic interactions is driven by the desolvation of the charged groups upon complex formation. Highly ordered solvent molecules are released into the bulk solvent thus resulting in a gain in entropy which is reflected in the positive value for the $T\Delta S^\circ$. The unfavorable value for ΔH° suggests that the energy needed to desolvate the charged groups overrides the energy gained by self-assembly process. The data obtained from the titration were successfully fitted to a 1:1 binding model giving an association constant K_a of $7.5 \times 10^5 \text{ M}^{-1}$.

ESI mass spectrometry provided further proof for the formation of the assembly **1•2**. The spectrum of an equimolar solution of **1** and **2** in MeOH shows the triply charged peak at m/z 998.6 corresponding to $[(\mathbf{1}\cdot\mathbf{2})+3\text{Na}]^{3+}$, together with a less intense peak at m/z 1486.5 attributable to the complex $[(\mathbf{1}\cdot\mathbf{2})+2\text{Na}]^{2+}$.

7.2.3 Formation of the molecular capsule at the surface

While ITC was used to detect the capsule formation in solution, surface plasmon resonance (SPR)³⁷ was utilized to study the assembly of **1•2** on a β -CD SAM on gold. Building the molecular capsule at the surface involves three different steps: the initial formation of a thioether β -CD SAM followed by the formation of an adsorbate layer of **2** through the inclusion of the adamantyl units in the cavities of the β -CD adsorbate molecules. Thereafter, the ionic interactions between **1** and **2** position the second building block at the surface (Figure 7.2).

SAMs of β -CDs were prepared to anchor the tetraguanidinium **2** to the surface through hydrophobic interactions between the adamantyl moieties of **2** and the β -CDs.³⁸ A prerequisite to study the reversible formation of the molecular capsule **1•2** is that **2** has to be “irreversibly” fixed to the substrate.

To prove that the formation of four Ad- β -CD interactions ensures a stable binding of the tetraguanidinium calix[4]arene onto the ‘molecular printboard’, the adsorption process of **2** onto a β -CD SAM was investigated by SPR. Figure 7.5 depicts the SPR sensogram obtained when partial replacements of a 4 mM solution of native β -CD on top of a β -CD monolayer, with a 0.1 mM solution of **2** in 4 mM β -CD solution are performed. The β -CD was used to compete with the β -CD cavities of the SAM for the complexation of the adamantyl moieties and to ensure a controlled adsorption of **2** at the surface in order to obtain a densely packed layer.³⁹ After the replacement with the solution of **2** in 4 mM β -CD, the system was equilibrated for 5-10 minutes, and subsequently rinsed with a 8 mM β -CD solution. The initial adsorption rate for the adsorption of **2** is fast as indicated by the rapid increase of the SPR signal upon addition of **2**. Afterwards, the SPR angle increases slowly in time, probably as a result of the reorganization of the monolayer and the adsorbed layer or as a consequence of nonspecific physisorption. Rinsing of the layer with a 8 mM β -CD solution did not lead to any decrease in the SPR signal. This indicates that **2** forms an extremely stable complex with the β -CD SAM as it cannot be removed from the surface even upon rinsing with a more concentrated β -CD concentration. The stable binding of **2** onto the ‘molecular printboard’ is attributed to the formation of four Ad- β -CD interactions. It was demonstrated recently that stable assemblies on surfaces could be achieved *via* multiple supramolecular interactions.⁴⁰ Thermodynamically

stable complexes at the surface are achieved when two or three Ad- β -CD interactions are formed.³⁵ Moreover, the adsorption of a tetraguanidinium bis(adamantyl)-calix[4]arene (analogous to compound **2**) onto a β -CD SAM has been investigated.^{39,41} These studies showed that a divalent Ad- β -CD binding also ensures a stable attachment of the calix[4]arene derivatives to the surface.

Therefore, the obtained result is in line with what could be expected for a tetravalent complex between **2** and β -CD SAMs⁴² and it demonstrates that **2** could be used as a suitable platform to study the **1•2** capsule formation at the surface.

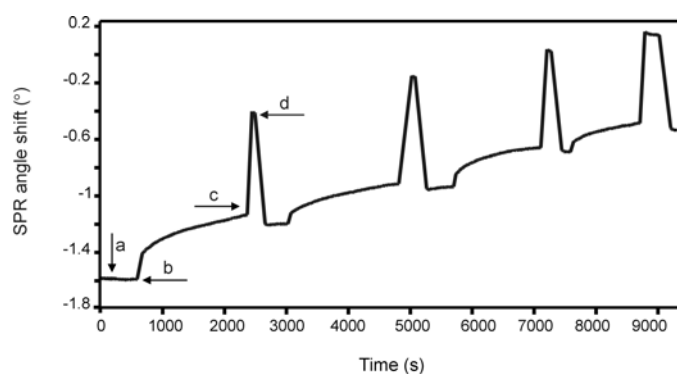


Figure 7.5. SPR sensogram for the adsorption of **2** followed by attempted desorption onto a β -CD SAM on a gold substrate. a) 4 mM β -CD; b) addition of **2** (0.1 mM in 4 mM β -CD); c) rinsing with 8 mM β -CD; d) replacement with 4 mM β -CD. All the solutions are in H₂O. (Four sequential injections of **2** (0.1 mM in 4 mM β -CD) over a β -CD SAM on a gold substrate).

Formation of the molecular capsule **1•2** at the surface was studied by titration of **1** to a β -CD SAM saturated with **2** using a KCl (1×10^{-2} M) solution as background electrolyte, similar to the studies performed in solution by microcalorimetry and ¹H NMR spectroscopy. Figure 7.6 depicts the SPR sensograms obtained for additions of increasing amounts of **1** to a β -CD SAM saturated with **2** (solid line) and a bare β -CD SAM (dotted line). The latter is used as a reference layer.

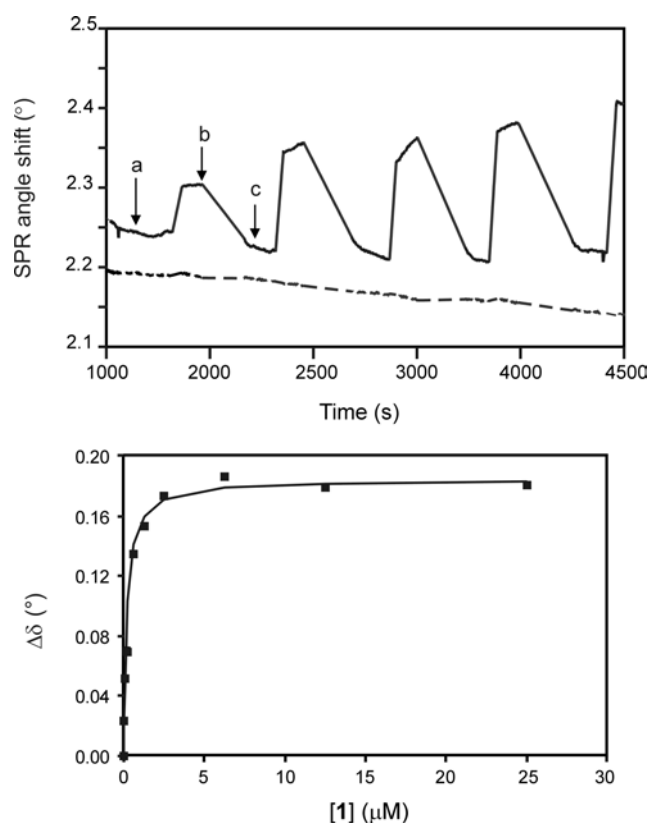


Figure 7.6. (Top) Part of the SPR sensogram for the titration of increasing amounts of **1** over a β -CD SAM saturated with **2** (solid line) and over a β -CD SAM (dashed line). Replacements of 20, 50, 100 and 200 μ l of the cell solution with 20, 50, 100 and 200 μ l of a 1×10^{-5} M solution of **1** are depicted. (All solutions in 1×10^{-2} M aqueous KCl). a) **2** adsorbed on a β -CD SAM; b) signal after addition of **1**; (c) signal after rinsing with 1 M KCl and replacement with 1×10^{-2} M KCl. (Bottom) Data points and best line fit for the change in SPR angle ($\Delta\delta$) of the monolayer of **2** as a function of the concentration of **1**.

Addition of **1** to the β -CD SAM saturated with **2** gives strong SPR responses, indicating the binding of **1** at the monolayer. In sharp contrast, the reference layer does not show any response at all upon addition of **1**. Rinsing of the cells with a 1×10^{-2} M KCl solution only led to a minor decrease in SPR signal (results not shown). Complete restoration of the SPR signals was instead obtained by rinsing the cells with a 1 M KCl solution. These results are indicative of the specific interaction between **1** and **2**. The incomplete restoration of SPR signals using a 1×10^{-2} M KCl solution implies slow dissociation rates at this background electrolyte concentration.⁴³ Fitting of the titration curves using a Langmuir isotherm gave a complexation constant of 3.5×10^6 M⁻¹. This association constant is in good agreement with the association

constant determined in solution by ITC, indicating a similar binding behavior in the bulk solution and at the interface.

Interestingly, the multistep strategy reported here allows the control of the self-assembly at two different levels. As shown the disassembly of half of the capsule is accomplished upon rinsing with a concentrated salt solution (1 M KCl) that weakens the guanidinium-sulfonate interactions. Additionally, the use of a β -CD-SAM as 'molecular printboard' and the reversible nature of the Ad- β -CD interactions offer the possibility to disassemble the adamantyl derivative from the solid support. This could be achieved upon rinsing with a solvent (i.e. ethanol) that weakens the hydrophobic interactions responsible for the Ad- β -CD binding.

7.3 Conclusions

In this chapter evidence was shown for the formation of a molecular capsule based on ionic interactions, both in aqueous solution and on a solid support.

At the surface the molecular capsule was built through a noncovalent, stepwise procedure which involves a multipoint attachment of one building block, functionalized with adamantyl units, onto a β -CD SAM followed by the successive binding of the second component. This approach is highly versatile as it opens the possibility to build large varieties of molecular capsules on a gold surface by simply functionalizing one of the building blocks with adamantyl units.

In conclusion, the results obtained indicate that the concept of building noncovalent molecular capsules based on ionic interactions, investigated so far only in the bulk solution, can also be extended to the surface.

7.4 Experimental Section

7.4.1 General information and instrumentation

All moisture sensitive reactions were carried out under nitrogen atmosphere. Most of the solvents and all reagents were obtained from commercial sources and used without further purification. All dry solvents were prepared according to standard procedures and stored over molecular sieves. ^1H NMR and ^{13}C NMR spectra were recorded on Bruker AC300 and Bruker AMX400 spectrometers. Spectra are reported in ppm downfield from TMS as an internal standard. Mass spectra by electrospray ionization (ESI) and chemical

ionization (CI) methods were recorded on a Micromass ZMD (or a Micromass LCT time-of-flight mass spectrometer) and on a Finnigan Mat SSQ710 spectrometer, respectively. MALDI-MS spectra were recorded with a PerSpective Biosystems Voyager-De-RP spectrometer. Elemental analyses were performed using a Carlo Erba EA1106. Analytical TLC was performed using Merck prepared plates (silica gel 60 F-254 on aluminium). Merck silica gel (40-63 μm) was used for flash chromatography. Compounds **2**, **3**, **5**, **6**, **7** were synthesized by Andrea Sartori.

Monolayer preparation. Gold substrates were obtained from Ssens B.V. (Hengelo, The Netherlands). SAMs monolayers of β -CD heptathioether were prepared as reported previously.³³

7.4.2 Binding studies

Calorimetric measurements. The titration experiments were carried out using a Microcal VP-ITC microcalorimeter with a cell volume of 1.4115 mL. The formation of the assemblies **1•2** has been studied adding aliquots of a 0.5 mM solution of **1**, in the burette, to a 0.05 mM solution of **2**, in the calorimetric cell, and monitoring the heat change after each addition. Dilution experiments showed that at the experimental concentrations employed here none of the species showed any detectable aggregation in water. The thermodynamic parameters given above are based on three independent calorimetric titrations. Titration curves were fitted with a 1:1 model using a least-squares fitting procedure and the association constant and enthalpy of binding as independent fitting parameters

SPR. SPR measurements were performed in a two-channel vibrating mirror angle scan setup based on the Kretschmann configuration, described by Kooyman and co-workers.⁴⁴ Light from a 2 mW HeNe laser is directed onto a prism surface by means of a vibrating mirror. The intensity of the light is measured by means of a large-area photodiode. This setup allows the determination of changes in plasmon angle with an accuracy of 0.0028. The gold substrate with the monolayer was optically matched to the prism using an index matching oil. All solutions were made using Millipore water and all solutions were filtered through nanopore filters prior to use.

In a typical experiment a cell placed on top of a β -CD monolayer was filled with 800 μ L of a 10 mM KCl solution. After stabilization of the SPR signals, the β -CD monolayer in one of the cells was saturated with **2** by replacing 720 μ L of the buffer solution with a 10 mM KCl buffer solution containing 0.1 mM of **2** and 5 mM of β -CD. The system was equilibrated while monitoring the SPR angle change. After stabilization of the SPR signal (typically 30 min.) both cells were rinsed with a 10 mM KCl solution by repeatedly replacing 720 μ L of the cell solutions with 720 μ L of the buffer solution (7 times). Titrations with **1** were performed by systematically replacing an increasing amount of buffer solution with of **1** (1-100 μ M) in 10 mM KCl for both cells. Between additions, the cells were rinsed by repeatedly replacing 720 μ L of the cell solution with 720 μ L of a 1 M KCl solution (7 times). The initial KCl concentration was restored by replacing 720 μ L of the cell solutions with 720 μ L Millipore water, and subsequent rinsing with 10 mM KCl using the procedure outlined above. Binding constants given above are based on three independent SPR titrations.

7.5 References and notes

1. Lawrence, D. S.; Jiang, T.; Levett, M. *Chem. Rev.* **1995**, *95*, 2229-2260.
2. MacGillivray, L. R.; Atwood, J. L. *Angew. Chem. Int. Ed.* **1999**, *38*, 1018-1033.
3. Jasat, A.; Sherman, J. C. *Chem. Rev.* **1999**, *99*, 931-967.
4. Greig, L. M.; Philp, D. *Chem. Soc. Rev.* **2001**, *30*, 287-302.
5. Higler, I.; Timmerman, P.; Verboom, W.; Reinhoudt, D. N. *Eur. J. Org. Chem.* **1998**, *12*, 2689-2702.
6. Prins, L. J.; Reinhoudt, D. N.; Timmerman, P. *Angew. Chem. Int. Ed.* **2001**, *40*, 2382-2426.
7. Conn, M. M.; Rebek, J. Jr. *Chem. Rev.* **1997**, *97*, 1647-1668.
8. Hof, F.; Craig, S. L.; Nuckolls, C.; Rebek, J. Jr. *Angew. Chem. Int. Ed.* **2002**, *41*, 1488-1508.

9. Rebek, J. Jr. *Chem. Soc. Rev.* **1996**, 25, 255-264.
10. Rebek, J. Jr. *Chem. Commun.* **2000**, 637-643.
11. Jacopozzi, P.; Dalcanale, E. *Angew. Chem. Int. Ed. Engl.* **1997**, 36, 613-615.
12. Radhakrishnan, U.; Schweiger, M.; Stang, P. J. *Org. Lett.* **2001**, 3, 3141-3143.
13. Takeda, N.; Umemoto, K.; Yamaguchi, K.; Fujita, M. *Nature* **1999**, 398, 794-796.
14. Fujita, M.; Umemoto, K.; Yoshizawa, M.; Fujita, N.; Kusukawa, T.; Biradha, K. *Chem. Commun.* **2001**, 509-518.
15. Wehner, M.; Schrader, T.; Finocchiaro, P.; Failla, S.; Consiglio, G. *Org. Lett.* **2000**, 2, 605-608.
16. Zadmard, R.; Schrader, T.; Grawe, T.; Kraft, A. *Org. Lett.* **2002**, 4, 1687-1690.
17. Zadmard, R.; Junkers, M.; Schrader, T.; Grawe, T.; Kraft, A. *J. Org. Chem.* **2003**, 68, 6511-6521.
18. Fiammengo, R.; Timmerman, P.; de Jong, F.; Reinhoudt, D. N. *Chem. Commun.* **2000**, 2313-2314.
19. Fiammengo, R.; Timmerman, P.; Huskens, J.; Versluis, K.; Heck, A. J. R.; Reinhoudt, D. N. *Tetrahedron* **2002**, 58, 757-764.
20. Corbellini, F.; Fiammengo, R.; Timmerman, P.; Crego-Calama, M.; Versluis, K.; Heck, A. J. R.; Luyten, I.; Reinhoudt, D. N. *J. Am. Chem. Soc.* **2002**, 124, 6569-6575.
21. Lehn, J.-M. *Science* **1996**, 35, 538-540.
22. Dubois, L. H.; Nuzzo, R. G. *Annu. Rev. Phys. Chem.* **1992**, 43, 437-463.
23. Arias, F.; Godinez, L. A.; Wilson, S. R.; Kaifer, A. E.; Echegoyen, L. *J. Am. Chem. Soc.* **1996**, 118, 6086-6087.
24. Hatzor, A.; Moav, T.; Cohen, H.; Matlis, S.; Libman, J.; Vaskevich, A.;

- Shanzer, A.; Rubinstein, I. *J. Am. Chem. Soc.* **1998**, *120*, 13469-13477.
25. Moav, T.; Hatzor, A.; Cohen, H.; Libman, J.; Rubinstein, I.; Shanzer, A. *Chem. Eur. J.* **1998**, *4*, 502-507.
26. Fragoso, A.; Caballero, J.; Almirall, E.; Villalonga, R.; Cao, R. *Langmuir* **2002**, *18*, 5051-5054.
27. Miura, Y.; Kimura, S. *Langmuir* **1998**, *14*, 2761-2767.
28. Yang, X.; McBranch, D.; Swanson, B.; Li, D. *Angew. Chem. Int. Ed. Engl.* **1996**, *5*, 538-540.
29. Huisman, B. H.; Rudkevich, D. M.; Farrán, A.; Verboom, W.; van Veggel, F. C. J. M.; Reinhoudt, D. N. *Eur. J. Org. Chem.* **2000**, *2*, 269-274.
30. Huisman, B. H.; Rudkevich, D. M.; van Veggel, F. C. J. M.; Reinhoudt, D. N. *J. Am. Chem. Soc.* **1996**, *118*, 3523-3524.
31. Levi, S.; Guatteri, P.; van Veggel, F. C. J. M.; Vancso, G. J.; Dalcanale, E.; Reinhoudt, D. N. *Angew. Chem. Int. Ed.* **2001**, *40*, 1892-1896.
32. Corbellini, F.; Di Costanzo, L.; Crego-Calama, M.; Geremia, S.; Reinhoudt, D. N. *J. Am. Chem. Soc.* **2003**, *125*, 9946-9947.
33. de Jong, M. R.; Huskens, J.; Reinhoudt, D. N. *Chem. Eur. J.* **2001**, *7*, 4164-4170.
34. Huskens, J.; Mulder, A.; Auletta, T.; Nijhuis, C. A.; Ludden, M. J. W.; Reinhoudt, D. N. *J. Am. Chem. Soc.* **2004**, *126*, in press.
35. Huskens, J.; Deij, M. A.; Reinhoudt, D. N. *Angew. Chem. Int. Ed.* **2002**, *41*, 4467-4471.
36. Kim, K. S.; Qian, L. *Tetrahedron Lett.* **1993**, *34*, 7677-7680.
37. Scuck, P. *Annu. Rev. Biophys. Biomol. Struct.* **1997**, *26*, 541-566.
38. Beulen, M. W. J.; Bügler, J.; de Jong, M. R.; Lammerink, B.; Huskens, J.;

- Schönherr, H.; Vancso, G. J.; Boukamp, B. A.; Wieder, H.; Offenhäuser, A.; Knoll, W.; van Veggel, F. C. J. M.; Reinhoudt, D. N. *Chem. Eur. J.* **2000**, *6*, 1176-1183.
39. Mulder, A.; Auletta, T.; Sartori, A.; Casnati, A.; Ungaro, R.; Huskens, J.; Reinhoudt, D. N. *J. Am. Chem. Soc.* **2004**, *126*, accepted.
40. Auletta, T. *Ph.D. Thesis*, University of Twente, The Netherlands, 2003.
41. Auletta, T.; Dordi, B.; Mulder, A.; Sartori, A.; Onclin, S.; Bruinink, C. M.; Péter, M.; Nijhuis, C. A.; Beijleveld, H.; Schönherr, H.; Vancso, G. J.; Casnati, A.; Ungaro, R.; Ravoo, B. J.; Huskens, J.; Reinhoudt, D. N. *Angew. Chem. Int. Ed.* **2004**, *43*, 369-373.
42. Estimation of the binding constant using the model presented in ref. 34 yields an association constant in the order of 10^{20} M^{-1} .
43. When the same experiment was repeated using a more concentrated solution of KCl (1 M) as rinsing solution, a faster response was obtained, nevertheless an accurate determination of the association constant was not possible.
44. Lenferink, A. T. M.; Kooyman, R. P. H.; Greve, J. *Sens. Act. B* **1991**, 261-265.

SUMMARY

The subjects of this thesis are synthesis, characterization and investigation of the binding properties of supramolecular capsules based on ionic interactions.

Chapter 1 has given a general introduction to the field of supramolecular chemistry and to the principles of molecular recognition and self-assembly, widely exploited in the synthesis of molecular containers.

In Chapter 2 an overview is given of the molecular containers obtained by covalent and noncovalent synthesis. In the first part of the chapter the most significant examples of (hemi)carcerands and cryptophanes resulting from the connection of two or more building blocks by means of covalent bonds are reported. The central part of the chapter focuses on the use of noncovalent forces, i.e. hydrogen bonds and metal-ligand interactions for the assembly of molecular capsules, cages and clusters. Some of the most important applications of molecular containers in chemistry (reaction chambers, isolation of reactive intermediates, and sensing) are highlighted in the last section of the chapter.

Chapter 3 describes the formation and characterization of a novel type of capsules resulting from the self-association between oppositely charged calix[4]arenes in MeOH and MeOH/H₂O solutions. The cationic building block is a calix[4]arene functionalized at the upper rim with four amidinium groups while the introduction of sulfonate, carboxylic acid, or phosphate moieties at the upper rim of the second calix[4]arene scaffold provides three different anionic building blocks. Despite the reasonable water solubility of the separate components, upon mixing the molecular capsules precipitated from water. The assemblies were characterized by ¹H NMR spectroscopy and mass spectrometry (ESI). It was demonstrated by isothermal titration calorimetry (ITC) that multiple ionic interactions ensure very stable assemblies in MeOH/H₂O solutions containing excess of salts (Bu₄NClO₄ and Na₂B₄O₇). The association constants K_a range from 10⁴ to 10⁷ M⁻¹ depending on the ion pairs involved in the assembly and on the ionic strength of the solution ($I = 0.01$ or 0.03 M). The assembly between the conformationally flexible thiacalix[4]arene and a tetraamidinium calix[4]arene was also investigated. While solution studies by ¹H NMR and ITC strongly suggested the formation of a 1:1 molecular capsule, the X-ray structure showed that in the solid state the two building blocks assemble into a more

complex 3D-network. Tetraamidinium calix[4]arenes bearing different amidinium side chains (propyl, isopropyl and heptyl) were synthesized and the formation of the molecular capsules with the oppositely charged tetrasulfonate calix[4]arene was investigated in Chapter 4. ^1H NMR studies in methanol- d_4 indicated that the different amidinium side chains affect the geometry of the resulting molecular capsules. While one of the short propyl or isopropyl chains can be included in the capsule's cavity, the long heptyl chain is too bulky to find accommodation in the capsule's cavity. ITC studies have shown that the length of the substituents of the amidinium moieties does not influence the thermodynamics of binding indicating that the assembly is essentially driven by the ionic interactions between the two oppositely charged building blocks.

An X-ray structure was obtained which confirmed the geometry proposed on the basis of solution studies (^1H NMR, 2D NMR), i.e. the inclusion of one of the propyl chains in the capsule's cavity. The included propyl chain was used as a probe to investigate the guest encapsulation properties of the molecular capsules. Upon addition of an excess of tetramethylammonium, acetylcholine, and *N*-methylquinuclidinium (chloride or iodide salt), to a solution of the capsule in methanol, the propyl chain was extruded from the capsule's cavity as a consequence of the inclusion of the ammonium cation. To obtain water solubility (poly)ethylene glycol chains of different lengths were introduced at the bottom rim of one of the building blocks of the capsule. In one case the self-assembly could be studied by ITC in aqueous solution. However, the solubility in water was still too poor to allow further investigations with other techniques.

Water solubility of the molecular capsules was obtained upon introduction of amino acid moieties at the upper rim of one of the building blocks as reported in Chapter 5. Two calix[4]arenes substituted at the upper rim with either alanine or lysine (Boc-protected on the side chain) moieties were synthesized and the formation of the molecular capsules with the oppositely charged tetraamidinium calix[4]arene was studied by ^1H NMR, ESI-MS and ITC. Microcalorimetric titrations in MeOH/H₂O and H₂O solution have demonstrated that although the association constants for the two assemblies are comparable ($K_a \sim 10^5$ - 10^6 M⁻¹), the side chain length of the different amino acidic moieties strongly influences the thermodynamic parameters of the binding. For comparison the self-assembly between a tetracarboxy and a tetraamidinium calix[4]arene was also investigated.

Molecular docking was used to predict potential guests for the tetraalanine-tetraamidinium molecular capsule. ^1H NMR confirmed that the capsule represents an effective host for both charged and neutral guest molecules such as *N*-methylquinuclidinium cation and 6-amino-2-methylquinoline.

Having established the success of multiple ionic interactions in constructing supramolecular capsules, the self-assembly of a molecular capsule from six independent components, two tetrasulfonate calix[4]arene and four bisbenzamidinium spacers was investigated in Chapter 6. ESI and FAB mass spectrometry suggested the self-association of the components into the 2:4 complex together with other aggregates having 1:1 and 1:2 stoichiometries. Solution studies, by ^1H NMR titrations, Job's plot analysis and ITC, suggested that the stoichiometry of the products depends on the solvent used in the experiments. The self-association of the monomeric units into the 1:1 complex is favored in water while in methanol the coexistence of 1:1, 1:2 and 2:4 complexes is most likely. X-ray crystallography showed that in the solid state the ternary complex of 1:2 stoichiometry is formed.

The self-assembly of a molecular capsule on a solid support was investigated in Chapter 7. The noncovalent strategy for building the molecular capsule at the surface involves two steps, the multipoint attachment of a tetraguanidinium calix[4]arene functionalized at the lower rim with adamantyl units onto a β -cyclodextrin self-assembled monolayer (β -CD SAM) followed by the successive binding of the second building block, a tetrasulfonate calix[4]arene, through ionic interactions. The assembly process was followed by surface plasmon resonance (SPR). This approach is highly versatile as it opens the possibility to build large varieties of molecular capsules on gold surfaces by simply functionalizing one of the building blocks with adamantyl units. ^1H NMR and ITC studies were performed to provide evidence for the formation of the assembly in solution. The comparable binding constants indicate a similar binding behavior in the bulk solution and at the interface.

SAMENVATTING

De onderwerpen van dit proefschrift zijn, de synthese, karakterisering en het onderzoek naar de bindings eigenschappen van supramoleculaire capsules gebaseerd op ionische interacties.

In Hoofdstuk 1 is een algemene introductie gegeven tot het gebied van de supramoleculaire chemie en de principes van moleculaire herkenning en zelf-assemblage, gebruikt in de synthese van moleculaire containers.

In Hoofdstuk 2 is een overzicht gegeven van moleculaire containers gemaakt door middel van covalente en niet-covalente synthese. In het eerste gedeelte van het hoofdstuk worden de belangrijkste voorbeelden van (hemi)carceranden en cryptofanen, resulterend uit de binding tussen twee of meer bouwstenen met behulp van covalente binding, gegeven. Het middengedeelte van het hoofdstuk richt zich op het gebruik van niet-covalente krachten, zoals waterstof bruggen en metaal-ligand interacties, voor the assemblage van capsules, kooien en clusters. Een aantal van de belangrijkste toepassingen van moleculaire containers in de chemie (reactie vaten, isolatie van reactieve intermediären, en sensoren) worden in het laatste gedeelte van dit hoofdstuk belicht.

Hoofdstuk 3 beschrijft de vorming en karakterisering van een nieuw soort capsules resulterend uit de zelf- associëring van tegenovergesteld geladen calix[4]arenen, in methanol en methanol/water oplossingen. De kationische bouwsteen is een calix[4]areen aan de bovenrand gefunctionaliseerd met vier amidinium groepen terwijl de introductie van sulfonaat, carboxylzuur, of fosfaat substituenten aan de bovenrand van de tweede calix[4]areen basis, voor drie verschillende anionische bouwstenen zorgt. Ondanks de redelijke wateroplosbaarheid van de componenten, konden de moleculaire capsules geïsoleerd worden door middel van precipitatie uit water. De assemblages zijn gekarakteriseerd met ^1H NMR en massa spectrometrie (ESI). Met isothermische titratie calorimetrie werd gedemonstreerd dat meervoudige ionische interacties zorgen voor zeer stabiele assemblages in methanol/water oplossingen met een overmaat van zouten (Bu_4NClO_4 en $\text{Na}_2\text{B}_4\text{O}_7$), met associatie constanten K_a variërend van 10^4 tot 10^7 M^{-1} , afhankelijk van de ionparen betrokken bij de assemblage en van de ion sterkte van de oplossing ($I = 0.01$ of 0.03 M). The assemblage van de conformationeel flexibele thiacalix[4]areen

met een tetrasulfonaat calix[4]areen is ook onderzocht. Terwijl studies in oplossing met ^1H -NMR en ITC sterk wezen op de vorming van een 1:1 moleculaire capsule, liet de kristal structuur zien dat de twee bouwstenen assembleerden in een gecompliceerder 3-dimensionaal netwerk.

Tetraamidinium calix[4]arenen met verschillende amidinium zijketens (propyl, isopropyl en heptyl) werden gesynthetiseerd en de formatie van moleculaire capsules met de tegengesteld geladen tetrasulfonaat calix[4]areen werd onderzocht in Hoofdstuk 4. ^1H NMR studies in methanol- d_4 gaven een indicatie dat de verschillende amidinium zijketens de geometrie van de gevormde moleculaire capsules beïnvloedden. Waar een van de korte propyl of isopropyl zijketens in de holte van de capsule kan worden omvat, neemt de lange heptyl keten te veel ruimte in beslag om de holte van de capsule te passen. ITC studies lieten zien dat de lengte van de substituenten van de amidinium groepen de thermodynamica van de binding niet beïnvloedt, wat er op duidt dat de assemblage hoofdzakelijk wordt gestuurd door ionische interacties van de twee tegenovergesteld geladen bouwstenen. Een X-ray kristalstructuur werd verkregen die de op basis van oplossingsstudies (^1H NMR, 2D NMR) verkregen geometrie bevestigde, namelijk de inclusie van een van de propyl ketens in de holte van de capsule. De ingesloten propyl-keten werd gebruikt als probe om de gast incapsulatie eigenschappen van de moleculaire capsule te onderzoeken. Na additie van een overmaat tetramethylammonium, acetylcholine, en N-methylquinuclidinium (chloride of iodide zout) aan een oplossing van de capsule in methanol, werd de propylketen uit de holte van de capsule geperst vanwege de inclusie van het ammonium kation. Om de capsule wateroplosbaar te maken werden (poly)ethyleen glycol ketens met verschillende lengtes aan de onderrand van een van de bouwstenen geïntroduceerd. In een geval kon met ITC de zelf-assemblage in waterige oplossing bestudeerd worden. De oplosbaarheid in water was echter zo laag dat verdere studies met andere technieken niet mogelijk waren.

Wateroplosbaarheid van de moleculaire capsules werd verkregen door introductie van aminozuur substituenten aan de bovenrand van een van de bouwstenen zoals staat beschreven in Hoofdstuk 5. Twee amine gesubstitueerde calix[4]arenen met of alanine of lysine (Boc-beschermd aan de zijketen) groepen werden gesynthetiseerd en de vorming van de moleculaire capsules met de tegenovergesteld geladen tetraamidinium calix[4]areen werd bestudeerd met ^1H NMR, ESI-MS en ITC. Microcalorimetrische titraties in methanol/water en water oplossingen lieten zien dat

ondanks dat associatie constanten van de twee assemblages vergelijkbaar zijn ($K_a \sim 10^5 - 10^6 \text{ M}^{-1}$), de lengte van de zijketens van de verschillende aminozuur groepen de thermodynamische bindingsparameters sterk beïnvloeden. Om te vergelijken werd de zelf-assemblage tussen een tetracarboxy en een tetraamidinium calix[4]areen ook onderzocht. Moleculaire docking experimenten werden gebruikt om potentiële gasten voor de tetraalanine-tetraamidinium moleculaire capsule te voorspellen. ^1H NMR bevestigde dat de capsule een effectieve gastheer voor geladen en neutrale gast moleculen, zoals het *N*-methylquinuclidinium kation en 6-amino-2-methylquinoline, is.

Nadat het succes van het gebruik van meervoudige ionische interacties voor het maken van supramoleculaire capsules werd vastgesteld, werd in Hoofdstuk 6 de zelfassemblage van een moleculaire capsule vanuit zes onafhankelijke componenten, twee tetrasulfonaat calix[4]arenen en vier bisbenzamidinium spacers, onderzocht. ESI en FAB massa spectroscopie suggereerden the zelfassociatie van de componenten in een 2:4 complex samen met andere aggregaten met 1:1 en 1:2 stochiometrieën. Oplossings studies, ^1H NMR en Job's plot analyse ITC, suggereerden dat de vorming van de producten met verschillende stochiometrieën afhangt van het oplosmiddel dat in de experimenten gebruikt werd. De zelfassociatie van de monomere eenheden tot het 1:1 complex is het gunstigst in water terwijl in methanol waarschijnlijk de 1:1, 1:2, 2:4 complexen samen voorkomen. X-ray kristallografie laat zien dat in de vaste fase het ternaire complex met 1:2 stochiometrie gevormd word.

The zelf-assemblage van een moleculaire capsule op een vaste drager werd in Hoofdstuk 7 behandeld. The niet covalente strategie om de capsule op een oppervlak op te bouwen behelst twee stappen, de meerpunts koppeling van een tetraguanidine calix[4]areen, aan de onderrand gefunctionaliseerd met adamantyl groepen , op een β -cyclodextrine zelf-geassembleerde monolaag (β -CD SAM) gevolgd door de binding van de tweede bouwsteen, een tetrasulfonaat calix[4]areen, door middel van ionische interacties. Het assemblage proces werd gevolgd door surface plasmon resonance (SPR). Deze aanpak is heel veelzijdig omdat het de mogelijkheid biedt om een heel scala aan moleculaire capsules op een goud oppervlak te binden door simpelweg een van de bouwstenen met adamantyl groepen te functionaliseren. ^1H NMR en ITC studies werden uitgevoerd om de assemblage in oplossing aan te tonen. De vergelijkbare bindingsconstanten indiceren dat een zelfde bindingsmode plaatsvindt in bulk oplossing en aan het oppervlak.

ACKNOWLEDGEMENTS

Many people have contributed, scientifically and not, to the realization of this thesis and made these four years a great experience.

First of all, I would like to express my appreciation to my promotor David Reinhoudt for giving me the privilege of working as a member of his group. You have given me enormous freedom to pursue my own research while at the same time providing the right amount of guidance to ensure that my efforts contribute to the achievement of the scientific goals of my project.

I would like to thank my supervisor Mercedes Crego Calama who, with her daily presence, ever-lasting optimism and contagious enthusiasm, has been my guide throughout this thesis. I really appreciate the effort you put to help find solutions for problems and to improve papers to satisfy referees. Thank you for the stimulating discussions and suggestions and for implementing the quality of this manuscript.

I would like to acknowledge Peter Timmerman under whose supervision I chose this topic and began the thesis. I am grateful for patiently guiding me through a completely new subject, providing encouragement and ideas for my project.

I am deeply indebted to Jurriaan Huskens for helping me anytime I knocked at his door. Thank you for your valuable time and criticism and for the substantial contribution to the work shown in Chapter 6.

The present thesis is also the result of fruitful collaborations: I am very grateful to Prof. Silvano Geremia and Luigi Di Costanzo for the X-ray analysis reported in Chapter 4 and 6. Thank you to Ronald Knegt and Peter Grootenhuis for the docking studies reported in Chapter 5. Prof. Albert Heck and Kees Versluis are acknowledged for the mass spectrometry measurements reported in Chapter 4. I would like to thank Huub Kooijman and Fijs van Leeuwen for the crystallographic work and for the clarifying discussions we had about the complicated structure reported in Chapter 3. Furthermore, I am indebted to Andrea Sartori for the synthetic work and to Alart Mulder and Manon Ludden for the SPR experiments reported in Chapter 7.

Tieme Stevens, Roel Fokkens, Bianca Snellink, Hannie Visser, Annemarie Montanaro deserve a special mention for their help with analytical techniques. Many thanks to Richard Egberink, for technical advice and above all for fixing all my computer's troubles. Marc Brouwer and Marcel de Bruine, thank you for helping me

to achieve a new record: Nobody else before ever used so many volumetric flasks and NMR tubes as me!

Becky, Leonard and Roberto, whom accepted to correct the concept thesis, thank you for managing to read the whole thesis thoroughly. Your meticulous review of this manuscript is invaluable. Thank you to Emiel who so kindly and patiently translated the summary into the samenvatting. I really appreciated that!

This project would not have been possible without the assistance and cooperation of Roberto. I have benefited from your expertise, appreciated your being a good “devil’s advocate”, and enjoyed your support and friendship.

I am convinced I was lucky to run this “marathon” with Alart. Thank you for providing me with all of the proper forms, for giving me stylistic advice, reminding me to be consistent! and for the friendly, sometimes nonsense, conversations we had during the breaks. I think I should also thank Steffen for putting up with my italianity!

The road to my Ph.D. degree has been long so I would like to thank not only the present SMCT group members, but also the people of the early days for providing a stimulating and pleasant environment. Kazu, Jessica, Stefano, Leo, Tommaso, Steve, Oskar, Jasper, Gerald, Menno, Juanjo, Paolo, Roberto, Christiaan, Mattijs, Joris, I have good memories of the time spent in and outside the lab.

There are some people who deserve special mention as they made this most intense four years of my life an equally pleasant and unforgettable time: Irene, Fernando, Lourdes, Olga, Alessio, Michel, Becky, Mirko, Soco, Andrea thank you for your friendship, for the fun we had together and for giving me extra strength to get the thesis done. Monica, Marco, Monica and Barbara I really appreciated your help and encouragement.

I had the good fortune of having a flatmate and friend like Marta. Thank you for your support and for helping me through the difficult times especially in this last year.

Maria, grazie per la bella amicizia che ci lega nonostante le nostre strade abbiamo preso direzioni diverse.

Michele e Francesco, paraninmfen, chi l’avrebbe mai detto! E’ un piacere poter avere due angeli custodi come voi. Grazie di cuore!

Infine, grazie alla mia famiglia per essere sempre il mio piu’ importante punto di riferimento.

Francesca

Curriculum Vitae

Francesca Corbellini was born in Leno (Italy) on October 26, 1975. In 1994 she obtained her diploma from the “Liceo Scientifico” B. Pascal, Ghedi (Italy). From 1994 till 1999 she studied Chemistry at the University of Parma (Italy).

Research conducted for her Master degree was based on the synthesis of chiral peptidic nucleic acids (PNAs) and studies of their diagnostic applications. The project centered on the study of the interaction of a PNA containing a “chiral box” with sequences of DNA and RNA of biomedical interest.

In January 2000 she joined the Supramolecular Chemistry and Technology group (SMCT) of Prof. Dr. Ir. David N. Reinhoudt at the University of Twente (The Netherlands). The results of her research conducted during the period 2000-2004 are described in this thesis.